U.S. Department of Energy
1000 Independence Avenue, S.W.
Washington, D.C. 20585

Fiscal Year 2017: Second Quarter

Progress Report
Advanced Battery Materials Research (BMR) Program

Revision 1: August 2017
for the period of January – March 2017

Approved by

Tien Q. Duong, Advanced Battery Materials Research Program Manager
Vehicle Technologies Office, Energy Efficiency and Renewable Energy

TABLE OF CONTENTS

TABLE OF FIGURES

TABLE OF TABLES

A MESSAGE FROM THE ADVANCED BATTERY MATERIALS RESEARCH PROGRAM MANAGER

This document summarizes the Advanced Battery Materials Research Program (BMR) investigator's activities performed from January 1, 2017, through March 31, 2017. Selected task highlights are summarized below:

- **Task 8.1 – New Lamination and Doping Concepts for Enhanced Li–S Battery Performance**

  Studies conducted at University of Pittsburg (Kumta's Group) have shown directly doped sulfur assembly (DDSA) electrodes with 1305 mAh/g and a very low fade rate of ~0.0014%/cycle.

- **Task 8.6 – Nanostructured Design of Sulfur Cathodes for High-Energy Li–S Batteries**

  Using sulfide catalysts, Li_2S electrodes were demonstrated with capacities (S-VS_2@G/CNT electrode) of 830 mA h g^{-1}, and the capacity remains at 701 mA h g^{-1} after 300 cycles with stabilized Coulombic efficiency above 99.5% (Stanford University, Cui's Group).

- **Task 1.3 – Electrode Architecture–Assembly of Battery Materials and Electrodes**

  Hydro–Quebec (Zaghib's Group) synthesized a SiO_x material consisting of nano-fibers and nano-particles that has cycled nearly 100 times in a half-cell with no capacity decay.

- **Task 9.3 – Li–Air Batteries**

  Argonne National Laboratory (Amine's Group) discovered that the hydrolysis of solid LiO_2 is significantly different from that of NaO_2 and KO_2, and a new approach has been developed that provides information on the composition of a discharge product in a Li-O_2 battery.

- **Task 4.5 – High Conductivity and Flexible Hybrid Solid–State Electrolyte**

  The University of Maryland (Wachsman's Team) synthesized ion insulating polymer PEO, ion conductive polymer PEO-LiTFSI, and *in situ* coated garnet nanofibers by polymer electrolyte. They found that Li-ion conductivity of cubic phase LLZO garnet pellet can reach as high as 10^{-3} S/cm, while the value for Li-salt-stuffed PEO is generally on the order of 10^{-6} to 10^{-9} S/cm at room temperature.

The U.S. Department of Energy (DOE) Annual Merit Review and Peer Evaluation (AMR) meeting was held at the Washington Wardman Park Hotel in Washington, D.C., on June 5 – 9, 2017. The meeting allowed our BMR investigators to review their plans and accomplishments over the previous 12 months and also provided an opportunity for industry, government, and academia to give input to the DOE. If you would like additional information regarding the BMR projects or our sister Advanced Battery Research (ABR) Program and Developer (USABC) programs, I invite you to visit the AMR website (https://www.annualmeritreview.energy.gov/).

Sincerely,

Tien Q. Duong

Tien Q. Duong
Manager, Advanced Battery Materials Research (BMR) Program
Energy Storage R&D
Vehicle Technologies Office
Energy Efficiency and Renewable Energy
U.S. Department of Energy

TASK 1 – ADVANCED ELECTRODE ARCHITECTURES

Summary and Highlights

Energy density is a critical characterization parameter for batteries for electric vehicles (EVs), as there is only so much room for the battery and the vehicle needs to travel over 200 miles. The U.S. Department of Energy (DOE) targets are 500 Wh/L on a system basis and 750 Wh/L on a cell basis. To meet these requirements not only entails finding new, high-energy-density electrochemical couples, but also highly efficient electrode structures that minimize inactive material content, allow for expansion and contraction for several thousand cycles, and allow full access to the active materials by the electrolyte during pulse discharges. In that vein, the DOE Vehicle Technologies Office (VTO) supports several projects in the Advanced Battery Materials Research (BMR) Program under the Advanced Electrode Architectures Task: (1) Higher Energy Density via Inactive Components and Processing Conditions and also Thermally Enhanced Lithium-Ion Cell Using Chemical Functionalization, both at Lawrence Berkeley National Laboratory (LBNL); (2) Electrode Architecture-Assembly of Battery Materials and Electrodes, Hydro–Quebec (HQ); and (3) Design and Scalable Assembly of High-Density, Low-Tortuosity Electrodes, Massachusetts Institute of Technology (MIT). These projects employ three different general engineering approaches to improving energy density. The first approach attempts to increase energy density by making thicker electrodes and reducing the overall amount of inactive components per cell. There is also an attempt at monitoring thermal efficiency *in situ*. The second approach attempts to increase energy density of Li-ion cells by replacing graphitic anodes with cyclable, high-capacity, Si-based active materials. The third approach attempts to make low-tortuosity electrodes by applying a magnetic field. All attempts involve establishing an appropriate methodology for introducing the changes.

One problem being addressed with the first approach is that as electrode thickness increases, the drying time can increase, which allows additional time for segregation of the electrode components. Another problem is that thick electrodes may still have to be wound around a mandrel in a cylindrical cell configuration. Both problems can result in delamination of the laminate from the current collector.

The problem being addressed by the second approach is that although silicon offers higher specific capacity for lithium, it experiences a 300% increase in volume during the lithiation process. The change in volume results in surface area being freshly exposed to electrolyte during the charging process and in a large amount of lithium ions to be consumed in forming the solid electrolyte interface (SEI) on the anode.

The problem being addressed by the third approach is that tortuosity plays an important role in the mass transfer limit of lithium ions across the cell. One way to increase the thickness and yet still discharge at high rates is to reduce the tortuosity.

Highlight. Zaghib's Group at HQ synthesized a SiO_x material consisting of nano-fibers and nano-particles that has cycled nearly 100 times in a half-cell with no capacity decay.

Task 1.1 – Thermally Enhanced Lithium-Ion Cell Using Chemical Functionalization
(Ravi Prasher and Vincent Battaglia, Lawrence Berkeley National Laboratory)

Project Objective. Effective heat dissipation in batteries is important for many reasons, such as performance, reliability, safety and fast charging. Currently, thermal management of battery cells is provided at the system level by either forced air or liquid cooling. This engineering solution has many shortcomings, such as a reduction in energy density and power density at the system level and also complex system-level designs that allow for fluid flow. This project is planned to overcome these challenges by increasing the effective thermal conductivity (k) of battery materials inside Li-ion cells. The overarching goal of this project is to increase the effective out-of-plane thermal conductivity of Li-ion battery cells by more than three to four times without affecting the electrical performance of Li-ion batteries.

Project Impact. An increased k of battery materials will reduce the burden on system-level cooling solutions significantly, leading to less complex and lower-cost Li-ion battery packs. Simpler system level solutions will also significantly increase the pack level energy density and power density.

Out-Year Goals. In the outgoing years, the project will measure thermal conductivity and resistance at the interface (R_{int}) of all materials within a functioning Li-ion battery cell in the presence and absence of electrolytes to identify and characterize individual sources of thermal resistance. To carry out these measurements, the project will employ state-of-the-art thermal characterization techniques, such as time-domain thermoreflectance (TDTR) and 3-omega. A number of interfacial chemistry methods will also be explored to reduce R_{int} within the Li-ion battery cell. The project will explore and optimize vapor-based techniques to functionalize different interfaces. It will also evaluate the success of the chemical and/or physical treatment of the cathode and the separator by using various microscopy and spectroscopy tools such as scanning electron microscopy (SEM), transmission electron microscopy (TEM), and X-ray photoelectron spectroscopy (XPS). The enhancement in adhesion between the interfaces before and after interfacial chemistry will be established by carrying out adhesion testing.

Collaborations. This project collaborates with Battaglia's Group at LBNL for electrode synthesis and electrical characterization.

Milestones

1. Fabricate metrology compatible battery material samples. (Complete)

Progress Report

The project has chosen the 3-omega technique to be its primary thermal metrology for battery material characterization for these reasons: it can measure thin materials (tens of microns via the traditional technique; tens of nanometers via the differential mode); it can achieve accuracies better than 5% even for high thermal conductance; it is robust against parasitic heat losses and interference from thermal signals generated by the battery itself; and it is easiest for compatibility in battery systems. The 3-omega technique works by using a heater line to provide periodic heating and temperature sensing at a sample surface, from which k of the materials and interfaces below can be measured. The project built a 3-omega system in its lab from scratch (Figure 1), verified its accuracy on control samples (glass, $k \sim 1.1$ W/m-K, and silicon, $k \sim 143$ W/m-K), and calibrated its sensitivity by accurately measuring k of 300-nm-thick glass and k of a 450-µm silicon wafer. The system, therefore, has a demonstrated sensitivity strong enough to measure conductance as high as ~ 0.3 MW/m^2-K (traditional measurement) and ~ 3.5 MW/m^2-K (in differential 3-omega mode).

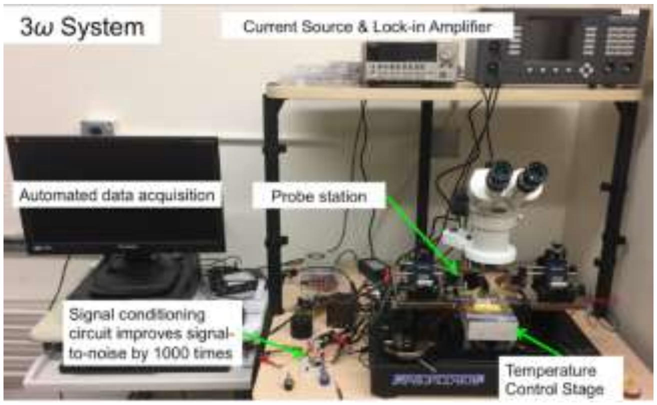

Figure 1. In-house 3-omega thermal metrology system.

To make battery samples compatible with this metrology, a 50-nm-thick, electrically insulating alumina layer was first deposited on the back side of the current collector of the battery electrode, using atomic layer deposition (ALD). Then, thin (300-nm thick) aluminum or gold heater lines (2 mm x 0.1 mm) were deposited on top of this passivation layer (Figure 2, left). Thin (60 µm), insulated, wire leads were attached to the heater-line contact pads and used for measurement. So far, these samples have been tested on the bench top by affixing cutout electrode pieces to support glass substrates (Figure 2, right).

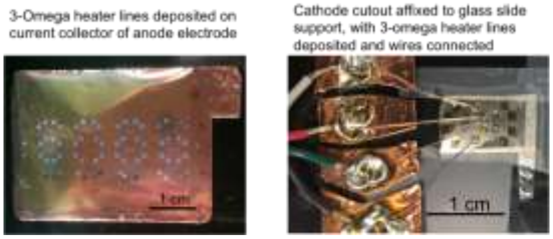

Figure 2. 3-omega lines on battery electrodes.

In the future, the project will cover the 3-omega heater lines with a protective, hollow, Teflon pocket, place those electrodes inside a full-battery pouch-cell with a separator and electrolyte, and run the 3-omega sensor wire leads out of the sealed, battery pouch-cell. So far, the project has successfully created a functioning, sealed, battery pouch-cell without 3-omega sensors (Figure 3, left) and has begun prototyping the hollow Teflon shields (Figure 3, right) to protect the 3-omega heater lines within the pouch cell.

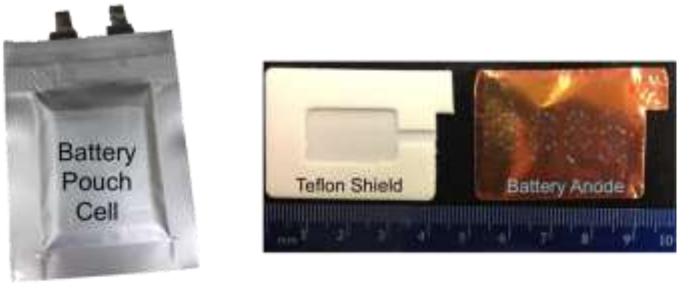

Figure 3. (left) In-house-made functioning battery pouch cell. (right) Hollow Teflon pocket.

Task 1.2 – Prelithiation of Silicon Anode for High-Energy Lithium Ion (Yi Cui, Stanford University)

Project Objective. Prelithiation of high-capacity electrode materials such as silicon is an important means to enable those materials in high-energy batteries. This study pursues two main directions: (1) developing facile and practical methods to increase first-cycle CE of Li-ion batteries, and (2) synthesizing fully lithiated silicon and other lithium compounds for pre-storing lithium.

Project Impact. The first-cycle CE of Li-ion batteries will be increased dramatically via prelithiation. Prelithiation of high-capacity electrode materials will enable those materials in next generation high-energy-density batteries. This project's success will make high-energy-density Li-ion batteries for EVs.

Out-Year Goals. Compounds containing a large quantity of lithium will be synthesized for pre-storing lithium ions inside batteries. First-cycle CE will be improved and optimized (over 95%) by prelithiation with the synthesized Li-rich compounds. The stability of prelithiation reagents in the air conditions and solvents will be improved.

Collaborations. This project collaborates with the following:

- BMR PIs,
- Stanford Linear Accelerator Center (SLAC): *In situ* X-ray, Dr. Michael Toney, and
- Stanford University: Prof. Nix, mechanics.

Milestones

1. Synthesize LiF/metal nanocomposite for cathode prelithiation with high capacity and good air stability (> 500 mAh/g). (March 2016 – Complete)
2. Synthesize Li_xSi-Li_2O composites for anode prelithiation with improved stability in ambient air with 40% relative humidity. (June 2016 – Complete)
3. Synthesize Li_xGe nanoparticles and Li_xGe-Li_2O composites for anode prelithiation with improved air-stability. (January 2017 – Complete)
4. Synthesize Li_xSn nanoparticles and Li_xSn-Li_2O composites for anode prelithiation with improved air-stability. (April 2017 – On going)

Progress Report

In the previous study, the team demonstrated that metallurgically synthesized Li_xSi nanoparticles (NPs) can serve as a high-capacity prelithiation reagent to effectively increase the first-cycle CE of anode materials. Group IV elements such as tin have relatively high specific capacities (993 mAh/g for tin) and similar volumetric capacities to silicon (2574 mAh/cm^3 for silicon, and 2111 mAh/cm^3 for tin), making them also suitable for pre-storing lithium. Tin NPs and SnO_2 nanoclusters were used as the starting materials to form the Li_xSn alloy and Li_xSn-Li_2O composite, respectively. The alloying temperature should be maintained between the melting points of lithium metal and tin NPs to ensure the preservation of the morphology of tin NPs. SEM was utilized to characterize the morphology of the tin NPs and SnO_2 nanoclusters before and after lithiation. SEM images confirm that the tin NPs have sizes less than 200 nm (Figure 4a). After metallurgical lithiation, the shape of the NPs is retained, whereas the particle sizes are larger due to volume expansion and some aggregation (Figure 4b).

XRD confirms transformation from tin (PDF no. 00-004-0673) to $Li_{22}Sn_5$ (PDF no. 01-081-6569) after thermal alloying with molten lithium (Figure 4c). The small amount of Li_2O arises from the intrinsic oxide SnO (PDF no. 04-005-4541) in tin NPs. The hydrothermal-synthesized SnO_2 nanoclusters are uniform both in size (~ 50 nm) and shape, as confirmed by SEM (Figure 4d). The monodisperse SnO_2 nanoclusters were utilized as the precursor for the Li_xSn-Li_2O composite. After thermal lithiation, the morphology of SnO_2 nanoclusters was preserved, whereas the size of the clusters slightly increased to 75 nm because of volume expansion (Figure 4e). XRD of lithiated SnO_2 shows the same final products as lithiated tin NPs with a higher percentage of the Li_2O phase.

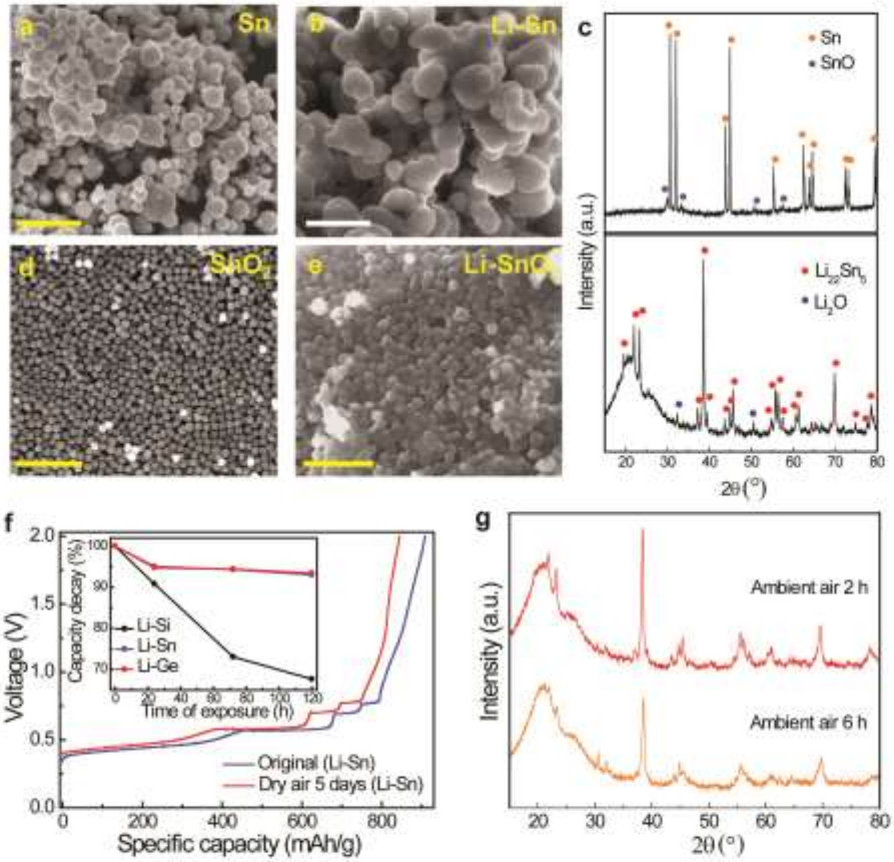

Figure 4. (a, b) Scanning electron microscopy (SEM) images of tin nanoparticles (NPs) (a) before (a) and after (b) thermal lithiation. Scale bar, 500 nm. (c) X-ray diffraction (XRD) patterns of tin NPs before (upper) and after (bottom) thermal lithiation. (d, e) SEM images of SnO_2 NPs before (d) and after (e) thermal lithiation. Scale bar, 500 nm. (f) First-cycle delithiation capacities of lithiated tin NPs before (blue) and after (red) exposure to dry-air condition for 5 days. The inset shows the trend of capacity decay of lithiated silicon (black), tin (purple) and germanium (red) NPs. (g) XRD patterns of lithiated tin NPs exposed to ambient-air condition for 2 h (upper) and 6 h (bottom).

To compare dry-air stability, different Li_xZ (Z = Si, Ge and Sn) alloys were stored in a dry room (dew point = −50°C) for 5 days. The remaining capacity of Li_xSn NPs exposed to dry air over many days was studied by charging the Li_xSn NPs electrodes to 2V at a low rate of C/20 (Figure 4f). After 5 days of exposure, Li_xSn NPs exhibit a high capacity of 845 mAh/g, corresponding to a capacity retention of 93%. The capacity decay for Li_xSn alloy and Li_xGe alloy is much slower compared with Li_xSi alloy. Among the Li_xZ alloys, Li_xGe shows the best dry-air stability with negligible (6.5%) capacity decay after 5 days of exposure.

No new peaks are present in the XRD pattern of Li_xSn NPs exposed to ambient air (~ 40% RH) for 2 h (Figure 4g, top). The XRD pattern reveals small peaks belonging to Li(OH)•H_2O (PDF no. 04-010-4336), and $Li_{22}Sn_5$ remains the major component after being exposed to ambient air for 6 h (Figure 4g, bottom). Because of the excellent air stability, the Li_xSn alloy and Li_xSn-Li_2O composites are potentially compatible to the industry battery fabrication process.

Patents/Publications/Presentations

Publication

- Zhao, J., and J. Sun, A. Pei, K. Yan, G. Zhou, Y. Liu, D. Lin, and Y. Cui.* "A General Prelithiation Approach for Group IV Elements and Corresponding Oxides." *Energy Storage Materials*. Under review.

Task 1.3 – Electrode Architecture-Assembly of Battery Materials and Electrodes (Karim Zaghib, Hydro–Quebec)

Project Objective. The project goal is to develop an electrode architecture based on nano-Si materials and design a full cell having high energy density and long cycle life. To achieve the objective, this project investigates the structure of nano-Si materials that provide acceptable volume change to achieve long cycle life, while still maintaining the high-capacity performance of silicon. The project scope includes control of the particle size distribution of nano-Si materials, crystallinity, silicon composition, and surface chemistry of the nano-Si materials. The focus is to develop electrode formulations and electrode architectures based on nano-Si materials, which require optimized nano-Si/C composites and functional binders, as well as a controlled pore distribution in the electrode and the related process conditions to fabricate the electrode.

Project Impact. Silicon is a promising alternative anode material with a capacity of ~4200 mAh/g, which is more than a magnitude higher than that of graphite. However, many challenges remain unresolved, inhibiting commercialization of silicon; this is mainly due to the large volume variations of silicon during charge/discharge cycles that result in pulverization of the particle and poor cycling stability. Successful development of highly reversible silicon electrodes with acceptable cost will lead to higher-energy-density and lower-cost batteries that are in high demand, especially for expanding the market penetration for EVs.

Approach. The project approach will encompass the following:

- Explore various synthesis methods to produce low-cost, nano-Si materials with controlled purity and particle morphology.
- Develop an appropriate silicon anode architecture that can tolerate volumetric expansion and provide an acceptable cycle life with low capacity fade.
- Identify a binder and electrode composition by investigating parameters that define the electrode structure, such as porosity, loading, and electrode density. The optimized Si-anode will be matched with a high-voltage NMC cathode to fabricate large format Li-ion cells.
- Use *in situ* techniques such as SEM and impedance spectroscopy to monitor the particle and electrode environment changes during cycling.
- Achieve cost reduction by moving from more costly silicon (> $50/kg) to metallurgical silicon, which is projected to be $3~$5/kg.

Out-Year Goals. Conduct failure mode analysis of nano-Si anodes before and after cycling. Use dual-beam (electron + ion) microscopy and TOF-SIMS (time-of-flight secondary ion mass spectrometry) techniques to analyze residual lithium contents in the structure of delithiated anodes. This analysis will help in understanding the failure mode of the anode and help guide efforts to improve particle morphology and electrode architecture.

Collaborations. This project collaborates with BMR PIs: V. Battaglia and G. Liu (LBNL), C. Wong and Jason Zhang (Pacific Northwest National Laboratory, PNNL), and J. Goodenough (University of Texas, UT).

Milestones

1. Analyze failure mode of the nano-Si/C composite electrode before and after cycling. Improve structure of the nano-Si/C composite based on results of failure mode analysis. (Q1 – Complete)
2. Explore new binder system with nano-Si/C composite; make new composite with electrospinning process. (Q2 – Complete)
3. Optimize electrode composition with nano-Si/C composite; evaluate electrochemical performance. (Q3 – In progress)
4. Verify performance in pouch-type full cell. *Deliverable*: 20g of nano-Si/C composite powder. (Q4 – In progress)

Progress Report

As part of an effort to mitigate ill effects of the volume expansion of silicon particles during charge/discharge, HQ synthesized SiO_x with a mixed morphology of nano fibers and nano particles. Figure 5 shows that the material is composed of randomly mixed nano fibers with a diameter 10 to 100 nm and nano particles less than 100 nm. The material is synthesized by a plasma process in one step without post treatment. Process parameters, such as precursor feeding rate, gas flow rate, and carrier gas concentration, were controlled to obtain morphologies with different fiber-to-particle ratios. Figure 5 shows the results from two different process conditions. For Condition A, a mixture of argon and helium was used as a plasma sheath gas, while for Condition B a mixture of argon and H_2 was used.

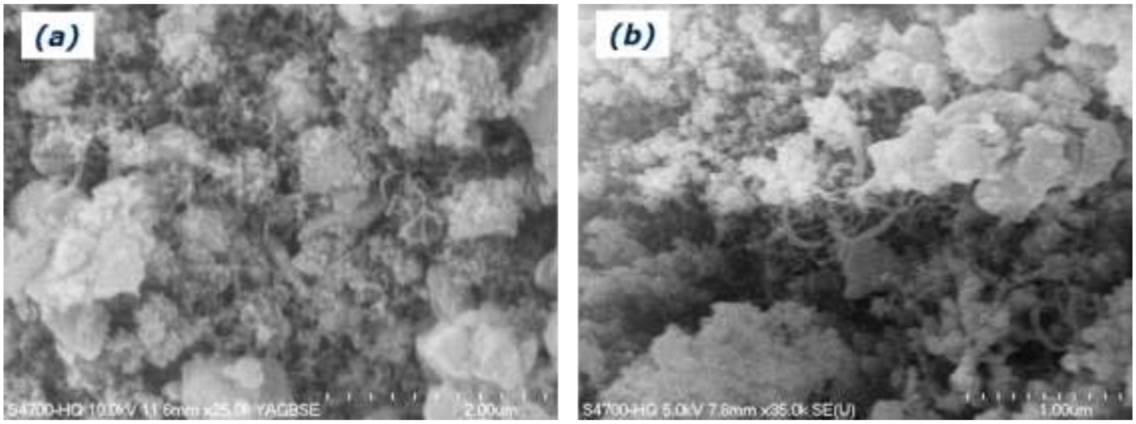

Figure 5. Scanning electron microscopy images of nano-SiO_x fibers for (a) Condition A and (b) Condition B.

The electrochemical performance was assessed in a coin-type half-cell with 1M $LiPF_6$–ethylene carbonate (EC)-diethyl carbonate (DEC)–10% fluoroethylene carbonate (FEC); the results are shown in Figure 6. The loading of active material (SiO_x) was around 0.5 mg/cm^2, and the electrode density was 0.7 g/cc. The composition of the nano-SiO_x electrode was 50%, with the other half a water-based binder. The measured capacity at C/24 was around 1050 mAh/g for Condition A and 1150 mAh/g for Condition B. After the first charging reaction, where a significant irreversible capacity results from the conversion reaction of SiO_x with Li^+, the Coulombic efficiency (CE) improved to greater than 95% for all subsequent cycles. The capacity retention was quite stable: no capacity loss after 90 cycles at C/6 (Figure 6b).

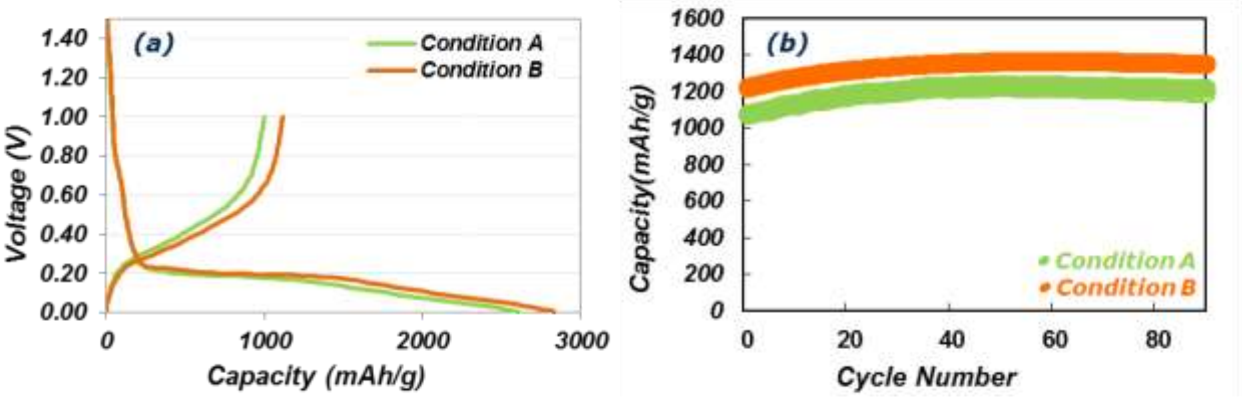

Figure 6. Electrochemical performance of (a) 1st charge/discharge voltage profile at C/24 between 1.0 V and 0.005 V and (b) cycle life at C/6 and room temperature.

The results show that the synthesized SiO_x is a promising material for a high-capacity anode. However, further effort is needed to obtain better morphology control and to improve the CE of the first cycle.

Task 1.4 – Design and Scalable Assembly of High-Density, Low-Tortuosity Electrodes
(Yet-Ming Chiang, Massachusetts Institute of Technology)

Project Objective. The project objective is to develop scalable, high-density, low-tortuosity electrode designs and fabrication processes enabling increased cell-level energy density compared to conventional Li-ion technology. It will also characterize and optimize the electronic and ionic transport properties of controlled porosity and tortuosity cathodes as well as densely-sintered reference samples. Success is measured by the area capacity (mAh/cm^2) that is realized at defined C-rates or current densities.

Project Impact. The high cost ($/kWh) and low energy density of current automotive Li-ion technology is in part due to the need for thin electrodes and associated high inactive materials content. If successful, this project will enable use of electrodes based on known families of cathode and anode actives, but with at least three times the areal capacity (mAh/cm^2) of current technology, while satisfying the duty cycles of vehicle applications. This will be accomplished via new electrode architectures fabricated by scalable methods with higher active materials density and reduced inactive content, and will in turn enable higher-energy-density and lower-cost EV cells and packs.

Approach. Two techniques are used to fabricate thick, high-density electrodes with low tortuosity porosity oriented normal to the electrode plane: (1) directional freezing of aqueous suspensions; and (2) magnetic alignment. Characterization includes measurement of single-phase material electronic and ionic transport using blocking and non-blocking electrodes with AC and DC techniques, electrokinetic measurements, and drive-cycle tests of electrodes using appropriate battery scaling factors for EVs.

Out-Year Goals. Identify anodes and fabrication approaches that enable full cells in which both electrodes have high area capacity under EV operating conditions. Anode approach will include identifying compounds amenable to same fabrication approach as cathode, or use of very high capacity anodes such as stabilized lithium or Si-alloys that in conventional form can capacity-match the cathodes. Use data from best-performing electrochemical couple in techno-economic modeling of EV cell and pack performance parameters.

Collaborations. Within BMR, this project collaborates with Antoni P. Tomsia (LBNL) in fabrication of low-tortuosity, high-density electrodes by directional freeze-casting, and with Gao Liu (LBNL) in evaluating silicon anodes. Externally, the project collaborates with Randall Erb (Northeastern University) on magnetic alignment fabrication methods for low-tortuosity electrodes.

Milestones

1. *Go/No-Go*: Fabricate and test half-cells and full Li-ion cell in which both cathode and anode are prepared by magnetic alignment, and in which at least one electrode is prepared by non-sintering process. Criteria: Measured area capacity of a half-cell is at least 10 mAh/cm^2 and of a full cell is at least 8 mAh/cm^2. (December 2016 – Complete)

Note. All milestones have been completed. This report provides additional results for preparation of low-tortuosity thick electrodes from other materials beyond those previously demonstrated, using the non-sintering magnetic alignment method. (March 2017 – Complete)

Progress Report

This quarter, additional results are reported for preparation of low-tortuosity thick electrodes from materials beyond $LiCoO_2$ (Umicore, average particle size 2–4 μm) and mesocarbon microbeads (MCMB) 6-28 (Osaka Gas, average particle size 6 μm), which were reported previously. The goal is to investigate whether the non-sintering magnetic alignment method can be generally applied to various electrode materials.

Commercially available electrode materials were chosen for this study: $LiFePO_4$ (LFP, MTI Corporation, D50 ~3.5 μm), OMAC-carbon (Osaka Gas), $LiNi_{1/3}Mn_{1/3}Co_{1/3}O_2$ (NMC-333, Toda, average particle size ~ 10 μm), $LiNi_{0.8}Co_{0.15}Al_{0.05}O_2$ (NCA, Toda, average particle size 2-5 μm), and MCMB (MTI Corporation, D50 ~ 18 μm). These materials were mixed with acetylene black, polyvinyl alcohol, water, and a small amount of ferrofluid (~5 vol%) and sonicated using an ultrasonic probe to make the emulsion-based slurries, whose formulations are similar to those used for $LiCoO_2$ (Umicore) and MCMB 6-28 (Osaka Gas) as reported previously. The slurries were then dried in silicone molds on top of magnets to make the electrodes. After initial drying, the electrodes were rinsed thoroughly using kerosene and acetone, and further dried at 100°C under vacuum.

The electrodes were cross-sectioned and examined using SEM (Figure 7). Figure 7a-b shows that vertically aligned pore channels are successfully introduced into LFP and OMAC-carbon electrodes. This demonstrates that the non-sintering magnetic alignment method can indeed work with electrode materials beyond the previously tested $LiCoO_2$ (Umicore) and MCMB 6-28 (Osaka Gas). The result with the NMC-333 electrode was less satisfactory (Figure 7c). Vertically aligned pore channels were observed, but they did not completely span the thickness of the electrode. For NCA and MCMB (MTI) electrodes, vertically aligned pore channels were not observed. The specific reasons are unclear, but particle size and surface chemistry may play important roles; these factors may be further investigated.

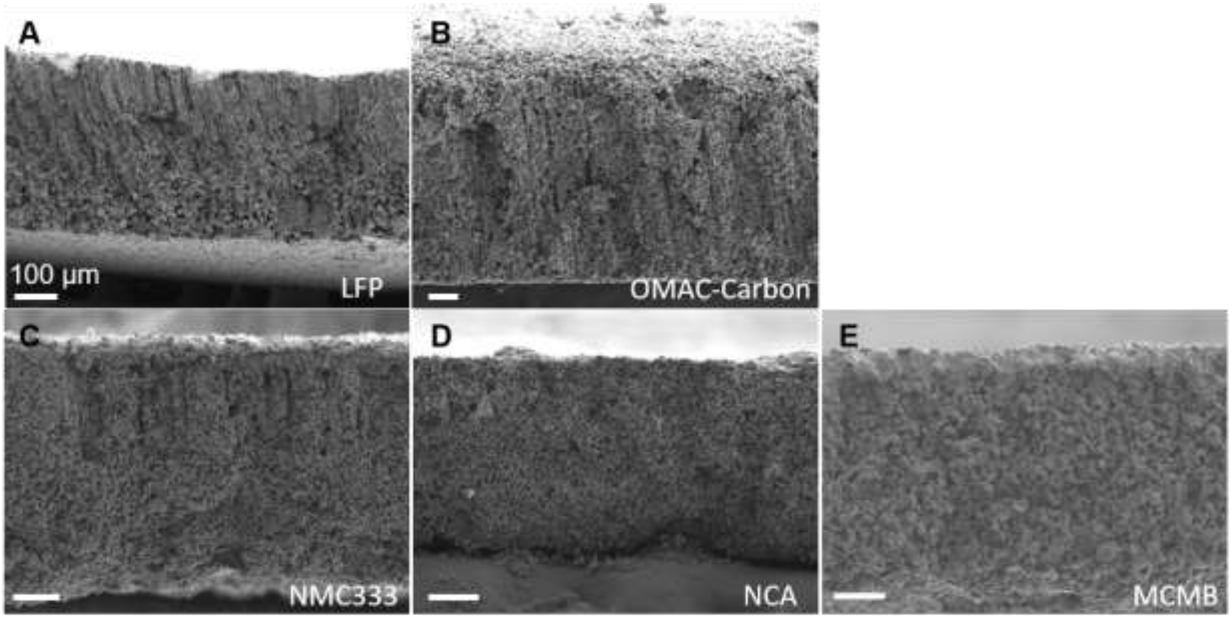

Figure 7. Electrodes of different materials prepared by the non-sintering magnetic alignment method. (a) LFP (MTI Corporation). (b) OMAC-carbon (Osaka Gas). (c) NMC-333 (Toda). (d) NCA (Toda). (e) Mesocarbon microbeads, or MCMB (MTI Corporation).

Task 2 – Silicon Anode Research

Summary and Highlights

Most Li-ion batteries used in state-of-the-art EVs contain graphite as their anode material. Limited capacity of graphite (LiC_6, 372 mAh/g) is one barrier that prevents the long-range operation of EVs required by the EV Everywhere Grand Challenge proposed by the DOE Office of Energy Efficiency & Renewable Energy (EERE). In this regard, silicon is one of the most promising candidates as an alternative anode for Li-ion battery applications. Silicon is environmentally benign and ubiquitous. The theoretical specific capacity of silicon is 4212 mAh/g ($Li_{21}Si_5$), which is 10 times greater than the specific capacity of graphite. However, the high specific capacity of silicon is associated with large volume changes (more than 300 percent) when alloyed with lithium. These extreme volume changes can cause severe cracking and disintegration of the electrode and can lead to significant capacity loss.

Significant scientific research has been conducted to circumvent the deterioration of Si-based anode materials during cycling. Various strategies, such as reduction of particle size, generation of active/inactive composites, fabrication of Si-based thin films, use of alternative binders, and the synthesis of one-dimensional silicon nanostructures have been implemented by several research groups. Fundamental mechanistic research also has been performed to better understand the electrochemical lithiation and delithiation processes during cycling in terms of crystal structure, phase transitions, morphological changes, and reaction kinetics. Although significant progress has been made on developing Si-based anodes, many obstacles still prevent their practical application. Long-term cycling stability remains the foremost challenge for Si-based anode, especially for the high loading electrode (> 3mAh/cm^2) required for many practical applications. The cyclability of full cells using Si-based anodes is also complicated by multiple factors, such as diffusion-induced stress and fracture, loss of electrical contact among silicon particles and between silicon and current collector, and the breakdown of SEI layers during volume expansion/contraction processes. The design and engineering of a full cell with a Si-based anode still needs to be optimized. Critical research remaining in this area includes, but is not limited to, the following:

- Low-cost manufacturing processes must be found to produce nano-structured silicon with the desired properties.
- The effects of SEI formation and stability on the cyclability of Si-based anodes need to be further investigated. Electrolytes and additives that can produce a stable SEI layer need to be developed.
- A better binder and a conductive matrix need to be developed. They should provide flexible but stable electrical contacts among silicon particles and between particles and the current collector under repeated volume changes during charge/discharge processes.
- The performances of full cells using Si-based anode needs to be investigated and optimized.

The main goal is to have a fundamental understanding on the failure mechanism on Si-based anode and improve its long-term stability, especially for thick electrode operated at full-cell conditions. Success of this project will enable Li-ion batteries with a specific energy of >350 Wh/kg (in cell level), 1000 deep-discharge cycles, 15-year calendar life, and less than 20% capacity fade over a 10-year period to meet the goal of the EV Everywhere Grand Challenge.

Highlight. Kumta of University of Pittsburgh (U Pitt) developed a commercially viable facile electrodeposition process with a nonaqueous ionic electrolyte consisting of silicon containing precursors and demonstrates an excellent capacity retention with a stable capacity of ~1870 mAh/g up to 70 cycles.

Task 2.1 – High-Capacity and Long Cycle Life Silicon Carbon Composite Materials and Electrodes (Gao Liu, Lawrence Berkeley National Laboratory)

Project Objective. This project will synthesize Si/C anode composite materials at 1,000 mAh/g capacity at a cost less than $10/kg and fabricate a long-cycle-life electrode similar to a graphite electrode for high-energy-density Li-ion batteries.

Project Impact. Low energy density and limited lifetime are two major drawbacks of the automobile Li-ion batteries for EV and plug-in hybrid electric vehicle (PHEV) applications. The project will develop high-capacity and long-life Si/C composite anodes to prolong battery cycling and storage lifetime, and to provide an in-depth understanding of silicon electrode design strategies to stabilize silicon material volume change and to prevent surface side reactions. This research effort will generate new intellectual properties based on the fundamental discovery of novel materials and new synthesis processes, and will bridge the research and development (R&D) gaps between the fundamental research and the applied materials discovery, to pave the way for the successful commercialization of silicon materials.

Approach. This work combines novel materials design and innovative synthesis process to synthesize mechanically robust and dimensionally stable Si/C composite materials. In addition, it will use low-cost Si/C precursor materials and a scalable process to generate low-cost Si/C product.

Out-Year Goals. The work progresses toward study of the physical and chemical properties and of electrochemical properties of the low-cost precursor materials. Novel synthesis strategy will be developed and used to fabricate materials to tailor the morphology, structure, composite component, and electrochemical properties of the Si/C composite materials. The morphologic and structural features and electrochemical properties will be characterized for the as-prepared Si/C composited with functional binder during electrochemical testing. The goal is to achieve a high-capacity, long-life Li-ion battery using this Si/C composite anode.

Collaborations. This project is a single investigator project. However, the proposed work requires extensive collaboration with DOE user facilities at national laboratories and industries. These include the National Center for Electron Microscopy (NCEM) and the Advanced Light Sources (ALS) program at LBNL, *in situ* electrochemical TEM facilities at the Environmental Molecular Sciences Laboratory (EMSL), the national user facility at PNNL, HQ's Research Institute (IREQ), General Motors (GM) R&D Center, and LBNL BMR laboratories. The project will also involve collaboration with BMR participants at LBNL, including Dr. Marca Doeff's group and Dr. Vince Battaglia's group.

Milestones

1. Set up the silicon materials and carbon precursors library, and finish characterizing the starting materials. (December 2016 – Complete)
2. Conduct preliminary tests to generate Si/C composite particles with the spray methods. (March 2017 – Complete)
3. Electron microscopy image analyses of the Si/C samples and development of functional binders based on Si/C composite structures. (June 2017 – On schedule)
4. Electrochemical analysis to demonstrate > 1000 mAh/g and > 3 mAh/cm^2 of the Si/C composite electrodes. (September 2017 – On schedule)

Progress Report

Preliminary tests were conducted using a spray method to synthesize Si/C composites particles, with a focus of controlling the spray conditions and understanding the morphology of the formed particles. A polymer adhesive was used as carbon precursor. The polymer solution and silicon nanoparticles were mixed to form viscous slurry. Different concentration of polymer was used to tune the viscosity of the slurry. When the slurry was sprayed into a non-solvent liquid pool, the slurry droplet precipitated into micron-sized spherical particles. Depending on the compositions of the slurry, a void space in the middle of the spherical composite particles could be formed. These hollow core spherical particles are composed of silicon nanoparticles and the polymer adhesive in the shell. The polymer adhesive glues the nanoparticles together to hold the hollow core shape of the micron-sized particles. Further, sintering these particles at elevated temperature affords hollow core Si/C micron-sized particle composites.

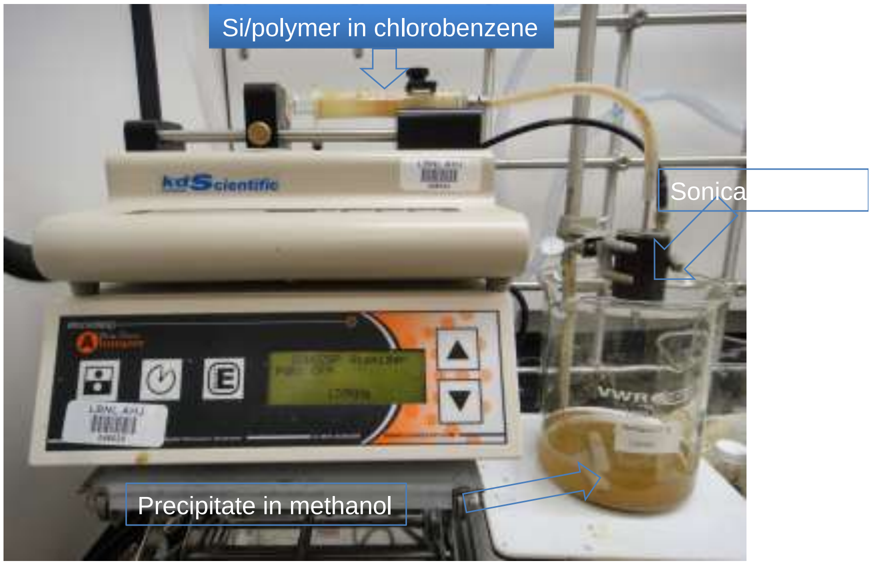

Figure 8. Photo image of the sonication spray-precipitation instrument setup for fabrication of Si/polymer secondary composite particles.

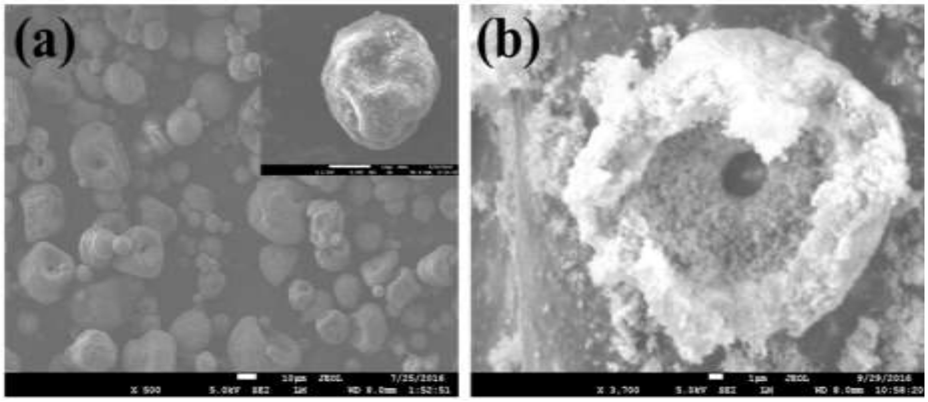

Figure 9. Scanning electron microscopy images of Si/polymer hollow particles made by spray method. (a) Si/polymer composite particles. The inset is single composite particle. (b) A broken particle shows the hollow core.

Task 2.2 – Stable Operation of Silicon-Based Anode for Lithium-Ion Batteries (Ji-Guang Zhang and Jun Liu, Pacific Northwest National Laboratory; Prashant Kumta, University of Pittsburgh)

Project Objective. The project objective is to develop a low-cost approach to prepare high-capacity Si-carbon composite anodes with good cycle stability and rate capability to replace graphite anode used in Li-ion batteries. In one approach, low-cost Si-graphite-carbon composite will be developed to improve the long-term cycling performance while maintaining a reasonably high capacity. Si-based secondary particles with a nano-Si content of ~10 to 15 wt% will be embedded in the matrix of active graphite and inactive conductive carbon materials. Controlled void space will be pre-created to accommodate the volume change of silicon. A layer of highly graphitized carbon coating on the outside will be developed to minimize the contact between silicon and electrolyte and hence minimize the electrolyte decomposition. New electrolyte additives will be investigated to improve the stability of SEI layer. In another approach, nanoscale silicon and Li-ion conducting lithium oxide composites will be prepared by *in situ* chemical reduction methods. The stability of Si-based anode will be improved by generating the desired nanocomposites containing nanostructured amorphous or nanocrystalline silicon as well as amorphous or crystalline lithium oxide ($Si+Li_2O$) by the direct chemical reduction of a mixture and variety of silicon sub oxides (SiO and SiO_x) and/or dioxides. Different synthesis approaches comprising direct chemical reduction using solution, solid-state, and liquid-vapor phase methods will be utilized to generate the $Si+Li_2O$ nanocomposites. The electrode structures will be modified to enable high utilization of thick electrode.

Project Impact. Si-based anodes have much larger specific capacities compared with conventional graphite anodes. However, the cyclability of Si-based anodes is limited because of the large volume expansion that is characteristic of these anodes. This work will develop a low-cost approach to extend the cycle life of high-capacity, Si-based anodes. The success of this work will further increase the energy density of Li-ion batteries and accelerate market acceptance of EVs, especially for PHEVs required by the EV Everywhere Grand Challenge proposed by DOE/EERE.

Out-Year Goals. The main goal of the proposed work is to enable Li-ion batteries with a specific energy of > 200 Wh/kg (in cell level for PHEVs), 5000 deep-discharge cycles, 15-year calendar life, improved abuse tolerance, and less than 20% capacity fade over a 10-year period.

Collaborations. This project collaborates with Xingcheng Xiao (GM): *In situ* measurement of thickness swelling silicon anode.

Milestones

1. Synthesize micron-sized silicon with the desired porosity and *in situ* grown graphene coating. (Q1 – Complete)
2. Synthesize low-cost Si-based nanocomposite anode materials using high-energy mechanical milling (HEMM) and other economical template derived methods. (Q2 – Complete)
3. Identify new electrolyte additive to improve the stable operation of Si-based anode. (Q3)
4. Fabricate and characterize Si-based anode with desired electrode capacity (~3 mAh/cm^2). (Q4)

Progress Report

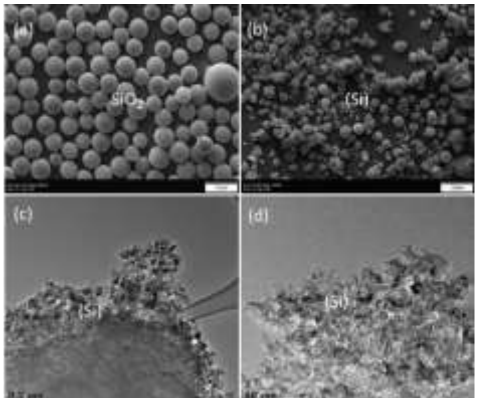

Figure 10. (a) Scanning electron microscopy (SEM) image of silica. (b) SEM image of the obtained silicon. (c-d) Transmission electron microscopy images of the obtained silicon.

This quarter, micro-sized silicon with porous structure was prepared by magnesium reduction and aluminum reduction methods. Silica microspheres were used as the precursor and morphology template. Efforts were made to retain the original morphology of silica after reduction. In the case of magnesium reduction method, different amounts of starting materials were investigated, and the corresponding characterization results were compared. The morphology of silica can be retained very well when the amount of starting materials is suitable. Typically, 0.4g silica, 0.4g magnesium, and 4g sodium chloride were mixed in a THINKY mixture and further ground in the agate mortar. Then, the mixture was placed in the ceramic boat, and heated and maintained at 650ºC (the melting point of magnesium) for 6 h under Ar/H_2 atmosphere to complete the reaction. The X-ray diffraction (XRD) patterns show that the pure silicon phase was obtained after reduction and acid etching. SEM images demonstrate that the as-prepared silicon basically maintains the morphology of silica (Figure109a-b). TEM images of Figure 10c-d confirm the mesoporous structure, in which the primary silicon crystallites with nano size are homogeously distributed. In an effort to further decrease reduction temperature, aluminum reduction method was used. The reaction temperature was further lowered to ~200ºC using a eutectic mixture of $ZnCl_2$ and $AlCl_3$ (melting point ~114°C).

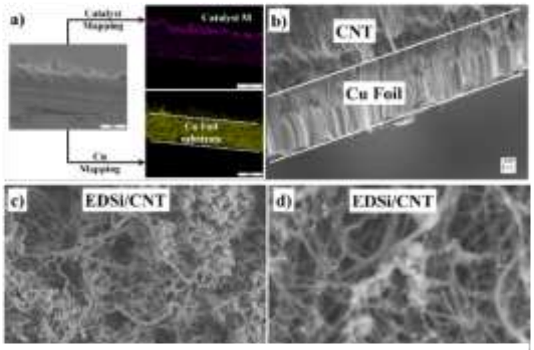

Figure 11. (a) Scanning electron microscopy (SEM) image and EDAX mapping of catalyst layer M on copper foil. (b) SEM of the carbon nanotube (CNT) forest. (c-d) Low and high magnification images of electro-deposition – Si/CNT.

Amorphous silicon was deposited on carbon nanotubes (CNT) using a commercially viable facile electrodeposition process with a nonaqueous ionic electrolyte consisiting of silicon-containing precursors. Figure 11 shows the SEM image and EDAX mapping of M-Cu, CNT forest, and amorphous silicon deposition. The silicon coating on the CNTs is uniform, and the size of the silicon particles is < 100 nm. The loading density of electrodeposited silicon (ED-Si) is ~0.25 mg/cm^2 – 0.31 mg/cm^2. The ED-Si on CNT/M-Cu (denoted as ED-Si/CNT) was tested as an anode in Li/Li$^+$ electrochemical cell without any further addition of additives. The ED-Si/CNT electrodes show a first-cycle discharge and charge capacity of ~ 3435 mAh/g and ~ 2050 mAh/g, respectively, with a first cycle irreversible (FIR) loss of ~ 35 – 45% (Figure 12) at a charge/discharge current rate of ~300 mA/g. The ED-Si/CNT also shows an excellent capacity retention with a stable capacity of ~1870 mAh/g up to 70 cycles (Figure 12). Efforts are under way to increase the ED-Si loading density by employing longer electrodeposition times as well as decrease the FIR loss by employing suitable surface coatings. In-depth characterization such as Raman spectroscopy, XRD, SEM, and TEM at various processing steps is also under way to study the ED-Si/CNT architecture, which will be reported in the future.

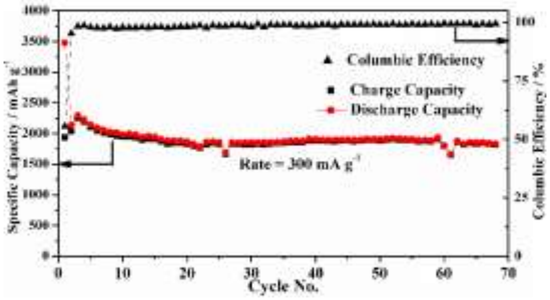

Figure 12. Specific discharge capacity versus cycle numbers for electrodeposition – Si/carbon nanotube nanostructured binder less electrode.

Patents/Publications/Presentations

Publications

- Li, Xiaolin, and Pengfei Yan, Xingcheng Xiao, Jae Ha Woo, Chongmin Wang, Jun Liu, and Ji-Guang Zhang. "Design of Porous Si/C-Graphite Electrodes with Long Cycle Stability and Controlled Swelling." *Energy Environ. Sci* (2017). doi: 10.1039/C7EE00838D.
- Gattu, Bharat, and Rigved Epur, Prashanth H. Jampani, Ramalinga Kuruba, Moni K. Datta and Prashant N. Kumta. "Silicon-Carbon Core-Shell (C@Si@C) Hollow Nanotubular Configuration - High Performance Lithium-Ion Anodes." *Journal of Physical Chemistry - C* (2017). In press.
- Gattu, Bharat, Prashanth H. Jampani, Moni K. Datta, and Prashant N. Kumta, "Water-Soluble Template Derived Nanoscale Silicon Nano-Flakes and Nano-Rods Morphologies: Stable Architectures for Lithium Ion Anodes." *Nanoresearch*. Under review.
- Gattu, B., and R. Epur, P. Shanti, P. H. Jampani, R. Kuruba, M. K. Datta, A. Manivannan, and P. N. Kumta. "Pulsed Current Electrodeposition of Silicon Thin Film Anodes for Lithium-Ion Battery Applications." *Inorganics* (2017). In press.

TASK 3 – HIGH-ENERGY-DENSITY CATHODES FOR ADVANCED LITHIUM-ION BATTERIES

Summary and Highlights

Development of high-energy-density, low-cost, thermally stable, and environmentally safe electrode materials is one of the key enablers for advanced batteries for transportation. High energy density is synonymous with reducing cost per unit weight or volume. Currently, one major technical barrier toward development of high-energy-density Li-ion batteries is the lack of robust, high-capacity cathodes. As an example, the most commonly used anode material for Li-ion batteries is graphitic carbon, which has a specific capacity of 372 mAh/g, while even the most advanced cathodes such as NMC or NCA have a maximum capacity of ~180 mAh/g. This indicates an immediate need to develop high capacity (and voltage) cathodes that have stable reversible capacities > 250 mAh/g. High volumetric energy density is also critical for transportation application. Alternative high-capacity cathodes such as those based on conversion compounds, lithium-sulfur, and metal-air chemistries still have fundamental issues that need to be addressed. Among oxide cathodes, Li-excess NMC and other cation disorder compositions provide a practical route toward high capacity at high redox voltage. Successful demonstration of practical high-energy cathodes will enable devices that meet or exceed the DOE cell level targets of 400 Wh/kg and 750 Wh/L with a system level cost target of $125/kWh.

During the last decade, many high-voltage cathode chemistries were developed under the BATT (now BMR) program including Li-rich NMC and Ni-Mn spinels. Current efforts are directed toward new synthesis methods and modifications for high-capacity, Ni-rich NMC to improve their structural and oxidative stability at higher voltage [Zhang, PNNL; Doeff & Tong, LBNL; Wang, Brookhaven National Laboratory (BNL)]. Thackeray and Croy's effort at Argonne National Laboratory (ANL) is focused on synthesis of composite layered-layered (LL) and layered-spinel (LS) high-voltage cathodes including Co- and Ni-based spinel phases. Nanda's effort at Oak Ridge National Laboratory (ORNL) is directed toward synthesis and stabilization of Li-excess disordered cathodes based on nickel, copper, molybdenum, chromium, and manganese. Whittingham's efforts at State University of New York (SUNY) at Binghamton are directed at high volumetric energy density Sn/Li_xVOPO_4 full cells and performance optimization.

Highlights. The highlights for this quarter are as follows:

- **Task 3.1.** Synthesized and characterized a Li-excess disordered cathode (Li_2MoO_3) and investigated its oxidative stability.
- **Task 3.2.** Demonstrated full cell cycling of a Sn_yFe/Li_xVOPO_4 redox couple.
- **Task 3.3.** Evaluated water as a solvent for surface modification of NMC and Ni-rich NMC materials.
- **Task 3.4.** Performed *in-situ* neutron diffraction studies to study the effect of cation disorder in Ni-rich NMC during synthesis.
- **Task 3.5.** Employed wet-chemical methods to test performance of Al-based treatments on lithium- and manganese-rich, layered-layered-spinel (LLS) cathodes powders.
- **Task 3.6.** Employed transmission X-ray microscopy (TXM) to study lithium distribution and heterogeneity in NMC-622 cathode material.
- **Task 3.7.** Developed general solid-state synthesis routes for Ni-rich transition metal (TM) oxide cathodes based on the electrochemical performance and cost.
- **Task 3.8.** Reported a low-temperature synthesis route for $Li_{1-x/2}(Co_{1-x}Mn_y)O_2$ and $Li_{1-x/2}(Co_{0.9-x}Ni_{0.1}Mn_x)O_2$ materials ($0 \leq x \leq 0.4$) via solid-state reaction at 400°C.

Task 3.1 – Studies on High-Capacity Cathodes for Advanced Lithium-Ion Systems (Jagjit Nanda, Oak Ridge National Laboratory)

Project Objective. The overall project goal is development of high-energy-density, lithium-ion battery electrodes for EV and PHEV applications that meet and/or exceed the DOE energy density and life cycle targets based on the USDRIVE/USABC roadmap. Specifically, this project aims to mitigate the technical barriers associated with high-voltage, high-capacity cathodes, including lithium-excess TM oxides and multi-lithium compositions such as $Li_2M_x^{I}M_{1-x}^{II}O_2$ and $Li_2M_x^{I}M_{1-x}^{II}O_3$ where M^{I} and $M^{II\ are}$ TMs that may or may not include manganese or cobalt. Major emphasis is placed on developing new materials and synthesis methods for stabilizing high-voltage cathodes to enable reversible capacities in the range of 250 mAh/g at an average voltage > 3.7 V versus Li/Li^+. Major technical barriers that will be addressed include (i) preventing structural transformations during repeated electrochemical cycling, (ii) improving the oxidative stability at higher redox potential by addressing interfacial stability, and (iii) reducing voltage hysteresis by facilitating reaction kinetics and mass transport at the materials level. The cathode synthesis and optimization will utilize various advanced characterization and diagnostic methods for studying cell and/or electrode degradation under abuse conditions. The techniques include electrochemical impedance spectroscopy (EIS), micro-Raman spectroscopy, mass spectrometry (MS), aberration corrected electron microscopy combined with electron energy loss spectroscopy (EELS), XPS, inductively coupled plasma atomic emission spectroscopy (ICP-AES), X-ray absorption near edge spectroscopy (XANES), and X-ray and neutron diffraction.

Project Impact. Short-term and long-term deliverables are directed toward VTO Energy Storage 2015 and 2022 goals. Work involves advanced electrode couples that have cell-level energy density targets exceeding 400 Wh/kg and 700 Wh/l for 5000 cycles. Increasing energy density per unit mass or volume ultimately reduces the cost of battery packs consistent with the DOE 2022 EV Everywhere Grand Challenge goal of $125/kWh.

Out-Year Goals. The goal is to develop new cathode materials that have high capacity, use low-cost materials, and meet the DOE roadmap in terms of safety and cycle life. Over the last few years, the principal investigator (PI) has worked on improving the performance of high-capacity, high-voltage cathodes by utilizing new synthesis and interfacial approaches such as surface modification. The cathode chemistries include lithium-manganese-rich NMC, multi-lithium TM oxides such as nickel-copper and manganese. In the coming years, the PI plans to improve the anionic (oxidative) stability of cathode compositions and develop new synthesis approaches to create disordered cathodes with improved structural and electrochemical stability. The tasks also include working in collaboration with researchers at Stanford Synchrotron Research Laboratory (SSRL) and Advanced Photon Source (APS) at LBNL to understand local changes in morphology, microstructure, and chemical composition under *in situ* and *ex situ* conditions.

Collaborations. This project collaborates with Johanna Weker, SSRL, SLAC: X-ray imaging and XANES; Pengfei and Chongmin Wang, PNNL: Electron Microscopy; Feng Wang, BNL: X-ray synchrotron spectroscopy and microscopy; and Jason Croy, ANL.

Milestones

1. Synthesize Ni-rich $Li_2Cu_xNi_{1-x}O_2$ cathodes with x = 0.2 and 0.3 and evaluate their high-voltage capacity and oxidative stability [> 225 mAh/g, 25 cycles]. (Q1 – In progress; 50%)
2. Complete *in situ* and *ex situ* X-ray, neutron, and spectroscopic studies of Ni-rich $Li_2Cu_xNi_{1-x}O_2$ and related high-voltage cathode compositions. (Q2 – In progress)
3. Synthesis of one particular class and composition of disordered cathodes-Li_2MoO_3 and Cr-substituted Li_2MoO_3. (Q3 – In progress)
4. Complete structural and electrochemical performance analysis of disordered cathodes including Li_2MoO_3 and Cr-substituted Li_2MoO_3. (Q4 – In progress)

Progress Report

This quarter, the project began work on Li-excess cathodes with cation disorder. It first investigated stability and oxygen activity of a stoichiometric two lithium composition, Li_2MoO_3. The goal of this specific study was not to use this composition as a high-voltage cathode candidate, but rather to consider this as one of the structural units for composite cathodes with the general formula $xLi_2MoO_3•(1-x)LiMO_2$. Li_2MoO_3 was synthesized by reducing Li_2MoO_4 at 675°C for 48 h under flowing Ar/H_2 (96/4) gas. The desired crystal structure of Li_2MoO_3 (spacegroup $R\bar{3}m$) was confirmed by XRD (results not shown). The electrochemical performance of Li_2MoO_3 was evaluated in half cells containing a Li-metal counter/reference electrode and liquid electrolyte (1.2 M $LiPF_6$ in EC/DMC 3/7). Cyclic voltammograms (Figure 13a) showed an irreversible oxidation process occurred during the first scan, and subsequent scans had a reversible redox peak near 2.5 V versus Li/Li^+ that is attributed to the Mo^{4+}/Mo^{5+} couple. Galvanostatic charge/discharge curves (Figure 13b) showed a sloping profile during the first delithiation cycle, and the electrode had a reversible capacity of 150 mA/g, which was stable over 10 cycles (Figure 13c). Overall, these results indicate that Li_2MoO_3 can reversibly cycle ~0.9 Li per Li_2MoO_3 formula unit at potentials ~2.5 V versus Li/Li^+, but some irreversible structural changes occur during the first cycle.

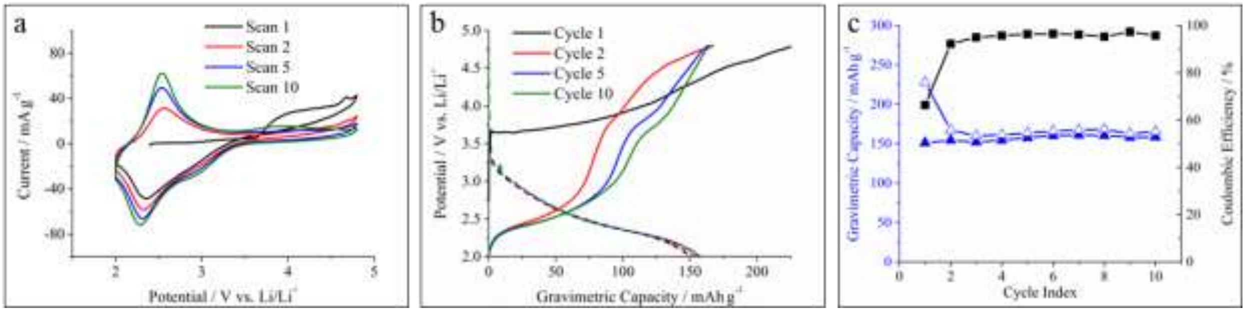

Figure 13. Electrochemical characterization of Li_2MoO_3 cathodes in half cells. (a) Cyclic voltammograms collected over 2.0 – 4.8 V at 0.1 mV/s. (b) Charge/discharge curves. (c) Cycling stability for coin cells cycled between 2.0 – 4.8 V at 10 mA/gLi_2MoO_3.

To investigate these cycling-induced structural changes, *ex situ* Raman and XRD analyses of pristine (that is, uncycled) and cycled Li_2MoO_3 cathodes were performed. Neither the pristine nor cycled electrodes were exposed to air during these measurements. XRD and Raman studies (not shown here) of cycled Li_2MoO_3 indicated the material underwent a crystalline to amorphous transition during cycling. Specifically, the pristine cathode had several Raman peaks in the range of 200 – 900 cm^{-1}, which corresponds well to that of Li_2MoO_3 reported in the literature. After cycling, these peaks were replaced by two very broad bands centered near 300 and 900 cm^{-1}, indicating the cycled electrode was amorphous. This result was confirmed through *ex situ* XRD. The pristine electrode had a diffractogram that matched that of Li_2MoO_3, but the cycled electrode had no apparent crystallinity, as evidenced by the absence of any significant diffraction signal. The project is investigating oxidative stability of Li_2MoO_3 electrodes at higher voltage by studying gas evolution using *in situ* MS. *Ex situ* and *in situ* X-ray and laser spectroscopy studies combined with electron microscopy are being pursued with collaborators at BNL and SSRL-SLAC to determine how the structure evolves as a function of state-of-charge during the first several cycles. Ultimately, the Li_2MoO_3 cathodes will be used to prepare disordered composite cathodes with the general formula $xLi_2MoO_3•$ $(1-x)LiMO_2$, where M is a TM such as chromium.

Patents/Publications/Presentations

Publication

- Ruther, R. E., and A. S. Pandian, P. Yan, J. N. Weker, C. Wang, and J. Nanda. "Structural Transformations in High-Capacity $Li_2Cu_{0.5}Ni_{0.5}O_2$ Cathodes." *Chem. Mater*. 29 (2017): 2997 – 3005.

Task 3.2 – High-Energy-Density Lithium Battery (Stanley Whittingham, SUNY Binghamton)

Project Objective. The project objective is to develop the anode and cathode materials for high-energy-density cells for use in PHEVs and EVs that offer substantially enhanced performance over current batteries used in PHEVs and with reduced cost. Specifically, the primary objectives are to:

- Increase the volumetric capacity of the anode by a factor of 1.5 over today's carbons
  - Using a SnFeC composite conversion reaction anode.
- Increase the capacity of the cathode
  - Using a high-capacity conversion reaction cathode, CuF_2, and/or
  - Using a high-capacity 2 lithium intercalation reaction cathode, $VOPO_4$.
- Enable cells with an energy density exceeding 1 kWh/liter.

Project Impact. The volumetric energy density of today's Li-ion batteries is limited primarily by the low volumetric capacity of the carbon anode. If the volume of the anode could be cut in half, and the capacity of the cathode to over 200 Ah/kg, then the cell energy density can be increased by over 50% to approach 1 kWh/liter (actual cell). This will increase the driving range of vehicles.

Moreover, smaller cells using lower cost manufacturing will lower the cost of tomorrow's batteries.

Out-Year Goals. The long-term goal is to enable cells with an energy density of 1 kWh/liter. This will be accomplished by replacing both the present carbon used in Li-ion batteries with anodes that approach double the volumetric capacity of carbon, and the present intercalation cathodes with materials that significantly exceed 200 Ah/kg. By the end of this project, it is anticipated that cells will be available that can exceed the volumetric energy density of today's Li-ion batteries by 50%.

Collaborations. The APS at ANL and, when available, the National Synchrotron Light Source II at BNL will be used to determine the phases formed in both *ex situ* and *operando* electrochemical cells. The University of Colorado – Boulder and University of Michigan will provide some of the electrolytes to be used.

Milestones

1. Determine cyclability of Sn/Li_xVOPO_4. (Q1 – Complete)
2. Demonstrate cyclability of Sn/CuF_2. (Q2 – In progress)
3. Choose optimum couple. (Q3 – Complete)
4. Supply cells to the DOE. (Q4)

Progress Report

The project goal is to synthesize tin-based anodes that have 1.5 times the volumetric capacity of the present carbons, and conversion and intercalation cathodes with capacities over 200 Ah/kg.

The major efforts in this second quarter of year three were to demonstrate the cyclability of the SnFe/two-electron cathode couple full cell containing the SnFe conversion anode and either a Li_xVOPO_4 or a CuF_2 cathode. The concentration was to be on CuF_2, but due to the challenges of Cu^+ transport into electrolyte, thereby minimizing the cyclability of CuF_2, the project focused on SnFe/Li_xVOPO_4 full cell with some low-level effort on suitable CuF_2 electrolyte.

Milestone 2 – "Demonstrate cyclability of the SnFe/CuF_2 couple. The cells will be cycled until failure. The results of this cell will be reported." The project previously demonstrated and reported challenges involved in cyclability of the high-energy density CuF_2. It was conclusively shown that Cu^+ ions diffuse readily in common Li-ion battery electrolytes and some solid electrolytes, resulting in copper metal being plated on the anode during charge, rather than reconversion to active CuF_2. To realize reversible cycling of CuF_2, a search for solid-state electrolytes that do not transport Cu^+ ion species is under way. Due to the dissolution challenge, there was limited effort on cyclability of SnFe/CuF_2 full cell. If the project achieves a breakthrough on suitable electrolytes, then it will place more effort on SnFe/new electrolyte/CuF_2.

The full-cell studies focus on SnFe/Li_xVOPO_4 couple due to excellent cycling behavior of SnFe and the high capacity and reversibility of Li_xVOPO_4. The project has achieved excellent rate behavior and long cycling performance of SnFe half cells (2016 Q3 report) with a reversible volumetric energy density of 1.2 Ah/cc, which is 1.5 times higher than that of graphite anode, 0.8 Ah/cc. The project has also made advances in improvement of the practical energy density, capacity retention, and rate capability of Li_xVOPO_4 by coating this cathode material with ionic and electronic conductors. It has achieved a capacity of around 250 mAh/g for over 70 cycles at a moderate current density of C/5 (Figure 14, left) compared to previous results in the first year, where practical capacity was around 200 mAh/g with poor cycling at low current densities, C/50.

Preliminary data has been obtained on the Sn_yFe/Li_xVOPO_4 electrochemical couple (Figure 14, right). The results indicate that the goal of attaining 4 mAh cells can be reached. The capacity fading is in part due to a mismatch in the capacities of the two electrodes. These cells will now be cycled more extensively.

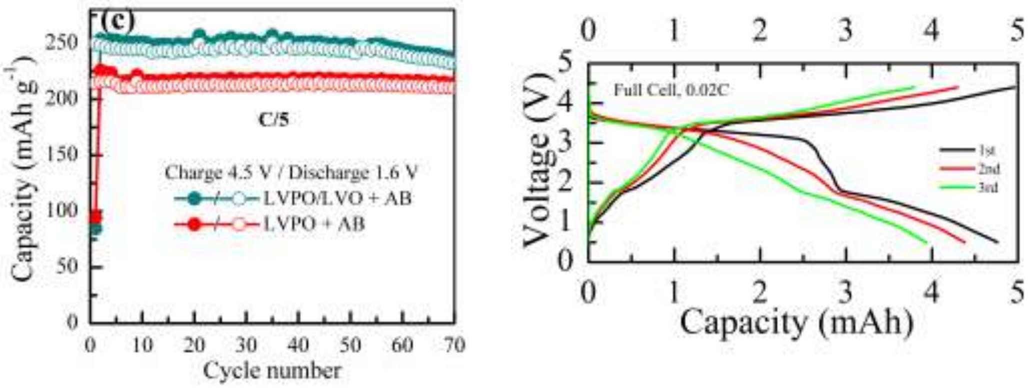

Figure 14. (left) The cycling behavior of the modified Li_xVOPO_4. (right) Full-cell cycling data for the Sn_yFe/Li_xVOPO_4 electrochemical couple.

Patents/Publications/Presentations

Presentations

- Lyceum, Vestal, New York (February 21, 2017): "The Future of Lithium Batteries"; M. Stanley Whittingham.
- Shimadzu Corporation, Kyoto, Japan (March 7, 2017): "Energy Storage, The Beginnings to Mass Transportation"; M. Stanley Whittingham.
- International Battery Association (IBA), Nara, Japan (March 9, 2017): "The Limits of High Energy Reactions for Lithium Batteries: The Electrolyte Challenge"; M. Stanley Whittingham.
- U.S. DOE Basic Research Needs Workshop, Gaithersburg, Maryland (March 27, 2017): "Electrical Energy Storage: Where Have We Come from and the Scientific Challenges Still Facing Us"; M. Stanley Whittingham.
- Presidential Session, Science for a Sustainable Energy Future, American Chemical Society (ACS) National Meeting, San Francisco (April 4, 2017): "Storing Energy in Lithium Batteries for a Sustainable Energy Future"; M. Stanley Whittingham.

Task 3.3 – Development of High-Energy Cathode Materials
(Ji-Guang Zhang and Jianming Zheng, Pacific Northwest National Laboratory)

Project Objective. The project objective is to develop high-energy-density, low-cost, cathode materials with long cycle life. The previous investigation demonstrates that synthesis condition, synthesis approach, and surface modification have significant effects on the performances of high-voltage spinel and LMR-NCM cathodes. These valuable understandings will be used to guide development of high-energy-density, enhanced long-term cycling stability of Ni-rich $LiNi_xMn_yCo_zO_2$ (NMC) cathode materials that can deliver a high discharge capacity with long-term cycling stability.

Project Impact. Although state-of-the-art layered structure cathode materials such as $LiNi_{1/3}Mn_{1/3}Co_{1/3}O_2$ and $LiNi_{0.4}Mn_{0.4}Co_{0.2}O_2$, have relatively good cycling stability at charge to 4.3 V, their energy densities need to be further improved to meet the requirements of EVs. This work focuses on the two closely integrated parts: (1) develop the high-energy-density NMC layered cathode materials for Li-ion batteries; and (2) characterize the structural properties of the NMC materials by various diagnostic techniques including scanning transmission electron microscopy (STEM)/EELS, energy dispersive X-ray mapping and SIMS, and correlate with the first part. The success of this work will increase energy density of Li-ion batteries and accelerate market acceptance of EVs, especially for PHEVs required by the EV Everywhere Grand Challenge.

Approach. In FY 2016, the compositions of NMC cathode materials and the charge cutoff voltage were optimized. Ni-rich NMC cathode materials with initial discharge capacity higher than 200 mAh g^{-1} and capacity retention of 90% after 100 cycles were successfully achieved. However, the long-term cycling stability is still unsatisfactory and requires further improvement. In FY 2017, several strategies will be carried out to further enhance the long-term cycling stability as well as the thermal stability of NMC cathode materials, including (1) cationic/anionic lattice doping; (2) surface modification; and/or (3) introduction of effective electrolyte formulas/additives.

Out-Year Goals. The long-term goal of the proposed work is to enable Li-ion batteries with a specific energy of > 96 Wh kg^{-1} (for PHEVs), 5000 deep-discharge cycles, 15-year calendar life, improved abuse tolerance, and less than 20% capacity fade over a 10-year period.

Collaborations. This project engages with the following collaborators:

- Dr. Bryant Polzin (ANL) – NMC electrode supply,
- Dr. X. Q. Yang (BNL) – *in situ* XRD characterization during cycling, and
- Dr. Kang Xu (U.S. Army Research Laboratory, ARL) − new electrolyte.

Milestones

1. Complete lattice doping to enhance cycling stability of NMC at high charge cutoff voltages, and identify the effect of dopants in NMC during cycling using quantitative atomic level mapping. (December 2016 – Complete)
2. Identify appropriate solvents for surface modification of NMC, and reveal the structural changes of different NMC materials after wash with water. (March 2017 – Complete)
3. Complete surface modification to enhance the cycling stability of NMC at high charge cutoff voltages. (June 2017 – In progress)
4. Achieve NMC performance improvement of 200 mAh g^{-1} and 80% capacity retention after 200 cycles. (September 2017)

Progress Report

This quarter's milestone was completed. To verify that water is a suitable solvent for surface modification of Ni-rich NMC cathodes, the stability of different Ni-rich NMC materials, including $LiNi_{0.6}Mn_{0.2}Co_{0.2}O_2$, $LiNi_{0.76}Mn_{0.14}Co_{0.10}O_2$, and $LiNi_{0.8}Mn_{0.1}Co_{0.1}O_2$, in water has been systematically investigated.

Figure 15a-b shows the cycling performances of $LiNi_{0.6}Mn_{0.2}Co_{0.2}O_2$ (Figure 15a) and $LiNi_{0.76}Mn_{0.14}Co_{0.10}O_2$ (Figure 15b) before and after water wash. The water-washed samples were prepared by stirring the cathode powder in water for 10 min, then filtered and dried at 120°C overnight. The cycling performance of water-washed samples were evaluated in coin-type cells with electrode loading similar to pristine material electrode (~ 4 mg cm^{-2}). Electrochemical performance results demonstrated that the Ni-rich NMC materials were not stable in water because the water leached the Li^+ ions out of the NMC cathode materials, damaging the material's crystal structure. During cycling, the water washed Ni-rich NMC cathode $LiNi_{0.76}Mn_{0.14}Co_{0.10}O_2$ exhibited dramatic increase in electrode polarization, as compared to pristine material (Figure 15c-d).

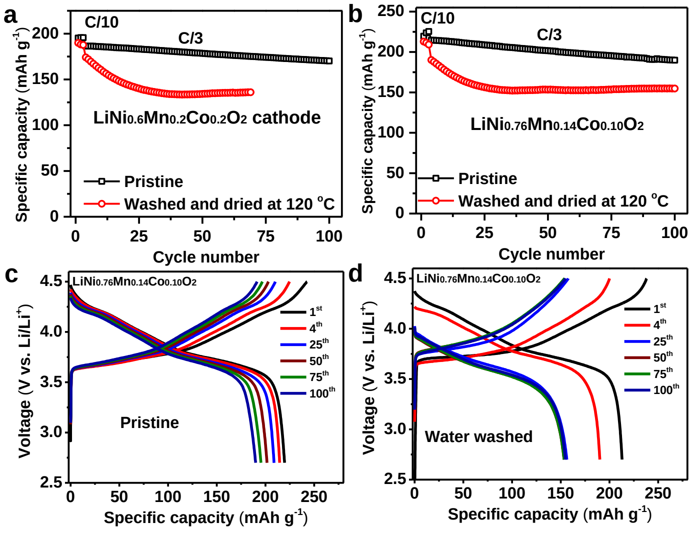

Figure 15. (a) Cycling performance of $LiNi_{0.6}Mn_{0.2}Co_{0.2}O_2$ before and after water wash. (b) Cycling performance of $LiNi_{0.76}Mn_{0.14}Co_{0.10}O_2$ before and after water wash. (c, d) Voltage profile evolutions of $LiNi_{0.76}Mn_{0.14}Co_{0.10}O_2$ (c) before and (d) after water wash.

The crystal structures of the Ni-rich NMC $LiNi_{0.76}Mn_{0.14}Co_{0.10}O_2$ before and after water wash were further characterized using XRD (Figure 16a-b). It was found that the XRD pattern of water-washed $LiNi_{0.76}Mn_{0.14}Co_{0.10}O_2$ did show clear difference as compared to pristine material. The intensity ratio between (003) and (104) diffraction peaks, the value of which indicates the Li/Ni cation disorder degree in the layered structure of NMC, decreased from 1.26 for pristine $LiNi_{0.76}Mn_{0.14}Co_{0.10}O_2$ to 1.11 for water-washed sample. The increase of Li/Ni cation disorder was related to the loss of Li^+ ions in water and the generation of Ni^{2+} species in the material crystal lattice. Moreover, the damage of the particle surface structure might significantly aggravate the interfacial reactions with the electrolyte, leading to accelerated capacity fade. In this regard, Ni-rich NMC cathode materials should be carefully stored in a dry atmosphere to avoid performance degradation. The results also illustrate that water is not a good solvent for surface modification of Ni-rich NMC cathodes. Appropriate solvents that do not leach out the Li^+ ions from NMC must be used for the surface modification. Currently, surface modifications using nonaqueous solvent are being carried out to enhance the structural integrity of secondary particles and hence improve long-term cycling stability of Ni-rich NMC cathodes.

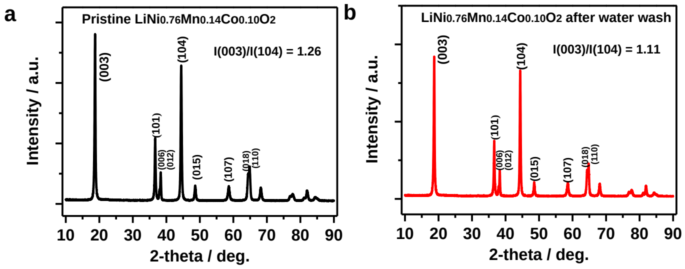

Figure 16. X-ray diffraction patterns of Ni-rich NMC cathode material $LiNi_{0.76}Mn_{0.14}Co_{0.10}O_2$ (a) before and (b) after water wash.

Patents/Publications/Presentations

Publication

- Yan, Pengfei, and Jianming Zheng, Meng Gu, Jie Xiao, Ji-Guang Zhang, and Chongmin Wang. "Intragranular Cracking as a Critical Barrier for High-Voltage Usage of Layer-Structured Cathode for Lithium-Ion Batteries." *Nature Communications* 8 (2017): 14101.

Task 3.4 – *In Situ* Solvothermal Synthesis of Novel High-Capacity Cathodes (Feng Wang and Jianming Bai, Brookhaven National Laboratory)

Project Objective. The goal is to develop novel high-capacity cathodes with precise control of the phase, stoichiometry, and morphology. Despite considerable interest in developing low-cost, high-energy cathodes for Li-ion batteries, designing and synthesizing new cathode materials with the desired phases and properties have proven difficult, due to complexity of the reactions involved in chemical synthesis. Building on established *in situ* capabilities/techniques for synthesizing and characterizing electrode materials, this project will undertake *in situ* studies of synthesis reactions under real conditions to identify the intermediates and to quantify the thermodynamic and kinetic parameters governing the reaction pathways. The results of such studies will enable strategies to "dial in" desired phases and properties, opening a new avenue for synthetic control of the phase, stoichiometry, and morphology during preparation of novel high-capacity cathodes.

Project Impact. Present-day Li-ion batteries are incapable of meeting the targeted miles of all-electric-range within the weight and volume constraints, as defined by the DOE in the EV Everywhere Grand Challenge. New cathodes with higher energy density are needed for Li-ion batteries so that they can be widely commercialized for plug-in electric vehicle (PEV) applications. The effort will focus on increasing energy density (while maintaining the other performance characteristics of current cathodes) using synthesis methods that have the potential to lower cost.

Out-Year Goals. This project is directed toward developing novel high-capacity cathodes, with a focus on Ni-rich layered oxides. Specifically, synthesis procedures will be developed for making $LiNiO_2$ and a series of Co/Mn substituted solid solutions, $LiNi_{1-x}M_xO_2$ (M=Co, Mn); through *in situ* studies, this project undertakes systematic investigations of the impact of synthesis conditions on the reaction pathways and cationic ordering processes toward the final layered phases. The structural and electrochemical properties of the synthesized materials will be characterized using scanning XRD, neutron scattering, TEM, EELS, and various electrochemical techniques. The primary goal is to develop a reversible cathode with an energy density of 660 Wh/kg or higher.

Collaborations. This project engages with the following collaborators: Lijun Wu and Yimei Zhu at BNL; Khalil Amine, Zonghai Chen, Yang Ren, and Chengjun Sun at ANL; Jagjit Nanda and Ashfia Huq at ORNL; Nitash Balsara, Wei Tong, and Gerbrand Ceder at LBNL; Scott Misture at Alfred University; Peter Khalifha at SUNY; and Kirsuk Kang at Seoul National University.

Milestones

1. Identify the synthesis reactions and involved structural ordering in both Ni-rich and Co-rich layered oxides through *in situ* synchrotron X-ray studies. (Q1 – Complete)
2. Develop neutron scattering-based techniques for *in situ* probing cation ordering in Ni-rich NMC layered oxides during synthesis under controlled atmosphere. (Q2 – Complete)
3. Identify synthesis procedures for kinetic control of the structural ordering in NMC layered oxides through combined *in situ/ex situ* synchrotron X-ray and neutron studies. (Q3)
4. Complete the evaluation of synthesis conditions, specifically identifying the effect of temperature and time on the structural ordering and electrode performance of Ni-rich NMC layered cathodes. (Q4)

Progress Report

This quarter, neutron scattering-based techniques were developed for *in situ* probing cation ordering in Ni-rich NMC layered oxides during synthesis under controlled atmosphere.

Starting with the cell design for XRD experiments, a new *in situ* reactor with configuration suited for neutron diffraction (ND) measurements was developed, with a gas-flow system integrated for probing solid-state reaction under controlled atmosphere. The functionality of the reactor has been tested in the POWGEN (powder diffractometer) beamline at the Spallation Neutron Source (SNS at ORNL) through *in situ* ND studies of synthesis reaction in preparing $LiNi_{0.7}Mn_{0.15}Co_{0.15}O_2$ (NMC-71515). Figure 17 shows one representative contour plot of temperature-resolved ND patterns from the measurements, revealing the entire reaction process, from the precursors (a mixture of Li/TM hydroxides) to intermediates, and then to the final layered NMC-71515. The results are consistent with the *in situ* XRD observation reported last quarter, but more details were obtained from *in situ* ND studies, particularly on cation ordering, owing to the unique capabilities of neutron scattering in detecting light elements (for example, lithium) and differentiating TMs (nickel, manganese, cobalt).

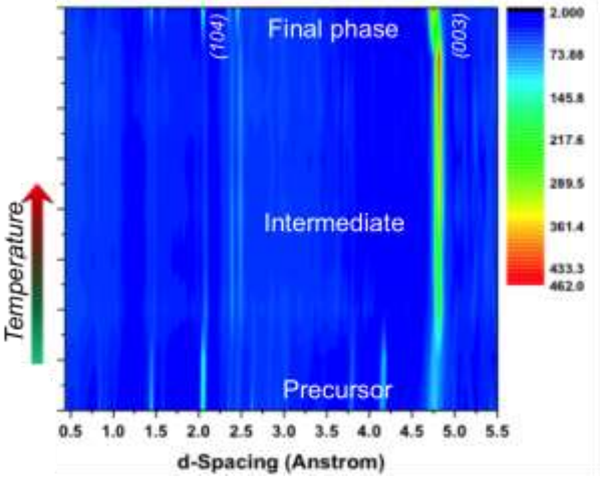

Figure 17. Contour plot of temperature-resolved *in situ* neutron diffraction patterns of intermediates during synthesis of $LiNi_{0.7}Mn_{0.15}Co_{0.15}O_2$ (NMC-71515).

Details of the synthesis reactions can now be obtained through joint refinement of *in situ* XRD and ND data acquired from the same system (as demonstrated in Figure 18), not only on the overall structural evolution, but the ordering of all the involved cations, thereby offering new insights into kinetic/thermodynamic parameters governing synthesis process in preparing Ni-rich layered oxides.

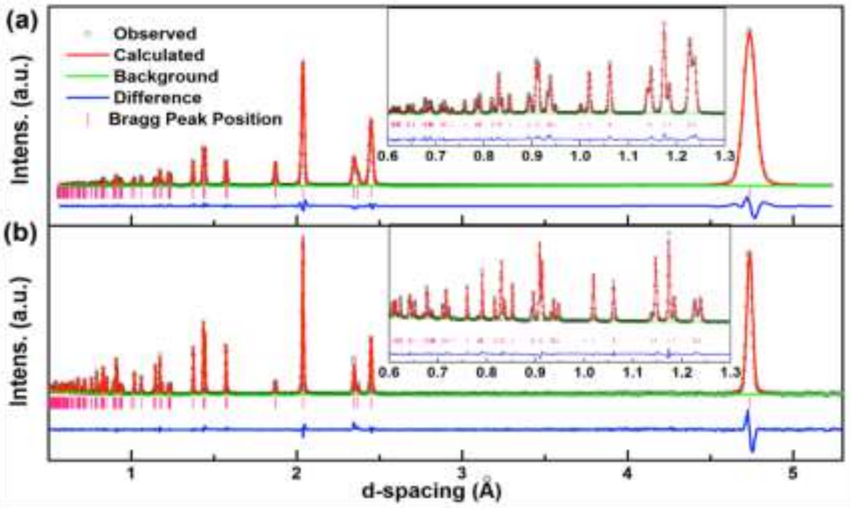

Figure 18. (a) Synchrotron X-ray and (b) neutron diffraction patterns of NMC-71515 in comparison to that from structure refinement. The enlarged spectra in small d−spacing range are shown in the inset. In the plots, open circles are used for the observed data; red lines for calculated data, pink bars for Bragg positions, blue lines for difference between observed and calculated data, and green lines for refined background.

Patents/Publications/Presentations

Publication

- Wang, D., and R. Kou, Y. Ren, C-J. Sun, H. Zhao, M-J. Zhang, Y. Li, A. Huq, J. Y. P. Ko, F. Pan, Y-K. Sun, Y. Yang, K. Amine, J. Bai, Z. Chen, and F. Wang. "Synthetic Control of Kinetic Reaction Pathway and Cationic Ordering in High−Ni Layered $LiNi_{0.7}Mn_{0.15}Co_{0.15}O_2$ Cathodes." *Adv. Mater.* Accepted.

Task 3.5 – Novel Cathode Materials and Processing Methods (Michael M. Thackeray and Jason R. Croy, Argonne National Laboratory)

Project Objective. The project goal is to develop low-cost, high-energy, and high-power Mn-oxide-based cathodes for Li-ion batteries that will meet the performance requirements of PHEVs and EVs. Improving the design, composition, and performance of advanced electrodes with stable architectures and surfaces, facilitated by an atomic-scale understanding of electrochemical and degradation processes, is a key objective.

Project Impact. Standard Li-ion battery technologies are unable to meet the demands of the next-generation EVs and PHEVs. Battery developers and scientists will take advantage of both the applied and fundamental knowledge generated from this project to advance the field. This knowledge should enable progress toward meeting DOE goals for 40-mile, all-electric range PHEVs.

Approach. Exploit the concept and optimize performance of structurally-integrated “composite” electrode structures with a primary focus on “layered-layered-spinel” materials. Alternative processing routes will be investigated; ANL’s comprehensive characterization facilities will be used to explore novel surface and bulk structures by both *in situ* and *ex situ* techniques in pursuit of advancing properties of state-of-the-art cathode materials. A theoretical component will complement the project’s experimental work.

Out-Year Goals. The out-year goals are as follows:

- Identify high-capacity (LL and LS) composite electrode structures and compositions that are stable to electrochemical cycling at high potentials (~ 4.5 V).
- Identify and characterize surface chemistries and architectures that allow fast Li-ion transport and mitigate or eliminate TM dissolution.
- Use complementary theoretical approaches to further understanding of electrode structures and electrochemical processes to accelerate progress of materials development.
- Scale-up, evaluate, and verify promising cathode materials in conjunction with scale-up and cell fabrication facilities at ANL.

Collaborators. This project engages with the following collaborators: Eungje Lee, Roy Benedek, Arturo Gutierrez, and Meinan He in Chemical Sciences and Engineering (CSE) at ANL.

Milestones

1. Explore the energy content, and stabilization thereof, of moderate Li_2MnO_3-content ($25\% < x < 50\%$) $y[xLi_2MnO_3•(1-x)LiMO_2]•(1-y)LiM_2O_4$ (M=Mn, Ni, Co), LL and LLS electrodes; target capacity ≥ 220 mAh/g. (Q4 – In progress)
2. Identify surface-treatment strategies that enable LLS electrodes to maintain high capacities (≥ 220 mAh/g) and high rate performance (~200 mAh/g at 1C). (Q4 – In progress)
3. Demonstrate oxide energy densities ≥ 750 Wh/kg_{oxide} in full-cell testing of surface-modified, LLS electrodes. (Q4 – In progress)

Progress Report

In a continued effort to explore and design unique surface structures that can enable stable cycling and high capacities (~200mAh/g) at 1C, aluminum-based surface treatments were investigated with respect to post-treatment annealing conditions. Aluminum, in the form of oxide coatings and dopants, has received much attention in the literature of Li-ion cathodes. However, the efficacy of aluminum treatments depends heavily on synthesis conditions as well as the underlying cathode material, in particular, cathode composition. Herein, wet-chemical methods are employed to test performance of Al-based treatments on Li- and Mn-rich LLS cathode powders.

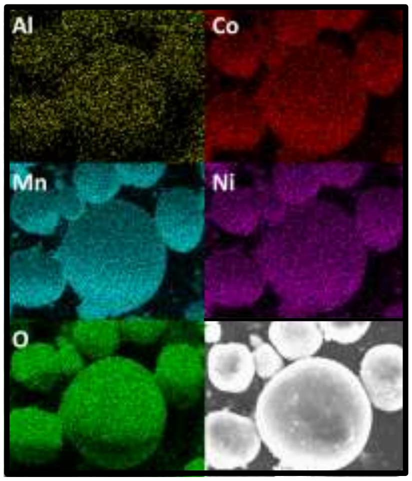

Figure 19. Scanning electron microscopy mapping of layered-layered-spinel particles treated in a 2 wt% (with respect to the cathode oxide) aluminum nitrate solution and annealed at 110°C.

Figure 19 shows SEM images of a $Li_{1.11}Ni_{0.25}Mn_{0.47}Co_{0.17}O_y$, LLS cathode powder after treatment in an aqueous solution of aluminum nitrate aimed at depositing ~2 wt% aluminum on the surface. Subsequent annealing experiments, between 110-750°C (in air for 6 h), unexpectedly showed that the lowest temperature of 110°C produced the best performance in terms of initial capacity, capacity retention, impedance rise with cycling, and rate. Figure 19 shows the sample prepared at 110°C and reveals an apparently uniform distribution of aluminum on the particles. Though the nature of surface phases formed are unknown, parallel characterization efforts are ongoing (See Task 5.8, Thackeray). Figure 20 (left) shows capacity versus cycle plots for untreated and Al-treated (110°C) samples between 4.45-2.5 V, after a first-cycle activation to 4.6 V (lithium half-cells, 15 mA/g, 30°C). Electrodes containing the treated LLS powders achieved a first-cycle efficiency ~94% and a stable capacity ~ 215 mAh/g over ~ 50 cycles. Electrodes fabricated from the untreated baseline powders achieved slightly less capacity and suffered more severe capacity fade. Subsequent impedance spectroscopy data (inset) showed that impedance rise after 50 cycles for the treated sample was minimal compared to the untreated electrode powders. Figure 20 (right) shows rate data for the untreated (black) and treated (red) electrodes, normalized to their respective discharge capacities at 15 mA/g. At rates of > 1C (> 150 mA/g discharge currents) the treated sample showed a clear improvement in discharge performance. These data suggest a possible advantage with respect to Al-based treatments, even at low temperatures, applied to Li- and Mn-rich, LLS electrodes. Further studies are in progress.

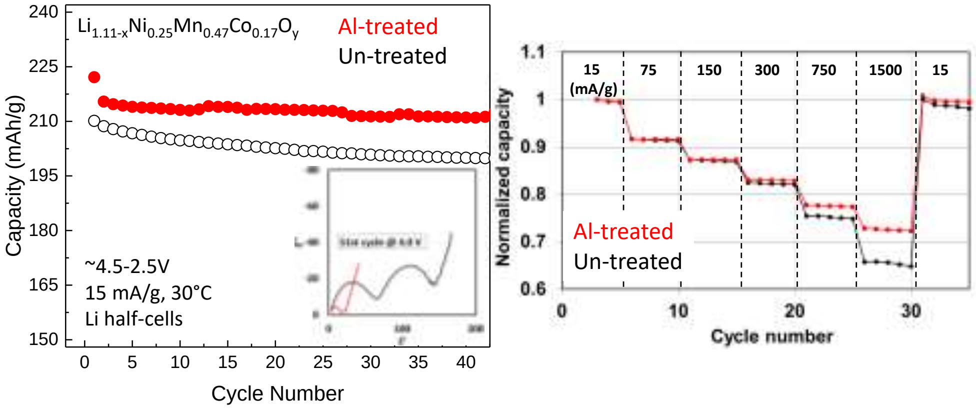

Figure 20. (left) Capacity versus cycle plots for the untreated and Al-treated (110°C) sample between 4.45 – 2.5 V, after a first-cycle activation to 4.6 V (lithium half-cells, 15 mA/g, 30°C). Inset shows impedance data conducted on the 51st cycle charge at 4.0 V. (right) Normalized rate data of treated (red) and untreated (black) samples (constant charge of 15 mA/g, 4.6 V, variable discharge rates as labeled).

Patents/Publications/Presentations

Patent

- Croy, Jason R., and Michael M. Thackeray, and Arturo Gutierrez. *Surface Treatment for Lithium Battery Electrode Materials*, U.S. Application, filed 62/466,0.

Publication

- IBA, Nara, Japan (March 7, 2017): "The Pursuit of High-Capacity Cathodes for High-Energy Lithium-Ion Cells"; Jason R. Croy, Mahalingam Balasubramanian, Daniel C. O'Hanlon, Kevin G. Gallagher, Arturo Gutierrez, Eungje Lee, and Michael M. Thackeray. Invited.

Task 3.6 – Advanced Cathode Materials for High-Energy Lithium-Ion Batteries (Marca Doeff, Lawrence Berkeley National Laboratory)

Project Objective. Microscopy and synchrotron X-ray absorption and photoemission techniques will be used to study the phenomenon of surface reconstruction to rock salt on NMC particle surfaces as a function of composition, synthesis method, surface chemistry, and electrochemical history. Because the surface reconstruction is implicated in capacity fading and impedance rise during high-voltage cycling, a thorough understanding of this phenomenon is expected to lead to principles that can be used to design robust, high-capacity NMC materials for Li-ion cells. The emphasis will be on stoichiometric NMCs with high nickel content such as 622 and 523 compositions.

Project Impact. To increase the energy density of Li-ion batteries, cathode materials with higher voltages and/or higher capacities are required, but safety and cycle life cannot be compromised. Ni-rich NMCs can provide higher capacities and lower cost in comparison with low nickel content NMCs, but surface reactivity is an issue. A systematic evaluation of the effects of synthesis method, composition, and cell history on the surface reconstruction phenomenon will lead to higher capacity, robust, and structurally stable positive electrode materials that result in higher-energy-density Li-ion cells than are currently available.

Out-Year Goals. The information generated by the in-depth characterization will be used to design robust NMC materials that can withstand cycling to high potentials and deliver > 200 mAh/g.

Collaborations. TXM was used this quarter to characterize NMC materials, with work done in collaboration with Yijin Liu (SSRL). Synchrotron and computational efforts continued in collaboration with Professor M. Asta (University of California – Berkeley, UCB); and Dr. Dennis Nordlund, Dr. Yijin Liu, and Dr. Dimosthenis Sokaras (SSRL). The TEM effort is in collaboration with Dr. Huolin Xin (BNL).

Milestones

1. Complete thermal characterization of Ni-rich NMC materials by TXM and X-ray Raman. (Q1 – Complete)
2. Synthesize Ti-substituted Ni-rich NMCs by conventional and spray pyrolysis methods. (Q2 – Ti substitued samples were prepared with both methods; however, conditions need to be further modified to get better performance. This will be completed, together with milestone 3, next quarter.)
3. Complete electrochemical characterization of Ti-substituted, Ni-rich NMCs. (Q3)
4. *Go/No Go:* Core-shell composites made by infiltration and re-firing of spray-pyrolyzed hollow spherical particles. (September 2016 – No-go decision made)

Progress Report

Partially delithiated $Li_{1-x}Ni_{0.6}Mn_{0.2}Co_{0.2}O_2$ particles were prepared using either chemical delithiation or electrochemical charge and discharge processes. Chemical delithiation is generally used to prepare large quantities of samples needed for certain synchrotron experiments. In addition, chemically delithiated samples are free from inactive components, such as binder and conductive carbon, which can complicate interpretation of results. However, it is necessary to determine whether the products of chemical delithiation accurately represent what occurs during electrochemical charge.

This quarter, the project employed TXM to determine the lithium distribution within NMC particles. Because nickel is the main redox element in NMC-622, it is reasonable to monitor the lithium distribution by mapping the nickel oxidation state. As shown in Figure 21a, both chemical delithiation and electrochemical charge and discharge (C/10 rates) led to a narrowing of the distribution of nickel oxidation states compared to the pristine state. The absolute oxidation state (peak center in Figure 21a) can be compared to ICP results for the chemically delithiated sample to determine lithium content. For electrochemically prepared samples, Coulometry can be used, but cell variation and parasitic reactions may lead to some over- or under-estimation of the lithium content. The absolute energy differences were also confirmed with hard X-ray absorption spectroscopy (XANES profile in Figure 21b). To directly compare lithium distributions among different samples, the peak center energy was used for color mapping. As shown in Figure 21c-f, chemical delithiation and electrochemical processes have similar heterogeneity in terms of lithium distributions. The relatively slow rates at which materials were charged and discharged (C/10 rate) for these experiments mean that kinetics should not be a determining factor of the heterogeneity observed.

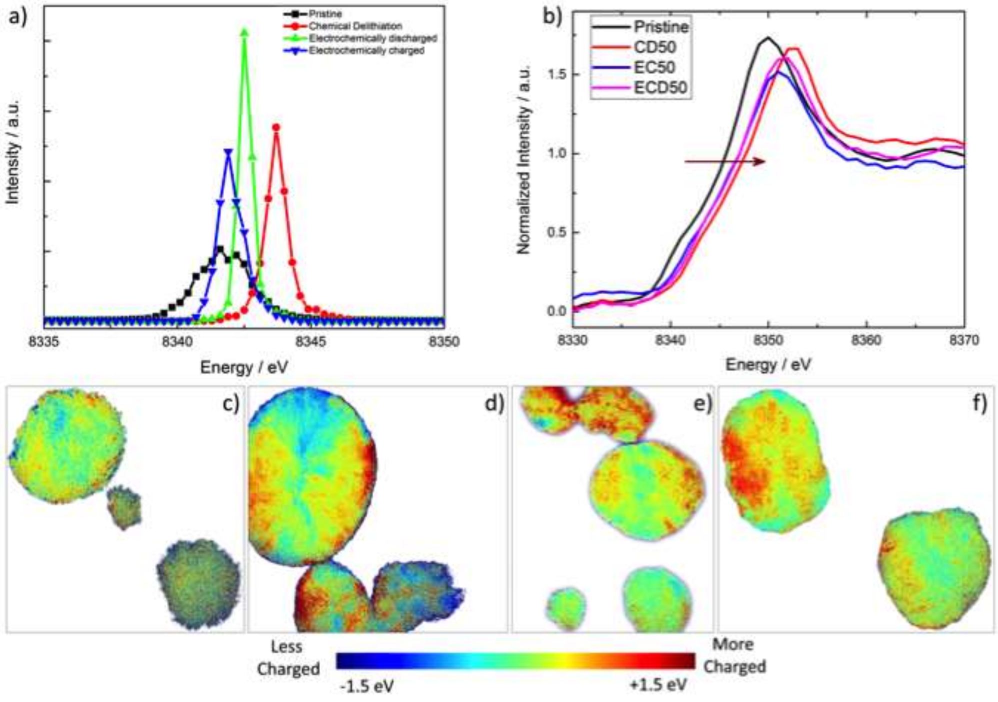

Figure 21. (a) Normalized histograms of the single-pixel nickel oxidation state relative to the particle median state of charge. (b) Nickel K-edge spectra for all the particles imaged in (c-f). (c-f) Two-dimensional state-of-charge mapping for: (c) pristine $Li_{0.5}Ni_{0.6}Mn_{0.2}Co_{0.2}O_2$ particles, and (d) chemically delithiated, (e) electrochemically discharged, and (f) electrochemically charged $Li_{0.5}Ni_{0.6}Mn_{0.2}Co_{0.2}O_2$ particles imaged at the nickel K-edge.

Patents/Publications/Presentations

Publication

- Cheng, Lei, and Huaming Hou, Simon Lux, Robert Kostecki, Ryan Davis, Vassilia Zorba, Apurva Mehta, and Marca Doeff. "Enhanced Lithium Ion Transport in Garnet-Type Solid State Electrolytes." *J. Electroceramics* (2017). doi: 10.1007/s10832-017-0080-3.

Presentations

- Bosch Research and Technology Center, North America, Palo Alto, California (April 13, 2017): "Studies on NMC and LLZO Materials for Lithium Batteries"; Marca M. Doeff. Invited.
- Materials Sciences and Engineering Colloquium, Fu Foundation School of Engineering and Applied Science, Columbia University, New York (March 24, 2017): "Materials for Next Generation Electric Vehicle Batteries." Invited.

Task 3.7 – Discovery of High-Energy Lithium-Ion Battery Materials (Wei Tong, Lawrence Berkeley National Laboratory)

Project Objective. This project aims to develop a cathode that can cycle >200 mAh/g while exhibiting minimal capacity and voltage fade. The emphasis will be on oxides with high nickel content. This task focuses on compositions in the Li-Ni-O phase space, which will be explored using a combinatorial materials approach to search for new high-capacity cathodes. The objectives are to: (1) investigate and understand the correlation between the synthesis and electrochemical performance of Ni-based compounds, and (2) design, synthesize, and evaluate potential new high-capacity cathodes within Li-Ni-O composition space using percolation theory as a guideline.

Project Impact. Energy density needs to be at least doubled to meet EV performance requirements (300 to 400 mile). Although capacities approaching 300 mAh/g have been reported in Li, Mn-rich layered oxide compounds, capacity decay and voltage fading in the long-term cycling are always observed. Therefore, new materials are urgently needed to make the breakthrough in Li-ion battery technology.

Approach. Recent discovery of high-capacity Li-excess cathodes provides new insight into material design principle. According to percolation theory, lithium excess is required to access 1 lithium exchange capacity in $LiTmO_2$ compounds. This seems to be independent of TM species and therefore could open a composition space for the search of new materials with high capacity. The interesting Ni^{2+}/Ni^{4+} redox is selected as the electrochemically active component, and a combinatorial materials design concept will be used to discover the potential cathode material candidates in the Li-Ni-O phase space.

Out-Year Goals. The long-term goal is to search new high-energy cathodes that can potentially meet the performance requirements of EVs with a 300- to 400-mile range in terms of cost, energy density, and performance. Work will progress from understanding of known compounds, $LiNiO_2$ and Li_2NiO_2, toward development of new Ni-based high-energy cathode oxides.

Collaboration. The PI closely collaborates with M. Doeff (LBNL) on soft X-ray absorption spectroscopy (XAS), C. Ban (NREL) on ALD coating, B. McCloskey (LBNL) for differential electrochemical mass spectrometry, and R. Kostecki (LBNL) for Raman spectroscopy. In addition, the project is collaborating with other PIs (X.-Q. Yang and F. Wang, BNL; and K. Persson, LBNL) for crystal structure evolution upon cycling and for material computation.

Milestones

1. Use Li-, Mn-rich oxide as the baseline material; develop synthesis that can be used to screen the second TMs for Li-rich, Ni-based oxides. (Q1 – Complete)
2. Design Li-rich, Ni-based oxide compositions and perform synthesis of designed compositions. (Q2 – Complete)
3. Complete electrochemical tests on synthesized Li-rich, Ni-based oxides; down select one composition that shows promising electrochemical performance with initial capacity of > 200 mAh/g. (Q3 – In progress)
4. Complete structural characterization of selected composition, and compare performance with Li-, Mn-rich oxide baseline. (Q4)

Progress Report

Different TMs (TM = Mn, Ru, Sn, Mo, Nb, Ti, V) with a general formula of $Li_{2-x-y}Ni_xTM_yO_2$ (0 < x, y <1) were synthesized via a solid-state reaction. Selection of the second TM was based on theoretical capacity and material cost. Stoichiometric amounts of lithium, nickel, and TM precursors were thoroughly mixed using the optimal synthesis condition identified last quarter for $Li_{1.2}Ni_{0.2}Mn_{0.6}O_2$. The as-milled precursor mixtures were annealed at various temperatures in the air. The XRD patterns of the as-produced samples are presented in Figures 22 and 23.

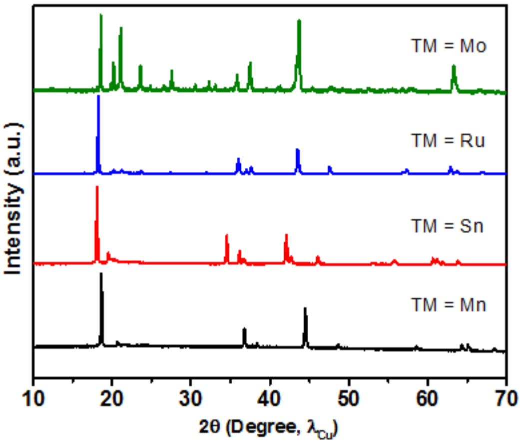

Figure 22. X-ray diffraction patterns of $Li_{2-x-y}Ni_xTM_yO_2$ (TM = Mn, Sn, Ru, Mo), exhibiting layered structure.

As can be seen in Figure 22, samples that incorporate ruthenium and those that incorporate tin showed very similar XRD patterns to that of $Li_{1.2}Ni_{0.2}Mn_{0.6}O_2$. A shift in XRD peaks was observed due to the difference in ionic radius of these three TM cations. For TM = Mo, more XRD peaks were observed; however, the major characteristic peaks of $Li_{1.2}Ni_{0.2}Mn_{0.6}O_2$ were reserved, along with more diffraction peaks in the two-theta region of 20 - 35°. It seems the crystal structure was somehow consistent with those of the samples with TM = Mn, Ru, Sn. A careful search and match of TM = Mo pattern in ICDD database showed consistency with Li_4MgWO_6, which belongs to the monoclinic crystal structure. Although the detailed structural characterization needs to be further performed, this is indeed close to the crystal structure of Li_2MnO_3 that the superstructure peaks around 21° in the XRD pattern of $Li_{1.2}Ni_{0.2}Mn_{0.6}O_2$ are typically assigned to.

For the other TMs tested, the crystal structure of the final products was very different. The XRD patterns are shown in Figure 23. For both titanium and niobium, the XRD patterns are very different from those of layered structure, where the major peak around 20° was absent. Instead, simple XRD patterns characterized by three major peaks around 37, 42, and 65° were observed for niobium and titanium. They can be easily assigned to the rock salt phase. Although NiO possesses a rock salt structure, the complete absence of any XRD peak that is related to lithium and TM precursors or byproducts suggests incorporating titanium and niobium very likely led to the formation of a rock salt phase in the final products. In fact, formation of a rock salt phase has been reported within Li-Ni-Nb-O, although the synthetic conditions and material compositions are very different from this project. As for TM = V, Li_3VO_4 was a thermodynamically favorable phase in synthesis and observed as the major phase along with NiO. The electrochemical properties of the as-produced samples will be tested next quarter, and one composition with good electrochemical performance will be selected for detailed characterization.

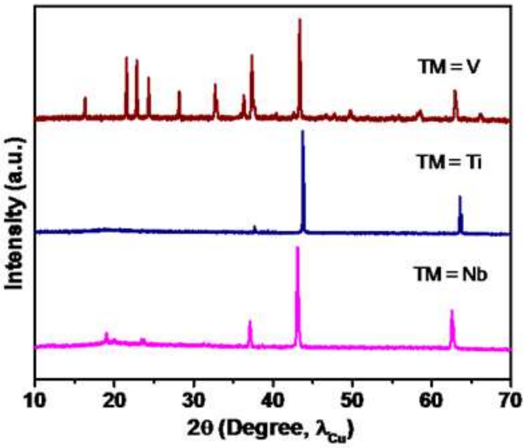

Figure 23. X-ray diffraction patterns of $Li_{2-x-y}Ni_xTM_yO_2$ (TM = Nb, Ti, V), exhibiting non-layered structure.

Patents/Publications/Presentations

Publication

- Ma, C., and J. Alvarado, J. Xu, R. Clément, M. Kodur, W. Tong, C. Grey, and Y. S. Meng. “Exploring Oxygen Activity in the High Energy P2-Type $Na_{0.78}Ni_{0.23}Mn_{0.69}O_2$ Cathode Material for Na-ion Batteries.” *Journal of the American Chemical Society*. doi: 10.1021/jacs.7b00164.
- Wu, F., and Y. Yan, R. Wang, H. Cai, W. Tong, and H. Tang. “Facile Synthesis of $LiNi_{1/3}Mn_{1/3}Co_{1/3}O_2$@Graphene Cathode for Lithium-Ion Batteries via Self-Assembled Polyelectrolyte Layers.” *Ceramics International*. doi: 10.1016/j.ceramint.2017.03.066.

Presentation

- LBNL/ETA Review, Berkeley, California (January 2017): “Development of High-Energy Li-Ion Battery Materials *via* Combinatorial Materials Approach”; W. Tong, poster presentation.
- 34th International Battery Seminar & Exhibit, Fort Lauderdale, Florida (March 2017): “Investigation of High-Capacity Ni-Based Layered Oxide Cathode for Li-ion Batteries”; W. Tong and J. Xu. Invited.
- 2017 SPIE Smart Structures/NDE, Portland, Oregon (March 2017): “Combinatorial Materials Approach to Accelerate Materials Discovery for Transportation”; Wei Tong.

Task 3.8 – Exploiting Cobalt and Nickel Spinels in Structurally Integrated Composite Electrodes (Michael M. Thackeray and Jason R. Croy, Argonne National Laboratory)

Project Objective. The project goal is to stabilize high capacity, composite 'layered-layered' electrode structures with lithium-cobalt-oxide and lithium-nickel-oxide spinel components (referred to as LCO-S and LNO-S, respectively), or solid solutions thereof (LCNO-S), which can accommodate lithium at approximately 3.5 V versus Li/Li^+. This approach and the motivation to exploit the electrochemical and structural LCO-S and LNO-S spinel structures, about which relatively little is known, is unique.

Project Impact. State-of-the-art Li-ion batteries are currently unable to satisfy the performance goals for PHEVs and EVs. If successful, this project will impact the advance of energy storage for electrified transportation as well as other applications, such as portable electronic devices and the electrical grid.

Approach. This work will focus on the design and synthesis of new spinel compositions and structures that operate above 3 V and below 4 V and on determining their structural and electrochemical properties through advanced characterization. This information will be subsequently used to select the most promising spinel materials as stabilizers in high-capacity composite electrode structures.

Out-Year Goals. The electrochemical capacity of most high-potential, Li-metal oxide insertion electrodes is generally severely compromised by structural instability and surface reactivity with the electrolyte at low lithium loadings (that is, at highly charged states). Although progress has been made by cation substitution and structural modification, the practical capacity of these electrodes is still restricted to approximately 160-170 mAh/g. This project proposes a new structural and compositional approach with the goal of producing electrode materials that can provide 200-220 mAh/g without significant structural or voltage decay for 500 cycles. If successful, the materials processing technology will be transferred to the ANL Materials Engineering and Research Facility for scale up and further evaluation.

Collaborations. This project collaborates with Eungje Lee, Arturo Gutierrez, and Roy Benedek (CSE, ANL); Mali Balasubramanian (APS, ANL); and V. Dravid and C. Wolverton (Northwestern University).

Milestones

1. Explore solution-based synthesis routes to optimize the structure and performance of Co-based spinel and structurally integrated LS electrodes. (Q4 – In progress; see text)
2. Determine structure/electrochemical property relationships of Co-based spinel materials and composite LS electrodes. (Q4 – In progress)
3. Investigate bulk and surface modifications of Co-based spinel and LS electrodes. (Q4 – In progress; see text)

Progress Report

Past reports have described the synthesis, structure, and electrochemistry of Co-based, lithiated spinel materials that have the general fomula Li($Co_{1-x-y}Ni_xMn_y$)O_2. These materials are typically prepared via solid-state synthesis routes using low-temperature (LT) firing conditions. After exploring a large area of the compositional space, it was found that nickel and manganese substitution improves the phase purity and electrochemistry of the lithiated spinel cathodes. However, impurity phases were easily formed during LT synthesis, and the range over which nickel and manganese substitution resulted in monophasic materials was limited.[1] The formation of impurity phases is related to the relative stability of possible oxide phases in a given overall composition. For example, in lithiated spinel Li($Co_{1-x}Mn_x$)O_2 compounds, the cobalt and TM manganese cations should maintain an overall oxidation state of +3 to satisfy charge neutrality conditions. However, Mn cations have a preference for +4 oxidaton and will drive the stabilization of a Li-Mn(IV)-O impurity phase, as shown in the previous examples of LT-Li($Co_{1-x-y}Ni_xMn_y$)O_2 materials with high manganese contents.

Therefore, in this quarter, a series of LT-$Li_{1-x/2}$($Co_{1-x}Mn_y$)O_2 and LT-$Li_{1-x/2}$($Co_{0.9-x}Ni_{0.1}Mn_x$)O_2 materials ($0 \leq x \leq 0.4$) have been synthesized via solid-state reaction at 400ºC. Different from the previous compounds that have a stoichiometric ratio of Li:TM=1 regardless of the TM compositions, the LT-$Li_{1-x/2}$($Co_{1-x}Mn_y$)O_2 and LT-$Li_{1-x/2}$($Co_{0.9-x}Ni_{0.1}Mn_x$)O_2 are designed to maintain manganese in the +4 oxidation state by decreasing the lithium content with manganese substitution. Figure 24a shows the XRD patterns of the LT-$Li_{1-x/2}$($Co_{0.9-x}Ni_{0.1}Mn_x$)O_2 powder samples. The x = 0.1 and 0.2 samples do not show an impurity phase related to Mn(IV) cations; however, the peaks for Co_3O_4 are clearly detected. The decreased lithium content in $Li_{0.95}$($Co_{0.8}Ni_{0.1}Mn_{0.1}$)O_2 and $Li_{0.9}$($Co_{0.7}Ni_{0.1}Mn_{0.2}$)O_2, which is devised to maintain the +4 oxidation state of manganese, actually induces the formation of a Co_3O_4 impurity phase. For the x = 0.4 sample, a third phase, denoted as LT-LMO, is observed in addition to the LT-spinel and Co_3O_4 phases. From the analysis of a LT-$LiMnO_2$, the LT-LMO phase observed for the x = 0.4 sample was identified as a Li_2MnO_3•$Li_4Mn_5O_{12}$ composite phase. The high-resolution XRD of a LT-$LiMnO_2$ (Figure 24b) shows a spinel structure, while the additional peak marked with an asterisk (2θ ~6°) suggests the superstructure ordering of Li/Mn as in Li_2MnO_3. The electrochemical behavior of LT-$LiMnO_2$ further confirms the composite structure by clearly exhibiting the characteristic voltage curves corresponding to Li_2MnO_3 and $Li_4Mn_5O_{12}$ spinel materials (Figure 24c). These results, combined with previous data, point to Co_3O_4 spinel, $Li_xNi_{1-x}O$ rocksalt, and Li_2MnO_3•$Li_4Mn_5O_{12}$ as the main impurity phases during the low-temperature synthesis of 'NMC spinel' materials. Therefore, alternative synthesis routes (for example, soft chemistry methods) that can mitigate the formation of stable impurity phases need to be explored.

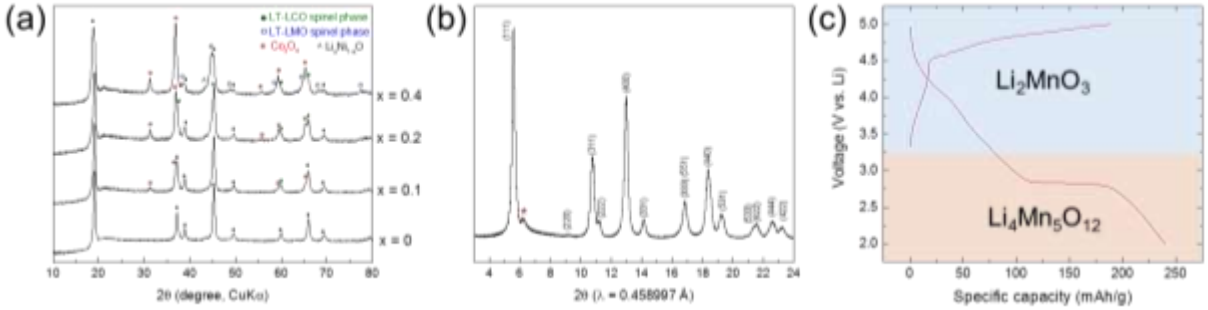

Figure 24. (a) X-ray diffraction (XRD) patterns of LT-$Li_{1-x/2}$($Co_{0.9-x}Ni_{0.1}Mn_x$)O_2. (b) High-resolution XRD of LT-$LiMnO_2$ (LT-LMO). (c) Electrochemistry of LT-LMO phase.

[1] Lee, E., and J. R. Croy, M. M. Thackeray et al., *ACS Appl. Mater. & Interfaces* 8 (2016): 27720.

TASK 4 – ELECTROLYTES

Summary and Highlights

The BMR Program goal is to develop long-life batteries superior to commercial Li-ion systems in terms of cost, vehicle range, and safety. The BMR Program addresses the fundamental problems of electrode chemical and mechanical instabilities that have slowed development of affordable, high performance, automotive batteries. The aim is to identify electrode/electrolyte materials that yield enhanced battery performance and lead to greater acceptance of EVs. Currently, the VTO supports seven projects in the BMR Program under the Electrolytes area. These projects can be categorized into three general topics:

- **Liquid.** The projects for liquid electrolyte aim to develop an atomic/molecular level understanding of the stability of electrochemical interfaces during charge-discharge cycling to stabilize solid /liquid interfaces in Li-ion batteries. In addition, electrolyte formulations, based on fluoro-chemistries, will be developed to achieve significantly improved operating voltage, increased durability, and increased energy density of Li-ion batteries at a reasonable cost.
- **Polymer.** The target of polymer electrolyte projects is mainly for use in Li-S batteries. Inorganic/polymer and polymer/gel hybrid electrolytes that have flexibility, mechanical strength, thermal stability, high ionic conductivity, stable interfaces against lithium metal, and polysulfide-trapping capability will be developed to enable energy densities twice that of the state-of-the-art Li-ion batteries, with comparable cycle life.
- **Self-Forming & Self-Healing.** The self-forming and self-healing electrolyte projects focus on developing and implementing Li-metal-based metal fluorite and metal iodide batteries, capable of energy densities > 400-500 Wh/kg and 1000 Wh/L.

Highlights. This quarter, the ANL group demonstrated their newly developed high-precision electrochemical measuring system for stability studies by revisiting the corrosion (or anodic dissolution) process of aluminum foils in nonaqueous electrolytes. Their data suggest that degradation of aluminum foil at high potentials is a coupled electrochemical-chemical reaction; that is, the electrochemical oxidation of organic solvents such as EC and ethyl methyl carbonate (EMC) at high potentials triggers the chemical corrosion of aluminum foils. Their density functional theory (DFT) calculations reveal that proton generated from the deprotonation reaction of EC^+ slowly reacts with the natural passivation layer, Al_2O_3, on aluminum, leading to an increase in the charge transfer reaction kinetics on the aluminum surface.

The Daikin group tested the cells from ANL and found that fluorocarbon electrolyte performs better than hydrocarbon up to 4.5 V, but the performance decreases when the upper voltage is extended to 4.6 V.

The University of Maryland group synthesized ion insulating polymer PEO, ion conductive polymer PEO-LiTFSI, and *in situ* coated garnet nanofibers by polymer electrolyte. They found that the Li-ion conductivity of cubic phase LLZO garnet pellet can reach as high as 10^{-3} S/cm, while the value for Li-salt-stuffed PEO is generally on the order of 10^{-6}-10^{-9} S/cm at room temperature. The flexible electrolyte combining conductive cubic LLZO garnet and lithium-PEO could therefore reach a reasonably high ionic conductivity of 2.5×10^{-4} S/cm at room temperature.

The University of Washington group investigated reaction conditions for successful formation of a gel network between poly(ethylene glycol) dimethacrylate (PEGDMA) of either M_n=750 Da or Mn=3500 Da in either N-methylpyrrolidone (NMP) or room-temperature ionic liquid (RTIL) solvent. They found that longer PEG chains impart improved elasticity to resultant gels (59.7% reversible elongation for Mn=3500 as opposed to 13.9% for an identical composition with Mn=750). Further, solid films of PENDI-C3 and Py Linker (with a 1:1 ratio between NDI and Py units) were prepared by drop casting from dichloromethane (DCM) solution. The film is self-healable. They successfully attached a primary amine functional group to mesoporous carbon samples; the surface modified carbon showed batter capacity retention, but with less than optimal kinetics.

The West Virginia University (WVU) group successfully fabricated molybdenum-doped lithium lanthanum zirconium oxide (LLMZO) nanofibers by an electrospinning process. In addition, they showed that the introduction of LLAZO nanofibers into the PEO/LiTFSI electrolyte increases the ionic conductivity.

The Stony Brook University (SBU) group measured AC impedance measurements as a function of temperature, for samples of AgI with various amounts of Al_2O_3 additive (5, 10, 20, 30%). It was determined that the highest conductivity was for the 20% and 30% Al_2O_3 at 9.6×10^{-5} S/cm and 1.0×10^{-4} S/cm at 30ºC, respectively.

At Rutgers University, baseline reactive current collectors and bi-ion conductors of ionic conductivity of the order of 1×10^{-5} S/cm identified in first-quarter work were successfully implemented into solid-state cells. These initial full-cell architectures were based on a baseline, and therefore, non-optimized design comprised of large inter- and intra- electrode diffusion lengths. Furthermore, they successfully implemented a mask-less scalable patterning technique to fabricate the solid-state cells described above. Such a mask-less scalable patterning technique offers a pathway to high throughput, low material loss fabrication of complex architectures.

Task 4.1 – Understanding and Mitigating Interfacial Reactivity between Electrode and Electrolyte (Khalil Amine, Larry A. Curtiss, and Nenad Markovic, Argonne National Laboratory)

Project Objective. This project aims to develop an understanding, at atomic/molecular levels, of the stability of electrochemical interfaces during charge-discharge cycling and to use the knowledge for stabilizing solid/liquid interfaces in Li-ion batteries. The goal is to improve stability of solid/liquid interfaces using insights into the atomic/molecular processes that limit stability during cycling. The core objective is to identify, rationalize, and understand the dynamics of the dissolution processes of 3D-TM cations in the cathode materials, stability of various commercial and highly purified electrolytes comprised of organic solvents, salts, and additives, and evolution of O_2 and other gaseous products formed from the electrode material or the electrolyte during the charging-discharging of the Li-ion battery.

Project Impact. The instability of the solid-liquid interfaces during cycling limits use of novel cathodes such as 6:2:2 and 8:1:1 NMC cathodes with higher voltage and higher power densities. Stabilization of solid/liquid interfaces in Li-ion batteries can lead to enhanced performance and increased safety.

Approach. This project follows an integrated program focused on solid-liquid interfaces in Li-ion batteries using state-of-the-art *in situ* characterization tools and computational modeling to understand and design interfaces with enhanced stability. The range of high-end analytical tools includes the following: (1) a three-electrode rotating disk electrode (RDE) setup; (2) ICP-MS; (3) Gas Chromatography with Triple Quadrupole MS (GC-QqQ) in Headspace sampling mode; and (4) differential electrochemical mass spectrometry (DEMS). High-precision electrochemical measurements in combination with *in situ* measurements and characterization are highly suitable to investigate correlation of stability with a number of electrochemical, structural, and compositional properties of the interfaces. Computational methods that provide reaction energies and barriers as well as structural information at the atomic level will be used to predict and test possible reactions that affect the stability of solid-liquid interfaces.

Out-Year Goals. Work will progress toward more comprehensive *in situ* characterization and integrated modeling capabilities with applications to solid liquid interfaces of electrolytes and 6:2:2 NMC cathodes. If the project can harness the complexity that governs interface instability, it should be able to move far beyond current state-of-the-art Li-ion systems and create new avenues to design and deploy cathode materials and electrolytes.

Collaborations. This project funds work at ANL and PNNL. Zonghai Chen, Sanja Tepavcevic, Pietro Papa Lopes, and Peter Zapol, all of ANL, contribute to the project.

Milestones

1. Perform first *ex situ* measurements of electrode/electrolyte decomposition products using ICP-MS and GC-MS. (Q1 – Complete)
2. Develop protocol for calculating electrochemical reactions at electrolyte-electrode interfaces. (Q1 – Complete)
3. Build a new 16-channel high-precision electrochemical measurement system dedicated to this project. (Q2 – Complete)
4. Benchmark the kinetics of direct electrochemical oxidation of baseline electrolyte at different potentials. (Q3)
5. Couple ICP-MS with electrochemical cell for direct *in situ* investigation of metal dissolution from the cathode. (Q4)

Progress Report

The project demonstrated its newly developed high-precision electrochemical measuring system for stability studies by revisiting the corrosion (or anodic dissolution) process of aluminum foils in nonaqueous electrolytes. It found that the measured static leakage current grows roughly exponentially with the applied potential, indicating an ongoing electrochemical oxidation of electrolyte on the carbon-coated aluminum foil. The hypothesis is that this reaction is related to the oxidation of EC.

To gain insight into the parasitic reactions, the project carried out XPS analysis for aluminum foils before and after anodic treatment. The XPS profiles are shown in Figure 25. The control experiment was carried out with bare aluminum foil, and a weak absorption peak was observed at about 73 eV. This corresponds to the binding energy of metallic aluminum. The strong peak at 75.6 eV in Figure 25 was assigned to a Al_2O_3 thin film on the surface of the aluminum foil. It shows that as-used nonaqueous electrolyte with the presence of possibly a trace amount of moisture was not enough to convert the Al_2O_3 layer into a more stable passivation layer of AlF_3. After anodic treatment at 3.9 V (20 hours), the absorption peak for Al_2O_3 at 75.6 eV disappears and a new peak at 77.2 eV appears. This new peak corresponds to the binding energy of AlF_3. A similar result was found for the sample anodized at 4.8 V for 20 h as shown in Figure 25.

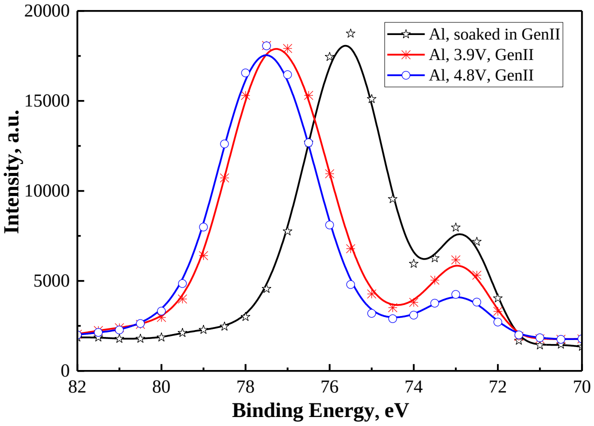

Figure 25. X-ray photoelectron spectroscopy profiles of aluminum foils before and after anodic treatment in 1.2 M $LiPF_6$ in EC/EMC (3:7 by weight).

A depth profile analysis of the XPS results revealed that the sample without anodic treatment was mostly covered by 15−25 nm of Al_2O_3; anodic treatment at 3.9 V led to a deposition of about 5 nm of AlF_3 on the top of the thinned Al_2O_3 layer (10−20 nm). Although a substantially higher parasitic current was measured at 4.8 V, no significant change of the thickness of the AlF_3 layer and embedded Al_2O_3 was observed. This indicates that the interface of the aluminum foil was stabilized by the AlF_3 coating that was electrochemically triggered by the oxidation of solvent to generate protons on the surface. After repeated cycling between 3.4 and 4.9 V for five cycles, it was observed that the open gap at about 3.9 V disappeared, primarily due to stabilization of the aluminum surface. In addition, the open gap associated with the corrosion of Al_2O_3 was pushed to a higher potential when EC was replaced with fluorinated EC. Also, the gap almost disappeared when both EC and EMC were replaced with a mixture of fluorinated carbonate and fluorinated ether, indicating that EMC also plays a major role in aluminum corrosion. These XPS results support the hypothesis that that the degradation of aluminum foil at high potentials is a coupled electrochemical-chemical reaction; that is, the electrochemical oxidation of organic solvents such as EC and EMC at high potentials triggers the chemical corrosion of aluminum foils.

DFT calculations were carried out on EC interacting with various models for the alumina surface. By itself, EC has a fairly high redox potential at about 7.2 V versus Li^+/Li according to the calculations, and in reasonable agreement with previous calculations. The proposed mechanism of EC oxidation in previous studies involved proton transfer to the carboxyl group of another EC molecule in solution, decreasing the oxidation potential to 5.94 V. Calculations were carried out on models of alumina shown in Figure 26. The DFT calculations indicate that the redox potential can decrease significantly when the proton is transferred to a hydroxyl attached to aluminum atom of the surface model. Calculations on either the hydroxyl group or a bridging oxygen site on larger and more realistic amorphous alumina models shown in Figure 26 similarly indicate that the alumina promotes the deprotonation reaction of the radical cation (EC^+), leading to an increase in the parasitic current at a low potential, as found in analysis of the voltage profiles. It is believed that the proton generated from the deprotonation reaction of EC^+ slowly reacts with the natural passivation layer, Al_2O_3, on aluminum, leading to an increase in the charge transfer reaction kinetics on the aluminum surface. At the same time, it is hypothesized that the presence of protons on the aluminum surface can also substantially promote decomposition of the PF_6 anion, forming proton-resistive AlF_3 on the surface of aluminum. After accumulation of enough protons from oxidation of EC, the surface of the aluminum foil can be stabilized by AlF_3 coating.

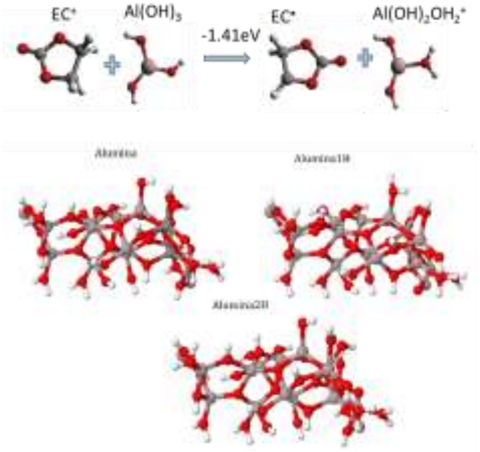

Figure 26. (top) Reaction of EC with $Al(OH)_3$. (bottom) Structure alumina models (Alumina, Alumina1H and Alumina2H) represented by clusters derived from a periodic model of amorphous alumina.

Patents/Publications/Presentations

Publication

- Ma, Tianyuan, and Gui-Liang Xu, Yan Li, Li Wang, Xiangming He, Jianming Zheng, Jun Liu, Mark H. Engelhard, Peter Zapol, Larry A. Curtiss, Jacob Jorne, Khalil Amine, and Zonghai Chen. "Revisiting the Corrosion of the Aluminum Current Collector in Lithium-Ion Batteries." *J. Phys. Chem. Lett*. 8, no. 5, (2017): 1072 – 1077. doi: 10.1021/acs.jpclett.6b02933.

Task 4.2 – Advanced Lithium-Ion Battery Technology: High-Voltage Electrolyte (Joe Sunstrom and Ron Hendershot, Daikin)

Project Objective. The overall project objective is to identify electrolyte formulations, based on fluoro-chemistries, that will allow significantly improved operating voltage, increased durability, and increased energy density of Li-ion batteries at a reasonable cost. The project objective is to understand the conditions under which the electrolyte degrades, the effect on battery performance, and solutions that can overcome current limitations of the electrolyte. The strategy is to select from a range of available fluorinated chemistries those combinations that provide the highest possible battery voltages, greater than 4.5 V, while keeping incremental battery cost increase as low as possible.

Project Impact. An understanding of the failure mechanisms for both state-of-the-art hydrocarbon and fluorocarbon electrolytes as they pertain to various cell chemistries is ultimately valuable in the design of future high-performance batteries. Electrolyte degradation has been a key limiting factor in development of new Li-ion technology. The ability to stop or significantly slow this degradation opens a whole new level of design for rechargeable batteries.

Approach. The evolving composition of the electrolyte in the battery will be examined by a variety of analytical instrumentation to study the gas (GC/MS), liquid chromatography (LC/MS), and solid (TOF-SIMS, thermogravimetric analysis (TGA)/ MS, XRD) electrolyte decomposition products during battery operation. In the first year, the team will address the gas composition and kinetics for both hydrocarbon and fluorocarbon as a function of several charge/discharge conditions that include (but are not limited to) electrode composition, operational voltage and current, temperature, and cycle number.

Out-Year Goals. Work will progress toward formulating rough mass balances of both the fluorinated and hydrocarbon electrolytes under the performance parameters suggested. Specifically, analysis of the liquid and solid decomposition products will be pursued. Understanding how the mass balance and kinetics change will give information on decomposition pathways and allow for solutions to be formulated to increase battery performance.

Milestones

1. Establish baseline and review current state-of-the-art. Compile baseline electrochemical and physical property specification for current best practice electrolyte. (Q2 – Complete)
2. Determination of gas composition. Failure mechanisms are understood and mitigation strategies/additives are selected for interim cells. (Q2 – In progress)

Progress Report

Final cell test results from ANL were received in March. The cycle testing results are shown in Figure 27 for:

- Group 1 (G1) hydrocarbon electrolyte cycled to 4.5 V,
- Group 2 (G2) fluorocarbon best practice electrolyte cycled to 4.5 V, and
- Group 3 (G3) fluorocarbon best practice electrolyte cycled to 4.6 V.

The results confirm Daikin internal results indicating that fluorocarbon electrolyte performs better than hydrocarbon up to 4.5 V (Figure 27, top), but there is a performance decrease when the upper voltage is extended to 4.6 V (bottom). This result fixes the study voltages to 4.2, 4.5, and 4.6 V, as initially proposed.

Gassing studies on the three in-house chemistries (LCO, NMC-111, NMC-622) have been completed. These initial static studies were completed by charging cells to the appropriate voltage, disassembling them charged, placing charged electrodes into pouches containing electrolyte, and monitoring cell volume increase upon storage at 60°C. Figure 28 shows an example of this for the charged cathodes at 3 weeks. The initial result shows extreme gassing for the 100% cobalt sample at 4.5 and 4.6 V. This is consistent with battery performance of these types of cathodes. The present goal is to identify the ratio of gases present and relate them back to either the electrolyte or the cathode surface (oxygen).

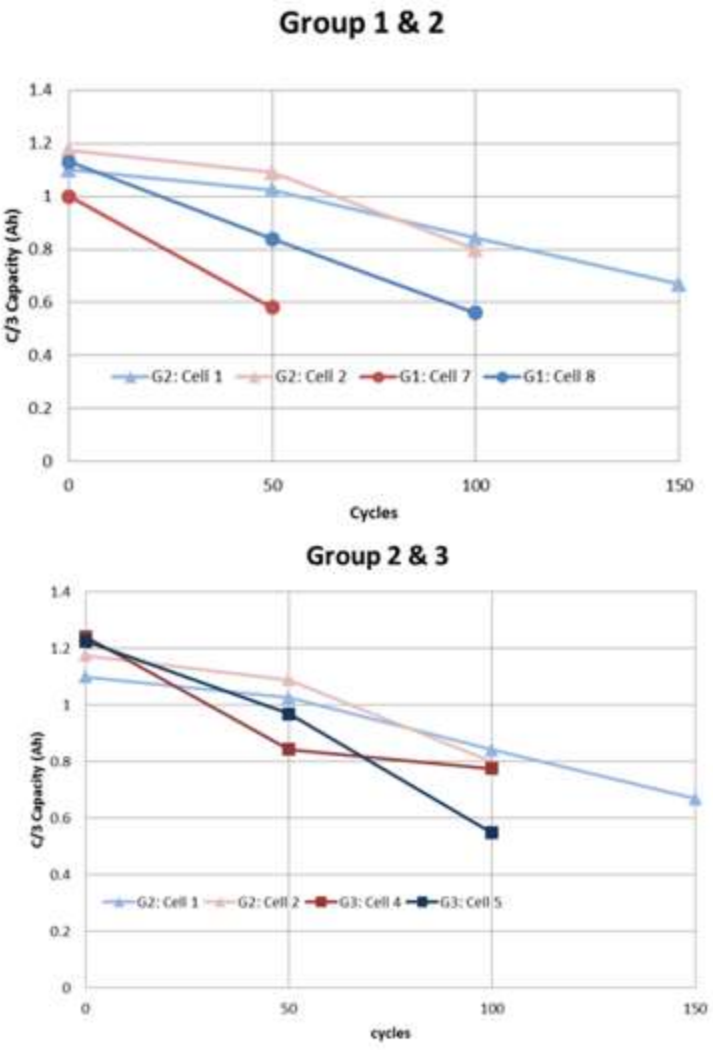

Figure 27. Cycle life curves showing HC and FC electrolyte at 4.5 V (top) and FC electrolyte at both 4.5 and 4.6 V (bottom).

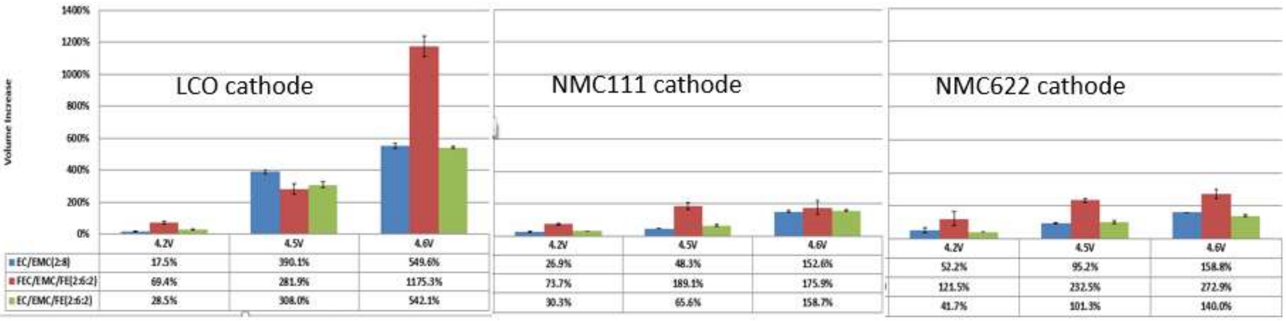

	LCO cathode			NMC111 cathode			NMC622 cathode		
	4.2V	4.5V	4.6V	4.2V	4.5V	4.6V	4.2V	4.5V	4.6V
■ EC/EMC(2:8)	17.5%	390.1%	549.6%	26.9%	48.3%	152.6%	52.2%	95.2%	158.8%
■ FEC/EMC/FE(2:6:2)	69.4%	281.9%	1175.3%	73.7%	189.1%	175.9%	121.5%	232.5%	272.9%
■ EC/EMC/FE(2:6:2)	28.5%	308.0%	542.1%	30.3%	65.6%	158.7%	41.7%	101.3%	140.0%

Figure 28. Volume increase due to gassing for three chemistries (LCO, NMC-111, and NMC-622 at three voltages—4.2, 4.5, and 4.6 V).

Task 4.3 – Multi-Functional, Self-Healing Polyelectrolyte Gels for Long-Cycle-Life, High-Capacity Sulfur Cathodes in Lithium-Sulfur Batteries
(Alex Jen and Jihui Yang, University of Washington)

Project Objective. The project objective is to develop self-healing and polysulfide-trapping polyelectrolyte gels containing RTIL for the Li-S battery system. The battery design will be capable of achieving gravimetric and volumetric energy densities of ≥ 800 Wh/kg and ≥ 1000 Wh/L, respectively.

Project Impact. The Li-S battery system is currently hampered by poor capacity retention, primarily caused by dissolution of polysulfide reaction intermediates in typical organic electrolytes, as well as poor electrical contact between insulating sulfur and the conductive carbon matrix. This project aims to produce a high-capacity, long-cycle-life Li-S battery system by using rational molecular design strategies to address each capacity loss mechanism directly. A long-cycle-life Li-S battery system with the capability of doubling Li-ion energy density would enable production of lighter, longer range EVs at a cost that is affordable to the average U.S. household.

Approach. The team will develop Li-S coin cells that utilize self-healing, interpenetrated ionomer gel electrolytes in both the cathode and separator. The team will synthesize necessary starting materials and fabricate components of these gels while testing their relevant electrochemical and mechanical properties. All components will be combined into interpenetrating structures, which will be tested both alone and in cell configurations. Device performance data will be collected and used to further optimize designs of both material and cell, culminating in an optimized Li-S battery design capable of doubling the energy density of traditional Li-ion batteries. During the first year, the team is focusing on (1) synthesis of a variety of precursors for gel electrolytes, (2) fabrication and testing of both baseline materials and novel materials made from these precursors, and (3) iterative validation and improvement of design principles through both materials and device testing.

Out-Year Goals. Work will progress toward developing structure-property relationships for the self-healing, interpenetrated gel ionomer electrolyte and its individual components, as well as successful incorporation of such an electrolyte into a working Li-S cell. The team plans to demonstrate significant improvements in both capacity and retention when using the project's novel materials, as compared to state-of-the-art baseline systems.

Collaborations. This project funds work at the University of Washington. Dr. Alex Jen (PI) focuses on the design, synthesis, and testing of novel materials, as well as device-based verification of design principles. Dr. Jihui Yang (Co-PI) focuses on optimization of device fabrication and testing, as well as investigation of failure mechanisms in devices using novel materials. Facilities at PNNL in Richland, Washington, will be used for detailed study of device operation.

Milestones

1. Synthesize organic starting materials, and demonstrate both an ionomer gel electrolyte and a self-healing film based on these materials. (Q3 – In progress)
2. Integrate S/C composites into Li-S coin cells, and cycle them both with an organic electrolyte system and with several novel gel electrolyte systems. (Q4 – In progress)

Progress Report

Facilities. Setup of a new facility for small-scale device testing, including a 1.65m^3 argon glovebox, 32-channel battery testing system with integrated EIS, and associated equipment, was completed in March 2017. The facility is now fully functional and in-use for testing of novel materials.

Figure 29. A free-standing gel produced using PEGDMA (Mw=750 Da), $Pyr_{13}TFSI$, and $(NBu_4)_2S_2O_8$ initiator.

Ionomer Gel Fabrication. Reaction conditions were investigated for successful formation of a gel network between poly(ethylene glycol) dimethacrylate (PEGDMA) of either M_n=750 Da or M_n=3500 Da in either N-methylpyrrolidone (NMP) or RTIL solvent. It was found that a gel can successfully be formed with PEGDMA (M_w=750 Da), $Pyr_{13}TFSI$, and $(NBu_4)_2S_2O_8$ radical initiator (Figure 29). Experiments varying the PEGDMA molecular weight, with NMP as the solvent, showed that longer PEG chains impart improved elasticity to the resultant gels (59.7% reversible elongation for M_n=3500, as opposed to 13.9% for an identical composition with M_n=750). More detailed mechanical tests, as well as fabrication of gels containing both LiTFSI and additional methacrylate components, are in progress.

Noncovalent Interactions and Self-Healing. UV Vis/dilution experiments were performed using the synthesized PENDI-C3 polymer along with Py Linker (Figure 30a). A new charge transfer absorption peak was found to emerge at 515 nm upon mixing in DCM solution, very similar to the peak previously observed at 500 nm for mixing of model single-molecule NDI and pyrene compounds. Their interaction strength, calculated based on Beer-Lambert law and dilution method, was found to be -12.44 kJ/mol, about 50% larger than that of the model single-molecule compounds (-8.19 kJ/mol). The project hypothesizes this is due to close proximity of NDI molecules in PENDI-C3, enabling most bound Py groups to stack with two NDI units at once, increasing overall measured interaction strength. Solid films of PENDI-C3 and Py Linker (with the ratio between NDI and Py units of 1:1) were prepared by drop casting from DCM solution. While films of PENDI-C3 are translucent green and crack easily, films of the mixture were a deep red color and continuous.

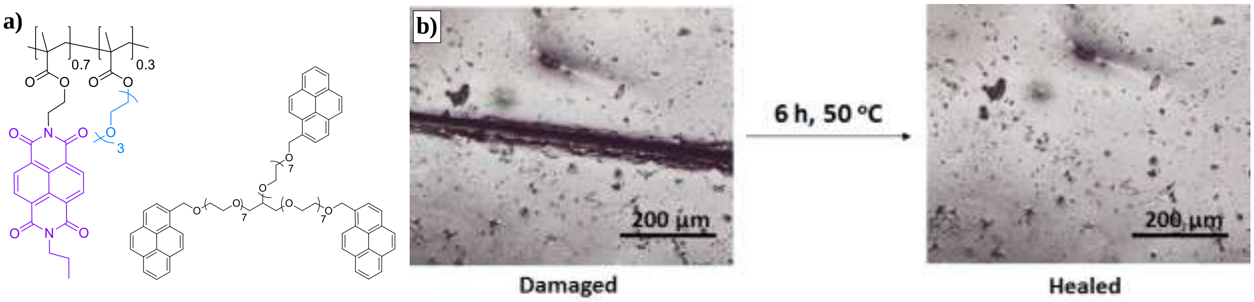

Figure 30. (a) Chemical structures of PENDI-C3 and Py Linker, respectively. (b) Observation of self-healing in a 1:1 PENDI-C3/Py Linker film after mild heating.

A self-healing test of the mixed film was performed by cutting the film into two pieces, then putting the pieces together and heating for 6 h at 50°C. Optical microscope images from before and after heating show complete self-healing of the cut (Figure 30b). The project continues to investigate properties of these materials.

Mesoporous Carbon Functionalization. To improve capacity retention, sulfur distribution, and/or reaction kinetics in S-based cathodes, the project is exploring chemical functionalization of mesoporous carbon surfaces prior to infiltration with sulfur. It has developed a chemical procedure based on well-studied diazonium chemistry (Figure 31a) to attach phenyl rings bearing customizable functional groups to unsaturated carbon surfaces. The project used this procedure to successfully attach a primary amine functional group to carbon samples, as confirmed by pore shrinkage determined through Brunauer-Emmett-Teller (BET) (Figure 31b), appearance of a nitrogen-associated peak in XPS analysis (Figure 31d), and weight loss during TGA (Figure 31c). Carbons used included MH00, a mesoporous carbon from Toyo Tanso possessing high surface area and well-ordered pores of ~4 nm. The project is investigating additional surface functional groups.

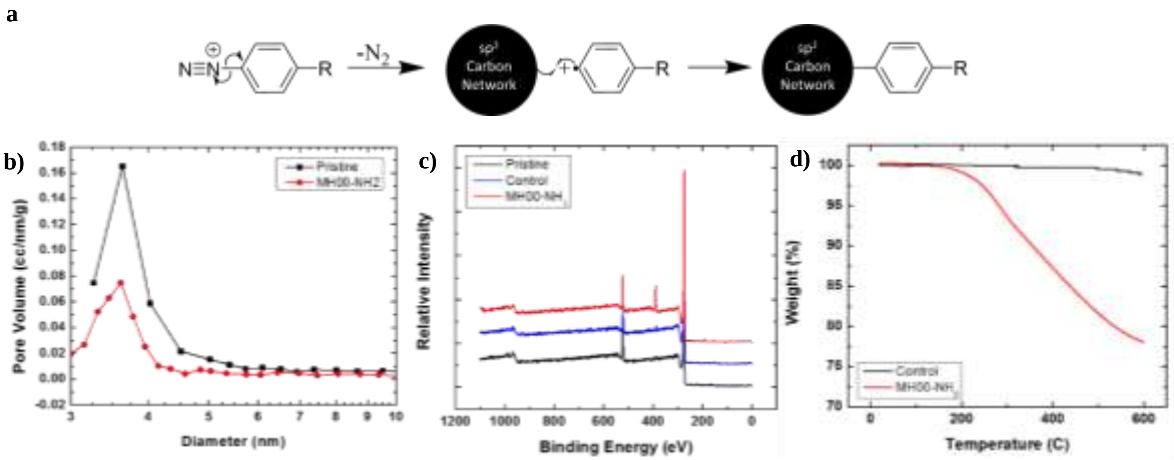

Figure 31. (a) Generalized reaction scheme for carbon functionalization using diazonium chemistry. (b) Brunauer-Emmett-Teller pore size analysis before and after functionalization, showing a decrease in overall pore volume and shrinkage of average pore size. (c) X-ray photoelectron spectroscopy data of MH00 carbon as-received (pristine), after chemical treatment absent diazonium (control), and after chemical functionalization including 1,4-phenylenediamine. The peak near 400eV is associated with nitrogen bonding. (d) Thermal gravimetric analysis data for both unfunctionalized and functionalized MH00, showing dramatically increased weight loss at 200°C due to decomposition of the functional group.

S/C Composite Synthesis. S/C composites were prepared with S_8 and MH00 carbons, both amine-functionalized and unfunctionalized, using a previously described melt-diffusion method. Successful infiltration was confirmed using BET analysis and XRD to confirm disappearance of the S_8 peak (Figure 32).

Li-S Concept Cell Testing. Li-S cells containing S/C composites, with both primary-amine-functionalized and unfunctionalized MH00 carbon containing 50 wt% sulfur, were fabricated and cycled at C/10 rate with organic electrolyte (1M LiTFSI in DOL:DME (50:50 vol) with 1 wt% $LiNO_3$) to investigate performance of these carbons in a cell environment. Initial results are shown in Figure 33a-c. Note that while amino surface functionalization dramatically improves both capacity and capacity retention of the cells over 20 cycles, it also introduces a significant additional overpotential to charge and discharge. The project hypothesizes that this could be a result of ion-dipole interactions between Li_2S_x species and the lone pair of the amino groups, which hinders escape of polysulfide into electrolyte, but also forces polysulfide reduction/oxidation to proceed largely through a kinetically-limited solid-state, rather than electrolyte-mediated, reaction mechanism. New types of functional groups being considered may be able to produce similar capacity retention while avoiding severe kinetic losses.

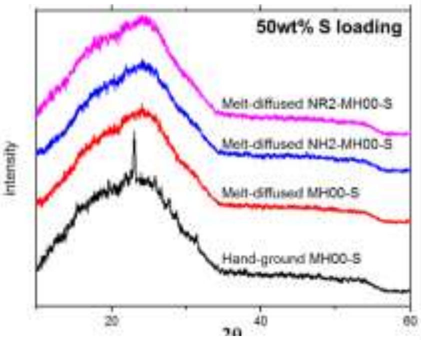

Figure 32. X-ray diffraction data of various C/S mixtures. Disappearance of the S_8 peak at 23° upon melt-diffusion indicates complete infiltration of sulfur into the carbon interior.

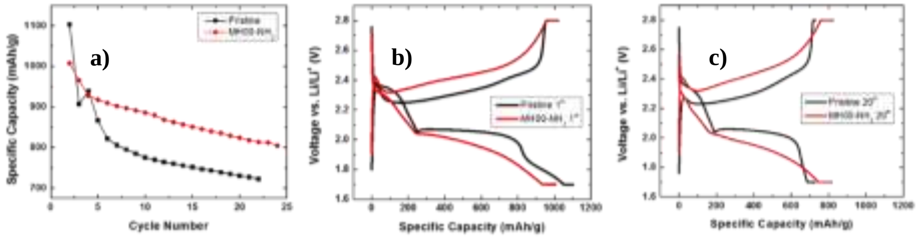

Figure 33. (a) Short-term cycling data (C/10) for S/C cathodes based on either amino functionalized or unfunctionalized MH00. (b) 1st cycle and (c) 20th cycle voltage traces for S/C cathodes both with and without functionalization. While capacity retention is improved, the cathodes based on functionalized carbon also show much higher overpotential during charge/discharge.

Patents/Publications/Presentations

Presentation

- DOE EERE BMR/ABR/Battery 500 Battery Research Information Exchange, Berkeley, California (January 18, 2017): "Multifunctional, Self-Healing Polyelectrolyte Gels for Long-Cycle, High-Capacity Sulfur Cathodes in Li-S Batteries"; Jihui Yang.

Task 4.4 – Development of Ion-Conducting Inorganic Nanofibers and Polymers
(Nianqiang (Nick) Wu, West Virginia University; Xiangwu Zhang, North Carolina State University)

Project Objective. The project objective is to develop solid-state electrolytes based on the highly-conductive inorganic nanofibrous network in the polymer matrix for lithium batteries.

Project Impact. The research team will conduct research and development on solid-state inorganic nanofiber-polymer composite electrolytes that will not only provide higher ionic conductivity, improved mechanical strength, and better stability than the polyethylene oxide polymer electrolyte, but also exhibit better mechanical integrity, easier incorporation, and better compatibility with the Li-metal anode than the planar ceramic membrane counterparts. The proposed inorganic nanofiber-polymer composite electrolytes will enable practical use of high-energy-density, high-power-density Li-metal batteries and Li-S batteries.

Approach. Integration of the highly Li^+-conductive inorganic nanofiber network into the polymer matrix not only provides the continuous Li^+ transport channels, but also kinetically inhibits the crystallization from the amorphous state of polymer electrolyte. The inorganic nanofibers will be fabricated with an electrospinning technique; and the ionic conductivity of inorganic nanofibers will be improved by chemical substitution or doping. Highly ionic-conductive polymers will be developed by cross-linking and/or creation of a block-copolymer structure; and the composition and microstructure of the composite electrolyte will be designed to suppress the lithium dendrite formation.

Out-Year Goals. Work will progress toward synthesis of the inorganic nanofibers and the polymer matrix. The goal is to find the optimal synthetic route to achieve the desirable conductivity.

Collaborations. This project funds work at WVU and North Carolina State University (NCSU). Dr. Nianqiang (Nick) Wu at WVU serves as PI, and Dr. Xiangwu Zhang at NCSU acts as Co-PI. Sujan Kasani (Ph.D. student at WVU), Hui Yang (Postdoctoral Fellow at WVU), Botong Liu (Ph.D. student at WVU), Chaoyi Yan (Ph.D. student at NCSU) and Mahmut Dirican (Postdoctoral Fellow at NCSU) contributed to the project.

Milestones

1. **Subtask 1.1.2.** Synthesize the inorganic nanofibers by the electrospinning technique. (Q2 – In progress, 50%)
2. **Subtask 1.1.3.** Characterize the chemical composition and microstructure of nanofibers, and identify the dopant site in the lattice. (Q2 – In progress, 50%)
3. **Subtask 1.1.4.** Test the temperature-dependence ionic conductivity of inorganic nanofibers, and the bulk and grain-boundary conductivity. (Q3 – In progress, 30%)
4. **Subtask 1.2.2.** Synthesize the ion-conducting polymers. (Q2 – In progress, 50%)
5. **Subtask 1.2.3.** Characterize the chemical composition, the phase, and the structure of ion-conducting polymers. (Q2 – In progress, 40%)

Progress Report

The project is synthesizing the inorganic nanofibers and the polymer matrix now. It has started the synthesis of inorganic nanofibers including the Perovskite-type lithium lanthanum titanate $Li_{0.33}La_{0.56}TiO_3$ (LLTO), NASICON-type $Li_{1.3}Al_{0.3}Ti_{1.7}(PO_4)_3$ and Garnet-type lithium lanthanum zirconium oxide $Li_7La_3Zr_2O_{12}$(LLZO) nanofibers. Synthesis of precursors and monomers for block co-polymers continues.

Task 1.1.2 - Synthesis of Inorganic Nanofibers

Lithium Lanthanum Zirconium Oxide (LLZO) Nanofibers. Aluminum-doped Garnet-type lithium lanthanum zirconium oxide (LLAZO) nanofibers were successfully produced, although small adjustment is still required to maintain a well-defined fiber network by optimizing the electrospinning solution composition.

The lithium-ion conductivity of PEO/LiTFSI/LLAZO nanofiber solid composite electrolytes was evaluated by EIS. Typical Nyquist plots and temperature dependence of ionic conductivity are shown in Figure 34. At room temperature, the calculated ionic conductivity of the composite electrolytes with 15 wt% LLAZO nanofibers was 3.47×10^{-5} S/cm. For comparison, the ionic conductivity of the PEO/LiTFSI electrolyte was 1.15×10^{-5} S/cm at room temperature, as shown in Figure 34b. The introduction of LLAZO nanofibers into the PEO/LiTFSI electrolyte increases the ionic conductivity.

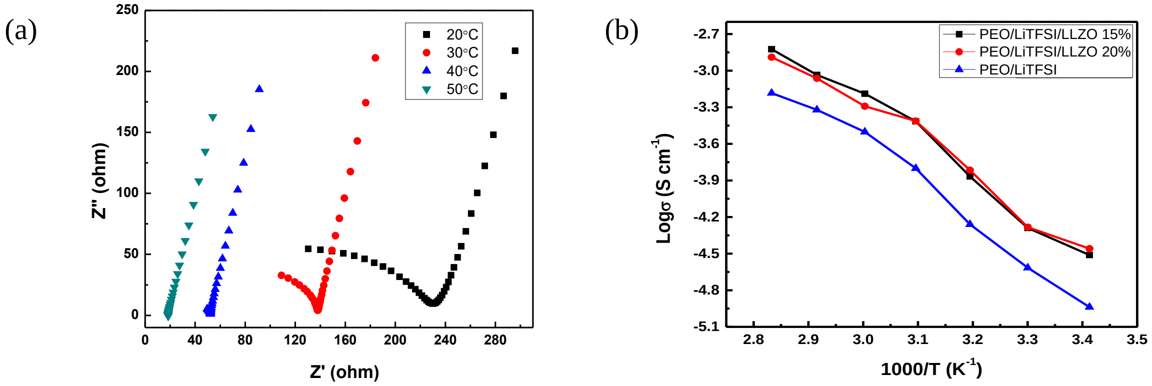

Figure 34. (a) Electrochemical impedance spectroscopy profiles of PEO/LiTFSI/LLAZO (15 wt%) electrolyte at different temperatures of 20°C, 30°C, 40°C, and 50°C. (b) Temperature dependence of ionic conductivity of PEO/LiTFSI/LLAZO electrolyte with different LALZO filler contents in the temperature range of 20 – 90 °C.

Lithium Lanthanum Titanate (LLTO) Nanofibers. Perovskite-type lithium lanthanum titanate $Li_{0.33}La_{0.56}TiO_3$ (LLTO) nanofibers were synthesized by electrospinning. The ionic conductivity of PEO/LiTFSI/LLTO solid composite electrolytes was measured by EIS. The PEO/LiTFSI/LLTO (15 wt%) composite electrolyte demonstrated the lowest resistance of 133.3 Ω, corresponding to the highest ionic conductivity of 4.76×10^{-5} S/cm at room temperature. Since a large electrochemical window is a desirable for application of any electrolyte in high-voltage lithium batteries, linear sweep voltammetry (LSV) was carried out to test the stability of PEO/LiTFSI/LLTO (15 wt%) composite electrolyte. As demonstrated in Figure 35, the PEO/LiTFSI/LLTO (15 wt%) composite electrolyte exhibited a stable voltage window up to 5 V versus Li/Li^+, indicating that this solid composite electrolyte could satisfy requirements of most high-voltage lithium batteries.

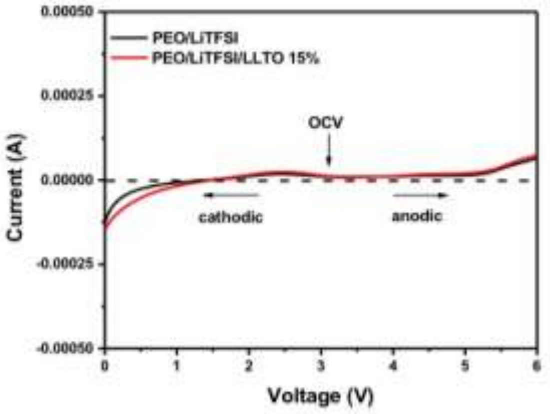

Figure 35. Linear Sweep voltammetry curve of PEO/LiTFSI/15 wt% LLTO composite electrolyte.

Lithium Aluminum Titanium Phosphate (LATP) Nanofibers. The NASICON-type $Li_{1.3}Al_{0.3}Ti_{1.7}(PO_4)_3$ fibers were prepared by electrospinning. Further tuning of phase and morphology of LATP nanofibers will be done in the future.

Task 1.2.2 - Synthesis of Polymer Matrix

Monomer (4-styrenesulfonyl) (trifluoromethanesulfonyl)imide (STFSI) was synthesized. Based on this, random copolymers potassium poly[(4-styrenesulfonyl) (trifluoromethanesulfonyl)imide-co-methoxy-polyethylene glycol acrylate] (K[PSTFSI-co-MPEGA]) copolymers with [EO]/[K^+] ratios (Table 1) were firstly synthesized. Substitution of K^+ ions in copolymers with Li^+ ions was carried out then.

The ionic conductivity of copolymer electrolyte Li[PSTFSI-co-MPEGA] (EO/Li^+ = 30) was 1.16×10^{-6} S/cm. The electrochemical performance measurements of Polymers 2 and 3 are still in progress and will be reported next quarter. The low ionic conductivity of copolymer electrolyte Li[PSTFSI-coMPEEGA] (EO/Li^+ = 30) was compensated by the fact that the copolymer is single lithium-ion conductor with a unity Li^+ transference number. In future work, the project will increase the ionic conductivity of copolymers by reducing the EO/Li^+ ratio and forming a block copolymer structure.

Table 1. EO/K^+ ratios of copolymers K[PSTFSI-co-MPEGA] and ionic conductivities of corresponding copolymers Li[PSITFSI-co-MPEGA].

Samples	Feed EO/K^+ Ratio	Actual EO/K^+ Ratio	Ionic Conductivity S/cm
Copolymer K[PSTFSI-co-MPEGA]			
Polymer 1	32.00	30.30	1.16×10^{-06}
Polymer 2	24.00	23.10	-
Polymer 3	16.00	20.26	-

Task 4.5 – High Conductivity and Flexible Hybrid Solid-State Electrolyte (Eric Wachsman, Liangbing Hu, and Yifei Mo, University of Maryland)

Project Objective. The project objective is to develop flexible hybrid electrolyte with garnet nanofibers to achieve the following: (1) flexible, with greater mechanical strength (~ 10 MPa) and thermal stability than polymer electrolytes; (2) high room temperature ionic conductivity, ~ 0.5 mS/cm; (3) stable interface with lithium metal and effective blocking of lithium dendrites at current densities up to 3 mA/cm^2; and (4) battery performance with Li-S chemistry with an energy density of ≥ 450 Wh/kg and (≥1000 Wh/L) and maintaining ≥ 80% of capacity up to 500 cycles.

Project Impact. Instability and/or high resistance at the interface of lithium metal with various solid electrolytes limit the use of the metallic anode for batteries with high energy density, such as Li-air and Li-S batteries. The critical impact of this endeavor will be focused on developing a new type of solid-state electrolyte (SSE) that is highly conductive, highly flexible, and electrochemically stable. In particular, the new SSE will enable Li-metal anodes with excellent interfacial impedance and blocking of lithium dendrite formation.

Approach. The project will synthesize garnet nanofibers, fill the porous region with polymer electrolyte, and characterize the flexible hybrid membrane properties. The flexible hybrid SSE microstructure will be determined using focused ion beam (FIB)/SEM and integrated with electrochemical methods to investigate the properties and stability with Li-metal anode.

Out-Year Goals. The project will develop a fundamental understanding of the mechanism of Li-ionic diffusion in garnet nanofibers and their mechanical properties, as well as these properties for hybrid garnet-fiber/polymer hybrids. Work will progress toward the study of the electrode assembly during electrochemical cycling of the anode.

Collaborations. This project funds work at University of Maryland, College Park. Dr. Eric D. Wachsman (PI) will focus on optimizing the garnet network to achieve high ionic conductivity and flexibility using FIB/SEM and EIS characterization. Dr. Liangbing Hu (Co-PI) focuses on synthesis of the hybrid electrolyte and test for Li-metal anode with the hybrid electrolyte. Dr. Yifei Mo (Co-PI) will lead efforts on computational modeling of the garnet nanofiber hybrid electrolytes for fundamental mechanistic understanding.

Milestones

1. Fabricate 4-cm by 4-cm garnet nanofiber membrane. (Q1 – Complete)
2. Synthesize ion-conductive polymers, synthesize ion-insulation polymers, and *in situ* synthesize polymer electrolyte coated garnet nanofibers. (Q2 – Complete)
3. Understand Li-ionic diffusion in garnet nanofibers and its response to mechanical deformation. (Q3 – In progress)
4. Achieve hybrid SSE with a high ionic conductivity (~0.5x10^{-3} S/cm), high electrochemical stability (~ 4.5V), and high mechanical property. (Q4)

Progress Report

Garnet-type $Li_{6.4}La_3Zr_2Al_{0.2}O_{12}$ (LLZO) nanofibers were prepared by electrospinning of polyvinylpyrrolidone (PVP) polymer mixed with relevant garnet LLZO salts, followed by calcination of the as-prepared nanofibers in air. Specifically, stoichiometric amounts of $LiNO_3$, $La(NO_3)_3 \cdot 6H_2O$, $ZrO(NO_3)_2 \cdot 6H_2O$, and $Al(NO_3)_3 \cdot 9H_2O$ were dissolved in dimethylformamide (DMF) with 15 vol% acetic acid. PVP (Mw~1,300,000) was dissolved in DMF with a concentration of 10 wt%. The salt solution and PVP solution were mixed at a 1:1 ratio in volume to prepare the precursor solution for electrospinning. During electrospinning, a high voltage of 20 kV was applied between the needle and the drum collector, between which the distance was 10 cm. The drum collector was covered with a thin nonwoven fabric to collect the as-spun nanofibers. The rotation speed was controlled and the humidity of the electrospinning chamber was no more than 20%. After electrospinning, the as-spun nanofibers were peeled off, dried in oven, and then calcined at 800°C for 2 h. After calcination, PVP polymer was removed and garnet nanofibers were crystallized. Figure 36 shows the morphology of Garnet nanofibers before and after sintering. The as-spun membrane consists of continuous nanofibers with diameters ranging from ~200 to 300 nm.

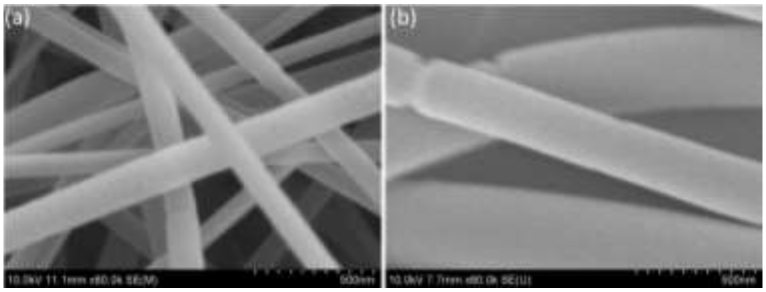

Figure 36. Scanning electron microscopy images of garnet nanofibers (a) before and (b) after calcination.

Polyethylene oxide (PEO, Mw~600,000) is an ionic insulating polymer. By adding lithium salt (LiTFSI) into PEO matrix, the ionic conductive polymer was obtained. The polymer electrolyte was coated onto the garnet nanofiber membrane by repeated wetting and drying to get a flexible solid-state membrane. The lithium salt/polymer composite solution was LiTFSI and polyethylene oxide (PEO, Mw~600,000) dissolved in acetone nitrile. The LiTFSI-PEO solution was dropped onto the garnet nanofiber membrane and dried first in a flow of dry air and then in a vacuum oven to remove the solvent. This wetting and drying process was repeated several times until the garnet nanofiber membrane was fully embedded in the PEO polymer matrix. The composite electrolyte was treated at 60°C to enable the *in situ* coating of PEO-LiTFSI polymer on the garnet nanofibers. Figure 37 shows the garnet nanofibers coated with the PEO-LiTFSI polymer electrolyte. The average diameter of the garnet nanofibers increased to 500 nm due to the PEO-LiTFSI ion-conductive polymer coating.

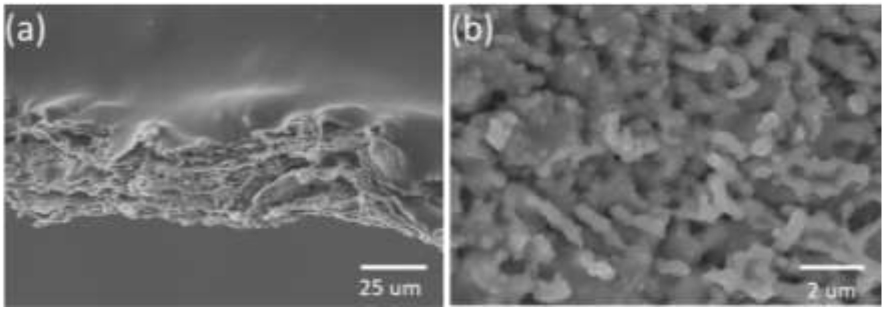

Figure 37. (a) Cross-sectional scanning electron microscopy (SEM) image. (b) Magnified SEM image of polymer electrolyte (PEO-LiTFSI) coated garnet nanofiber.

The project has synthesized ion insulating polymer PEO, ion conductive polymer PEO-LiTFSI, and *in situ* coated garnet nanofibers by polymer electrolyte. As reported, the Li-ion conductivity of cubic phase LLZO garnet pellet can reach as high as 10^{-3} S/cm, while the value for Li-salt-stuffed PEO is generally on the order of 10^{-6}-10^{-9} S/cm at room temperature. The project's flexible electrolyte combining conductive cubic LLZO garnet and lithium-PEO could therefore reach a reasonably high ionic conductivity of 2.5×10^{-4} S/cm at room temperature.

Task 4.6 – Self-Forming Thin Interphases and Electrodes Enabling 3D Structured High-Energy-Density Batteries
(Glenn Amatucci, Rutgers University)

Project Objective. The project objective is to develop and implement a novel *in situ* formed lithium-metal-based metal fluoride battery that will enable packaged 10 mAh batteries of energy densities > 1000 Wh/L and >400 Wh/kg at 12V.

Approach. The project focuses on the coalescence of three main aspects of the baseline technology, corresponding to the three sub-tasks of the project: the self-forming chemistry comprised of electrodes and electrolyte, electrode and electrolyte fabrication, and cell design.

Impact. Successful realization of 3D batteries formed *in situ* with a practical approach to large-scale fabrication would address some of the DOE EV performance goals, including: (1) areal capacity increase, (2) improved rates, and (3) designs to enable high-voltage unit cells.

Milestones

1. Establish positive reactive current collector compositions that achieve 50% of the theoretical energy density. (September 2017 – In progress)
2. Establish negative reactive current collector compositions with uniform lithium plating after *in situ* formation showing < 30% variation of the plated-Li thickness. (March 2017 – In progress)
3. Establish a bi-ion solid-state conducting glass composition with ionic conductivity >$1\text{x}10^{-4}$ S/cm prior to *in situ* formation (June 2017 – Concluded in Q1). > $1\text{X}10^{-5}$ S/cm achieved pre-formation, > $1\text{X}10^{-4}$ S/cm achieved post formation. No additional focus on this milestone this year, as achieved results are sufficient for stated goals.
4. Establish cell-stack design to achieve the 1st Go/No-Go point with 50% utilization of the positive reactive current collector. (December 2016 – In progress)
5. *Go/No Go*: Achieve self-formed cell-stack with > 500 Wh/L and 200 Wh/kg at a rate of C/10, and > 80% capacity retention after 25 cycles. (September 2017)

Full Cell Implementation. This quarter, baseline reactive current collectors and bi-ion conductors of ionic conductivity of the order of $1\text{X}10^{-5}$ S/cm identified in first quarter work were successfully implemented into solid-state cells. The viability of the *in situ* formation of the entire electrochemical cell was demonstrated with limited cycling at output voltages of approximately 2 V. These initial full-cell architectures were based on a baseline, and therefore, non-optimized design comprised of large inter- and intra- electrode diffusion lengths.

Implementation of Scalable Patterning. This quarter, the project successfully implemented a mask-less scalable patterning technique to fabricate the solid-state cells described above. Such mask-less scalable patterning technique offers a pathway to high throughput, low material loss fabrication of complex architectures. All other fabrications pathways were eliminated this quarter to pursue this option based on the initial results obtained.

Task 4.7 – Dual Function Solid-State Battery with Self-Forming, Self-Healing Electrolyte and Separator
(Esther Takeuchi, Stony Brook University)

Project Objective. The project objective is to demonstrate a solid-state rechargeable battery based on a Li-metal anode and iodine cathode with a self-forming, self-healing electrolyte and separator. The resulting rechargeable self-assembled metal/iodine solid state battery will provide an energy density of ≥ 560 Wh/kg and ≥ 1536 Wh/kg.

Project Impact. This program will enable demonstration of the proposed rechargeable battery with improved power capability, high energy density, and a self-forming, self-healing solid-state electrolyte / separator. Technical insight will be gained regarding improved conductivity of the solid lithium iodide (LiI) based electrolyte, power capability of the proposed system, the self-healing nature of the LiI layer, the nature of the electrode-electrolyte interfaces, and feasibility of the system to reach the EV Everywhere Grand Challenge targets.

Approach. The proposed concept is a dual function rechargeable solid-state battery utilizing LiI combined with silver iodide (AgI) as the electrolyte with lithium metal (and small quantities of silver metal) as the anode and iodine as the cathode with a self-forming, self-healing separator/electrolyte. The battery will be assembled in the discharged state where the anode and cathode will be created during the first formation (charge) step. Initially, silver ion (Ag^+) will diffuse toward the negative electrode and be reduced to silver metal (Ag^0), and iodine ion (I^-) will be oxidized to elemental iodine (I_2) at the cathode side. As the formation of the battery continues, lithium ion (Li^+) will form a Li-metal layer at the anode, with generation of iodine at the cathode. LiI will remain and serve as both the separator and electrolyte.

Out-Year Goals. This is a multiyear program where the effort is divided into three major tasks.

- Year 1 involves electrolyte preparation and characterization including preparation of solid state electrolytes and conductivity measurements.
- Year 2 will focus on cell construction and testing including both *in situ* and *ex situ* analysis.
- Year 3 will focus on cell characterization. Under the program, cycle life, efficiency, energy density, and the functional capacity of cells will be determined.

Collaborations. This project collaborates with Amy Marschilok and Kenneth Takeuchi of SBU.

Milestones

1. Reagents procured; composition, purity, and water content verified. (Q1 – Complete)
2. Develop methodology for AC impedance measurement as a function of temperature. (Q2 – Complete)
3. Identify the four most conductive silver-containing LiI solid electrolytes for further study. (Q3 – In progress)
4. At least one electrolyte with conductivity ≥ 10^{-3} S/cm. (Q4)

Progress Report

Methodology for AC Impedance Measurements as a Function of Temperature. The milestone this quarter was development and demonstration of repeatable measurements of resistance over a range of temperatures for solid electrolytes. The project used AC EIS methodology to measure the resistance of the solid electrolytes and validated by application of the measurement to known materials with reported results. It achieved reproducible results by repeating measurements of the same material over a range of temperatures, compared the values with those in the literature, and found the values consistent with prior reports. For all material types, either pristine material (AgI, LiI) or composite (AgI_*x* % Al_2O_3), measurements were performed at least in triplicate, and resistance values collected as a function of temperature were analyzed quantitatively by equivalent circuit modeling. The same circuit model was used both in analysis of AgI, LiI, and AgI_*x* % Al_2O_3 materials.

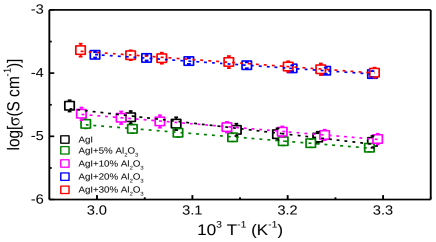

Figure 38. Conductivity of AgI_*x*%Al_2O_3 including error bars.

Preparation and Measurement of AgI Containing Conductor. Samples of AgI with various amounts of Al_2O_3 additive (5, 10, 20, 30%) were prepared using a reproducible process, and conductivities were determined, as shown in Figure 38, Figure 39, and Table 2. It was determined that the highest conductivity was for the 20% and 30% Al_2O_3 at 9.6×10^{-5} S/cm and 1.0×10^{-4} S/cm at 30°C, respectively.

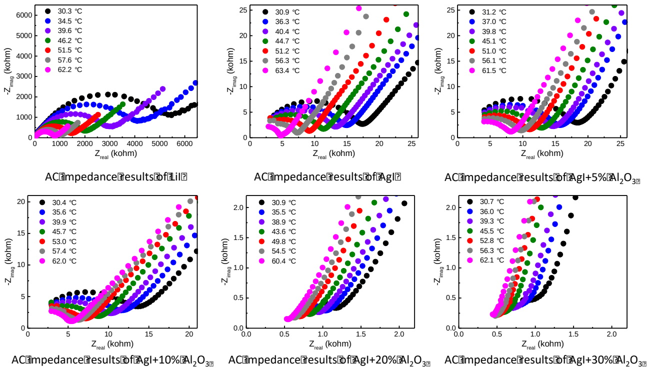

AC impedance results of LiI

AC impedance results of AgI

AC impedance results of AgI+5% Al_2O_3

AC impedance results of AgI+10% Al_2O_3

AC impedance results of AgI+20% Al_2O_3

AC impedance results of AgI+30% Al_2O_3

Figure 39. Electrochemical impedance spectroscopy for AgI + *x*% Al_2O_3 as a function of temperature.

$RbAg_4I_5$ was synthesized and determined to be phase pure (Figure 40). Using the developed impedance measurement methodology, composites of LiI_*x*%$RbAg_4I_5$ (*x* = 10, 20) were measured (Figure 41).

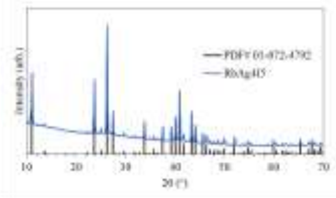

Figure 40. X-ray diffraction of $RbAg_4I_5$.

Table 2. Conductivity values of pristine materials and composites at 30°C.

Material	σ (S/cm, 30 °C)	E_a (eV)
AgI	8.2×10^{-6}	0.35
AgI+5% Al_2O_3	6.6×10^{-6}	0.25
AgI+10% Al_2O_3	9.0×10^{-6}	0.25
AgI+20% Al_2O_3	$\mathbf{9.6 \times 10^{-5}}$	0.21
AgI+30% Al_2O_3	$\mathbf{1.0 \times 10^{-4}}$	0.22
LiI	3.5×10^{-8}	0.57

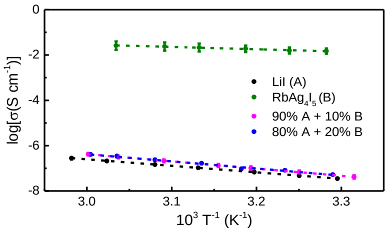

Figure 41. Conductivity as a function of temperature for LiI_*x*%$RbAg_4I_5$ (*x* = 10, 20).

Patents/Publications/Presentations

Presentation

- DOE EERE BMR/ABR/Battery 500 Research Information Exchange, Berkeley, California (January 17 - 19, 2017): “Dual Function Solid-State Battery with Self-Forming Self-Healing Electrolyte and Separator”; E. Takeuchi, A. Marschilok, and K. Takeuchi.

TASK 5 – DIAGNOSTICS

Summary and Highlights

To meet the goals of the VTO Multi-Year Program Plan and develop lower-cost, abuse-tolerant batteries with higher energy density, higher power, better low-temperature operation and longer lifetimes suitable for the next-generation of HEVs, PHEVs and EVs, there is a strong need to identify and understand structure-property-electrochemical performance relationships in materials, life-limiting and performance-limiting processes, and various failure modes to guide battery development activities and scale-up efforts. In the pursuit of batteries with high energy density, high cell operating voltages and demanding cycling requirements lead to unprecedented chemical and mechanical instabilities in cell components. Successful implementation of newer materials such as silicon anode and high-voltage cathodes also requires better understanding of fundamental processes, especially those at the solid/electrolyte interface of both anode and cathode.

This Task takes on these challenges by combining model system, *ex situ*, *in situ*, and *operando* approaches with an array of state-of-the-art analytical and computational tools. Four subtasks are tackling the chemical processes and reactions at the electrode/electrolyte interface. Researchers at LBNL use *in situ* and *ex situ* vibrational spectroscopy, far- and near-field scanning probe spectroscopy and laser-induced breakdown spectroscopy (LIBS) to understand the composition, structure, and formation/degradation mechanisms of the SEI at silicon anode and high-voltage cathodes. The University of California – San Diego (UCSD) combines STEM/EELS, XPS and *ab initio* computation for surface and interface characterization and identification of instability causes at both electrodes. At the University of Cambridge, nuclear magnetic resonance (NMR) is being used to identify major SEI components, their spatial proximity, and how they change with cycling. Subtasks at BNL and PNNL focus on the understanding of fading mechanisms in electrode materials, with the help of synchrotron-based X-ray techniques (diffraction and hard/soft X-ray absorption) at BNL and high-resolution transmission electron microscopy (HRTEM) and spectroscopy techniques at PNNL. At LBNL, model systems of electrode materials with well-defined physical attributes are being developed and used for advanced diagnostic and mechanistic studies at both bulk and single-crystal levels. These controlled studies remove the ambiguity in correlating material's physical properties and reaction mechanisms to performance and stability, which is critical for further optimization. The final subtask takes advantage of the user facilities at ANL that bring together X-ray and neutron diffraction, X-ray absorption, emission and scattering, HRTEM, Raman spectroscopy, and theory to look into the structural, electrochemical, and chemical mechanisms in the complex electrode/electrolyte systems. The diagnostics team not only produces a wealth of knowledge key to developing next-generation batteries, it also advances analytical techniques and instrumentation that have a far-reaching effect on material and device development in a variety of fields.

Highlights. The highlights this quarter are as follows:

- LBNL (Chen's group) demonstrated significant morphology damage during lithium extraction of a novel, high-capacity, Li-excess TM oxide cathode involving oxygen redox activities.
- Cambridge (Grey's Group) investigated sodium dendrite using an *in situ* ^{23}Na NMR technique and found more severe dendrite formation for Na-metal anodes in comparison to that of Li-metal anodes. Significant dendrite/microstructure forms even at low current densities that may be partially removed on reversing the current.

Task 5.1 – Model System Diagnostics for High-Energy Cathode Development (Guoying Chen, Lawrence Berkeley National Laboratory)

Project Objective. This project will use a rational, non-empirical approach to design and synthesize next-generation high-energy, high-voltage cathode materials. Combining a suite of advanced diagnostic techniques with model cathode materials and model electrode/electrolyte interfaces, the project will perform systematic studies to achieve the following goals: (1) obtain new insights into solid-state chemistry, particularly cationic and/or anionic redox activities during charge and discharge of high-capacity Li-TM oxides, (2) gain fundamental understanding on cathode/electrolyte interfacial chemistry and charge transfer process as a function of operating voltage, (3) reveal performance- and stability-limiting properties and processes in high-energy, high-voltage cathodes, and (4) develop strategies to mitigate the structural and interfacial instabilities.

Project Impact. The project will improve the commercial viability of next-generation high-energy cathode materials. The findings will enable more stable high-voltage cycling of existing Li-TM oxides as well as development of novel high-capacity cathode materials for advanced Li-ion batteries.

Approach. Prepare crystal samples of Li-stoichiometric and Li-excess TM oxides with well-defined physical attributes. Perform advanced diagnostic and mechanistic studies at both bulk and single-crystal levels. Global properties and performance of the samples will be established from the bulk analyses, while the single-crystal-based studies will utilize time- and spatial-resolved analytical techniques to probe the material redox transformation process and failure mechanisms under battery operating conditions.

Out-Year Goals. Obtain fundmental knowledge on performance-limiting physical properties, phase transition mechanisms, parasitic reactions, and transport processes that prevent cathode materials from delivering higher capacities and achieving more stable cycling at high voltages. Develop approaches to mitigate cathode structural and interfacial instabilities during high-voltage operation. Design and synthesize optimized Li-TM oxide cathodes as well as novel high-energy electrode materials.

Collaborations. This project collaborates with the following: G. Ceder, K. Persson, M. Doeff and P. Ross (LBNL); V. Srinivasan (ANL); Simon Mun, (Gwangju Institute of Science and Technology, GIST); Y. Liu (SSRL); J. Guo (ALS); C. Wang (PNNL); C. Grey (Cambridge); and A. Huq and J. Nanda (ORNL).

Milestones

1. Synthesize model Li-TM oxide cathode materials with several different chemical compositions and/or morphologies. (Q1 – Complete)
2. Investigate the bulk activities of TM and oxygen redox centers in Li-TM oxides as a function of state of charge and temperature. (Q2 – Complete)
3. *Go/No-Go*: Investigate synthesis methods for preparing single crystals of Li-excess TM oxides with previously reported reversible oxygen redox activities. *No-Go* if high-quality crystals of the oxide cannot be made. (Q3 – On schedule)
4. Determine the activities of lattice oxygen and TM on particle surface and the impact of cathode chemistry and surface facet. (Q4 – On schedule)

Progress Report

This quarter, studies were performed to understand the redox activities in the bulk of high-capacity Li-excess TM oxides. Uniform micron-sized $Li_{1.3}Nb_{0.3}Mn_{0.4}O_2$ ($Li_{1.3}$NMO) crystals were previously synthesized by a molten salt method. Lithium extraction and insertion in the crystal sample were achieved by both electrochemical charge/discharge and chemical methods. For the former, composite electrodes were prepared by first ball-milling $Li_{1.3}$NMO crystals with a carbon black (20 wt%) followed by mixing the powder with additional carbon black and a PVDF binder in a weight ratio of 70:20:10. The electrodes were assembled into half-cell coin cells with a 1.0 M $LiPF_6$ EC/DEC electrolyte and cycled at room temperature at a constant current of 10 mA/g between 1.5 and 4.8 V. Figure 42a shows the voltage profiles of the first 4 cycles. An activation plateau was observed in the first cycle which becomes slopy in the following cycles. Both voltage and capacity fade occurred during cycling. A large discharge capacity of 260 mAh/g was obtained in the first cycle, of which ~120 mAh/g can be accounted for by the Mn redox of Mn^{3+}/Mn^{4+}, corresponding to the extraction of 0.4 Li^+ per formula unit or a residual lithium content of 0.9 in the sample. The source of the additional capacity (~140 mAh/g) is not fully understood.

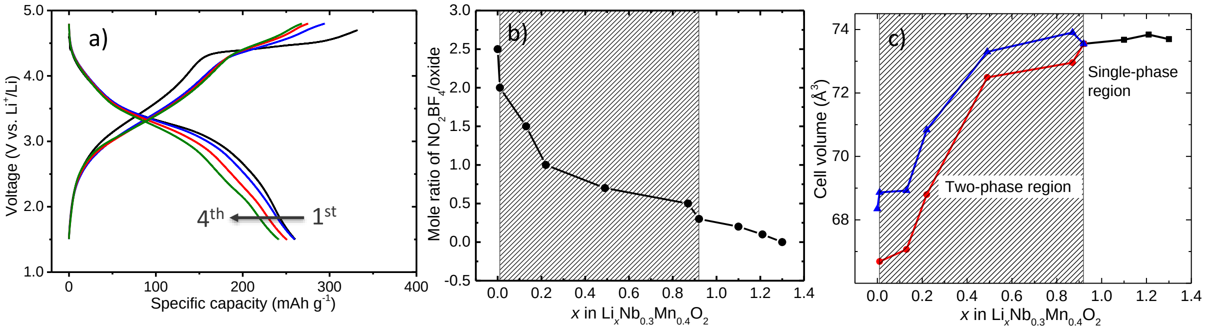

Figure 42. (a) Voltage profiles of electrochemical charge/discharge of $Li_{1.3}Nb_{0.3}Mn_{0.4}O_2$. (b) Relationship between the content of residual lithium and amount of oxidant used during chemical delithiation of the crystals. (c) Cell volume as a function of x in $Li_xNb_{0.3}Mn_{0.4}O_2$.

As electrochemical methods do not produce the large quantities of samples needed for several analytical studies, chemical oxidation was used to extract various amounts of lithium from $Li_{1.3}$NMO crystals. The residual lithium content (x) in the delithiated oxides was controlled by the mole ratio between the oxidizing agent (NO_2BF_4 solution in acetonitrile), as shown in Figure 42b. While a near linear relationship was observed in $0.9 < x < 1.3$, the kinetic behavior becomes more complex when x is below 0.9. Rietveld refinement of the synchrotron XRD patterns collected on various delithiated samples was performed, and the unit cell volume as a function of x is shown in Figure 42c. Two separate regions (a single rock-salt phase region following Vegard's law, and a two-phase region with rock-salt phases of different lattice dimensions) were observed, suggesting a distinct transition in redox activities from cation redox involving Mn^{3+}/Mn^{4+} in the single-phase region to more complex oxygen redox in the two-phase region around x=0.9. Figure 43 shows the changes in particle morphology along with the decrease of x in $Li_xNb_{0.3}Mn_{0.4}O_2$ crystals. The particles with a lithium content above 0.9 remain intact, but significant cracking was observed when the lithium content is less than 0.9, likely a combined effect of cell volume change (7.3% total) and oxygen evolution during the process.

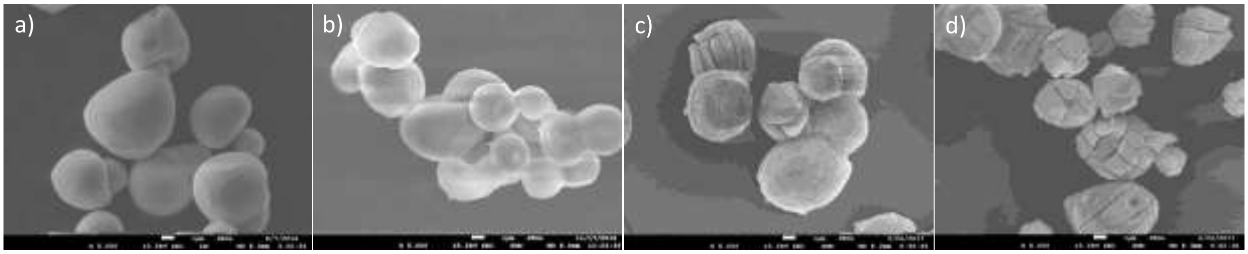

Figure 43. Scanning electron microscopy images of chemically delithiated $Li_xNb_{0.3}Mn_{0.4}O_2$ crystal samples: (a) x=1.3, (b) x=1.1, (c) x=0.76, and (d) x=0.13.

Patents/Publications/Presentations

Publications

- Ma, Y. , and Y. Zhou, C. Du, P. Zuo, X. Cheng, L. Han, D. Nordlund, Y. Gao, G. Yin, H. L. Xin, M. M. Doeff, F. Lin, and G. Chen. "A New Anion Receptor for Improved Interface between the Lithium- and Manganese-Rich Layered Oxide Cathode and the Electrolyte." *Chemistry of Materials* 29, no. 5 (2017): 2141. doi: 10.1021/acs.chemmater.6b04784.
- Kuppan, S., and Y. Xu, Y. Liu, and G. Chen. "Phase Transformation Mechanism in $LiMn_{1.5}Ni_{0.5}O_4$ Cathode Particles Revealed by Single-Crystal Hard X-Ray Microscopy." *Nature Communications* 8 (2017): 14309. doi: 10.1038/ncomms14309.

Presentations

- Energy Technology Area Lab Town Hall Meeting, Berkeley, California (March 2017): "Rational Design and Development of Advanced Lithium Battery Materials"; J. Kan and G. Chen. Invited.
- Energy Technology Area Lab Director's Review, Berkeley, California (January 2017): "Rational Design and Development of Advanced Lithium Battery Materials"; J. Kan, T. Yan, and G. Chen. Invited.

Task 5.2 – Interfacial Processes – Diagnostics
(Robert Kostecki, Lawrence Berkeley National Laboratory)

Project Objective. This collaborative project involves developing and applying advanced experimental methodologies to study and understand the mechanism of operation and degradation of high-capacity NMC materials for Li-ion cells for PHEV and EV applications. The main objective is to apply *in situ* and *ex situ* far- and near-field optical multifunctional probes to obtain detailed insight into the active material structure and the physicochemical phenomena at electrode/electrolyte interfaces of stoichiometric NMCs with high nickel contents such as 622 and 523 composition materials at a spatial resolution that corresponds to the size of basic chemical or structural building blocks. The primary goal of these studies is to unveil the structure and reactivity at hidden or buried interfaces and interphases that determine material, composite electrode, and full-cell electrochemical performance and failure modes.

Project Impact. Instability and/or high resistance at the interface of high-voltage Li-ion cathodes limits electrochemical performance of high-energy density batteries. A better understanding of the underlying principles that govern these phenomena is inextricably linked with successful implementation of high-energy-density materials such as silicon and high-voltage cathodes in Li-ion cells for PHEVs and EVs. The proposed work constitutes an integral part of the concerted effort within the BMR Program, and it supports development of new cathode materials for high-energy Li-ion cells.

Approach. The pristine and cycled NMC powders and electrodes will be probed using a variety of surface- and bulk-sensitive techniques, including Fourier transform infrared (FTIR), attenuated total reflection (ATR)-FTIR, near-field infrared and Raman spectroscopy and microscopy, and scanning probe microscopy to identify and characterize changes in materials structure and composition. Novel *in situ/ex situ* far- and near-field optical multifunctional probes in combination with standard electrochemical and analytical techniques are developed to unveil the structure and reactivity at interfaces and interphases that determine materials electrochemical performance and failure modes.

Out-Year Goals. Determine the degradation mechanism(s) of high-voltage cathodes; propose and test effective remedies to intrinsic interfacial instability of these materials and composite electrodes.

Collaborations. NMC materials and composite electrodes tested under different cycling regimes by M. Doeff (LBNL) and C. Ban (NREL) will be studied. The diagnostic studies will be carried out in sync with differential electrochemical MS analysis by B. McCloskey (LBNL) and other diagnosticians in the BMR program. He will also work closely with V. Battaglia (LBNL) to obtain samples from full-cell cycling experiments.

Milestones

1. Determine relationship between surface reconstruction and aging/cycling of NMC powders/electrodes. (Q1– Complete)
2. Complete *in situ* atomic force microscopy (AFM) characterization of interfacial activity of the model NMC material in organic carbonate electrolytes. (Q3 – On schedule)
3. Determine composition of surface film and its effect on electrochemical performance of NMC electrodes. (Q3 – On schedule)
4. Determine relationship between surface reconstruction, film formation, and metal dissolution in NMC electrodes. (Q4 – On schedule)

Progress Report

This quarter, the project evaluated the effect of an artificial surface reconstruction layer (see last report) on the electrochemical performance of the nickel-rich NMC (Ni:Mn:Co=5:3:2) cathode and its effect on the degradation mechanism of the NMC electrode. The project used XAS in total electron yield mode (XAS-TEY) to probe the valence state of TM ions in NMC at shallow depths (2-5 nm) from the particle surface. Figure 44 shows XAS-TEY spectra of the pristine nickel-rich NMC powder and NMC/R powder samples after surface modification process at nickel, cobalt, and manganese L-edge. The absorption peaks at 852.5 eV and 854 eV correspond to Ni^{2+} and Ni^{3+}, respectively. NMC/R exhibits lower Ni^{3+}/Ni^{2+} peak ratio than pristine NMC, which indicates that NMC/R material has higher concentration of Ni^{2+} at the surface. Cobalt and manganese L-edge spectra display Co^{2+} and Mn^{2+} shoulders at 778 eV and 639 eV next to the main Co^{3+} and Mn^{4+} peaks at 780.5 eV and 642.5 eV, respectively. Higher intensities of Co^{2+} and Mn^{2+} peaks in NMC/R spectra also point toward surface enrichment with Co^{2+} and Mn^{2+}. In other words, XAS-TEY spectra provide direct evidence of a surface reconstruction layer, which was artificially created in NMC/R particles upon long-term exposure to the electrolyte at elevated temperatures. The (II) valance state of nickel, cobalt, and manganese at the surface is consistent with the presence of a rock salt structure thin-film, as has been reported by different groups.

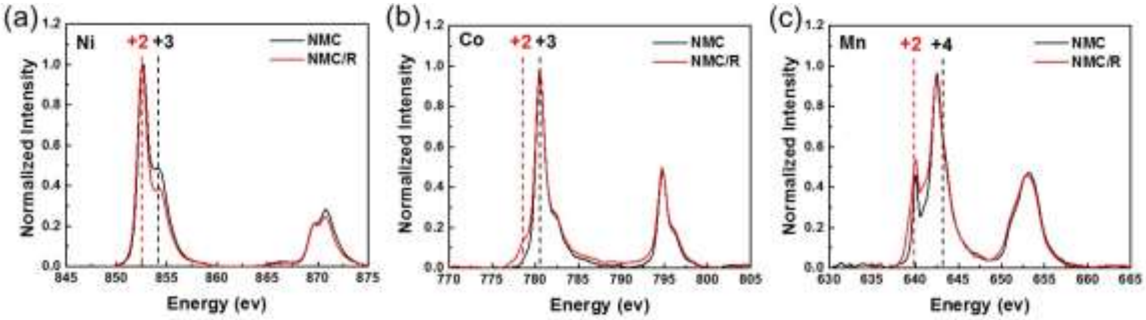

Figure 44. X-ray absorption spectroscopy total electron yield of NMC and NMC/R powders on the range L-edge of (a) nickel, (b) cobalt, and (c) manganese.

Composite cathodes were fabricated with pristine NMC and NMC/R powders and then cycled at 0.5 C between 2 – 4.7 V in coin cells equiped with lithium anode and 1M $LiPF_6$ EC/DEC (1:2 wt%) electrolyte. The cycled cathodes were washed in DEC and dried in vacuum. Figure 45 shows XAS spectra of the cycled electrodes at nickel, cobalt, and manganese L-edge. The nickel L-edge spectrum of the NMC electrode shows a notable decrease of the Ni^{3+} peak at 854 eV after cycling, whereas the cycled NMC/R electrode shows no such change. Interestingly, the surface composition of the NMC and NMC/R electrodes after cycling becomes almost the same. Cobalt and manganese L-edge spectra show increased peak intensities at 778 eV, 639 eV and 641eV, which is associated with higher surface concentrations of Co^{2+}, Mn^{2+} and Mn^{3+}, respectively. However, the extent of surface reduction in NMC/R is much smaller than in NMC after cycling. It appears that the rate of formation of the reconstruction layer and associated processes (for example, dissolution, surface film formation) during cycling is strongly dependent on the initial state of the surface.

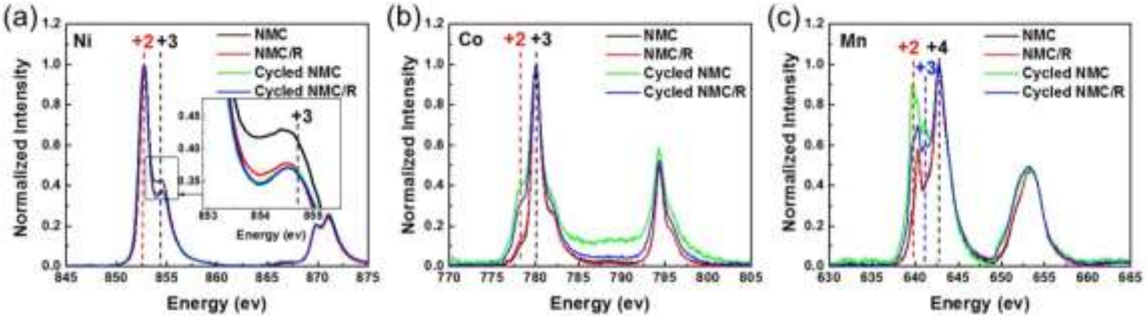

Figure 45. (a) X-ray absorption spectroscopy total electron yield of cycled NMC and NMC/R electrodes on the range L-edge of (a) nickel, (b) cobalt, and (c) manganese.

Task 5.3 – Advanced *In Situ* Diagnostic Techniques for Battery Materials (Xiao-Qing Yang and Seongmin Bak, Brookhaven National Laboratory)

Project Objective. The primary project objective is to develop new advanced *in situ* material characterization techniques and to apply these techniques to support development of new cathode and anode materials for the next generation of Li-ion batteries for PHEVs. To meet the challenges of powering the PHEV, Li-ion batteries with high energy and power density, low cost, good abuse tolerance, and long calendar and cycle life must be developed.

Project Impact. The VTO Multi-Year Program Plan describes the goals for battery: "Specifically, lower-cost, abuse-tolerant batteries with higher energy density, higher power, better low-temperature operation, and longer lifetimes are needed for the development of the next-generation of HEVs, PHEVs, and EVs." The knowledge gained from diagnostic studies through this project will help U.S. industries develop new materials and processes for new generation Li-ion batteries in the effort to reach these VTO goals.

Approach. This project will use the combined synchrotron-based *in situ* X-ray techniques (XRD, and hard and soft XAS) with other imaging and spectroscopic tools such as HRTEM and MS to study the mechanisms governing the performance of electrode materials.

Out-Year Goals. Complete the first-stage development of diagnostic technique to study effects of micro-structural defects on performance fading of high-energy-density LMR cathode materials for Li-ion batteries using pair distribution function (PDF), XRD, and XAS combined with STEM imaging and TXM. Apply these techniques to study the structural changes of various new cathode materials.

Collaborations. The BNL team will work closely with material synthesis groups at ANL (Drs. Thackeray and Amine) for the high-energy composite; and at PNNL for the Si-based anode materials. The project will also collaborate with industrial partners at GM and Johnson Controls, as well as with international collaborators.

Milestones

1. Complete the structure studies of $Li_2Ru_{0.5}Mn_{0.5}O_3$, as a model compound for Li- and Mn- rich (LMR) high-energy-density cathode materials using PDF to correlate the voltage and capacity fading with micro-structural defects in this type of material. (Q1 – Complete)
2. Complete the structure studies $Li_2Ru_{0.5}Mn_{0.5}O_3$, as a model compound for LMR high-energy-density cathode materials using STEM to correlate the voltage and capacity fading with micro-structural defects in this type of material. (Q2 – Complete)
3. Complete the XRD and XAS studies of $Li_2Ru_{0.5}Mn_{0.5}O_3$ cathode material samples with different cycle history (charge and discharge limit and cycle numbers). (Q3 – In progress)
4. Complete the structure studies of $Li_{1.2}Ni_{0.15}Co_{0.1}Mn_{0.55}O_2$ for LMR high-energy-density cathode materials using STEM to correlate the voltage and capacity fading with micro-structural defects in this type of material. (Q4 – In progress)

Progress Report

The milestones for this quarter have been completed. BNL has been focused on structure studies of $Li_2Ru_{0.5}Mn_{0.5}O_3$, as a model compound for Li- and Mn- rich (LMR) high-energy-density cathode materials using STEM to correlate the voltage and capacity fading with micro-structural defects in this type of material. Microstructure changes and nano-sized microstructural defects created by prelithiation process can be directly observed by comparing the Z-contrast annular dark-field STEM (ADF-STEM) images taken on pristine and prelithiated samples. Figure 46a (left panel) shows the atomic-resolution ADF-STEM image of the pristine material, indicating good crystallinity with typical features of the layered structure. After prelithiation, the material (right panel, Figure 46a) shows great loss of the crystallinity, forming domains that orient differently from each other with a large amount of additional grain boundaries created. It can be seen that these domains are at the scale of several nanometers, confirming previous analysis of XRD and PDF results. The process is illustrated in Figure 46b.

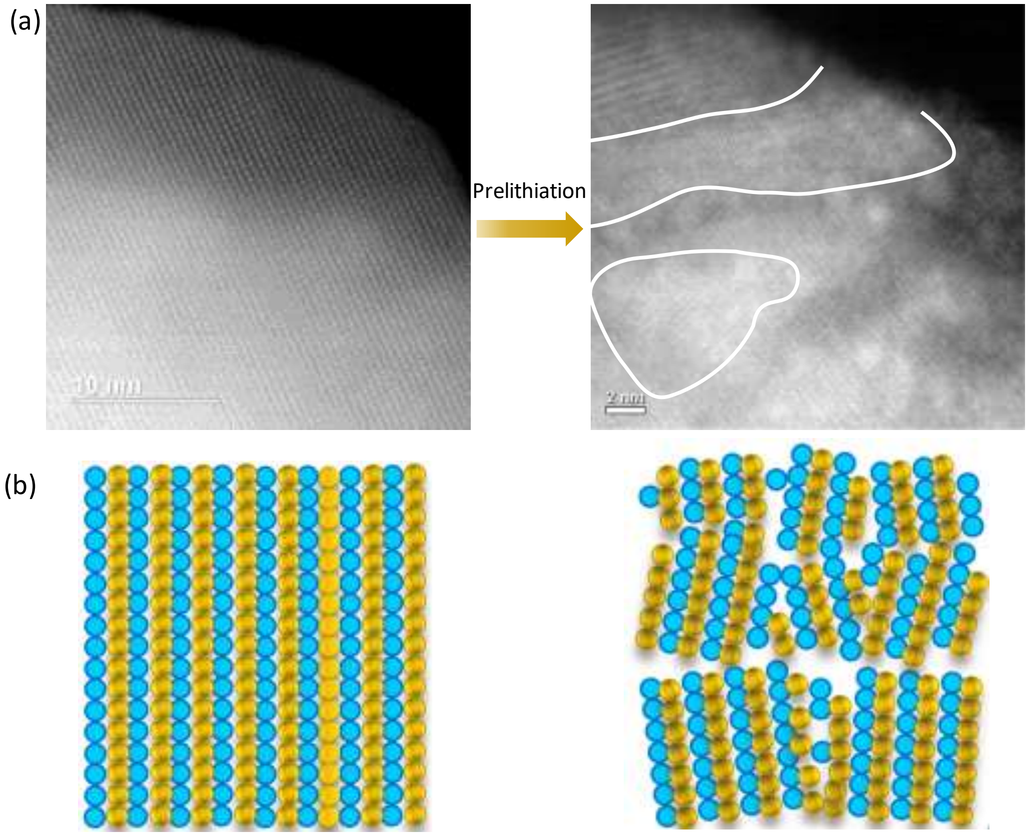

Figure 46. (a) Z-contrast scanning transmission electron microscopic images of pristine sample and "OCV—1V—3V" sample. In the "OCV—1V—3V" sample, a few selected domains are circled out by the white lines. (b) Illustration of the microstructure changes caused by prelithiation process.

Patents/Publications/Presentations

Publication

- Kim, Ji-Young, and Sang Hoon Kim, Dong Hyun Kim, Dieky Susanto, Se Young Kim, Won-Young Chang, Byung Won Cho, Won-Sub Yoon, Seong Min Bak, Xiao Qing Yang, Kyung Wan Nam*, and Kyung Yoon Chung.* "Electronic Structural Studies on the Improved Thermal Stability of $Li(Ni_{0.8}Co_{0.15}Al_{0.05})O_2$ by ZrO_2 Coating for Lithium Ion Batteries." *Appl Electrochem* (2017). First online: March 21, 2017; doi:10.1007/s10800-017-1062-5.

Task 5.4 – Nuclear Magnetic Resonance and Magnetic Resonance Imaging Studies of Solid Electrolyte Interphase, Dendrites, and Electrode Structure
(Clare Grey, University of Cambridge)

Project Objective. The growth of a stable SEI on most electrode materials is key to long-term capacity retention of a working Li-ion battery. On anodes such as silicon, this is particularly critical because the continual expansion and contraction of this intermetallic upon alloying with lithium exposes fresh, reactive surfaces that result in further electrolyte decomposition and SEI growth. This project will perform a detailed multinuclear NMR study of the SEI that forms on silicon, where thick SEIs typically grow and where SEI stability is a key aspect hindering commercialization of this technology. The focus will be to determine how additives (for example, FEC) and charging parameters (for example, voltage) influence the composition and stability of the SEI. Fundamental studies of SEI structure *in operando* will be complemented by a synthetic program aimed at preparing new silicon coatings based on phosphazene (P-N) elastomeric polymers to increase CE. Further, the nature of the SEI is one factor that appears to control the type of lithium microstructures that form on lithium metal during cycling. To test this hypothesis, the project will use magnetic resonance imaging (MRI) to investigate lithium dendrite versus moss formation in different electrolytes as a function of salt concentration and with different additives. Finally, it will compare lithium and sodium metal anode chemistries to determine the composition, morphology, and stability of local structures that form on sodiating anodes such as tin and hard carbons.

Project Impact. The first impact of this project will be a molecular-level understanding of how factors such as applied voltage and electrolyte additives modify the SEI that forms on silicon anodes. The insight gained from these studies will guide the design of new P-N coatings for silicon. A rationally designed surface coating has the potential to improve SEI stability, and thus increase CE for silicon and beyond. A description of how SEI composition influences lithium microstructures will provide the foundation to mitigate dendrite formation during cycling that currently limits the safety of many promising electrode materials. These approaches will be extended to study Na-ion battery electrodes to provide an understanding of how to chemically manipulate both electrodes as well as the electrolyte to avoid adverse failure mechanisms in next-generation batteries.

Out-Year Goals. The project goals are as follows: (a) determine the effect of voltage and additives (for example, FEC) on the composition of the silicon SEI; (b) synthesize and test new inorganic coatings to increase the CE seen on cycling silicon; (c) identify correlations between SEI structure and thickness and Li-metal dendrite formation; and (d) determine the local and long-range structures formed on cycling sodium anode materials and compare with lithium. To facilitate these goals, the project will prepare ^{13}C-enriched FEC for ^{13}C NMR multinuclear studies to investigate the SEI that forms on silicon during cycling. It will synthesize new P-N polymers for coating silicon nanoparticles and probe changes in performance in the presence of these coatings. In addition, the project will use MRI to correlate lithium dendrite formation with the nature of the SEI. Finally, it will apply the methods developed to study lithium chemistries to investigate sodium electrodes.

Collaborations. This project collaborates with B. Lucht (University of Rhode Island); J. Cabana, (University of Illinois – Chicago); Y. Shirley Meng (UCSD), S. Whittingham (SUNY – Binghamton); P. Bruce (St. Andrews); S. Hoffman and A. Morris (Cambridge); and P. Shearing (University College London).

Milestones

1. Synthesis of ^{13}C FEC. (Q1 – Complete)
2. Preparation of P-N coatings on silicon; Develop *in situ* ^{19}F NMR studies of FEC. (Q2 – In progress)
3. Multinuclear NMR studies of SEI coatings on silicon with FEC. (Q3 – In progress)
4. Testing of P-N coatings; MRI/dendrite studies of two ionic liquids. (Q4 – In progress)

Progress Report

In situ ^{23}Na NMR studies have been performed on the sodium dendrites that form on Na-metal anodes to complement previous work on lithium microstructural growth in the group.[1,2,3] Quantification of the ^{23}Na NMR signal during electrochemical cycling indicates that Na-metal deposits with a morphology associated with an extremely high surface area (Figure 47), and that the deposits continuously accumulate, even in the case of galvanostatic cycling at low currents (for example, 0.5 mA cm^{-2}, Figure 48b orange).

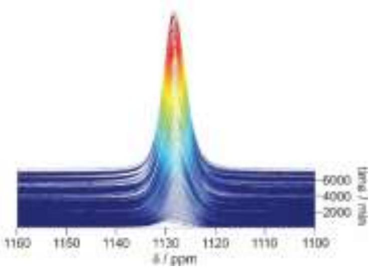

Figure 47. ^{23}Na NMR spectra as a function of time during galvanostatic cycling at 2 mA cm^{-2}, showing high surface area Na-metal deposits growing in.

Two distinct regimes for electrochemical cycling of sodium metal are observed that have implications for application of sodium anodes. At low currents (0.5 mA cm^{-2}), sodium deposits are partially removed upon reversing the current (Figure 48, orange), while at higher currents (1 and 2 mA cm^{-2}) there is essentially no removal of the deposits in the initial stages (Figure 48, blue and black, respectively). At longer times, high currents show a significantly greater accumulation of deposits during cycling, again indicating a much lower efficiency of removal of these structures when the current is reversed. Analysis of current–time transients performed in a separate experiment were interpreted in terms of a change in the mechanism of nucleation from a progressive (time dependent) nucleation mechanism at the overpotentials observed for the lower current density of 0.5 mA cm^{-2} to instantaneous at higher currents. For instance, the fraction of high surface area Na-metal deposits measured with NMR compared to the accumulated mass calculated from Faraday's law revealed that at low currents, smooth deposition and stripping occurs, while at high currents, rough deposition and less efficient removal is present (Figure 49). It is proposed that the different and fewer microstructures formed at lower currents are more readily removed on cycling.

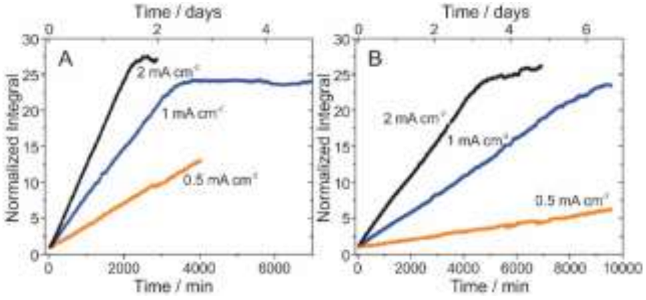

Figure 48. Integral of the normalized ^{23}Na metal resonance for (a) continuous galvanostatic deposition and (b) galvanostatic cycling at three different current densities.

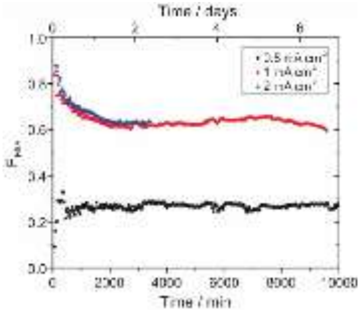

Figure 49. Fraction of high surface area (FHSA) sodium during galvanostatic cycling at various current densities. A ratio of 1 indicates completely rough deposition, and 0 indicates smooth deposition.

Unfortunately, despite differences in the nucleation and growth processes, both mechanisms yield microstructures that continue to grow as cycling progresses. Overall, dendrite formation appears to be more severe for Na-metal anodes in comparison to Li-metal anodes, with significant dendrite/microstructure formation occurring at low current densities, as probed by *in situ* ^{23}Na NMR experiments. However, the microstructures that form at low currents can be partially removed on reversing the current, which is not the case for the dendrites formed at higher currents. Differences in the mechanisms of nucleation of dendrites may account for some of these differences. Further investigation into the role of SEI in both sodium and lithium dendrite formation will be key to elucidating the physical origin underpinning the differences observed between these two systems.

[1] Chandrashekar, S., and N. M. Trease, H. J. Chang, L.-S. Du, C. P. Grey, and A. Jerschow. *Nat. Mater.* 11 (2012): 311.

[2] Chang, H. J., and A. J. Ilott, N. M. Trease, M. Mohammadi, A. Jerschow, and C. P. Grey. *J. Am. Chem. Soc.* 137 (2015): 15209.

[3] Ilott, A. J., and M. Mohammadi, H. J. Chang, C. P. Grey, and A. Jerschow. *Proc. Natl. Acad. Sci. USA* 113 (2016): 10779.

Patents/Publications/Presentations

Publications

- Clément, R. J., and J. Xu, D. S. Middlemiss, J. Alvarado, C. Ma, Y. S. Meng, and C. P. Grey. "Direct Evidence for High Na^+ Mobility and High Voltage Structural Processes in P2-$Na_x[Li_yNi_zMn_{1-y-z}]O_2$ (x,y,z ≤ 1) Cathodes from Solid-State NMR and DFT Calculations." *J. Mater. Chem. A* 5 (2017): 4129.
- Dally, R., and R. J. Clément, R. Chisnell, S. Taylor, M. Butala, V. Doan-Nguyen, M. Balasubramanian, J. W. Lynn, C. P. Grey, and S. D. Wilson. "Floating Zone Growth of α-$Na_{0.90}MnO_2$ Single Crystals." *J. Cryst. Growth* 459 (2017): 203.
- Ma, C., and J. Alvarado, J. Xu, R. J. Clément, M. Kodur, W. Tong, C. P. Grey, and Y. S. Meng. "Exploring Oxygen Activity in the High Energy P2-type $Na_{0.78}Ni_{0.23}Mn_{0.69}O_2$ Cathode Material for Na-ion Batteries." *J. Am. Chem. Soc.* 139 (2017): 4835.

Presentations

- Joint seminar, Chemistry and Physics Departments, St Andrews (February 2017).
- International Workshop on Advanced Materials: IWAM-2017, Ras al Khaimah (February 2017).
- IBA, Nara, Japan (March 2017).
- 58th Experimental NMR Conference, Monterey, California (March 2017).
- ACS, San Francisco, California (April 2017): Talks in the Presidential and Synthesis & Characterization of Materials for Energy Applications Symposia, and the 2016 E.V. Murphree Award in Industrial & Engineering Chemistry Symposium in honor of Michael M. Thackeray.
- Applied Materials, Palo Alto, California (April 2017).

Task 5.5 – Optimization of Ion Transport in High-Energy Composite Cathodes (Shirley Meng, University of California – San Diego)

Project Objective. This project aims to probe and control the atomic-level kinetic processes that govern the performance limitations (rate capability and voltage stability) in a class of high-energy composite electrodes. A systematic study with a powerful suite of analytical tools [including atomic resolution STEM (a-STEM) and EELS, neutron, XPS and first principles (FP) computation] will elucidate approaches to optimize ion transport. Ultimately, this will hone in on the optimum bulk compositions and surface characteristics to improve the mechanistic rate and cycling performance of high-energy composite electrodes. Moreover, it aims to develop the large-scale synthesis efforts to produce materials with consistent performance. The surface-sensitive characterization tools will be extended to diagnose various silicon anode types.

Project Impact. If successful, this research will provide a major breakthrough in commercial applications of the class of high-energy-density cathode material for Li-ion batteries. Additionally, it will provide in-depth understanding of the role of surface modifications and bulk substitution in the high-voltage composite materials. The diagnostic tools developed here can also be leveraged to study a wide variety of cathode and anode materials for rechargeable batteries.

Approach. This unique approach combines STEM/EELS, XPS, and *ab initio* computation as diagnostic tools for surface and interface characterization. This allows for rapid identification of surface interphases that provide surface instability or stability in various types of electrode materials including both high-voltage cathodes and low-voltage anodes. Neutron enables the characterization of bulk material properties to enhance and further optimize high-energy electrode materials.

Out-Year Goals. The goal is to control and optimize Li-ion transport, TM migration, and oxygen activity in the high-energy composite cathodes and to optimize electrode/electrolyte interface in silicon anodes so that their power performance and cycle life can be significantly improved.

Collaborations. This work funds collaborations on EELS (Miaofang Chi, ORNL); molecular layer deposition (MLD, Chunmei Ban, NREL); neutron diffraction (Ken An, ORNL); soft XAS (Marca Doeff, LBNL); and XPS, TOF-SIMS characterization (Keith Stevenson, UT Austin). It supports collaborative work with Zhaoping Liu and Yonggao Xia at Ningbo Institute of Materials Technology and Engineering in China.

Milestones

1. Quantify structural change and its correlation with oxygen activities in Li-rich layered oxide during electrochemical cycling. (Q2 – In progress)
2. Investigate on structural reversibility based on the proposed anionic activities in Li-rich layered cathode to stabilize the operating voltage. (Q2 – In progress)
3. Study the effects of PAA and CMC (cycled in ionic liquid) on the morphological and compositional changes of SEI after various cycle numbers using STEM – energy dispersive X-ray spectroscopy (STEM-EDS) and XPS. (Q2 – In progress)

Progress Report

Identifying the Strain Formation and Its Correlation with Oxygen Activity in Li-Rich Layered Oxides

It has been confirmed previously that anionic activity is involved in the electrochemistry of Li-rich layered oxides besides the cationic redox process, by which extra capacity is obtained. Lithium ion removal together with oxygen loss from the lattice facilitates cation migration and structural rearrangement, which can finally lead to a considerable amount of strain formation in the bulk. To quantify the microstrain development during electrochemical cycling in Li-rich layered oxides, *operando* synchrotron X-ray diffraction (SXRD) patterns were collected at the APS at ANL. The wavelength of the X-ray source was 0.11165 Å. Williamson−Hall analysis of all peaks in SXRD patterns was carried out for a better quantification of microstrain changes during initial cycling process. The instrumental broadening was corrected based on the standard sample CeO_2. As shown in Figure 50, the strain in the material gradually increases within the slope region during the charging process mainly due to removal of lithium from the lithium layer, causing a concentration gradient in the structure. The increase is more rapid after the beginning of the plateau region, indicating large non-uniformity when lithium ions in the TM layer are removed simultaneously with oxygen oxidation. As the discharge step begins, the strain keeps stable first, then decreases to a value matching that observed from the pristine state. During the discharging step, the material has a clear strain and stress relief mechanism via lithium re-entering the structure and reversible oxygen activity. The results presented underline the flexibility of the structure of Li-rich layered oxides: a material able to undergo large structural variations without significant negative impacts on the electrochemical performance. The link between microstrain formation and oxygen activity holds promise for advanced control of oxygen activity and enabling reversible structure transformation by defect engineering.

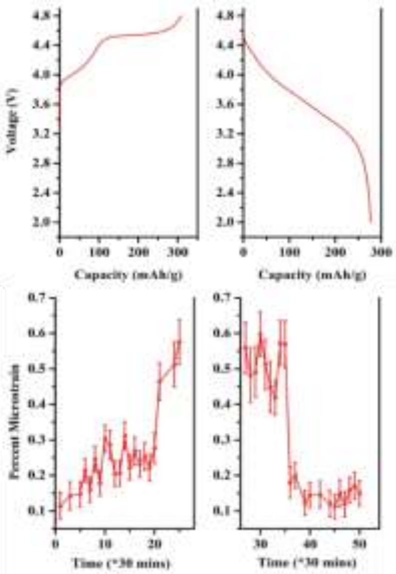

Figure 50. Initial electrochemical profile with corresponding microstrain analysis for $Li[Li_{0.144}Ni_{0.136}Co_{0.136}Mn_{0.544}]O_2$. The battery was cycled at a current density of 25 mA/g.

Investigating the Effect of Polymer Binders and Coating on High Loading Silicon Anode Electrochemistry

Polymer binders can have a direct impact on the silicon electrochemical performance. Here, the effect of different binders on silicon nanoparticles cycled in ionic liquid (LiFSI /EMIFSI) is studied, as ionic liquid provides the highest rate capability compared to the carbonate-based electrolyte. Interestingly, PAA provides higher cycling performance compared to CMC, suggesting that FSI-based IL electrolyte with PAA binder could be considered as an alternative electrolyte and a binder for silicon anodes. The ADF-STEM image of the Si-PAA after 5 cycles and their corresponding EDS mappings are shown in Figure 51. It is revealed that the SEI is located at the edge of the electrodes. The ADF-STEM images of both systems did not show significant changes upon cycling.

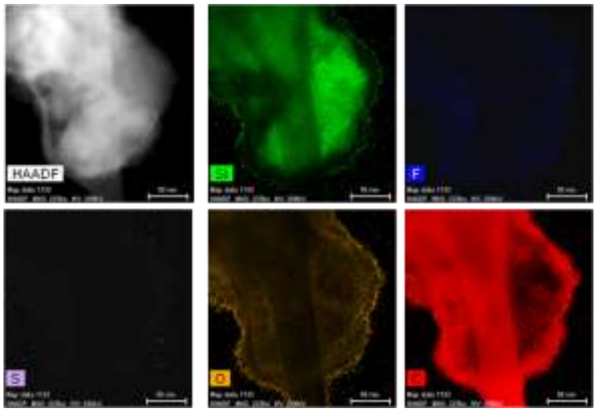

Figure 51. High-angle annular dark field – scanning transmission electron microscopy image, and the corresponding energy-dispersive X-ray spectroscopy maps of silicon, fluorine, silicon, oxygen, and carbon.

Patents/Publications/Presentations

Publications

- Qiu, B., and M. Zhang, Y. Xia, Z. Liu, and Y. S. Meng. “Understanding and Controlling Anionic Electrochemical Activity in High-Capacity Oxides for Next Generation Li-Ion Batteries.” *Chemistry of Materials* 29 (2017): 908.
- Shobukawa, H., and J. Alvarado, Y. Yang, and Y. S. Meng. “Electrochemical Performance and Interfacial Investigation on Si Composite Anode for Lithium Ion Batteries in Full Cell.” *Journal of Power Sources* (2017). Accepted.

Presentation

- Electric Vehicle and Battery Technology Information Exchange, Zhuhai, China (April 2017): “Characterization and Optimization of SEI Composition and Morphology in High Si Loading Anode”; Y. S. Meng. Invited.

Task 5.6 – *In Situ* Diagnostics of Coupled Electrochemical-Mechanical Properties of Solid Electrolyte Interphases on Lithium Metal Rechargeable Batteries

(Xingcheng Xiao, General Motors; Brian W. Sheldon, Brown University; Yue Qi, Michigan State University; and Y. T. Cheng, University of Kentucky)

Project Objective. The project objective is to develop a comprehensive set of *in situ* diagnostic techniques combined with atomic/continuum modeling schemes to investigate and understand the coupled mechanical/chemical degradation of the SEI layer/lithium system during lithium cycling. The goal of this understanding is to develop a new coating design strategy to achieve high cycle efficiency/dendrite free and extend the cycle life of high-energy-density batteries with lithium as the anode for EV application.

Project Impact. The fundamental understanding of the coupled mechanical/chemical degradation of the SEI layer during lithium cycling will enable the project to identify the desirable mechanical properties on SEI/lithium as a system and the specific transport properties that enable the homogenous lithium stripping/plating while avoiding the mossy structure. Furthermore, it will allow the project to develop a highly impactful strategy to protect lithium metal and achieve dendrite-free high cycle efficiency, which can dramatically increase the energy density of lithium batteries for EV applications.

Approach. Different *in situ* techniques, including AFM, nanoindentor, dilatometer, and stress-sensor, will be developed to investigate the mechanical compatibility between SEI and soft lithium and the relationship between surface morphology and current density distribution that results in an inhomogeneous lithium plating/stripping process. Multiple strategies will be developed to tailor the mechanical and transport properties of SEI and to properly engineer the protective coating/lithium interface.

Out-Year Goals. The project will first develop a lithium film model-system with well-controlled thickness, roughness, and textures for different *in situ* diagnostic tools and cycle performance tests. Then, a comprehensive set of *in situ* diagnostic tools will be adapted from the previous work to characterize the mechanical behavior of both SEI and lithium electrodes. In parallel, the advanced electrochemical characterization and postmortem analysis will be used to characterize the electrochemical performance, composition, and microstructure of the SEI and lithium.

Collaborations. Prof. Huajian Gao (Brown University) and Dr. Peng Lu (GM) will be the key researchers involved in continuum simulation and postmortem analysis. Dr. Chongmin Wang (PNNL), Dr. Wangli Yang (LBNL), and Dr. Jie Xiao will be collaborators on advanced *in situ* analysis and electrolyte additives.

Milestones

1. Lithium film electrodes with controlled thickness and roughness developed. (Q1 – Complete)
2. Composition map of representative SEI as a function of current density and capacity established. (Q2 – In progress)
3. The results from different tools correlated with SEI microstructure, transport properties, and cycle performance. (June 2017)
4. *Go/No-Go*: Decision based on information obtained from *in situ* and *ex situ* experiments demonstrated to be complementary and coherent. (September 2017)

Progress Report

Develop *In Situ* Nanoindentation Technique to Investigate the Mechanical Properties of Lithium Metal

Mechanical properties of porous lithium produced by lithium electroplating have been investigated using the nanoindentation system in a glovebox. Without the electrolyte, the indentation depth of porous electroplated lithium is about half of that of the bulk lithium under identical nanoindentation condition (shown in Figure 52). Likewise, the creep depth of porous electroplated lithium is only about 10% of that in the bulk lithium. The porous electroplated lithium is thus stiffer than bulk lithium under the dry condition. These are unexpected results considering the porosity present in the electroplated lithium.

Nanoindentation measurements of bulk and porous electroplated lithium in the electrolyte environment will be conducted in the next phase of the project using the specially designed *in situ* cell for nanoindentation to help understand the differences in mechanical behavior of bulk and porous electroplated lithium metals.

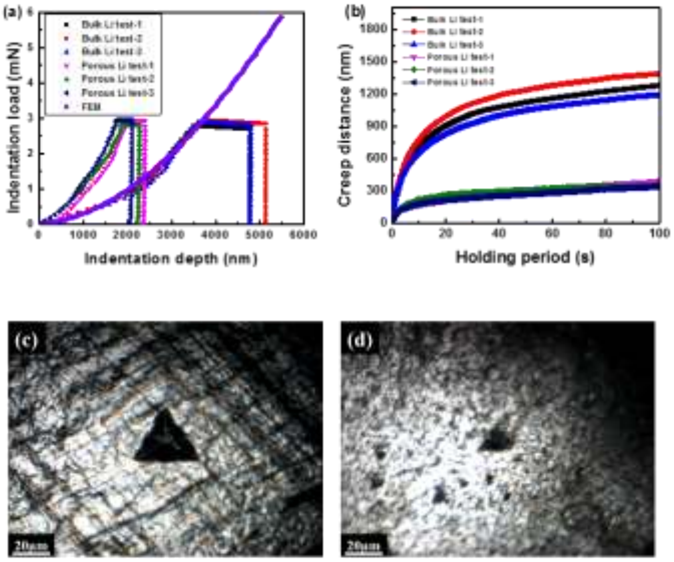

Figure 52. (a) Nanoindentation load-displacement curves of bulk lithium and porous electroplated lithium under dry condition. (b) The creep depth-time profile; and the image of the indent of (c) bulk lithium and (d) porous electroplated lithium.

Interfacial Integration between SEI and Li Metal- Void Nucleation at the Li|Li_2CO_3 Interface. Using density-functional tight-binding (DFTB) method, a Li(001)| Li_2CO_3(001)|EC slab model was constructed. The reduced state is represented by a perfect Li-metal slab, covered by 4 layers of Li_2CO_3 with 32 EC liquid molecules. The optimized Li| Li_2CO_3 interface undergoes obvious atomic relaxation. Oxidized states were obtained by removing Li^+ ions from Li-metal slab one by one and dissolving them into the EC electrolyte, while the electrons and vacancies were left on the lithium metal. Various locations of the vacancies were tested, such as one vacancy at the surface versus at the bulk and two or three vacancies that are far away or next to each other. The minimized energy for the structure with one vacancy at the Li-metal surface is 0.3eV lower than that inside the bulk, suggesting Li^+ will be stripped from the surface first. The second Li^+ may be removed around (case 1) or far away from (case 2) the first lithium vacancy (Figure 53b). The minimized energy for the structures with two vacancies next to each other is 0.58eV, lower than that far away, indicating the second Li^+ will be stripped

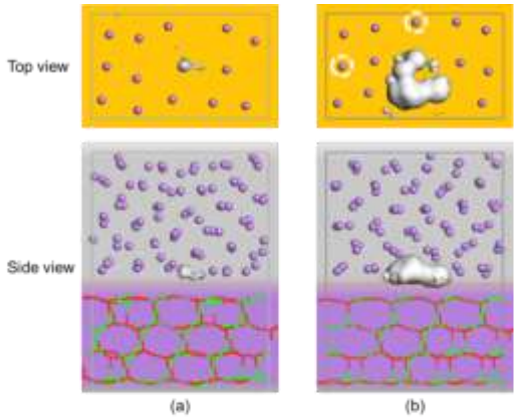

Figure 53. The minimized Li|Li_2CO_3 interface structure after (a) 1 Li^+ and (b) 3 Li^+ ions were stripped. The white volume indicates the location of the void.

next to the first lithium vacancy. Similarly, the minimized energy also shows three vacancies agglomerate on the Li-metal surface is the most stable structure. Therefore, lithium ions will be stripped from the surface non-uniformly and prefer to form a void at the Li-metal and Li_2CO_3 interface. Considering the work of adhesion of Li(001)|Li_2CO_3(001) and Li(110)|Li_2CO_3(001) interfaces is only 0.167 J/m^2 and 0.124 J/m^2, respectively. Interface delamination is expected without any compression stress.

A Preliminary Theoretical Model of SEI Wrinkling on Lithium Metal. In coordination with the multi-beam optical stress sensor (MOSS) measurements of stress evolution in Li-metal electrodes conducted by experimental colleagues, the project is developing a tentative theoretical model of wrinkling of SEI on lithium metal induced by lithium deposition. The mechanical and electrochemical responses have been integrated by combining a stress analysis of the wrinkled SEI and the kinetic model developed by Monroe and Newman. Since lithium diffusion in SEI is several orders of magnitudes faster than the interfacial reactions of lithium ions, the process of lithium plating is controlled by the current density normal to the SEI/Li interface. The model predicts that the normal current density at the wrinkle peak (i_{peak}) is less than that at the valley (i_{valley}) if there exists an initial surface perturbation, which means lithium deposition resists further SEI wrinkling. Other electrochemical processes besides SEI wrinkling could also contribute to the observed stress evolution in MOSS experiments. Further experimental evidences will enrich and improve this theoretical model.

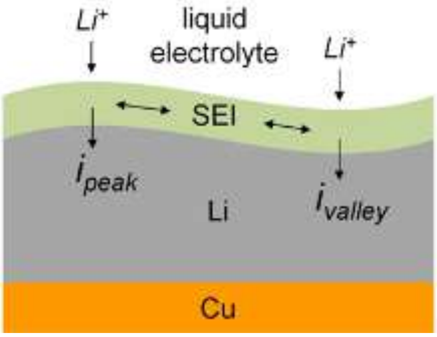

Figure 54. Schematic of a growing Li-metal electrode and a wrinkled solid electrolyte interface (SEI). i_{peak} and i_{valley} are current densities normal to the Li/SEI interface at the wrinkle peak and the valley, respectively.

Patents/Publications/Presentations

Publication

- Zhang, Q., and L. Han, J. Pan, Z. Chen, and Y. Cheng. "Chemically Stable Artificial SEI for Li-Ion Battery Electrodes." *Appl. Phys. Lett.* 110 (2017): 133901.

Presentations

- Electronic Materials and Applications 2017, American Ceramic Society, Orlando, Florida (January 20, 2017): "Stress Evolution and Degradation Mechanisms at Interfaces in Energy-Related Ceramics"; B. W. Sheldon.
- The Minerals, Metals, and Materials Society (TMS) Annual Meeting, San Diego, California (March 2, 2017): "Mechanical Degradation and Optimization of Solid Electrolyte Interphases in Li-Ion Batteries"; B. W. Sheldon.

Task 5.7 – Microscopy Investigation on the Fading Mechanism of Electrode Materials (Chongmin Wang, Pacific Northwest National Laboratory)

Project Objective. The objective will be using a combination of *ex situ*, *in situ*, and *operando* HRTEM and spectroscopy to probe the fading mechanism of layer structured cathode under high-voltage operating condition. To complement the high-resolution TEM study, *in situ* liquid cell SIMS and atom probe tomography (APT) will also be used to gain structural and chemical evolution of electrodes and correlate the structural and chemical evolution with battery performance.

Project Impact. The proposed characterization work focused on atomic level structural and chemical analysis and direct correlation with battery fading properties. The work can be directly used to guide the designing of electrode materials with tailored microstructure and chemistry for enhanced properties of increasing the energy density of Li-ion batteries and to accelerate market acceptance of EV, especially for PHEV required by the EV Everywhere Grand Challenge.

Approach. This project will use the unique *ex situ* and *in situ* TEM methods to probe the structure of Li-ion batteries, especially a biasing liquid electrochemical cell that uses a real electrolyte in a nano-battery configuration. It will also use various microscopic techniques, including *ex situ*, *in situ*, and especially the *operando* TEM system, to study the fading mechanism of electrode materials in batteries. This project will be closely integrated with other research and development efforts on high-capacity cathode and anode projects in the BMR Program to: (1) discover the origins of voltage and capacity fading in high-capacity layered cathodes, and (2) provide guidance for overcoming barriers to long cycle stability of electrode materials.

Out-Year-Goals. This project has the following out-year goals:

- Multi-scale (ranging from atomic-scale to meso-scale) *ex situ*/*in situ* and *operando* TEM investigation of failure mechanisms for energy-storage materials and devices. Atomic-level *in situ* TEM and STEM imaging to help develop fundamental understanding of electrochemical energy-storage processes and kinetics of electrodes.
- Extend the *in situ* TEM capability for energy storage technology beyond lithium ions, such as Li-S, Li-air, Li-metal, sodium ions, and multi-valence ions

Collaborations. This project collaborates with Michael M. Thackeray and Jason Croy (ANL); Guoying Chen (LBNL); Jagjit Nanda (ORNL); Chunmei Ban (NREL); Khalil Amine (ANL); Donghai Wang (Penn State), Arumugam Manthiram (UT Austin), Wei Tong (LBNL), Gao Liu (LBNL); Yi Cui (Stanford University); Jason Zhang (PNNL); Jun Liu (PNNL); Xingcheng Xiao (GM), Shirley Meng (UCSD), and Stan Whittingham (SUNY –Binghamton).

Milestones

1. Void formation mechanism and its correlation with ionic mobility in the lattice upon high-voltage cycling; exploring lattice stability with dopant such as tin, silicon, and phosphorous. (March 2017 – Complete)
2. Atomic-level identification of the behavior of nickel, manganese, cobalt, and aluminum in the NCM and NCA when cycled at high voltage; correlate with fading mechanism. (June 2017)
3. Environmental TEM (ETEM) studies of the nickel segregation characteristics, and correlation with materials processing temperature. (September 2017)

Progress Report

A key question on the Li-O_2 battery system is why the reaction product shows unique morphological features, ranging from hollow spheres to toroidal structure. This question is addressed by using an aberration-corrected *in situ* ETEM under oxygen environment. The morphology and phase evolution on the CNT cathode of a working solid-state Li-O_2 nano-battery are directly correlated with electrochemical reaction. The present *in situ* observation provides insight for understanding how the toroidal structure forms in Li-O_2 system.

The capacity, CE, rate, and cyclability of a Li-O_2 battery critically depend on the electrode reaction mechanism and the structure/morphology of the reaction product as well as their spatial and temporal evolution, which are all further complicated by the choice of different electrolyte. For the case of aprotic cell, little is known on the formation mechanism of the perplexing morphology of the reaction product. For the case of Li-O_2 battery using solid electrolyte, neither electrode reaction mechanism nor the nature of the reaction production is known.

For the present work, a solid-state nano-battery was constructed through a two-probe configuration. The CNTs/RuO_2 cathode was loaded on a Pt probe, and brought to a Li_2O covered Li-metal anode anchored on the other tungsten probe through precise nano-manipulation inside the ETEM. The oxygen gas environment around the sample was maintained at a pressure of 0.1 mbar throughout the *in situ* experiments. The electrochemical reaction is driven by external biasing, that is, a negative bias applied on the Pt end to drive the Li^+ to cross the Li_2O layer to react with oxygen, which corresponds to the oxygen reduction reaction (ORR) during the discharging of the Li-O_2 battery; a positive bias drives the Li^+ ions back to the Li_2O/Li end, leading to the decomposition of the discharged product, which is oxygen evolution reaction (OER) during the charging of the battery. Real-time visualization of the structural and phase changes of the air cathode in a working Li-O_2 battery can be directly correlated to the electrochemical reactions based on the above configuration.

It is observed that ORR on CNTs initially produces LiO_2, which subsequently evolves to Li_2O_2 and O_2 through disproportionation reaction. It is interesting to note that it is the releasing of O_2 that inflates the particles to a hollow structure with a Li_2O outer surface layer and Li_2O_2 inner-shell, demonstrating that, in general, accommodation of the released O_2 coupled with the Li^+ ion diffusion and electron transport paths across both spatial and temporal scales critically governs the morphology of the discharging/charging product in Li-O_2 system. It would be expected that the determination of Li-O_2 reaction mechanisms sets a foundation for quantitative understanding/modeling of the electrochemical processes in the Li-O_2 system, enabling rational design of both solid-state and aprotic Li-O_2 batteries.

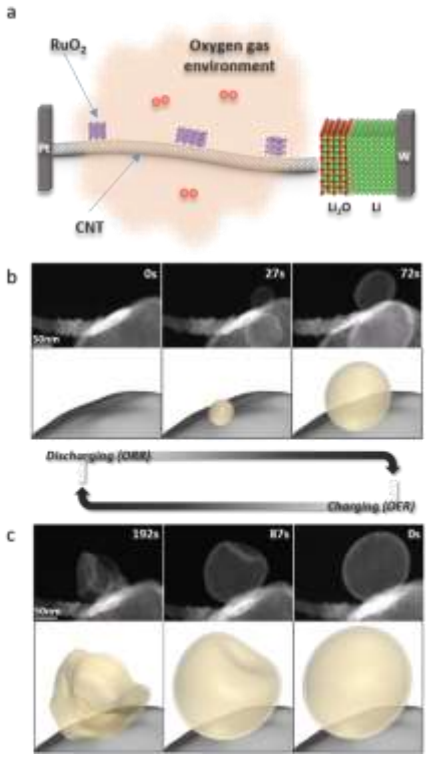

Figure 55. Experimental set up of the Li-O_2 nano-battery and the *in situ* scanning transmission electron microscopy (STEM) observation of morphological evolution of the reaction products upon discharge-charge cycling of the Li-O_2 battery. (a) Schematic drawing to illustrate configuration of the Li-O_2 nano-battery in the environmental transmission electron microscopy chamber. (b) The time-resolved high-angle annular dark field STEM images depict the morphological evolution of the discharging product (oxygen reduction reaction), which is featured by formation of hollow structure (illustrated by the bottom panel). (c) The images illustrate the morphological evolution upon charging (oxygen evolution reaction), which is featured by the collapsing of the hollow structure as illustrated by the bottom panel.

Patents/Publications/Presentations

Publications

- Yan, Pengfei, and Jianming Zheng, Meng Gu, Jie Xiao, Ji-Guang Zhang, and Chongmin Wang. "Intragranular Cracking as a Critical Barrier for High-Voltage Usage of Layer-Structured Cathode for Lithium-Ion Batteries." *Nat. Commun.* 8 (2017): 14101. doi: 10.1038/ncomms14101.
- Lu, Xiaotang, and Yang He, Scott X. Mao, Chong-min Wang, and Brian A. Korgel. "Size Dependent Pore Formation in Germanium Nanowires Undergoing Reversible Delithiation Observed by *In Situ* TEM." *J. Phys. Chem. C* 120 (2016): 28825–28831.

Presentation

- 41st International Conference and Expo on Advanced Ceramics and Composites (ICACC), Daytona Beach, Florida (January 22 – 27, 2017): Symposium 6: Advanced Materials and Technologies for Direct Thermal Energy Conversion and Rechargeable Energy Storage; Chongmin Wang. Invited.

Task 5.8 – Characterization and Computational Modeling of Structurally Integrated Electrodes (Michael M. Thackeray and Jason R. Croy, Argonne National Laboratory)

Project Objective. The primary project objective is to explore the fundamental, atomic-scale processes that are most relevant to the challenges of next-generation, energy-storage technologies, in particular, high-capacity, structurally integrated electrode materials. A deeper understanding of these materials relies on novel and challenging experiments that are only possible through unique facilities and resources. The goal is to capitalize on a broad range of facilities to advance the field through cutting-edge science, collaborations, and multi-disciplinary efforts to characterize and model structurally integrated electrode systems, notably those with both layered and spinel character.

Project Impact. This project capitalizes on and exploits DOE user facilities and other accessible national and international facilities (including skilled and trained personnel) to produce knowledge to advance Li-ion battery materials. Specifically, furthering the understanding of structure-electrochemical property relationships and degradation mechanisms will contribute significantly to meeting the near- to long-term goals of PHEV and EV battery technologies.

Approach. A wide array of characterization techniques including X-ray and neutron diffraction, X-ray absorption, emission and scattering, HRTEM, Raman spectroscopy, and theory will be brought together to focus on challenging experimental problems. Combined, these resources promise an unparalleled look into the structural, electrochemical, and chemical mechanisms at play in novel, complex electrode/electrolyte systems being explored at ANL.

Out-Year Goals. The out-year goals are as follows:

- Gain new, fundamental insights into complex structures and degradation mechanisms of high-capacity composite cathode materials from novel, probing experiments carried out at user facilities and beyond.
- Investigate structure-property relationships that will provide insight into the design of improved cathode materials.
- Use knowledge and understanding gained from this project to develop and scale up advanced cathode materials in practical Li-ion prototype cells.

Collaborators. This project collaborates with the following: J. R. Croy, A. Gutierrez, R. Benedek, and F. Dogan (CSE, ANL); M. Balasubramanian and Y. Ren (APS, ANL); Ashfia Huq (SNS); V. Dravid, C. Wolverton, and Soo Kim (Northwestern University); Chongmin Wang (PNNL); and Rose Ruther, and Harry Meyer (ORNL).

Milestones

1. Characterize bulk and surface properties of structurally integrated electrode materials using the DOE User Facilities at ANL, including the APS, Electron Microscopy Center, and Argonne Leadership Computing Facility (ALCF), along with facilities elsewhere (for example, SNS), The EMSL at PNNL, and the Northwestern University's Atomic and Nanoscale Characterization Experimental Center (NU*ANCE*). (September 2017 – In progress; see text)
2. Use complementary theoretical approaches to further the understanding of structural and electrochemical properties of LS electrodes and protective surface layers. (September 2017 – In progress)
3. Analysis, interpretation, and dissemination of collected data for publication and presentation. (September 2017 – In progress)

Progress Report

Previous reports on the integration of a spinel component into lithium- and manganese-rich oxides to produce y[xLi_2MnO_3•(1-x)$LiMO_2$]•(1-y)LiM_2O_4 (M=Mn,Ni,Co), LLS, composite structures have proven promising. Specifically, high first-cycle efficiency, good rate capability, and stable capacities at practical voltages (for example, ~210 mAh/g at ~4.4V versus graphite) can be achieved. However, the surfaces of LLS cathode particles are prone to instabilities similar to other lithiated oxide materials including oxygen evolution and TM dissolution. Many strategies have been proposed for protection of particle surfaces, but no consensus exists as to the efficacy of any given strategy. The difficulty, in part, in identifying specific trends in the literature is strong dependence of surface modifications on properties of the underlying cathode particles. For example, composition, morhphology, porosity, and the conditions of synthesis under which surface modifications are carried out can all play a role. Herein, the project revisits the effects of Al-based surface treatments for improving the surface properties of cathode materials as they apply to Li- and Mn- rich LLS particles.

Complementary studies found that treatment of LLS particles in an aqueous solution of aluminum nitrate, followed by annealing between 110-750°C, led to a decrease in performance with increasing temperature. Figure 56a shows ^{27}Al NMR spectroscopy of LLS particles after aluminum treatment, followed by annealing at 550°C (blue) and 110°C (red) along with an Al_2O_3/Al(OH) reference (green). At the lowest temperature (110°C), the aluminum coordination is clearly different than that of Al_2O_3/Al(OH), instead resembling a distorted 4-fold coordination environment. By 550°C (blue) the diamagnetic peak near ~0 ppm completey disappears. This could be due to the presence of lattice aluminum and/or three-coordinate surface/interface aluminum. Figure 56b shows XPS of the untreated LLS (black) and the Al-treated LLS powders after annealing at 110°C (red), 400°C (blue), and 550°C (green). A small surface impurity (for example, carbonate) can be seen in the untreated sample. After aluminum treatment and annealing at 110°C, a large peak forms at ~532 eV, in agreement with Al-O bonding. Upon annealing to higher temperature, this feature decreases and virtually disappears by ~550°C, consistent with the NMR data. Figure 56c shows the aluminum content (atomic %) derived from the XPS data as a function of temperature. As shown, increasing annealing temperatures led to less detectable surface aluminum. These data sets suggest that small amounts of aluminum might be doped into the bulk of LLS particles after surface treatments and high-temperature annealing, an important finding considering the decrease in performance with higher annealing temperatures. Furthermore, preliminary conclusions of this study are inconsistent with similar studies reported for Mn-rich, layered materials. This reiterates the important role of cathode composition with respect to surface modifications.

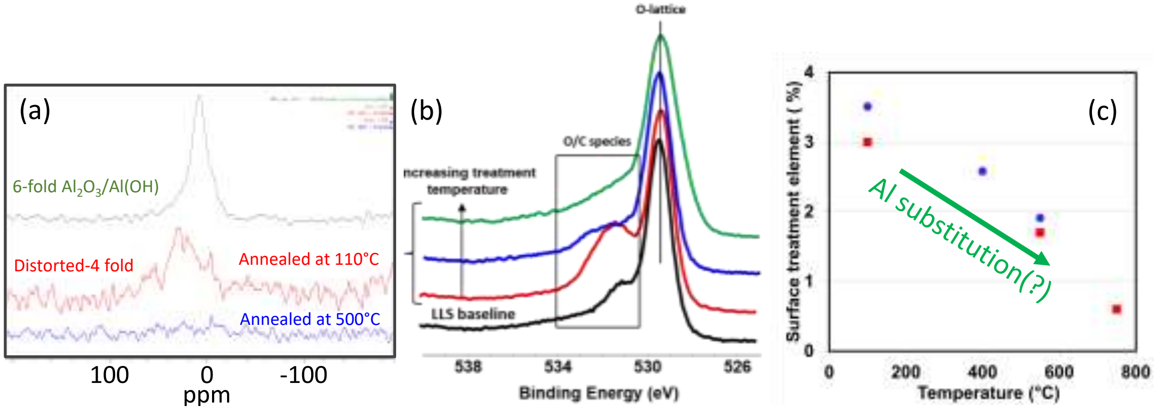

Figure 56. (a) ^{27}Al magic angle spinning nuclear magnetic resonance of Al-treated samples annealed at 110°C (red) and 550°C (blue) and an Al_2O_3/Al(OH) reference (green). (b) X-ray photoelectron spectroscopy (XPS) of layered-layered-spinel, followed by aluminum treatment and annealing at 110°C (red), 400°C (blue), and 550°C (green). (c) Aluminum content (at. %) as a function of annealing temperature, determined by XPS. Red squares represent samples previously (before aluminum treatments) exposed to air; blue circles are samples not exposed to air. Similar results were obtained with both sample sets.

Task 5.9 – Advanced Microscopy and Spectroscopy for Probing and Optimizing Electrode-Electrolyte Interphases in High-Energy Lithium Batteries (Shirley Meng, University of California – San Diego)

Project Objective. This project aims to develop advanced microscopy and spectroscopy tools to probe, understand, and optimize the anion activities that govern performance limitations such as capacity and voltage stabilities in high-energy, Li-excess TM (nickel, cobalt, manganese, etc.) oxides cathode materials. The approach uniquely combines a-STEM, EELS, *operando* Bragg coherent diffraction imaging (BCDI), and first principles computation to probe anion redox and oxygen evolutions in Li-excess NMC materials. Furthermore, the project will track the lithium and oxygen dynamics under electrochemical testing via *operando* neutron diffraction that will enhance understanding of the overall structural changes due to anion activities. Ultimately, this will hone in on the synthesis efforts to produce modified materials with optimum bulk compositions and surface characteristics at large scale for consistently good performance. The above-mentioned characterization tools will be extended to diagnose various anode types, such as Li-metal anode.

Project Impact. If successful, this research will enable *operando* imaging at the single-particle level by advanced microscopy imaging and high energy resolution O K-edge EELS. This work will provide an in-depth understanding of anion activities in high-voltage electrode materials, which can lead to significant improvement in stabilizing operation voltage and electrode-electrolyte interface for future generation high-energy-density electrodes.

Approach. This unique approach combines STEM/EELS, operando BCDI, and *ab initio* computation as diagnostic tools for probing anion redox and oxygen evolutions in Li-excess NMC materials. This allows for pinning down the atomistic/molecular mechanism of anion oxidation and determining speciation compositions and surface characteristics for enabling high rate and long life in the proposed materials. Neutron enables the characterization of bulk material properties to enhance and further optimize high-energy electrode materials.

Out-Year Goals. The goal is to probe and control oxygen activity in the high-energy composite cathodes and to characterize electrode/electrolyte interface in Li anodes so that their cycle life and efficiency can be significantly enhanced.

Collaborations. This work funds collaborations on EELS (Miaofang Chi, Oakridge National Lab); neutron diffraction (Ken An, ORNL); soft XAS (Marca Doeff, Lawrence Berkeley National Laboratory). It supports collaborative work with Zhaoping Liu and Yonggao Xia at Ningbo Institute of Materials Technology and Engineering China.

Milestones

1. Choose the Li-excess layered NMC baseline materials with various compositions; benchmark electrode performance. (Q1 – Complete)
2. XPS and DEMS characterization of cathode electrolyte interphase on Li-excess NMC. (Q2 – On track)
3. BCDI Characterization of Li-excess NMC single particle. (Q3 – On track)
4. STEM/EELS Characterization of Li-excess NMC single particle. (Q4 – On track)

Progress Report

Stabilizing Oxygen in Li-rich Layered Oxide Cathode Materials. Through the incorporation of excess lithium in the TM layer, the role of oxygen has extended beyond its essential role as a structural component in classical layered oxide cathodes, exhibiting electrochemical activity and enhancing the capacities of layered oxides through anionic redox mechanisms. Commensurate with the enhanced activity of the oxygen comes its instability in the form of oxygen loss, which is associated with irreversible voltage decay and capacity fade. To develop an understanding of this irreversible loss and to increase the stability of lattice oxygen, DFT is used to calculate oxygen vacancy formation energies, E_f, in Li-rich layered oxides for a variety of dopants, noting an increased stability upon doping of 4d elements. Motivated by these findings, representative dopants aluminum, cobalt, and titanium are doped into Li-rich NiMn, showing behavior consistent with calculations (Figure 57), and similarly other 4d elements are doped into Li-rich NiMnCo, showing notably reduced voltage decay and capacity fade. First principles calculations suggest this is due to a notable change in charge density distribution on incorporation of 4d elements, altering local band structure and stabilizing the lowest E_f site in the structure.

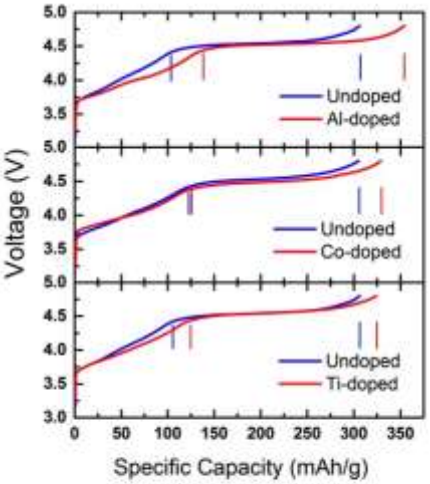

Figure 57. First cycling data for Al-, Co-, and Ti-doped NiMn.

Feasibility of Cryo-TEM to Characterize Li-metal Dendrite Formation. Basic understanding of lithium growth mechanism is important to prevent detrimental dendrites formation. Although much work has been done to explore growth of lithium dendrite by various characterizations, such as optical microscopy, SEM, and AFM. Its growth mechanism is still unclear and controversial. Furthermore, little attention is paid on the structure of plated lithium metal, especially at the atomic scale. Compared with other characterization tools, TEM provides insight related to both microstructural and chemical evolutions with a superior spatial resolution. The challenge of probing lithium metal under TEM is the low dose tolerance (high beam sensitivity) of lithium metal. It is difficult to handle lithium metal without contamination and damage. Figure 58 shows the morphology changes of the lithium metal as a function of the beam exposure time under room temperature. At room temperature, the dendritic lithium metal is quite unstable: quickly drifted, shrunk, and evaporated under TEM beam exposure. Holes are created in the lithium metal (Figure 58c). One of the promising approaches to stabilize the beam-sensitive samples is the cryo technique. This project will apply the cryo method (low-temperature) and low-dose electron microscopy and specialized camera to enable characterization of the lithium metal.

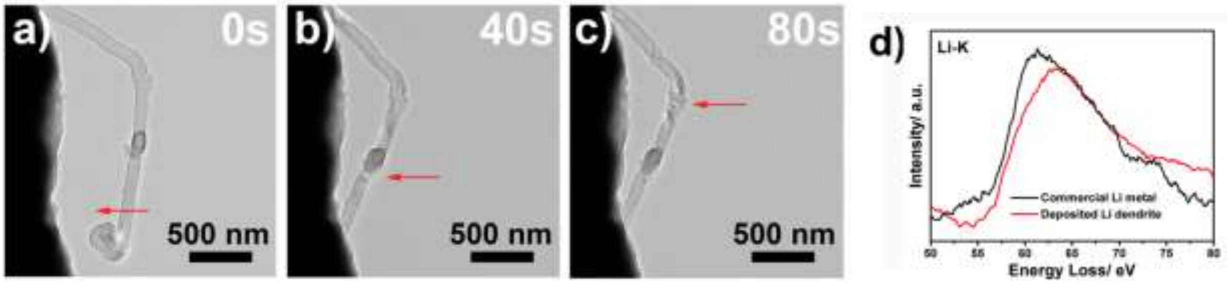

Figure 58. Morphology changes of the dendritic lithium metal as a function of the beam exposure time under room-temperature transmission electron microscopy. The electron energy loss spectroscopy spectrum of the deposited lithium dendrite is considerably different from that of commercial Li-metal foil.

TASK 6 – MODELING ADVANCED ELECTRODE MATERIALS

Summary and Highlights

Achieving the performance, life, and cost targets outlined in the EV Everywhere Grand Challenge will require moving to next generation chemistries, such as higher capacity Li-ion intercalation cathodes, silicon and other alloy-based anodes, Li-metal anode, and sulfur cathodes. However, numerous problems plague development of these systems, from material-level challenges in ensuring reversibility to electrode-level issues in accommodating volume changes, to cell-level challenges in preventing cross talk between the electrodes. In this task, a mathematical perspective is applied to these challenges to provide an understanding of the underlying phenomenon and to suggest solutions that can be implemented by the material synthesis and electrode architecture groups.

The effort spans multiple length sales from *ab initio* methods to continuum-scale techniques. Models are combined with experiments, and extensive collaborations are established with experimental groups to ensure that the predictions match reality. Efforts are also focused on obtaining the parameters needed for the models, either from lower-length scale methods or from experiments. Projects also emphasize pushing the boundaries of the modeling techniques used to ensure that the task stays at the cutting edge.

In the area of intercalation cathodes, the effort is focused on understanding the working principles of the high nickel layered materials with an aim of understanding structural changes and the associated changes in transport properties. Coatings, an effective strategy for high-voltage operation, are being explored with the aim of providing a rational design approach for new coating materials. In addition, focus is paid to the assembling of porous electrodes with particles to predict the conduction behavior and developing tools to measure electronic conduction. This quarter, the project has shown preliminary calculations that suggest that the facet has an effect on the propensity for doping. More progress is also being made in developing the electronic-conductivity tool.

In the area of silicon anodes, the effort is in trying to understand the interfacial instability and suggest ways to improve the cyclability of the system. This quarter, progress was made in understanding the connection between the silicon expansion and SEI cracking. In addition, a phase diagram was developed that shows the various failure modes for silicon.

In the area of Li-metal anodes, the focus is on understanding how materials can be designed to prevent dendrite growth at high current densities using continuum modeling approaches. The results are used to guide materials development by providing the properties needed to prevent dendrites while also achieving the energy and power goals. This quarter, models have focused on incorporating the plastic deformation of the lithium and the protection layer into the models so as to enable better predictions under real-world conditions. Models are also starting to examine the role of the SEI on the morphology of the dendrite.

Task 6.1 – Predicting and Understanding Novel Electrode Materials from First Principles (Kristin Persson, Lawrence Berkeley National Laboratory)

Project Objective. This project supports VTO programmatic goals by developing next-generation, high-energy cathode materials and enabling stable cathode operation at high voltages through target particle morphology design, functional coatings, and rational design of electrolytes. The end-of-project goals include: (1) novel disordered, high-rate Li-excess cathodes, (2) new fundamental understanding of the cathode/electrolyte interface and the factors that control the interfacial chemistry and interfacial impedance, (3) critical surface and coating design and optimization strategies that will improve cycling of Li-ion battery cathodes, and finally (4) understanding of the factors that govern stability in nonaqueous electrolytes for Li-ion and Li-S systems.

Project Impact. To enhance the performance of Li-ion systems, improvements on the cathode and the electrolyte side are needed. This project is aimed to result in an improved understanding of the atomistic mechanisms underlying the surface behavior and performance of the Li-ion cathode materials with the ultimate goal being to suggest strategies, such as coatings, surface protection, and particle morphology design. Furthermore, fundamental studies of electrolyte stability, as a function of solvent and salt concentrations, and components will be conducted.

Out-Year Goals. Stable interfaces will be determined by focusing initially on degradation mechanisms related to the release of surface oxygen at high charge. Tuning particle morphology and coating materials—both of crystalline as well as amorphous structure—will be explored using the Materials Project. For the electrolyte development, work will be aimed toward understanding the atomistic interactions underlying the performance of lithium electrolytes specifically elucidating the solvation structure (as a function of salt concentration) and its impact on the stability of different liquid constituent species.

Collaborations. This project is highly collaborative between BMR PIs G. Chen (LBNL), G. Ceder (LBNL) and V. Srinivasan (ANL). Cathode design and synthesis will be performed by Chen and Ceder, surface design by Persson, and electrolyte design and testing by Persson and Srinivasan.

Milestones

1. Provide matrix of surface candidate dopants based on literature search and practical considerations. (December 2016 – Complete)
2. Benchmark calculations of amorphous coating materials, that is, Al_2O_3/SiO_2. (March 2017 – Complete)
3. Present first screening of surface dopants. (May 2017 – In progress)
4. *Go/No-Go*: New strategies are identified. Stop this approach if facet stabilization cannot be achieved. (May 2017 – In progress)
5. Evaluate two electrolyte benchmark formulations for Li-S and Li-ion for stability and diffusion. (September 2017 – In progress)

Progress Report

The current BMR project is aimed toward the study of surface stabilization strategies of the Li-excess layered materials using first-principles calculations. The investigation is focused on the end member of the Li-excess, Mn-rich layered cathodes; for example, Li_xMnO_3 provides a useful model, 'worst-case' system. The project has previously established that Li_xMnO_3 is rendered unstable toward *surface* oxygen release for a fairly low amount of lithium removal ($x_{Li} = 1.7$). First-cycle surface oxygen release will cause cation densification and structural reconstruction of the surface region, leading to impeded ionic transport and increased impedance. Hence, surface protection strategies, such as surface dopants and coatings, are being explored.

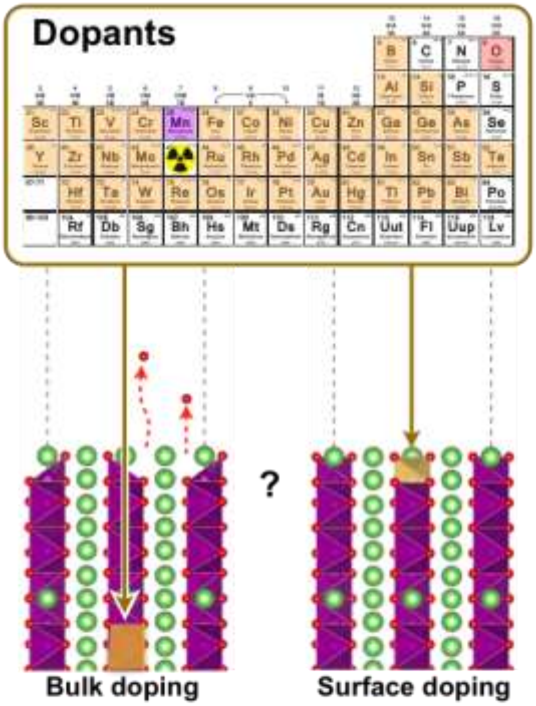

Figure 59. Illustration of the initial screening process including the range of considered elements and the preference of surface dopant occupancy to enhance oxygen retention at the surface.

As a first possible strategy, the project screens for suitable surface dopant elements, where the dopant is designed to increase surface oxygen retention. Previous work showed that the Li_xMnO_3 equilibrium particle shape exhibits five stable facets; two dominant surfaces [(001) and (010)] and three sub-dominant surfaces [(100), (110), and (111)]. To identify the best candidate surface doping elements, the project systematically investigates possible dopants on all five stable facets. Dopant candidates include TMs, post-TMs, and metalloids (yellow colored elements on the Periodic table in Figure 59). The project expects the element to be added during the synthesis process, which requires consideration of not only the oxygen retention capabilities of the dopant candidates, but also removal of elements that may preferentially occupy the bulk of the material. Hence, the project first examines the defect segregation energy defined as,

$$E_S = \Delta E^{bulk} - \Delta E^{surface}$$

where ΔE^{bulk} represents the energy difference between the doped and undoped bulk, and $\Delta E^{surface}$ shows the equivalent quantity for surface. In this way, a positive E_S indicates a dopant that preferentially occupies the surface. The calculations show that the defect preferences depend somewhat on the specific surface chemistry and morphology. For example, Zn doping in the bulk is preferred compared to doping at the (001) surface but less preferred than doping on the (110) surface. Therefore, best candidate dopants would segregate to the surface across dominant surface facets.

Task 6.2 – Addressing Heterogeneity in Electrode Fabrication Processes (Dean Wheeler and Brian Mazzeo, Brigham Young University)

Project Objective. The project goal is to better understand connections between fabrication conditions and undesired heterogeneity of thin-film electrodes by means of new nondestructive inspection techniques and computer models. Two nondestructive inspection techniques will be developed or improved to characterize electrochemical and mechanical uniformity of the electrodes. The first tool will be a flexible contact probe on a polymer substrate for rapidly measuring local electrical conductivity across electrodes of any geometry. The second tool will be a new acoustic probe that measures local elasticity and density of the composite film. These two prototyping efforts will be tied together by a particle-based microstructure model that allows prediction and correlation of electrode conductive and mechanical properties with fabrication conditions.

Project Impact. This work will result in new diagnostic and modeling tools for rapidly and conveniently interrogating how well homogeneity has been maintained in electrodes during fabrication and in subsequent cycling. Real-time measurement of heterogeneity will enable manufacturer quality control improvements. The measurement and modeling tools will further enable researchers to compare different electrodes, improve formulations and processes, and anticipate cell performance of new designs.

Out-Year Goals. This project was initiated October 2016 and concludes September 2018. Overall goals by fiscal year are as follows:

- **2017.** Fabricate first-generation flexible conductivity probe and proof-of-concept of acoustic probe; improve microstructure model to match experiment.
- **2018.** Integrate flex probe with test fixtures suitable for assessment of large or continuous samples; demonstrate measurement of localized ionic conductivity.

Collaborations. Ram Subbaraman (Bosch), Daniel Abraham (ANL), Steve Harris (LBNL), Bryant Polzin (ANL), and Karim Zaghib (HQ) have provided battery materials for analysis. Other collaborations and the transfer of this technology to interested parties are being pursued.

Milestones

1. Complete flex probe prototype and demonstrate that measurements match those for the previous rigid probe. (Q1 – Complete)
2. Integrate the flex probe with existing high-precision positioning system and make measurements on 3 different electrode materials. (Q2 – Complete**)**
3. Demonstrate that the dynamic particle packing (DPP) model can predict effective conductivities that match experiment for 3 different electrode materials. (Q3)
4. Complete prototype of localized acoustic probe and associated model. *Go/No-Go*: Determine whether to continue developing the acoustic method by assessing sensitivity to film stiffness. (Q4)

Progress Report

The second milestone of FY 2017 was to further demonstrate that the micro-flex-line probe (µFLP), which is the flexible variant of the micro-N-line probe (µNLP), can be used to make measurements of electrode-film electronic conductivity. The primary value of the flex probe is that it can be used to test much larger samples than the previous design, which will allow extension of this testing technology eventually to on-line measurement during the electrode manufacturing process.

Specifically, for this milestone, the flex probe results are to be performed for three different electrode samples while the probe is mounted on the high-precision positioning system. Table 3 shows results for three different commercial-grade electrodes provided by ANL. The first two are cathodes, while the last is an anode. At least nine spatially separated points were used to obtain the averages and confidence intervals.

Table 3: Experimental conductive property results (with 95% confidence intervals) from using µFLP on the three electrode samples.

	AC005	C015	AA002
Conductivity (mS/cm)	241±15	198±5	3962±681
Contact Resistance (Ω cm^2)	0.146±0.021	0.198±0.010	0.053±0.011

As during the previous quarter, the design and materials used to construct the µFLP were iterated and improved to increase reliability of the measurements, and further improvements in future quarters are likewise anticipated. As further validation of the results, the values in Table 3 have been compared to previous measurements using other methods (such as 4-line probe and the van der Pauw method) where available. The comparative results are consistent, though additional investigations are planned for ongoing validation.

During this and the prior quarter, additional samples were obtained from other researchers. Investigations are in progress to use the current suite of tools to assess effects of formation and cycling on changes in electronic and ionic conductivity of electrodes. Additional work will also study the effect of different mixing processes on resulting electrode conductivities. It is anticipated that these studies will provide insight into what manufacturing practices can most efficiently increase needed conductivities and increase power and accessible energy of Li-ion batteries.

Significant progress was also made on upcoming milestones. These will be described in future reports, including at the DOE Annual Merit Review meeting in June 2017.

Patents/Publications/Presentations

Publication

- Nevers, D. R., and F. R. Brushett, and D. R. Wheeler. "Engineering Radical Polymer Electrodes for Electrochemical Energy Storage." *J. Power Sources* 352 (2017): 226–244.

Task 6.3 – Understanding and Strategies for Controlled Interfacial Phenomena in Lithium-Ion Batteries and Beyond

(Perla Balbuena, Jorge Seminario, and Partha Mukherjee, Texas A&M University)

Project Objective. The project objective is to evaluate and characterize interfacial phenomena in lithiated silicon and Li-metal anodes and to develop guidelines for potential solutions leading to controlled reactivity at electrode/electrolyte interfaces of rechargeable batteries using advanced modeling techniques based on first-principles.

Project Impact. Understanding SEI growth on constantly evolving silicon surfaces and on highly reactive Li-metal surfaces is expected to define the electrolyte properties required in high performance cells. Strategies to control the silicon anode instability and pulverization issues and the well-known safety and short effective lifetimes of Li-metal anodes will be developed by tuning the electrolyte composition, structure, dynamic, and stability, as well as that of the electrode morphology and interactions with the electrolyte, on the basis of multiple characterizations of interfacial phenomena.

Approach. A comprehensive multiscale modeling approach including first-principles *ab initio* static and dynamics, classical molecular dynamics, and coarse-grained mesoscopic models will focus on the roles of the electrolyte chemical, structural, and dynamical properties and of the electrode micro- and nanostructure on the formation and evolution of the SEI layer and associated electrochemical performance on silicon and on Li-metal anodes.

Out-Year Goals. Work will progress toward characterizing lithiation and SEI formation at silicon surfaces as well as the subsequent cracking and reforming events under the most realistic modeling conditions. Similarly, the project will investigate electrolyte effects on reactivity and dendrite formation in Li-metal surfaces. The project aims to capture how the chemistry of the various components of the electrolyte (mainly liquids, but also solid polymers and gels) affects the main issues that influence the electrode performance.

Collaborations. This project funds work at Texas A&M University (TAMU). Dr. Chunmei Ban (NREL), Dr. Xiaolin Li (PNNL), and Dr. Kevin Leung (Sandia National Laboratories, SNL) may also contribute.

Milestones

- Characterize SEI nucleation and modes of cracking as functions of SEI composition on lithiated silicon nanoparticles. (Q1 – Complete)
- Identify and quantify Li-ion transport mechanisms through SEI blocks. (Q2 – In progress)
- Evaluate and quantify the relative influence of mechanical and chemical degradation interplay in silicon active particles. (Q3 – In progress)
- Characterize SEI growth as a function of SEI composition. Compare the SEI rate growth with experimental trends in the literature and from collaborators; if there is any disagreement, revise respective modeling approach. (Q4)

Progress Report

Molecular dynamics simulations of cracking phenomena were performed on ~8-nm silicon particles covered by a LiF layer of ~1.8 nm. Upon lithiation, the core expands, and it is observed that cracking in the shell starts when the alloy core expands up to 1.5 times its original volume. The stress on the SEI layer increases during the Li_xSi_y core expansion until reaching a limit in which the crack on the SEI layer takes place. The study evaluated the induced stress and subsequent cracking at different current rates.

The impact of high volumetric expansion during lithiation in silicon on the damage stochastics inside a larger 500-nm diameter particle and in the SEI film is also studied with a mesoscopic model. Figure 61 shows the lithium transport induced damage characteristics in crystalline (Figure 61a) and amorphous (Figure 61b) silicon particle covered by SEI film. It is evident that fracture in the crystalline silicon particle exhibits significantly higher fracture due to two-phase diffusion, as compared to a single-phase diffusion in amorphous silicon, which generates large mismatch in volumetric strain between the core and surface. The SEI film shows complete rupture for both scenarios due to large stress from the expanding silicon particle. Si-particle diameter below 200–300 nm is preferable, which can reduce the microcrack-induced damage inside the particle as well as in the SEI film. This suggests that an appropriate combination of the mechanical properties of the SEI film and silicon active particle may enable better strain accommodation.

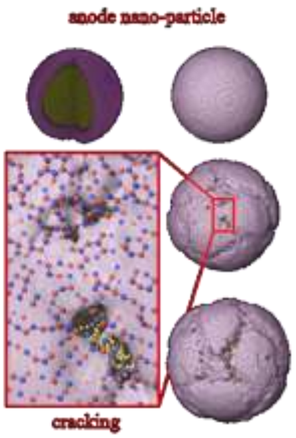

Figure 60. Molecular dynamics simulations of cracking of a silicon nanoparticle of ~4 nm radius, covered by a LiF film of ~1.8-nm thickness. Stress-induced bond breaking in the shell leads to formation of holes that then result in extended cracks.

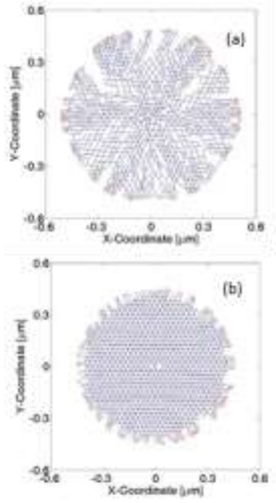

Figure 61. Effect of core structure on cracking: (a) crystalline core, and (b) amorphous core. A solid electrolyte interface film covers the particle.

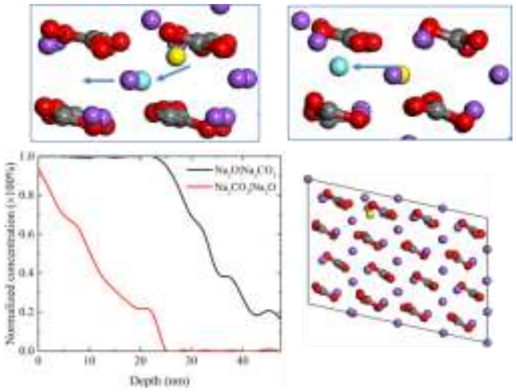

Figure 62. Diffusion of Na^+ ions through Na_2CO_3 crystals (top) via knock-off mechanism. Bottom (left) shows concentration profile through an assembly of Na_2O/Na_2CO_3 blocks from the electrolyte towards the anode (see text).

DFT calculations are used to characterize ionic diffusion through various SEI blocks. Figure 62 (top) shows a sodium ion diffusing through a Na_2CO_3 block via a knock-off mechanism where one ion pushes another one in the crystalline lattice and induces motion. The DFT calculated barriers are then fed into a mesoscale model able to evaluate ion diffusion through blocks assembled in a given configuration. Figure 62 (bottom) shows the Na^+ concentration profile in two configurations of a hetero-structured SEI film. In the Electrolyte|Na_2O|Na_2CO_3|Anode configuration, a concentration jump is observed at the defective Na_2O|Na_2CO_3 interface, which is attributed to the facilitated Na^+ diffusion in a defective Na_2O phase. On the other hand, in the Electrolyte|Na_2CO_3|Na_2O|Anode configuration, a significant concentration drop is observed at the Na_2CO_3|Na_2O interface, suggesting an interfacial resistance. It is worth noticing that the concentration at the anode interface of the Electrolyte|Na_2CO_3|Na_2O|Anode configuration is much higher. It can be inferred that the second configuration deters Na^+ diffusion through the hetero-structured SEI film.

Patents/Publications/Presentations

Publications

- Galvez-Aranda, D. E., and V. Ponce, and J. M. Seminario. ‘‘Molecular Dynamics Simulations of the First Charge of a Li-Ion—Si-Anode Nanobattery.” *J. Mol. Model.* 23 (2017): 120.
- Hankins, Kie, and Fernando A. Soto, and Perla B. Balbuena. “Insights into the Lithium Intercalation and SEI Formation on LiSi Nanoclusters.” Submitted, March 2017.
- Benitez, L., and J. M. Seminario. “Ion Diffusivity through the Solid Electrolyte Interphase in Lithium-Ion Batteries.” Submitted, March 2017.

Task 6.4 – First Principles Modeling of SEI Formation on Bare and Surface/Additive Modified Silicon Anode (Perla Balbuena, Texas A&M University)

Project Objective. This project aims to develop fundamental understanding of the molecular processes that lead to formation of an SEI layer due to electrolyte decomposition on silicon anodes, and to use such new knowledge in a rational selection of additives and/or coatings. The focus is on SEI layer formation and evolution during cycling and subsequent effects on capacity fade through two concatenated problems: (1) SEI layers formed on lithiated silicon surfaces, and (2) SEI layers formed on coated surfaces. Key issues being addressed include the dynamic evolution of the system and electron transfer through solid-liquid interfaces.

Project Impact. Finding the correspondence between electrolyte molecular properties and SEI formation mechanism, structure, and properties will allow identification of new/improved additives. Studies of SEI layer formation on modified surfaces will allow identification of effective coatings able to overcome the intrinsic deficiencies of SEI layers on bare surfaces.

Approach. Investigating the SEI layer formed on modified silicon surfaces involves the following: (1) analysis of the interfacial structure and properties of specific coating(s) deposited over the silicon anode surface, (2) characterization of the corresponding surface properties before and after lithiation, especially how such modified surfaces may interact with electrolyte systems (solvent/salt/additive), and (3) what SEI layer structure, composition, and properties may result from such interaction. This study will allow identification of effective additives and coatings able to overcome the intrinsic deficiencies of SEI layers on bare surfaces. Once the SEI layer is formed on bare or modified surfaces, it is exposed to cycling effects that influence its overall structure (including the anode), chemical, and mechanical stability.

Out-Year Goals. Elucidating SEI nucleation and electron transfer mechanisms leading to growth processes using a molecular-level approach will help establish their relationship with capacity fading, which will lead to revisiting additive and/or coating design.

Collaborations. Work with Chunmei Ban (NREL) consists in modeling the deposition-reaction of alucone coating on silicon surfaces and their reactivity. Reduction of solvents and additives on silicon surfaces were studied in collaboration with K. Leung and S. Rempe from SNL. This project collaborates with Professor Jorge Seminario (TAMU) on electron and ion transfer reactions and with Dr. Partha Mukherjee (TAMU) focusing on development of a multi-scale model to describe SEI growth on silicon anodes.

Milestones

1. Determining matching and chemistry of solid-solid interfaces including possible cracking effects. Further force-field development and test for solid-liquid interfaces. (Complete)
2. Perform further computational studies on SEI formed in alucone coating including some experimental tests by Chunmei Ban and Clare Grey. (In progress)

Progress Report

Electron Transfer at the Anode/SEI/Electrolyte Interface. The project has investigated the electron transport on various SEI products and oxides in four lithiation stages of the anode using a DFT Green's function approach to understand early stages of SEI nucleation and growth. Results indicated that, in all Li_xSi_y cases, the current is significantly reduced with the addition of the SEI components, as compared with the systems where no SEI element is present. Moreover, increasing the thickness of the SEI layer also resulted in a reduction of the electron transfer. Results also indicate that at high voltages of ~5 V, $Li_2Si_2O_5$ presents a much higher resistance to electron transfer than Li_2CO_3 and SiO_2. The current decreases exponentially as the SEI layer thickness increases, thus implying higher electron transport at initial SEI formation stages and then significantly slower steady growth. These results were published in *JPCC*, 2016.

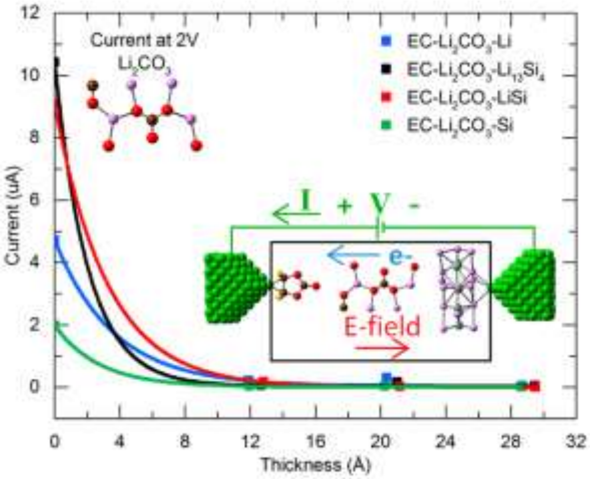

Figure 63. Leakage current from the anode to the solvent through the solid electrolyte interface under an external voltage between two nanotips (green).

Ionic Transport through the SEI. Classical molecular dynamics simulations were used to determine ionic diffusion coefficients through individual SEI components: LiF, Li_2O, and Li_2CO_3. In the absence of an electric field, the predominant diffusion mechanisms observed were vacancy-assisted and knock-off in LiF, direct exchange in Li_2O, and vacancy-assisted and knock-off in Li_2CO_3. When an electric field was applied, diffusion occurred via knock-off in LiF, and via vacancies in Li_2O and Li_2CO_3. These results will be used in a Kinetic Monte Carlo model to analyze diffusion through combination of these blocks. These results were published in the *Journal of the Electrochemical Society*, 2017.

Reactivity of Alucone Coating. In previous collaboration work in with NREL, the project examined behavior of an alucone coating deposited on a silicon anode. Here, the project studied reactivity of the film. Adsorption of solvent molecules (EC) and salt ($LiPF_6$), and reduction by two mechanisms depending on the lithium content of the film (yielding open EC adsorbed on the film or C_2H_4 + CO_3^{2-}) take place near the film/electrolyte and film/anode interfaces. The products of the reaction incorporate to the structure of the film creating a new kind of solid-electrolyte interphase layer. The project finds that there are two main mechanisms by which EC molecules can be reduced and interact with the film near its interface with the electrolyte and with the silicon surface.

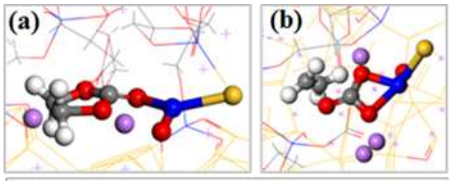

Figure 64. EC reduction and ring opening in adsorbed state. (a) EC molecule adsorbed on aluminum receives 2 e^- and breaks into (b) carbonate anion adsorbed on aluminum/silicon and ethylene. Oxygen (red), lithium (purple), carbon (grey), helium (white), aluminum (blue), and silicon (yellow).

These mechanisms involve electron transfer from the film or anode surface to EC to yield adsorbed open EC (1 e- mechanism) or C_2H_4 and CO_3^{2-} (2 e- mechanism). Reaction products from both mechanisms may adsorb on the film and modify its structure. Preliminary inspection of the effect of Li-ion loading of the film and the presence of salt near the film/electrolyte interface seems to indicate favoring or inhibition of either mechanism. The project continues investigating those effects and seeks to elucidate structural changes in the alucone film and its transformation as a new SEI layer can be formed due to interactions with electrolyte components and their reduction products, which will provide understanding of the behavior of the protective film and fundamental information to help engineer these materials. A letter has been submitted for publication. The project is now preparing a new manuscript combining the main theoretical findings regarding the identification of the coordination number of aluminum in the film, and its oxidation state, and changes in the film structure, with experimental NMR and XPS results from NREL.

Patents/Publications/Presentations

Publications

- Benitez, L., and J. M. Seminario. “Electron Transport and Electrolyte Reduction in the Solid-Electrolyte Interphase of Rechargeable Lithium Ion Batteries with Silicon Anodes.” *J. Phys. Chem. C* 120 (2016): 17978–17988.
- Benitez, L., and J. M. Seminario. “Ion Diffusivity through the Solid Electrolyte Interphase in Lithium-Ion Batteries.” *J. Electrochem. Soc.* In press.
- Gomez Ballesteros, J. L., and P. B. Balbuena. “Reduction of Electrolyte Components on a Coated Silicon Anode of Lithium-Ion Batteries.” Submitted.

Task 6.5 – A Combined Experimental and Modeling Approach for the Design of High Current Efficiency Silicon Electrodes (Xingcheng Xiao, General Motors; Yue Qi, Michigan State University)

Project Objective. The use of high-capacity, Si-based electrode has been hampered by its mechanical degradation due to large-volume expansion/contraction during cycling. Nanostructured silicon can effectively avoid silicon cracking/fracture. Unfortunately, the high surface-to-volume ratio in nanostructures leads to an unacceptable amount of SEI formation and growth, and thereby low current/CE and short life. Based on mechanics models, the project demonstrates that artificial SEI coating can be mechanically stable despite the volume change in silicon, if the material properties, thickness of SEI, and the size/shape of silicon are optimized. Therefore, the project objective is to develop an integrated modeling and experimental approach to understand, design, and make coated silicon anode structures with high current efficiency and stability.

Project Impact. The validated model will ultimately be used to guide synthesis of surface coatings and optimization of silicon size/geometry that can mitigate SEI breakdown. The optimized structures will eventually enable a negative electrode with a 10x improvement in capacity (compared to graphite), while providing > 99.99% CE; this could significantly improve the energy/power density of current Li-ion batteries.

Out-Year Goals. The out-year goal is to develop a well-validated mechanics model that directly imports material properties either measured from experiments or computed from atomic simulations. The predicted SEI induced stress evolution and other critical phenomena will be validated against *in situ* experiments in a simplified thin-film system. This comparison will also allow fundamental understanding of mechanical and chemical stability of artificial SEI in electrochemical environments and correlation between CE and the dynamic process of SEI evolution. Thus, the size and geometry of coated silicon nanostructures can be optimized to mitigate SEI breakdown, providing high current efficiency.

Collaborations. This project engages in collaboration with LBNL, PNNL, and NREL.

Milestones

1. Identify critical mechanical and electrochemical properties of the SEI coating that can enable high current efficiency. (Q1 – Complete)
2. Design a practically useful silicon electrode where degradation of the SEI layer is minimized during lithiation and delithiation. (Q2 – Complete)
3. Construct an artificial SEI design map for silicon electrodes, based on critical mechanical and transport properties of desirable SEI for a given silicon architecture. (Q3 – Complete)
4. Validated design guidance on how to combine the SEI coating with a variety of silicon nano/microstructures. *Go/No-Go:* Decision based on whether the modeling guided electrode design can lead to high CE > 99.9%. (Q4 – Complete; Go)

Progress Report

A New Strategy has been Developed to Stabilize the SEI and Si-Based Electrode. By controlling the cycle potential window, the project has demonstrated excellent cycle performance of columnar Si-film electrode paired with Li $\text{Ni}_{0.6}\text{Mn}_{0.2}\text{Co}_{0.2}\text{O}_2$ counter electrode. It has been demonstrated that the controlled potential window leads to half of the mechanical stress and it was retained at compressive state, when the Li-Si electrode is operated between 0.13 and 0.55 V versus a lithium reference. The deformation of silicon electrode is maintained at elastic region, and no plastic flow is observed during cycling. The combining effects can mitigate mechanical degradation, therefore leading to significantly improved cycle life. The full cells have 90% capacity retention of the initial cell capacity even after 400 cycles, as shown in Figure 65. Figure 66 shows the cross-section of Si-film electrode after different cycles. Although the thickness has increased to 10 µ from 3 µ, the film still retains the mechanical integrity and good adhesion to current collectors. The constraint from the current collector leads to silicon expansion along the thickness direction. The SEI has been observed along the boundary of the columnar structure, indicating silicon has become porous, which can effectively accommodate volume expansion and reduce stress. In addition, the thickness of Si-film electrode does not show significant change after the first 10 cycles, which provides useful information for battery cell design.

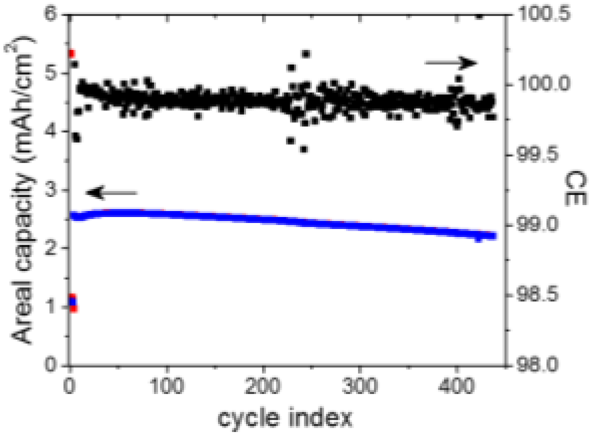

Figure 65. Full cell performance of Si-film electrode paired with He-NMC positive electrode.

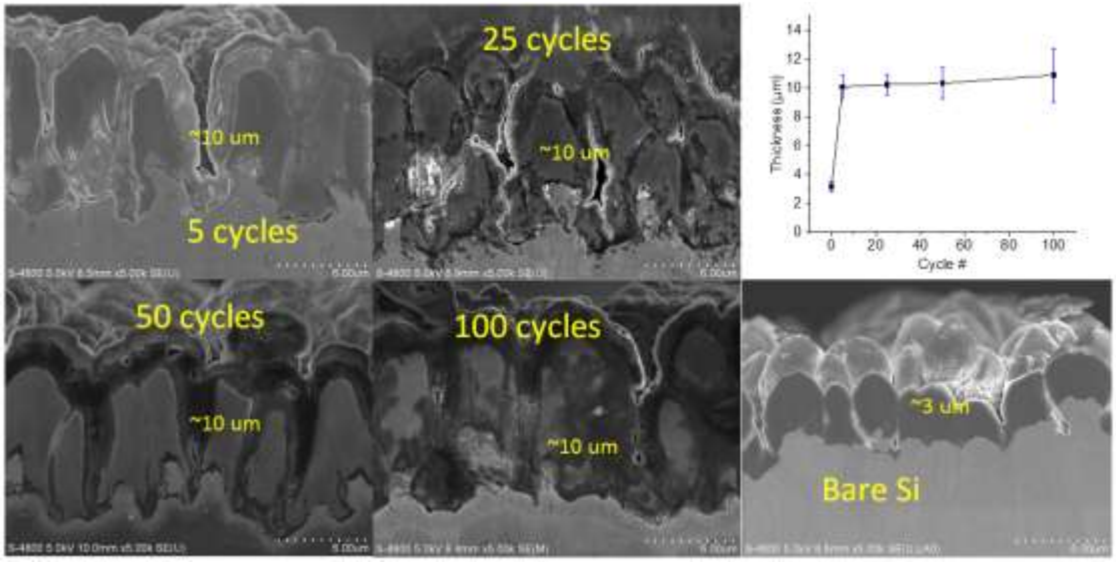

Figure 66. Cross-section images of Si-film electrode after different cycles.

Patents/Publications/Presentations

Publication

- Verbrugge, M., and X. Xiao, Q. Zhang, M. Balogh, K. Raghunathan, and D. Baker. "Fabrication and Characterization of Lithium-Silicon Thick-Film Electrodes for High-Energy-Density Batteries." *J. Elec. Soc.* 164, no. 2 (2017): A156–A167.

Presentation

- Electronic Materials and Applications 2017, American Ceramic Society, Orlando, Florida (January 20, 2017): "Stress Evolution and Degradation Mechanisms at Interfaces in Energy-Related Ceramics"; B. W. Sheldon.

Task 6.6 – Electrode Materials Design and Failure Prediction
(Venkat Srinivasan, Argonne National Laboratory)

Project Objective. The project goal is to develop a continuum-based mathematical model to (1) investigate the impact of mechanical stress on growth of dendritic protrusions and (2) elucidate competition between transport and mechanical means for preventing dendrite growth. Effectiveness of protective layers in preventing growth of dendritic protrusions will also be studied. The focus will be to develop a microscale model that can capture the mechanical stresses and transport processes within lithium metal and adjacent electrolyte/protective layer. Impact of surface energy on growth of dendrites will be investigated. Possibility of plastic deformation within lithium metal and/or solid electrolyte material will also be elucidated along with its effect on propagation of dendrites. Propensity of fracture within the SEI layer (or the protective layer) and its impact on dendrite growth will be explored.

Project Impact. The next-generation Li-ion batteries are expected to use Li-metal based anodes, which offer low reduction potential and superior specific capacity. The biggest drawback preventing widespread usage of Li-metal anodes is formation of dendrites over multiple cycles during operation at higher current densities. Insight gained from this project will provide guidance in designing solid polymer electrolytes (or protective layers) that prevent growth of dendrites on lithium metal.

Out-Year Goals. At the end of this project, a mathematical model will be developed that can capture the mechanical stress field, concentration, and potential profiles around a dendritic protrusion. This model will allow estimation of the propensity for growth of such a protrusion and provide guidance in design of solid polymer electrolytes (or protective layers) for prevention of lithium dendrites.

Milestones

1. Develop mathematical model to understand the proper stress state that exists within lithium metal and adjacent electrolyte during electrochemical deposition of lithium. (Q1 – Complete)
2. Develop mathematical models to investigate and capture possibility of plastic deformation within lithium metal. Impact of plasticity on effective exchange current density will also be explored. (Q2 – Complete)
3. Combine the impact of elasto-plastic stress evolution with transport of lithium within the electrode-electrolyte system. If unsuccessful in combining both elastic and plastic deformation with the transport process, consider only elastic deformation of lithium and electrolyte. (Q3 – In progress)
4. Report on the electrolyte shear modulus required for successful prevention of dendrites. The coupled mechanics and transport framework will be used to analyze the Li-electrolyte system. (Q4 – In progress)

Progress Report

Several researchers have argued that growth of dendritic protrusions during deposition of lithium metal can be prevented by application of externally applied mechanical stress. This project is exploring this concept. Last quarter, it was determined that the components of typical Li/solid electrolyte/Li cells are in stress-free states prior to assembly, which has significant implications for the evolution of tensile and compressive stress at the Li-electrolyte interface. This quarter, work has built on this finding to investigate the effectiveness of a PEO-type polymer-based electrolyte in preventing growth of dendritic protrusions. This has demonstrated that plastic deformation of lithium metal and polymer electrolyte must also be considered. Figure 67a depicts the computational mesh for lithium metal with a dendritic protrusion and a PEO-based electrolyte, before and after cell assembly. Figure 67b demonstrates that, under the assumption of only elastic deformation, the compressive stress that evolves within the lithium and polymer greatly exceeds the yield limits in both regions, over much of the interfacial region. Hence, proper elastic-plastic stress-strain constitutive relations must be used to correctly predict the hydrostatic and deviatoric stresses within the lithium and polymer regions.

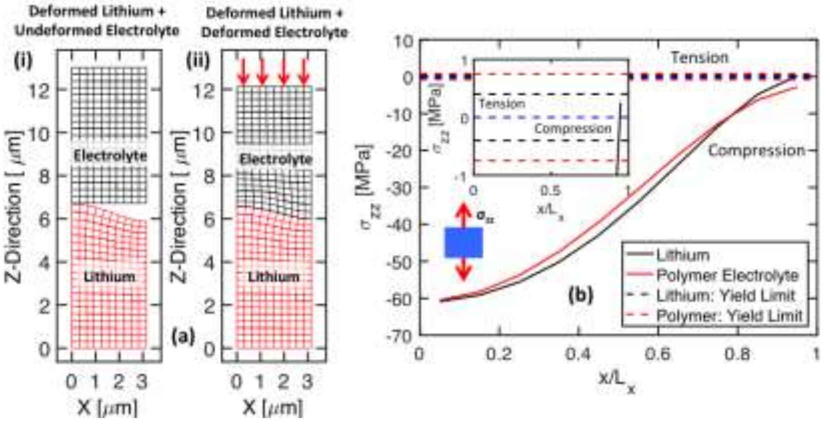

Figure 67. (a) Lithium and polymer electrolyte regions (i) before assembly and (ii) after the regions are fully in contact. Both lithium and polymer have deformed plastically. (b) Stresses within lithium metal and polymer electrolyte regions under the assumption of only elastic deformation. The stresses exceed the elastic limits across much of the domain.

Nonlinear, isotropic elastic-plastic constitutive models including strain-hardening have been adopted to capture the stress-strain relationships observed in lithium metal and PEO-based polymers. Comparisons between the experimental data (obtained from literature) and the computational models for lithium and pure PEO are shown in Figure 68a and Figure 68b, respectively. The ratio of effective exchange current densities at the protrusion peak and valley as a function of the electrolyte shear modulus is shown in Figure 68c, with the model including plasticity clearly predicting a much smaller current ratio. Development of the elastic-plastic model for lithium and polymer satisfies the second quarter milestone.

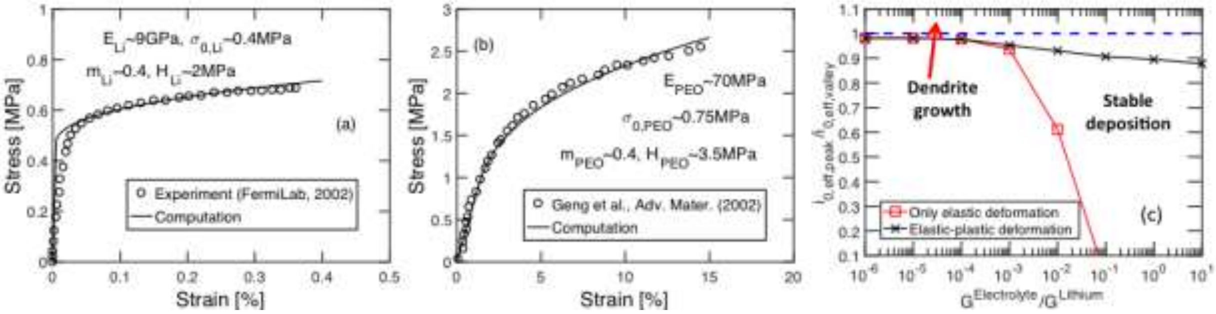

Figure 68. (a) Computational model compared with elastic-plastic stress-strain experimental data. (b) Experimental stress-strain curve for PEO polymer and corresponding numerical model. (c) Ratio of effective exchange current density at the protrusion peak over that at the valley using purely elastic (squares) or elastic-plastic (crosses) models.

Task 6.7 – First Principles Calculations of Existing and Novel Electrode Materials (Gerbrand Ceder, Lawrence Berkeley National Laboratory)

Project Objective. The main project objectives are as follows: (1) develop very high-capacity, layered cathodes with high structural stability (> 250 mAh/g) and high surface stability; (2) clarify the role that Li-excess and cation disorder play in capacity and structural stability; (3) develop predictive modeling of oxygen charge transfer and oxygen loss, and find ways to make oxygen redox beneficial in terms of increase capacity; and (4) develop materials with engineered surface passivation that does not lead to impedance increase.

Project Impact. The project will lead to insight in how Li-excess materials work and ultimately to higher capacity cathode materials for Li-ion batteries. The project will help in the design of high-capacity cathode materials that are tolerant to TM migration.

Out-Year Goals. Future goals include the following: (1) develop higher capacity Li-ion cathode materials, and novel chemistries for higher energy density storage devices, and (2) guide the field in the search for higher energy density Li-ion materials.

Collaborations. This project collaborates with K. Persson (LBNL), C. Grey (Cambridge), V. Srinivasan (ANL), and G. Chen (LBNL).

Milestones

1. Computational approach to predict cation disorder and synthesis temperature. (Q1 – Complete)
2. Comparison of electronic structure modeling with experimental spectra (for example, XAS, XPS, or EELS). (Q2 – Complete)
3. Use modeling to come up with a new cation-disordered material. (Q3 – On target)
4. Demonstrate reduced surface oxygen loss by surface modification of a disordered cathode material using DEMS or TEM. (Q4 – On target)

Progress Report

Reversible oxygen redox in the solid state has the potential to enable high energy density as it can deliver excess capacity beyond the theoretical TM redox capacity at a high voltage. This theoretical study shows that specific chemical and structural features in Li-excess metal oxides introduce labile oxygen electrons that can be easily extracted and participate in the practical capacity of these materials. Experimental O K-edge XAS of various Li-excess cathode materials has been reported to demonstrate oxygen redox processes, but interpretations are very limited. This project investigated O K-edge XAS for cation-disordered $Li_{1.25-x}Mn_{0.5}Nb_{0.25}O_2$ using first principles calculation.

To prepare the atomic structure of cation-disordered $Li_{1.25}Mn_{0.5}Nb_{0.25}O_2$, all possible cation arrangements within the primitive unit cell of Li_3NbO_4 were created by the enumeration method. The lowest energy structure of this material was determined from the generalized gradient approximation (GGA)+U energies of 50 cation arrangements with low electrostatic energies. Figure 69 represents the atomic structure of most stable structure of $Li_{1.25}Mn_{0.5}Nb_{0.25}O_2$, showing that it has various oxygen local environments.

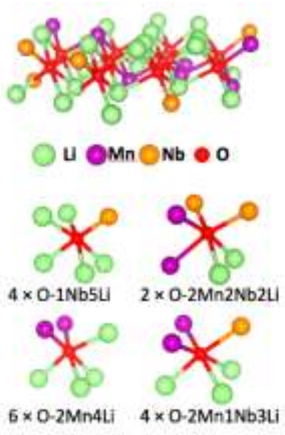

Figure 69. Atomic structure of $Li_{1.25-x}Mn_{0.5}Nb_{0.25}O_2$ and its various oxygen local environments.

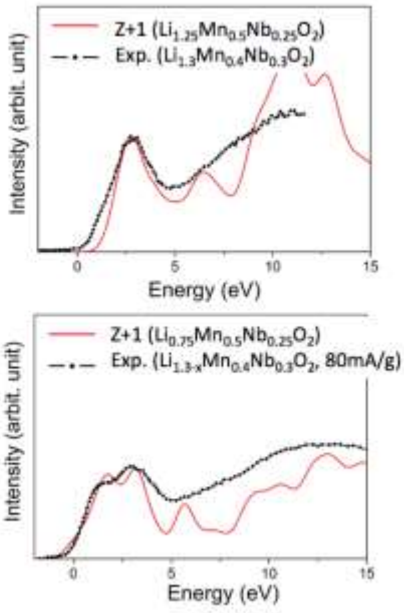

Figure 70. Computed O K-edge X-ray absorption spectroscopy of $Li_{1.25-x}Mn_{0.5}Nb_{0.25}O_2$ (x = 0 and 0.5).

HSE06 hybrid functional was adopted to describe the relative energy level of metal and oxygen states accurately. The Z+1 approximation was employed to treat the core hole effect of XAS. O K-edge XAS of all individual oxygen atoms in $Li_{1.25}Mn_{0.5}Nb_{0.25}O_2$ and $Li_{0.75}Mn_{0.5}Nb_{0.25}O_2$ were calculated and summed for total O K-edge XAS. The resolution of the computed spectra was reduced by convolution with Gaussian distribution and 1 eV of full width at half maximum to consider an instrumental broadening of XAS. Computed and experimental spectra were aligned at the first peak to compare each other. Results of computed O K-edge XAS of $Li_{1.25}Mn_{0.5}Nb_{0.25}O_2$ and $Li_{0.75}Mn_{0.5}Nb_{0.25}O_2$ are in a good agreement with experimental ones, as shown in Figure 70, validating the method used for computing O K-edge EELS spectra. The small discrepancy between computed and experimental XAS may be attributed to a slightly different composition.

Task 6.8 – Dendrite Growth Morphology Modeling in Liquid and Solid Electrolytes (Yue Qi, Michigan State University)

Project Objective. The ultimate goal of this project is to develop a validated model to predict lithium dendrite morphology evolution in both liquid and solid electrolytes during electrodeposition and stripping, in order to accelerate the adoption of Li-metal electrodes in current and emerging battery technologies. To achieve this goal, the project has four objects: (1) formulate a general framework that captures the electrochemical-mechanical driving forces for lithium morphology evolution; (2) consider the role of the nm-thin SEI in liquid-electrolytes as well as the microstructures of mm-thick solid-electrolytes for lithium morphology evolution; (3) connect micron-scale phase-field models and atomic-scale DFT-based simulations via parameter- and relationship-passing to predict lithium dendrite nucleation and growth kinetics and morphology; and (4) validate the key input parameters and main conclusions of the multi-scale model as new capabilities being developed step-by-step.

Project Impact. This atomically informed, fully coupled, electrochemical-mechanical dendrite morphology evolution model will allow us to design the desired properties of artificial SEI coatings, the microstructure of solid electrolyte materials, and the corresponding battery operating conditions, so as to avoid dendrite growth during cycling. It will accelerate design of durable and safe Li-anodes for Li-S, Li-air, and all-solid Li-ion batteries. Thus, it directly impacts emerging technologies, such as Li-S, Li-air, and all-solid Li-ion batteries, which aim to meet the DOE target of the high-energy-density battery cells (> 350 Wh/kg) for EV applications and to push the cost below \$100/kWh$_{\text{use}}$.

Out-Year Goals. The goal this year is to illuminate the role of SEI kinetics on lithium dendrite growth in liquid electrolytes. To achieve this goal, a phase-field model will be developed to capture the electrochemical driven dendrite morphology evolution in a liquid electrolyte. The role of SEI will be modeled both implicitly and explicitly. The kinetic properties, as well as lithium diffusion coefficient along the Li/SEI interface will first be computed from DFT- and DFTB- based atomic simulations. The validation of the model will come from experiments to correlate the distinctively different transport properties of artificial SEI layers with their impact on lithium dendrite morphology.

Collaborations. This project collaborates with the University of Maryland, SNL–Albuquerque, PNNL, and the University of Arkansas.

Milestones

1. Computational approach to predict cation disorder and synthesis temperature. (Q1 – Complete)
2. Comparison of electronic structure modeling with experimental spectra (for example, XAS, XPS, or EELS). (Q2 – Complete)
3. Use modeling to come up with a new cation-disordered material. (Q3 – On target)
4. Demonstrate reduced surface oxygen loss by surface modification of a disordered cathode material using DEMS or TEM. (Q4 – On target)

Progress Report

Atomic Modeling. A new set of DFTB parameters for lithium, hydrogen, cobalt, and oxygen interactions was developed, verified, and used to compute the charge transfer reaction energetics on an SEI covered Li-metal surface, under an applied potential. Figure 71 shows the Li^+ ion energy change when it desolvates from the EC solvents, diffuses through the 4 layers of Li_2CO_3 (a model SEI layer), and gets reduced by electrons on the Li-metal slab. The energy of the oxidized state with electron density of 0.002 e/$Å^2$ on Li-metal surface is 1.42 eV lower than the reduced state, in good agreement from the thermodynamics cycle predicted value of 1.2 eV. The Li^+ ion coordinates to 5 EC molecules to form $Li^+(EC)_5$. With the increase of electron density on Li-metal surface (lower potential), the energy of the Li^+ in the electrolyte increased gradually. This energy landscape provides an important input for thermodynamics based on phase-field model of lithium plating and dendrite morphology evolution.

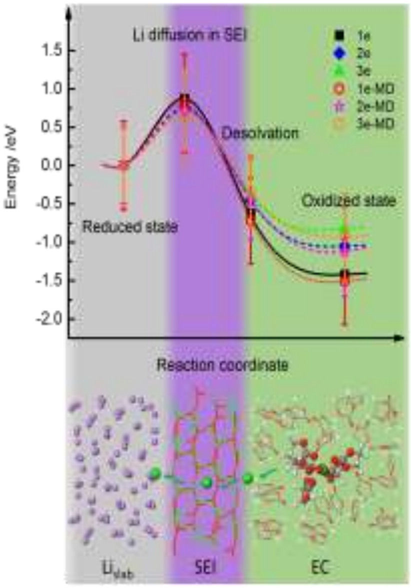

Figure 71. Energy for Li^+ transport from electrolyte to Li-metal slab under different potential.

Coupled Morphology Evolution Model. The previously developed dendrite growth model was extended to implicitly include the effect of SEI by parametric study of the metallic Li/liquid electrolyte binary phase field model. The key parameters closely associated with lithium plating behavior in the model are: interfacial energetics and anisotropy (formulated in κ), Li-ion diffusion coefficients (D^{eff}), charge transfer rate (normalized in L_η), and double-well energy profile ($g'(\xi)$). This information was obtained from previous DFT results and current DFTB calculations. The parametric studies revealed that the SEI charge transfer rate constant (L_η) plays a more dominating role on the evolution kinetics and final plating morphology than other parameters. As shown in Figure 72, the plating at Li-metal anode covered by Li_2CO_3 as SEI layer results in a dendritic and mossy morphology, while that covered by LiF takes on a thick and chunky morphology. Based on this result, it can be preliminarily concluded that LiF is a more advantageous component in SEI for Li-metal anodes in terms of suppressing dendrite growth and enhancing battery cyclability. Note, this model is not coupled with mechanical effect yet.

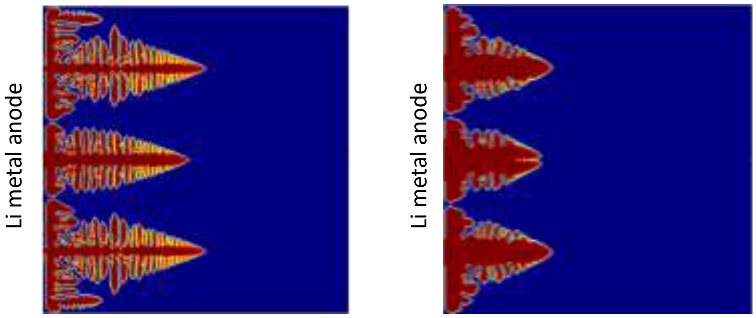

Li_2CO_3 as SEI: mossy Li dendrite

LiF as SEI: chunky Li dendrite

Figure 72. The implicit solid electrolyte interface (SEI) phase field model parametric study results: the lithium plating morphology comparison of Li_2CO_3 and LiF as SEI layer covering Li-metal anodes.

Patents/Publications/Presentations

Presentation

- Mechanical & Materials Engineering, University of Nebraska, Lincoln, Nebraska (March 2017): "Modeling of the Interface and Interphases in Li-Ion Batteries"; Yue Qi. Invited seminar.

TASK 7 – METALLIC LITHIUM AND SOLID ELECTROLYTES

Summary and Highlights

The use of a metallic lithium anode is required for advanced battery chemistries like Li-air and Li-S to realize dramatic improvements in energy density, vehicle range, cost requirements, and safety. However, the use of metallic lithium with liquid and polymer electrolytes has so far been limited due to parasitic SEI reactions and dendrite formation. Adding excess lithium to compensate for such losses effectively negates the high-energy density for lithium in the first place. For a long lifetime and safe anode, it is essential that no lithium capacity is lost either (1) to physical isolation from roughening, dendrites, or delamination processes, or (2) to chemical isolation from side reactions. The key risk and current limitation for this technology is the gradual loss of lithium over the cycle life of the battery.

To date there are no examples of battery materials and architectures that realize such highly efficient cycling of metallic lithium anodes for a lifetime of 1000 cycles due to degradation of the Li-electrolyte interface. A much deeper analysis of the degradation processes is needed, so that materials can be engineered to fulfill the target level of performance for EV, namely 1000 cycles and a 15-year lifetime, with adequate pulse power. When projecting the performance required in terms of just the lithium anode, this requires a high rate of lithium deposition and stripping reactions, specifically about 40 μm of lithium per cycle, with pulse rates up to 10 and 20 nm/s (15mA/cm^2) charge and discharge, respectively. This is a conservative estimate, yet daunting in the total mass and rate of material transport. While such cycling has been achieved for state-of-the-art batteries using *molten* sodium in Na-S and zebra cells, solid sodium and lithium anodes are proving more difficult.

The efficient and safe use of metallic lithium for rechargeable batteries is then a great challenge, and one that has eluded research and development efforts for years. This Task takes a broad look at this challenge for both solid-state batteries and batteries continuing to use liquid electrolytes. For the liquid electrolyte batteries, PNNL researchers are examining the use of dual lithium salts and organic additives to the typical organic carbonate electrolytes to impede lithium corrosion and dendrite formation at both the lithium and graphite anodes. If successful, this is the simplest approach to implement. At Stanford, novel coatings and 3D structures are applied to the lithium surface and appear to suppress roughening and lengthen cycle life. A relatively new family of solid electrolytes with a garnet crystal structure shows super-ionic conductivity and good electrochemical stability. Four programs chose this family of solid electrolytes for investigation. Aspects of the processing of this ceramic garnet electrolyte are addressed at the University of Maryland and at the University of Michigan (UM), with attention to effect of flaws and the critical current density. Computational models will complement their experiments to better understand interfaces and guide reduction of the lithium and cathode area specific resistance (ASR). At ORNL, composite electrolytes composed of ceramic and polymer phases are being investigated, anticipating that the mixed phase structures may provide additional means to adjust the mechanical and transport properties. The last project takes on the challenge to use nano-indentation methods to measure the mechanical properties of the solid electrolyte, the Li-metal anode, and the interface of an active electrode. Each of these projects involves a collaborative team of experts with the skills needed to address the challenging materials studies of this dynamic electrochemical system.

Highlights. The highlights for this quarter are as follows:

- In a hybrid solid/liquid Li-S battery, the lithium is protected with the LLZO garnet ceramic electrolyte. Utilizing a freshly conditioned LLZO pellet showed much smaller hysteresis in the voltage profile compared to LLZO that was stored two weeks to two months in an inert glovebox.
- The mechanical hardness of Li-metal films characterized by nanoindentation of thin film displays unique size and strain rate dependence; this is leading to a diffusional-creep-based model capable of describing the change in stress with strain rate and indentation depth.

- Stable cycling of a solid-state Li-S battery was realized by using a bi-layer $Li_7La_{2.75}Ca_{0.25}Zr_{1.75}Nb_{0.25}O_{12}$ (LLCZNO) garnet electrolyte; one layer is dense to function as the separator, and the second layer is porous to store the sulfur cathode.
- The “solid-liquid” hybrid behavior of Silly Putty, a popular children’s toy, provides an interfacial layer over the Li-metal anodes that can reversibly switch between its “liquid” and “solid” properties in response to the rate of lithium growth. This provides uniform surface coverage and dendrite suppression.
- Electroplated lithium metal forms smooth and uniform films of lithium nanorods when cycled in the $LiPF_6$/PC electrolyte containing mixtures of additives; mixtures of VC+X and FEC+X perform better than any of the additives alone.
- A new perovskite solid electrolyte $Li_{3/8}Sr_{7/16}Hf_{1/4}Ta_{3/4}O_3$ (LSHT) was fired by spark plasma sintering (SPS) to 99.9% density. The LSHT electrolyte has a room-temperature Li-ion conductivity of $\sigma = 4.4 \times 10^{-4}$ S cm^{-1}, an activation energy of 0.33 eV, and good stability in air.
- Cycling of lithium using an open cell foam current collector composed of a structurally isomorphous alloy (Li-SIA) proved to be more stable for Li-metal plating/de-plating than for a copper foil.

Task 7.1 – Mechanical Properties at the Protected Lithium Interface
(Nancy Dudney, Oak Ridge National Laboratory; Erik Herbert, Michigan Technological University; Jeff Sakamoto, University of Michigan

Project Objective. This project will develop the understanding of the Li-metal SEI through state-of-the-art mechanical nanoindentation methods coupled with solid electrolyte fabrication and electrochemical cycling. The goal is to provide the critical information that will enable transformative insights into the complex coupling between the microstructure, its defects, and the mechanical behavior of Li-metal anodes.

Project Impact. Instability and/or high resistance at the interface of lithium metal with various solid electrolytes limit the use of the metallic anode for high-energy-density batteries, such as Li-air and Li-S. The critical impact of this endeavor will be a much deeper analysis of the degradation so that materials can be engineered to fulfill the target level of performance for EV batteries, namely 1000 cycles and 15-year lifetime, with adequate pulse power.

Approach. Mechanical properties studies through state-of-the-art nanoindentation techniques will be used to probe the surface properties of the solid electrolyte and the changes to the lithium that result from prolonged electrodeposition and dissolution at the interface. An understanding of the degradation processes will guide future electrolyte and anode designs for robust performance. In the first year, the team will address the two critical and poorly understood aspects of the protected Li-metal anode assembly: (1) the mechanical properties of the solid electrolyte, and (2) the morphology of the cycled lithium metal.

Out-Year Goals. Work will progress toward study of the electrode assembly during electrochemical cycling of the anode. The project hopes to capture the formation and annealing of vacancies and other defects in the lithium and correlate this with the properties of the solid electrolyte and the interface.

Collaborations. This project funds work at ORNL, Michigan Technological University, and UM. Asma Sharafi (UM, Ph. D. student) and Dr. Robert Schmidt (ORNL) also contribute to the project. Steve Visco (PolyPlus) will serve as a technical advisor.

Milestones

1. Characterize *in situ* changes in lithium anode from a single stripping and plating half cycle. (Q2 – In progress)
2. Measure the Li-LLZO interface strength as a function of surface treatment using the Instron and EIS capability. (Q3 – In progress, initial results recorded)
3. Examine lithium anode *in situ* during extended electrochemical plating, stripping, and relaxation to assess defect formation and annealing. (Q4 – Completed, by profilometry of lithium thin-film cell)
4. Determine the physical properties of electrolyte failures, the nature of material reduction or lithium incursion/pileup, using indentation and X-ray tomography. Samples obtained from other Task 7 projects. (Q4)

Progress Report

Recent nanoindentation experiments performed on vapor deposited lithium films reveal a remarkable length scale dependence in the measured hardness. (Hardness in this study is the resistance to permanent or plastic deformation; this is highly relevant to the mechanics of successfully confining the lithium anode.) Figure 73a shows a unique inflection point in the hardness that coincides with an abrupt change in the mechanism that controls the plastic flow of lithium. Hardness data to the right of the inflection point are consistent with the well-documented indentation size effect. Differences in the hardness between the 5- and 18- μm thick films are generally consistent with Hall-Petch strengthening due to the smaller grain size of the thinner film. Hardness data to the left of the inflection point, on the other hand, are entirely unique. While an increase in hardness with increasing indentation depth has been observed in BCC iron, unlike iron, this observation in lithium is not the result of dislocation interaction with a nearby grain boundary. Figure 73b shows 20 residual hardness impressions in the grain interior and 68 impressions in close proximity to a grain boundary. As shown in Figure 73c, there is no discernable difference in the measured hardness at these positions relative to the boundary and the grain interior (red and green). The difference in hardness between the bulk arrays (yellow) and data obtained within the grain and near the boundary (Figure 73c) is potentially due to plastic anisotropy. In addition to the length scale dependence, Figure 73d shows the hardness near the free surface also depends on the strain rate. As the data show, the rate effect is most pronounced near the free surface, it diminishes with increasing indentation depth and is completely exhausted by the inflection point. To rationalize these unique experimental observations, an effort is in progress to develop a diffusional-creep-based model capable of describing the change in stress with strain rate and indentation depth.

Initial results of the lap shear measurements to assess the mechanical properties of a Li-metal anode with the $Li_7La_3Zr_2O_{12}$ were recorded. So far, results show that the adhesive strength of the interfaces associated with low interfacial resistance exceed the yield strength of the lithium metal itself. This poses a challenge for the study, and alternative sample configurations and much thinner lithium contacts will be considered.

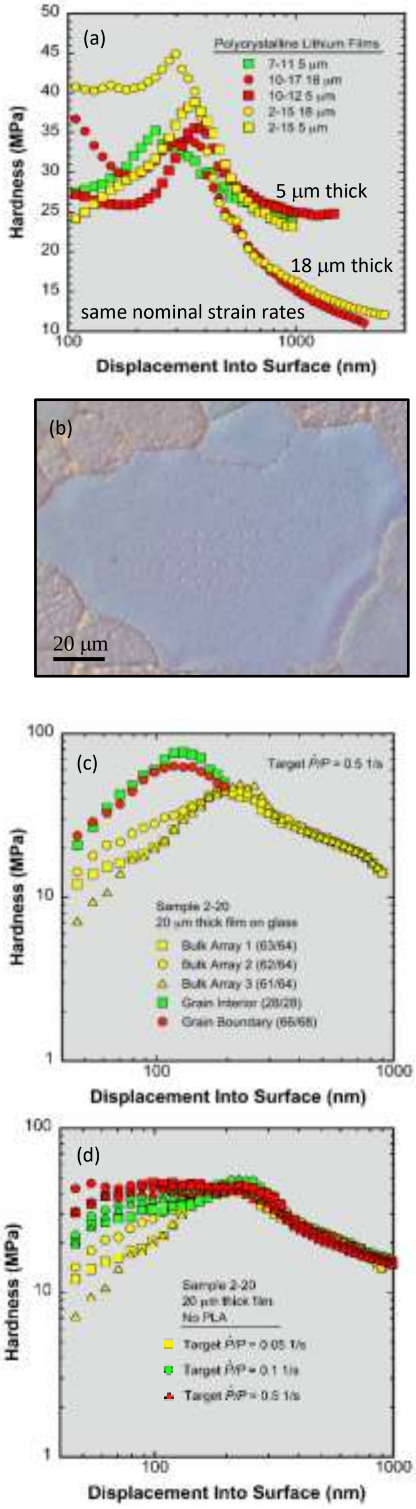

Figure 73. (a, c, d) Hardness as a function of indentation depth, deposition date, film thickness, location, and strain rate. (b) Micrograph of residual hardness impressions in lithium.

Patents/Publications/Presentations

Publication

- Dudney, Nancy J. "Evolution of the Lithium Morphology from Cycling of Thin Film Solid-State Batteries." *Journal of Electroceramics*. Invited for Solid State Batteries Issue; published on-line.

Presentation

- ACS meeting, San Francisco (March 2017): "Stability and Cycling of Metallic Lithium with an Inorganic Solid Electrolyte"; Nancy J. Dudney, Miaofang Chi, Jeff Sakamoto, and Erik Herbert. Invited presentation.

Task 7.2 – Solid Electrolytes for Solid-State and Lithium–Sulfur Batteries (Jeff Sakamoto, University of Michigan)

Project Objective. *Enable advanced Li-ion solid-state and lithium-sulfur EV batteries using LLZO solid-electrolyte membrane technology*. Owing to its combination of fast ion conductivity, stability, and high elastic modulus, LLZO exhibits promise as an advanced solid-state electrolyte. To demonstrate relevance in EV battery technology, several objectives must be met. First, LLZO membranes must withstand current densities approaching ~1 mA/cm^2 (commensurate with EV battery charging and discharging rates). Second, low ASR between lithium and LLZO must be achieved to obtain cell impedance comparable to conventional Li-ion technology (~10 Ohms/cm^2). Third, low ASR and stability between LLZO and sulfur cathodes must be demonstrated.

Project Impact. The expected outcomes will: (1) enable Li-metal protection, (2) augment DOE access to fast ion conductors and/or hybrid electrolytes, (3) mitigate Li-polysulfide dissolution and deleterious passivation of Li-metal anodes, and (4) prevent dendrite formation. Demonstrating these aspects could enable Li-S batteries with unprecedented end-of-life, cell-level performance: > 500 Wh/kg, > 1080 Wh/l, > 1000 cycles, and lasting > 15 years.

Approach. This effort will focus on the promising new electrolyte known as LLZO ($Li_7La_3Zr_2O_{12}$). LLZO is the first bulk-scale ceramic electrolyte to simultaneously exhibit the favorable combination of high conductivity (~1 mS/cm at 298K), high shear modulus (61 GPa) to suppress lithium dendrite penetration, and apparent electrochemical stability (0-6 V versus Li/Li$^+$). While these attributes are encouraging, additional R&D is needed to demonstrate that LLZO can tolerate current densities in excess of 1mA/cm^2, thereby establishing its relevance for PHEV/EV applications. This project hypothesizes that defects and the polycrystalline nature of realistic LLZO membranes can limit the critical current density. However, the relative importance of the many possible defect types (porosity, grain boundaries, interfaces, and surface and bulk impurities), and the mechanisms by which they impact current density, have not been identified. Using experience with the synthesis and processing of LLZO (Sakamoto and Wolfenstine), combined with sophisticated materials characterization (Nanda), this project will precisely control atomic and microstructural defects and correlate their concentration with the critical current density. These data will inform multi-scale computation models (Siegel and Monroe), which will isolate and quantify the role(s) that each defect plays in controlling the current density. By bridging the knowledge gap between composition, structure, and performance, this project will determine if LLZO can achieve the current densities required for vehicle applications.

Milestones

1. Establish a process to control the microstructural defect that governs the critical current density (CCD) to achieve > 1 mA/cm^2. (Q1 – Complete)
2. Establish a process to control the atomic-scale defect that governs the CCD to achieve > 1 mA/cm^2. (Q1 – Complete)
3. Design, fabricate, and test beginning of life performance of hybrid Li-LLZO-liquid-S+carbon cells. (Q2 – Complete)
4. Extended cycling of hybrid Li-LLZO-liquid-S+carbon cells. (Q3 – In progress)
5. Experimentally evaluate the CCD, based on the dominant defects (atomic and or microstructural) identified in years 1 and 2, as a function of Q, temp, and pressure. Also characterize the CE (Q4)
6. Cycling Li-LLZO-liquid-SOA Li-ion cathode to demonstrate hybrid electrolyte concept can cycle at $\geq$ 1 mA/cm^2. (Q4)

Progress Report

Highlight. Milestones 3 (complete) and 4 (in progress): Cycling of hybrid Li-LLZO-liquid-S+carbon cells.

First generation (Gen 1) Li-LLZO-Sulfur+carbon cells were tested in hybrid configuration with a cathode of 46% S, 37% KJB, 8.5% PVDF, 8.5% Super P, all in wt%. The cells were cycled at 0.06 mA/cm^2 in 1M LiTFSI, DOL: DME on the cathode side. Electrodes were ~30-35 µm thick; 0.8 mg$_{(S)}$/cm^2 loading. The previous report showed that cycling such hybrid LLZO/liquid cells is possible and the efficiency was found to be close to 100%, which is much higher than all-liquid Li-S cells. Extended cycling for more than 50 cycles (Figure 74a) showed lasting high CE, but the capacity continuously faded (after 50 cycles the capacity was 28% of the initial capacity). Photographs of the LLZO after cycling (Figure 74b) showed dark discoloration on the LLZO surface facing the cathode. However, by gently wiping the surface, a visually clean LLZO surface could be seen (Figure 74b, bottom photograph). This indicates that there is no significant deterioration for the LLZO surface after cycling, at least as observed by naked eye. To ensure reproducibility, a new cell was assembled and tested, but the hysteresis between the lithiation and delithiation was much larger than Gen 1 (green plots in Figure 74c). The only difference between Gen 1 (blue plot in Figure 74c) and that new cell is the time LLZO was kept in the glovebox; the new cell has more aged LLZO (aged LLZO was kept for more than 2 months in in the glovebox, while Gen 1 was kept in the glovebox for less than 2 weeks). When a freshly conditioned LLZO pellet (red plot in Figure 74c) was tested in the same configuration as Gen 1, it showed much smaller hysteresis in the voltage profile compared to the aged LLZO. The EIS shown in Figure 74d can explain this observation, since the aged LLZO (green) exhibited an order of magnitude higher resistance than the freshly conditioned LLZO (red). It is worth noting that while the first cycle capacity is comparable for both Gen 1 and Fresh LLZO, the capacity fade is much lower for fresh LLZO.

Efforts are under way to address the capacity fade by studying the LLZO/catholyte interface and engineering the catholyte.

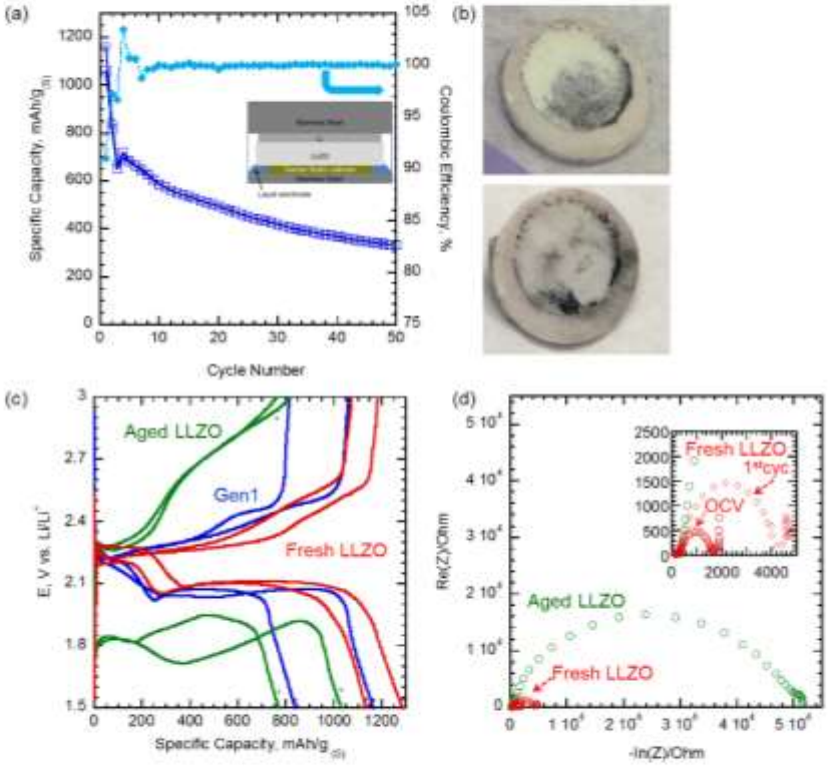

Figure 74. (a) Sulfur specific capacity versus cycle number, and Coulombic efficiency versus cycle number. The inset shows a schematic diagram of test cell. LLZO membrane physically isolated lithium from the liquid electrolyte. (b) Photographs after electrochemical cycling of LLZO showing the surface that was in contact with C/S cathode and liquid electrolyte. The bottom photograph is after gently wiping the surface using Kimwipe paper. Specific capacities normalized by grams of sulfur. (c) Voltage profile for the first two cycles comparing Gen 1 (blue), aged LLZO (green), and fresh LLZO (red).

Patents/Publications/Presentations

Patent

- Sakamoto, J., and A. Sharafi, and T. Thompson. Patent Application, “System and Method for Treating the Surface of Solid Electrolytes.” U.S. Utility Patent Application, 62/480/080 (March 31, 2017).

Presentation

- BMW Workshop, Munich, Germany (March 14–15, 2017): “Solid-State Electrolytes Enabling beyond Li-ion Cell Chemistries”; J. Sakamoto.

Task 7.3 – Composite Electrolytes to Stabilize Metallic Lithium Anodes (Nancy Dudney and Frank Delnick, Oak Ridge National Laboratory)

Project Objective. Prepare composites of representative polymer and ceramic electrolyte materials to achieve thin membranes that have the unique combination of electrochemical and mechanical properties required to stabilize the metallic lithium anode while providing for good power performance and long cycle life. Understand the Li-ion transport at the interface between polymer and ceramic solid electrolytes, which is critical to the effective conductivity of the composite membrane. Identify key features of the composite composition, architecture, and fabrication that optimize the performance. Fabricate thin electrolyte membranes to use with a thin metallic lithium anode to provide good power performance and long cycle life.

Project Impact. A stable lithium anode is critical to achieve high energy density with excellent safety, lifetime, and cycling efficiency. This study will identify the key design strategies that should be used to prepare composite electrolytes to meet the challenging combination of physical, chemical, and manufacturing requirements to protect and stabilize the Li-metal anode for advanced batteries. By utilizing well characterized and controlled component phases, the design rules developed for the composite structures will be generally applicable toward substitution of alternative and improved solid electrolyte component phases as they become available. Success in this project will enable these specific DOE technical targets: 500-700 Wh/kg, 3000-5000 deep discharge cycles, and robust operation.

Approach. This project seeks to develop practical solid electrolytes that will provide stable and long-lived protection for the Li-metal anode. Current electrolytes all have serious challenges when used alone: oxide ceramics are brittle, sulfide ceramics are air sensitive, polymers are too resistive and soft, and many electrolytes react with lithium. Composites provide a clear route to address these issues. This project does not seek discovery of new electrolytes; rather, the goal is to study combinations of current well-known electrolytes. The project emphasizes investigation of polymer-ceramic interfaces formed as bilayers and as simple composite mixtures where the effects of the interface properties can be readily isolated. In general, the ceramic phase is several orders of magnitude more conductive than the polymer electrolyte, and interfaces can contribute an additional source of resistance. Using finite element simulations as a guide, composites with promising compositions and architectures are fabricated and evaluated for Li-transport properties using AC impedance and DC cycling with lithium in symmetric or half cells. General design rules will be determined that can be widely applied to other combinations of solid electrolytes.

Out-Year Goal. The out-year goal is to use advanced manufacturing processes where the architecture of the composite membrane can be developed and tailored to maximize performance and cost-effective manufacturing.

Collaborations. Work is conducted by Dr. A. Samuthira Pandian. Dr. Jihua Chen (ORNL) assisted with electron microscopic characterization and Dr. Rose Ruther (ORNL) with Raman spectroscopy. Electrolyte powders are obtained from Ohara corporation and Prof. Sakamoto (University of Michigan). Dr. Sergiy Kalnaus has provided finite element simulations.

Milestones

1. For spray-coated composites with high ceramic loading, vary the salt, plasticizer, and ceramic content to achieve facile ion transport across phase boundaries and 10^{-5} S/cm. (Q2 – In progress)
2. Assess the lithium/electrolyte interface resistance. Adjust the composition or add a barrier coating to reduce the ASR and passivate the interface. (Q3 – In progress)
3. Fabricate a full battery using aqueous spray coating for both the composite electrolyte and cathode incorporating a protected Li-metal anode. Demonstrate lithium cyclability. (Q4 – Stretch goal)

Progress Report

Aqueous slurry containing PEO-based polymer dispersed with Ohara glass ceramic powders was spray coated following the earlier reports. The TEGDME is an ideal plasticizer for improving the properties for the composite electrolyte coating, including uniform and crack-free structure, wetting on metal foils, thermal stability and lithium stability of the polymer; however, the conductivity of the composite remains too low, well below the target of 10 mS/cm. This molecule clearly does not facilitate Li^+ ion transport across the interface between the Ohara ceramic and the PEO polymer in the composite electrolyte. Investigations of other possible candidates for plasticizer were conducted attempting to improve the interface between the ceramic particle and polymer electrolyte.

Diethyleneglycol dibutylether (DEGDBE) has fewer ether-oxygen compared to tetraglyme (TEGDME) and consequently was expected to coordinate more weakly with Li^+ ions. It has a similarly low vapor pressure compared to TEGDME, so is not lost when drying the spray-coated membrane. A second molecule hexamethylphosphoramide (HMPA) was also examined as a possible plasticizer, being more compact with a high negative charge at the oxygen. Some properties are given in the table. These were incorporated at the same molar ratio as used for the tetraglyme.

Table 4. Properties of possible candidates for plasticizer being investigated to improve the interface between the ceramic particle and polymer electrolyte.

Property	*TEGDME*	*HMPA*	*DEGDBE*	*DMC*
Molecular formula	$C_{10}H_{22}O_5$	$C_6H_{18}N_3OP$	$C_{12}H_{26}O_3$	$C_3H_6O_3$
MW	222	179	218	90
Solubility in water	Miscible	Miscible	Immiscible	
Vapor pressure (20°C)	<0.01 torr	0.03 mmHg	<0.01 mmHg	18 mmHg
Boiling point	275°C	232°C	256°C	90°C

Results for the conductivities of the composite coatings with 50 vol% Ohara powder and the new candidate plasticizer molecules are shown in Figure 75. Unfortunately, the composites remain rather resistive, and the conduction path is limited to the polymer phase. To date only DMC and water appear to provide the pathway for Li^+ to access the ceramic phase giving a conductivity for the composite that is orders of magnitude higher than for the ceramic-free plasticized polymer electrolyte.

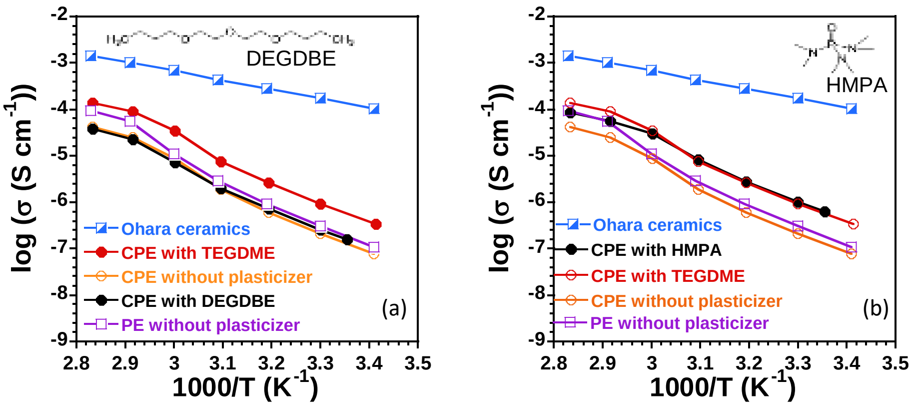

Figure 75. Comparison of spray-coated composite containing DEGDBE (a) and HMPA (b) as plasticizer with earlier results obtained using TEGDME as plasticizer. Conductivity of composite and polymer that does not contain plasticizer and Ohara ceramics is also presented.

In other experiments, the mechanical strength of the 50vol% ceramic composite coating was demonstrated under uniaxial pressure to 3.5 ton/cm^2 (300 MPa). A thin glassy coating over the composite was well supported and able to withstand this pressure without cracking or extrusion of the polymer component.

Patents/Publications/Presentations/Presentations

Publication

- “Composite Polymer Ceramic Electrolyte for High Energy Lithium Secondary Batteries.” In preparation.

Presentation

- Pacific Rim Meeting on Electrochemical and Solid-State Science (PRiME) Meeting of Electrochemical Society, Hawaii (2016): “Composite Polymer-Ceramic Electrolyte for High Energy Lithium Secondary Batteries”; Amaresh Samuthira Pandian, Frank Delnick, and Nancy Dudney.

Task 7.4 – Overcoming Interfacial Impedance in Solid-State Batteries
(Eric Wachsman, Liangbing Hu, and Yifei Mo, University of Maryland College Park)

Project Objective. The project objective is to develop a multifaceted and integrated (experimental and computational) approach to solve the key issue in solid-state, Li-ion batteries (SSLIBs), interfacial impedance, with a focus on garnet-based SSEs, the knowledge of which can be applied to other SSE chemistries. The focus is to develop methods to decrease the impedance across interfaces with the solid electrolyte, and ultimately demonstrate a high power/energy density battery employing the best of these methods.

Project Impact. Garnet electrolytes have shown great promise for intrinsically safer batteries with high energy density. The success of the proposed research can lead to dramatic progress on the development of SSLiBs based on garnet electrolytes. With regard to fundamental science, the methodology of combining computational and experimental methods can lead to an understanding of the thermodynamics, kinetics, and structural stability of SSLiBs with garnet electrolytes. Garnet electrolyte particles are naturally brittle and hard due to their ceramic nature, and thus typically have poor contact between electrolyte particles and with electrode materials. A fundamental understanding of the particle interfaces at the nanoscale and through computational methods, especially with interface layers, can guide improvements to the SSE and battery design and eventually lead to the commercial use of SSLiB technology.

Approach. Electrode/electrolyte interfaces in SSLiBs are typically planar, resulting in high impedance due to low specific surface area. Attempts to make high surface area 3D interfaces (for example, porous structure) can also result in high impedance due to poor contact at the electrode-electrolyte interface that hinders ion transport or degrades due to expansion/contraction with voltage cycling. This project will experimentally and computationally determine the interfacial structure-impedance relationship in SSLiBs to obtain fundamental insight into design parameters to overcome this issue. Furthermore, it will investigate interfacial modification (layers between SSE and electrode) to extend these structure-property relationships to demonstrate higher performance SSLiBs.

Collaborations. This project collaborates with Dr. Venkataraman Thangadurai on garnet synthesis. It will collaborate with Dr. Leonid A. Bendersky (Leader, Materials for Energy Storage Program at NIST) and use neutron scattering to investigate the lithium profile across the bilayer interface with different charge-discharge rates. The project is in collaboration with Dr. Kang Xu, ARL, with preparation of perfluoropolyether (PFPE) electrolyte.

Milestones

1. Fabricate and test SSLiBs with Li-NMC Chemistry. (Q1 – Complete)
2. Fabricate and test SSLiBs with Li-S Chemistry. (Q2 – Complete)
3. Develop models to investigate interfacial transport for Li-S and Li-NMC SSLiBs. (Q3 – In progress)
4. Achieve full cell (Li-S or Li-NMC) performance of 350-450 Wh/kg and 200 cycles. (Q4)

Progress Report

Solid-State Lithium-ion Batteries with Li-S Chemistry

Solid-state Li-ion batteries with a sulfur cathode, garnet SSE, and Li-metal anode were fabricated. The SSE was realized by a bi-layer $Li_7La_{2.75}Ca_{0.25}Zr_{1.75}Nb_{0.25}O_{12}$ (LLCZNO) garnet, comprising one dense layer functioning as separator and one porous layer to store sulfur cathode. The structure of the bi-layer garnet and the sulfur cathode is shown by the cross-section SEM image (Figure 76a). The sulfur fills the pores of garnet in the porous layer, as confirmed by EDS in Figure 76b. Li-metal anode was coated on the dense side of the bi-layer garnet, with a polymer interface for better contact.

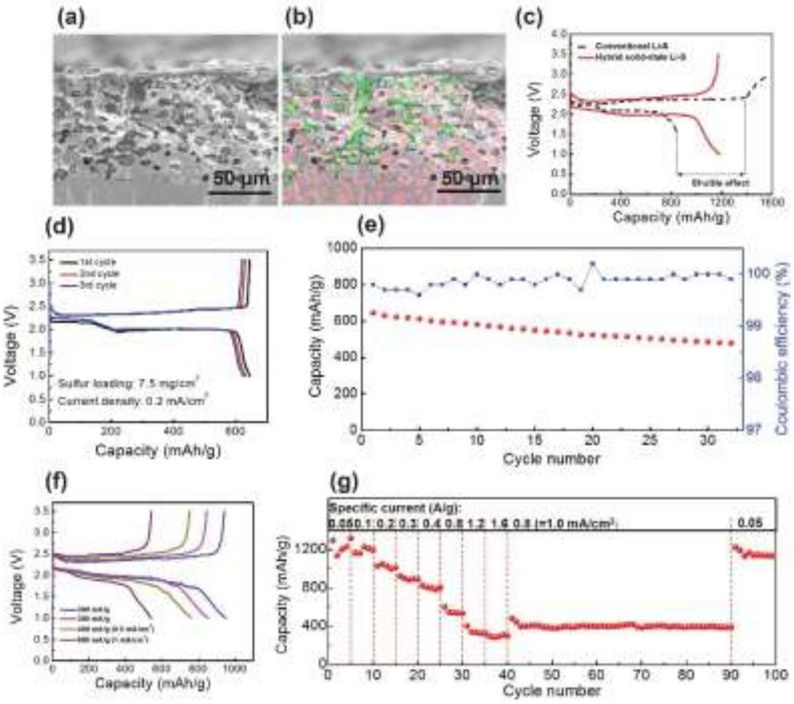

Figure 76. Characterizations of bi-layer garnet and performances of Li-S battery. (a) Cross sectional scanning electron microscopy of bi-layer garnet filled with sulfur. (b) Energy-dispersive X-ray spectroscopy of sulfur (green) and lanthanum (red) distribution in bi-layer garnet. (c) Comparison of charge and discharge curves of Li-S cells with conventional and garnet electrolyte. (d-e) Voltage profile and cycling performance of the solid-state Li-S cell with a loading of 7.5 mg/cm² at 0.2 mA/cm². (f) Charge and discharge curves of the solid-state Li-S cell at different current densities. (g) Rate performance of the solid-state Li-S cell.

Figure 76c shows that the SSE can effectively prevent the polysulfide shuttling effect and provide a higher battery efficiency than conventional electrolytes because of the dense layer garnet. Figure 76d shows the discharge and charge voltage profiles of the solid-state Li-S cell. The first-cycle discharge capacity is 645 mAh/g with a high CE of 99.8%. The cycling performance is shown in Figure 76e. The CE remains > 99%, confirming that no shuttling effect occurs in the hybrid design. The hybrid bilayer Li-S cell with a sulfur mass loading of 7.5 mg/cm^2 has an energy density of 280 Wh/kg on the basis of the cathode, lithium anode, and electrolytes. Figure 76f shows the discharge and charge curves of the cell at different current densities. At a current density of 200 mA/g, the sulfur cathode delivers a specific capacity of ~1000 mAh/g with a ~100% CE. At a current density of 800 mA/g the specific capacity is 550 mAh/g, and the cell still maintains a high CE close to 100%. The rate performance is shown in Figure 76g. The solid-state cell shows a good cycling stability at elevated current densities (up to 800 mA/g) and a good capacity retention when further cycled at a current density of 50 mA/g.

Task 7.5 – Nanoscale Interfacial Engineering for Stable Lithium-Metal Anodes
(Yi Cui, Stanford University)

Project Objective. This study aims to render Li-metal anode with high capacity and reliability by developing chemically and mechanically stable interfacial layers between lithium metal and electrolytes, which is essential to couple with sulfur cathode for high-energy, Li-S batteries. With the nanoscale interfacial engineering approach, various kinds of advanced thin films will be introduced to overcome issues related to dendritic growth, reactive surface, and virtually "infinite" volume expansion of Li-metal anode.

Project Impact. Cycling life and stability of Li-metal anode will be dramatically increased. The success of this project, together with breakthroughs of sulfur cathode, will significantly increase the specific capacity of lithium batteries and decrease cost as well, therefore stimulating the popularity of EVs.

Out-Year Goals. Along with suppressing dendrite growth, the cycle life, CE, and current density of Li-metal anode will be greatly improved (that is, no dendrite growth for current density up to 3.0 mA/cm^2, with CE greater than 99.5%) by choosing the appropriate interfacial nanomaterial along with rational electrode material design.

Milestones

1. Rational design of composite artificial SEI for the stabilization of 3D nanoporous Li-metal anode. (December 2016 – Complete)
2. Explore novel materials and their properties as artificial SEI layer on lithium metal. (March 2016 –Complete)

Progress Report

Previously, the project has employed the nanoscale interfacial engineering approach using inter-connected hollow carbon spheres, 2D boron nitride, and graphene on copper current collectors as stable artificial SEI for lithium metal. The strategies effectively suppressed lithium dendrite growth and greatly enhanced the CE during cycling. Recently, the project has continued to explore the different coating materials in search for better surface protections on Li-metal anode. This quarter, the project took advantage of the "solid-liquid" hybrid behavior of Silly Putty (SP), a popular children's toy, as the interfacial layer for Li-metal anodes. SP can reversibly switch between its "liquid" and "solid" properties in response to the rate of lithium growth to provide uniform surface coverage and dendrite suppression, respectively, therefore enabling the stable operation of Li-metal electrodes.

The idea is illustrated schematically in Figure 77. SP, primarily comprised of polydimethylsiloxane (PDMS) crosslinked by transient boron-mediated bonds, is technically termed as a "shear thickening material." Namely, the rigidity of SP increases significantly as the deformation rate increases. It can even temporarily become an elastic solid if the deformation rate is too fast for the dynamic crosslinks to temporally break and reconnect. Therefore, when coated on the surface of lithium metal, SP flows on the time scale of each charging and discharging circle and can uniformly cover the electrode surface to serve as a stable interface between the lithium metal and the electrolyte. However, if occasionally there are some "hot-spots" where the deposition and expansion of lithium is faster than at other places on the electrode, the stiffness of the local SP coating consequently increases. As such, SP acts as a clamping layer to help eliminate fast local overgrowth or expansion of lithium metal and the SEI breakage, effectively suppressing lithium dendrite growth.

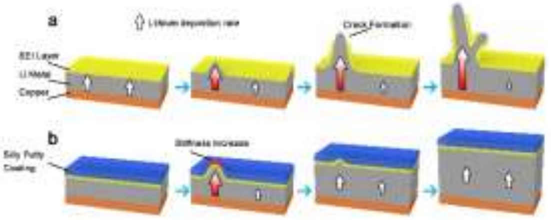

Figure 77. Schematic showing the design of Silly Putty modified lithium anode.

The viscoelastic behavior of the SP was first studied by rheometer. As shown in Figure 78, when the stain rate is low (<10^{-2} s^{-1}), the loss modulus (G'', which represents the viscous property), is significantly larger than the storage modulus (G', which represents the elastic property), indicating that the viscous property dominates the behavior and the SP behaves more like a flowable liquid. As the strain rate increases, G' increases significantly, indicating that the SP becomes stiffer. G' even exceeds G'' by almost an order of magnitude at high strain rates (>10^{-2} s^{-1}), at which SP exhibits more elastic solid-like behaviors. Therefore, as expected, SP indeed possesses the interesting viscoelastic behavior that makes it a favorable candidate as artificial SEI for Li-metal anode.

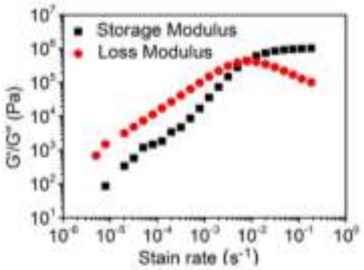

Figure 78. The rheological study of Silly Putty.

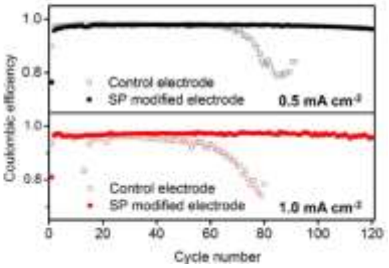

Figure 79. Coulombic efficiency of lithium deposition/stripping (1 mAh cm^{-2}) on Silly Putty-modified electrodes and control copper electrodes at different current densities.

The lithium stripping/plating CE of SP-coated copper electrode was tested. The SP-coated electrode showed good cycling performance, maintaining an average CE of 97.6% for over 120 cycles at 0.5 mA cm^{-2}. In comparison, control electrodes without SP coatings exhibited poor performance, with CE dropping below 90% after only 75 cycles. At a higher current density of 1 mA cm^{-2}, the SP-modified electrode achieved an average CE of 97.0% over 120 cycles, while the control electrodes maintained CE of over 90% for only 65 cycles.

Patents/Publications/Presentations

Publication

- Liu, K., et al. "Solid-Liquid-Like Dual Properties of Silly Putty for the Stable Cycling of Lithium Metal Anodes." *J. Am. Chem. Soc.* 139 (2017): 4815–4820.

Task 7.6 – Lithium Dendrite Suppression for Lithium-Ion Batteries
(Wu Xu and Ji-Guang Zhang, Pacific Northwest National Laboratory)

Project Objective. The project objective is to enable lithium metal to be used as an effective anode in rechargeable Li-metal batteries for long cycle life at a reasonably high current density. The investigation will focus on the effects of various lithium salts, additives, and carbonate-based electrolyte formulations on Li-anode morphology, lithium CE, and battery performances in terms of long-term cycling stability at room temperature and elevated temperatures and at various current density conditions, rate capability, and low-temperature discharge behavior. The surface layers on lithium anode and cathode will be systematically analyzed. The properties of solvates of cation-solvent molecules will also be calculated to help explain the obtained battery performances.

Project Impact. Lithium metal is an ideal anode material for rechargeable batteries. Unfortunately, dendritic lithium growth and limited CE during lithium deposition/stripping inherent in these batteries have prevented practical applications. This work will explore new electrolyte additives that can lead to dendrite-free lithium deposition with high CE. The success of this work will increase energy density of Li-metal batteries and accelerate market acceptance of EVs, especially for PHEVs required by the EV Everywhere Grand Challenge.

Out-Year Goals. The long-term goal of the proposed work is to enable lithium and Li-ion batteries with > 120 Wh/kg (for PHEVs), 1000 deep-discharge cycles, 10-year calendar life, improved abuse tolerance, and less than 20% capacity fade over a 10-year period.

Collaborations. This project collaborates with the following: Bryant Polzin (ANL) on NMC electrodes, Chongmin Wang (PNNL) on characterization by TEM/SEM, and Zihua Zhu (PNNL) on TOF-SIMS.

Milestones

1. Verify formation of a transient high Li^+-concentration electrolyte layer during fast discharging by direct microscopic observation. (Q1 – Complete)
2. Identify effects of dual-salt electrolytes on Li-metal protection during fast charging. (Q2 – Complete)
3. Identify new electrolytes that are stable with both lithium and high-voltage cathode. (Q3 – In progress)
4. Increase the CE of lithium cycling in the new electrolyte to be more than 99%. (Q4)

Progress Report

This quarter, the effects of additives in the $LiPF_6$/PC electrolyte on the morphologies of deposited lithium metal and the cycling performance of Li||NMC cells were investigated, and the morphological results are shown in Figure 80. It is seen that the baseline electrolyte leads to disordered and dendritic lithium growth. Adding VC or FEC can eliminate lithium dendrite formation, but the surface of deposited lithium is rough. Adding additive X gives ordered lithium nanorods growth, but the lithium surface is still rough. When using the additive mixtures of VC+X and FEC+X, the lithium surface is smoother and uniform and the lithium nanorods are more compact and well aligned. Detailed studies are under way and will be reported in next quarter.

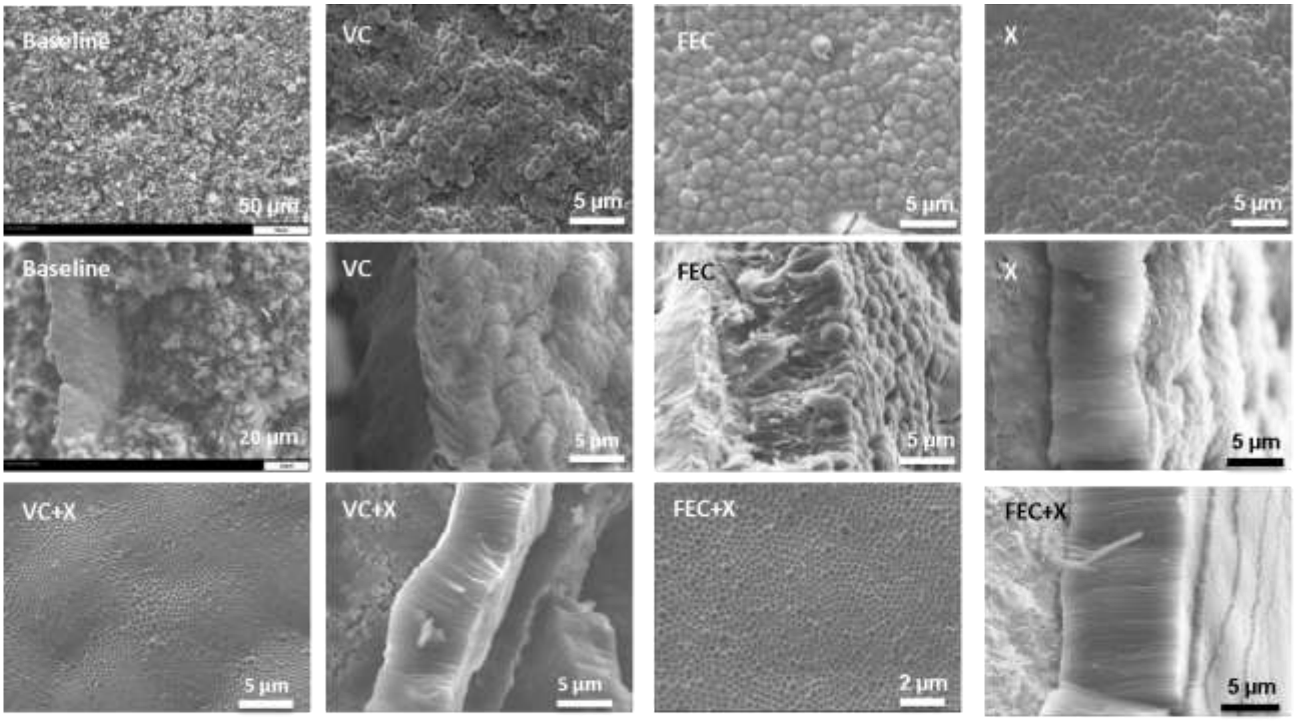

Figure 80. Scanning electron microscopy images (surface and cross-section views) of the deposited lithium metal on copper foils in electrolytes of 1 M $LiPF_6$/PC with different additives (VC, FEC, and X) and additive mixtures (VC+X and FEC+X) at 0.1 mA cm^{-2} for 15 hours.

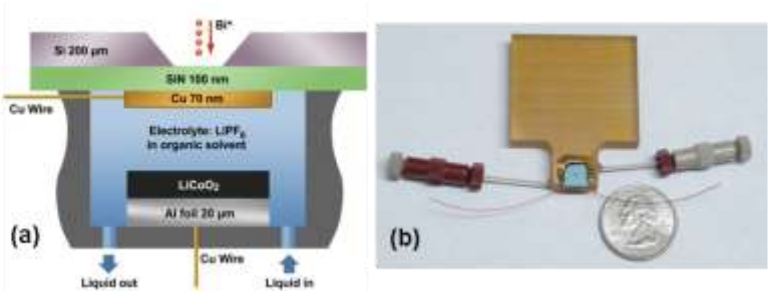

Figure 81. (a) A schematic drawing of the liquid cell device with both anode and cathode integrated into the liquid cell. (b) A photo of the real device.

The composition of the surface passivation layer of lithium anode during fast and slow discharge rates of the Li||$LiCoO_2$ cells was characterized by *in situ* TOF-SIMS. The electrolyte was 1.0 M $LiPF_6$ in EC-EMC. The schematic configuration and a photo of the cell are shown in Figure 81. The Cu||$LiCoO_2$ cell was charged first to deposit lithium on copper substrate at slow rate, and then the cell was discharged at fast (1C) and slow (C/5) rates. The composition of the surface layers formed on lithium anode was analyzed *in operando* by TOF-SIMS. Test results indicate that the difference in Li^+-content in SEI formed on lithium anode during fast and slow discharge rates (1C vs. C/5) is not significant enough to show whether a concentrated Li^+ electrolyte is formed during fast discharge (lithium stripping). This is probably because of technical limitations of the electrochemical cell and/or *in situ* TOF-SIMS.

Patents/Publications/Presentations

Publication

- Zheng, J., and M. H. Engelhard, D. Mei, S. Jiao, B. J. Polzin, J.-G. Zhang,* and W. Xu.* “Electrolyte Additive Enabled Fast Charging and Stable Cycling Lithium Metal Batteries.” *Nature Energy* 2 (2017): 17012.

Task 7.7 – Lithium Batteries with Higher Capacity and Voltage
(John B. Goodenough, University of Texas – Austin)

Project Objective. The project objective is to develop an electrochemically stable alkali-metal anode that can avoid the SEI layer formation and the alkali-metal dendrites during charge/discharge. To achieve the goal, a thin and elastic solid electrolyte membrane with a Fermi energy above that of metallic lithium and an ionic conductivity $\sigma > 10^{-4}$ S cm^{-1} will be tested in contact with alkali-metal surface. The interface between the alkali-metal and the electrolyte membrane should be free from liquid electrolyte, have a low impedance for alkali-metal transport and plating, and keep a good mechanical contact during electrochemical reactions.

Project Impact. An alkali-metal anode (lithium or sodium) would increase the energy density for a given cathode by providing a higher cell voltage. However, lithium is not used as the anode in today's commercial Li-ion batteries because electrochemical dendrite formation can induce a cell short-circuit and critical safety hazards. This project aims to find a way to avoid the formation of alkali-metal dendrites and to develop an electrochemical cell with dendrite-free alkali-metal anode. Therefore, once realized, the project will have a significant impact by an energy-density increase and battery safety; it will enable a commercial Li-metal rechargeable battery of increased cycle life.

Approach. The project will design, make, and test cells. The key approach is to introduce a solid-solid contact between an alkali metal and a solid electrolyte membrane. Where SEI formation occurs, the creation of new anode surface at dendrites with each cycle causes capacity fade and a shortened cycle life. To avoid the SEI formation, a thin and elastic solid electrolyte membrane would be introduced, or the solid electrolyte should not be reduced by, but should be wet by, a metallic alkali-ion anode.

Out-Year Goals. The out-year goal is to develop coin cells that are safe and low-cost with a long cycle life at a voltage $V > 3.0$ V.

Collaborations. This project collaborates with A. Manthiram at UT Austin, and Karim Zaghib at HQ.

Milestones

1. Demonstrate the cycle life and capacity of a Li-S cell. (Q1 – Complete)
2. Demonstrate a high-voltage cell containing the glass electrolyte. (Q2 – In progress)
3. Demonstrate a new battery concept. (Q3)
4. Test energy density, cycle life, rate of charge/discharge of the new battery concept. (Q4)

Progress Report

A solid Li-ion electrolyte with a small interfacial resistance for Li-ion transfer is a key component of an all-solid-state Li-ion battery. The project has introduced a 99.9% dense perovskite electrolyte $Li_{3/8}Sr_{7/16}Hf_{1/4}Ta_{3/4}O_3$ (LSHT) fired by SPS. LSHT has a room-temperature Li-ion conductivity $\sigma = 4.4 \times 10^{-4}$ S cm^{-1} and a small activation energy of 0.33 eV from 298 to 420 K (Figure 82). Another advantage of LSHT is its good stability in air; unlike the garnet electrolyte which reacts with moist air to form Li_2CO_3, there is no Li_2CO_3 detectable with a Raman shift at 1080 cm^{-1}on the surface of a perovskite LSHT pellet after exposure to air for three months.

Because of its stability, LSHT shows a small interfacial resistance with a solid polymer electrolyte and commercial organic electrolyte; moreover, it is chemically and electrochemically stable with polysulfide catholyte. An all-solid-state Li/$LiFePO_4$ battery with LSHT as electrolyte had a small resistance, high CE of 99.5–100%, and long cycling life (Figure 83). A Li-S battery with dense LSHT as a separator that blocks the polysulfide transport towards the Li-metal delivered an initial discharge capacity of 1100 mAh g^{-1}, had a high CE of 99.5%, and kept 93% capacity after 400 cycles.

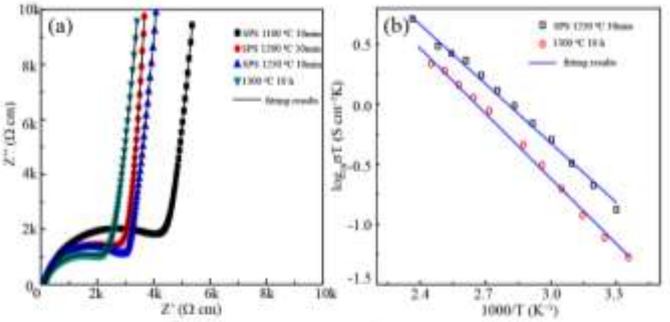

Figure 82. (a) Impedance spectra and (b) Arrhenius plot of LSHT pellet fired by spark plasma sintering.

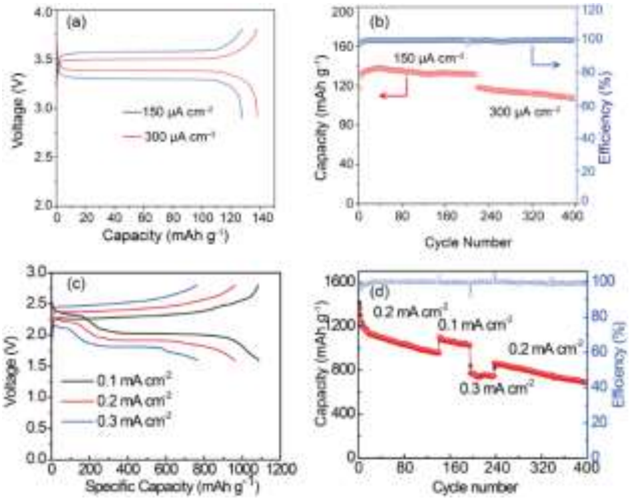

Figure 83. (a) Charge and discharge voltage profiles of Li/LSHT/$LiFePO_4$ at 150 and 300 μA cm^{-2}. (b) Capacity retention and cycling efficiency of $LiFePO_4$/Li cells. (c) Charge and discharge voltage profiles of Li-S battery with LSHT at different current densities. (d) Capacity retention and cycling efficiency of Li–S battery.

Task 7.8 – Advancing Solid-State Interfaces in Lithium-Ion Batteries
(Nenad Markovic and Larry A. Curtiss, Argonne National Laboratory)

Project Objective. The project objectives are multifaceted, including: (1) development of a new mechanically and chemically stable Li-selective solid "membrane" capable of protecting the metal lithium anode during the discharge process in commercially available liquid electrolytes (hereafter denoted as a S_{Li}-S_M-E_L system); and (2) development of a mechanically/chemically stable and Li-ion conductive ($\geq 2 \times 10^{-4}$ S/cm at 298K) solid electrolyte for a solid-state battery encompassing a metal lithium anode and nonflammable solid electrolyte that can operate at cathode potentials > 5 V (denoted as a S_{Li}-S_{EL}-S_C system).

Project Impact. Protective organic and inorganic compounds can enhance stability of interface, improve Li-ion interfacial transport, minimize dendrite formation, and increase safety in Li-ion batteries.

Approach. The project proposes to develop and use interdisciplinary, atomic-/molecular-level insight obtained from integrating both experimental- and computational-based methodologies to define the landscape of parameters that control interfacial properties for a new generation of the Li-ion solid-solid battery systems. The strategy will involve transferring knowledge gained from well-characterized thin-film materials to real-world materials. This strategy forms a closed loop wherein the knowledge gained from model systems is used to design more complex, real-world materials and vice-versa. The work will focus on utilizing existing in-house synthesis and characterization methods to enable rapid transition from fundamental science to realistic cells.

Out-Year Goals. The out-year goals are to use and develop the physical and chemical synthesis methods for design of solid-solid interfaces with unique chemical/mechanical/conductivity properties of S_{Li}-S_M-E_L and S_{Li}-S_{EL}-S_C systems. The proposed work will develop and exploit a variety of *ex situ* and *in situ* experimental optical and surface sensitive techniques and electrochemical methods to explore and explain bulk and interfacial properties of the selected materials. The results will serve to unravel many puzzling bulk and interfacial properties of S_{Li}-S_M-E_L and S_{Li}-S_{EL}-S_C materials.

Collaborations. This project funds work at ANL and University of Illinois at Chicago (Prof. Amin Salehi). It will establish collaboration with Jeff Sakamoto at University of Michigan.

Milestones

1. Development of new synthesis and characterization methods for controlled deposition of lithium on well-defined $SrTiO_3$ single crystals. (Q1 – In progress)
2. Use ultra high vacuum (UHV)-based experimental techniques in combination with computational methods to investigate parameters that control interaction of lithium anode with individual components of $Li_{6.5}La_3Zr_{1.5}M_{0.5}O_2$ (M = Nb, Ta) and Li_2CO_3 "membrane." (Q2 – In progress)
3. Design and develop *in situ* evaluation of stability of both Li_2CO_3 "membrane" (ICP-MS) and selected organic electrolytes during charge-discharge processes (DEMS). (Q3)
4. Investigate the CE of as well as the charge-discharge cyclability for selected S^{Li}-S_M-E_L and S_{Li}-S_{EL}-S_C systems. (Q4)

Progress Report

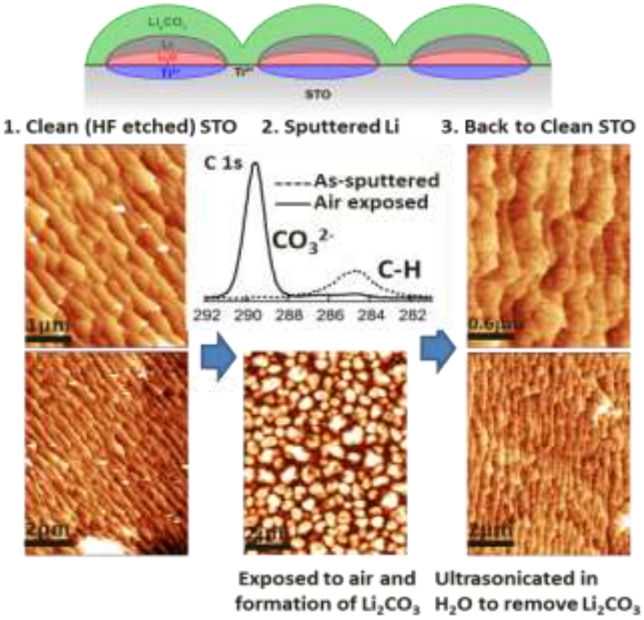

Figure 84. Atomic force microscopy and X-ray photoelectron microscopy results confirmed that lithium interaction with STO is rather weak, suggesting island growth of lithium atoms.

Interaction of lithium with $SrTiO_3$ (STO) single crystal substrate is explored by utilizing a combination of AFM and XPS. As summarized in Figure 84, from AFM analysis the project found that lithium deposition (sputtering in UHV) on STO (001) follows Stranski-Krastanov growth mechanism. Exposing to air leads to formation of $LiCO_3$, detected by XPS, which can be removed in water. Importantly, AFM image shows that after removal of $LiCO_3$, the terraces of STO are the same as in the case of as-prepared STO, suggesting weak interaction of lithium with the substrate.

The importance of experimental results goes well beyond the model Li-STO systems and, in the future, will be used for understanding lithium interaction with $Li/Li_{6.5}La_3Zr_{1.5}M_{0.5}O_2$ (M = Nb) interfaces, as summarized further below.

First, the project developed UHV sputter/characterization method for studying Li/LLZO interfaces. Figure 85 summarizes XPS results, which in contrast to Li/STO system, reveal that there is no chemical interaction between Li- and Al-doped LLZO components (see previous report). These results are further confirmed by XAS experiments performed at APS; see *total electron yield spectra* in the upper part of Figure 86. Notice that bulk *total fluorescence yield spectra* in the bottom part of Figure 86 indicate differences in surface and bulk chemistry and/or electronic structure, but the origin of these differences is unclear. Therefore, it will be of paramount importance to introduce well-defined LLZO interfaces (as in the case of STO) to understand Li/LLZO interfacial and bulk properties.

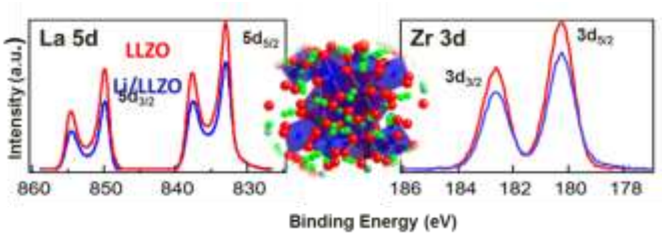

Figure 85. X-ray photoelectron microscopy results for lanthanum 5d and zirconium 3d peaks before and after lithium deposition on LLZO are the same, indicating weak chemical interactions.

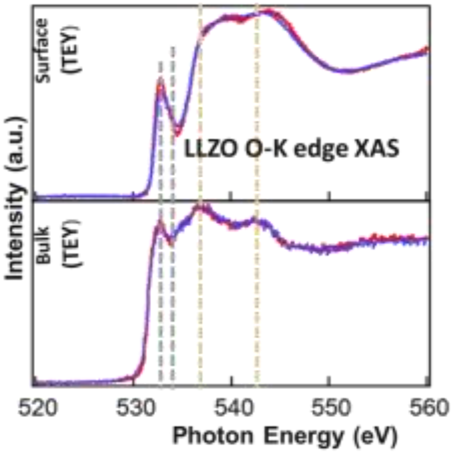

Figure 86. X-ray absorption spectroscopy results for monitoring surface and bulk properties of the Li-LLZO system.

Task 7.9 – Engineering Approaches to Dendrite-Free Lithium Anodes (Prashant Kumta, University of Pittsburgh)

Project Objective. This project will yield Li-metal anodes with specific capacity ≥ 2000 mAh/g (≥ 10 mAh/cm^2), ~ 1000 cycles, CE loss ≤ 0.01%, and CE ≥ 99.99% with superior rate capability. The goal is to (1) systematically characterize different approaches for generation of dendrite-free Li-metal anodes while also providing an understanding of the scientific underpinnings, and (2) evaluate the microstructure and electrochemical performance of the dendrite free Li-metal anodes. Generation of high-performance, dendrite free Li-metal anodes will successfully demonstrate generation of novel sulfur cathodes, affording the fabrication of Li-S batteries meeting the targeted gravimetric energy densities ≥ 350 Wh/kg and ≥ 750Wh/l with a cost target $125/kWh and cycle life of at least 1000 cycles for meeting the EV Everywhere Grand Challenge blueprint.

Project Impact. Dendrite formation in electrochemical systems occurs due to inhomogeneous current densities coupled with local diffusion gradients, surface roughness, and kinetic roughening. Lithium dendrite formation and growth are, however, not well-understood; adding to the complexity is the SEI formation. Control and elimination of Li-metal dendrite formation is a veritable challenge. If overcome, it would render the universal adoption of Li-anode batteries for stationary and mobile applications. The current project is a scientific study of novel approaches to address dendrite formation in Li-anode batteries, electrolyte decomposition, and associated cell failure. Development of dendrite-free, high-performance lithium anodes will enable the use of Li-free cathodes, opening myriad possibilities of pushing the envelope in terms of cathode capacity and battery energy density.

Out-Year Goals. This multi-year project comprises three major phases to be successfully completed in three years:

- Phase 1 (year 1) – Synthesis, characterization, and scale up of suitable PF (porous foams) for use as current collectors for lithium anodes and Li-ion conductor (LIC) materials to prepare multilayer porous foams (MPFs).
- Phase 2 (year 2) – Development of Li-rich SIA anodes, and generation of composite multilayer anodes.
- Phase-3 (year 3) – Advanced high-energy-density, high-rate, extremely cyclable cell development.

Collaborations. The project will involve collaboration with Dr. Moni Kanchan Datta (U Pitt) and Dr. Oleg I. Velikokhatnyi (U Pitt) as co-PIs, and Dr. Prashanth Jampani Hanumantha (U Pitt) as senior research personnel. In addition, collaboration will be undertaken with Dr. D. Krishnan Achary (U Pitt) for solid-state magic angle spinning nuclear magnetic resonance (MAS-NMR) characterization.

Milestones

1. Delegate tasks and convene the technical aspects between partners. (October 2016 – Complete)
2. Determine electrode and cell design parameters for achieving the targeted energy density. (October 2016 – Complete)
3. Identify and synthesize materials with high electronic conductivity, electrochemical stability that can be generated as porous architectures. (Q3 – In progress)
4. Prepare doped LIC with improved ionic conductivity for coating of PFs to prepare MPFs. (Q4 – In progress)

Progress Report

Phase 1 of the current project is aimed at development of PF materials and multilayer PFs with the aim of reducing orthogonal lithium nucleation and growth. Figure 87 shows attempts at the use of innovative architectural design to inhibit the formation of Li-dendrite during cycling, that is, porous metal alloy foams (PMFs) as novel dendrite resistant electrodes. PFs were prepared with varying amounts of hierarchical porosity/wall roughness. The effects of these factors on dendrite formation is still under study. Figure 88 shows the effect of using structurally isomorphous alloys (Li-SIA) as electrodes for Li-metal plating/de-plating. It can be seen in Figure 88a that upon cycling lithium metal on a copper current collector (cyclic voltammetry), most of the lithium is consumed via dendrite formation and SEI occurrence. On the other hand, Figure 88b-c shows that the Li-SIA electrodes exhibit both excellent charge retention and CE over extended cycling at high current densities on the order of ~80-100 mA/cm^2.

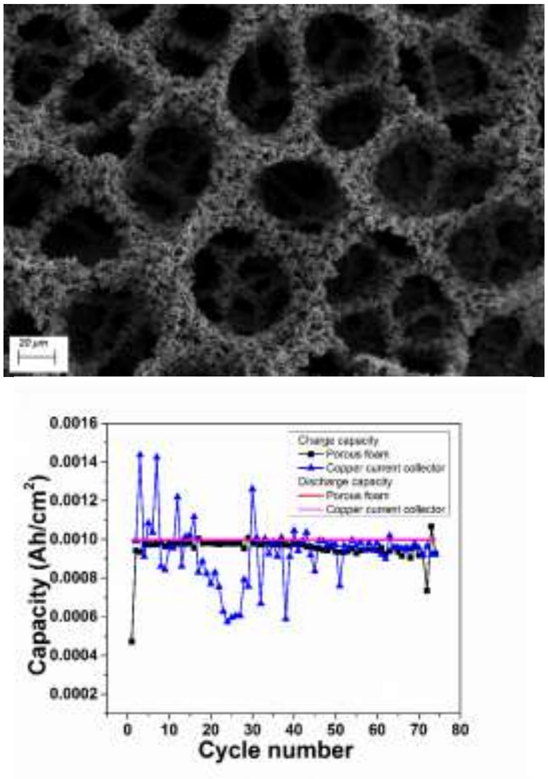

Figure 87. (a) Porous foams (PFs) with hierarchical porosity. (b) Improvement in Coulombic efficiency of lithium afforded by use of PFs.

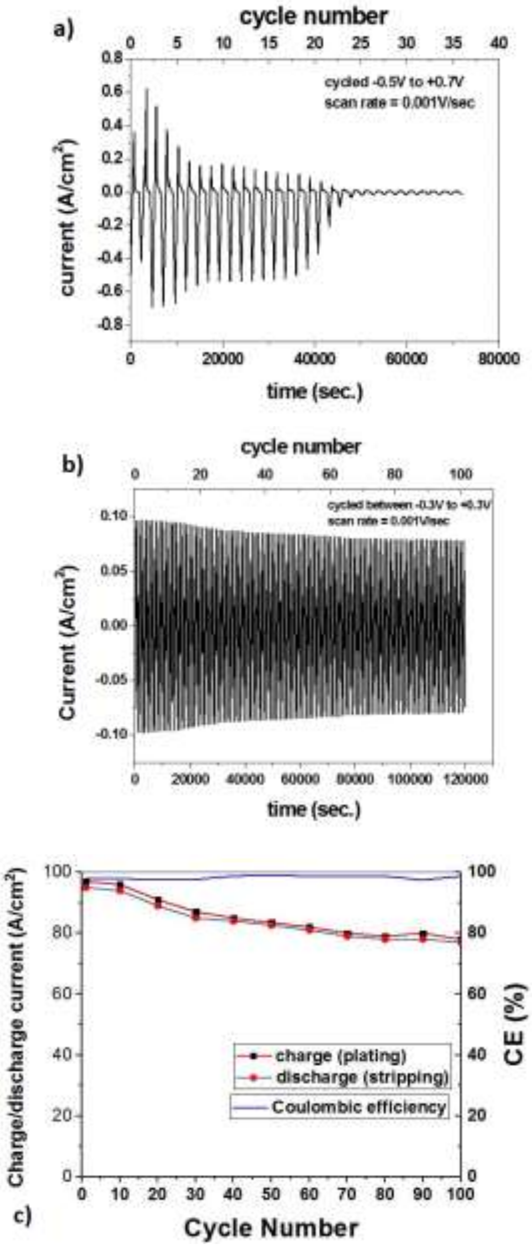

Figure 88. Current-time profiles of cyclic voltammetry of (a) lithium-copper current collector cell and (b) lithium-Li-SIA cell; (c) Coulombic efficiency of Li-SIA cell showing stability thereof.

Patents/Publications/Presentations

Publication

- Jampani, P. H., and P. M. Shanthi, B. A. Day, B. Gattu, O. I. Velikokhatnyi, M. K. Datta, and P. N. Kumta. "Lithium Metal Anode Based Rechargeable Batteries: Recent Advances and Challenges for the Future." *Progress in Materials Science* (2017). Under review.

Task 7.10 – Self-Assembling and Self-Healing Rechargeable Lithium Batteries (Yet-Ming Chiang, Massachusetts Institute of Technology; Venkat Viswanathan, Carnegie Mellon University)

Project Objective. The project objectives are as follows: (1) investigate formation of lithium halide containing SEI, (2) characterize the structure and composition of the SEI surface film and morphology of the electrochemically deposited lithium, and (3) develop combinations of electrolytes (solvents + salts) and electrolyte additives that produce a highly Li-ion conducting, mechanically robust, and self-healing SEI to suppress lithium dendrite formation and improve CE.

Project Impact. Efforts to achieve the practical use of the Li-metal anode in rechargeable lithium batteries have long been plagued by lithium dendrite formation and low CE. Lithium dendrites cause battery short-circuits, leading to serious safety hazards. The low CE of Li-metal anodes demands use of excess lithium to offset the lithium loss during cycling, which lowers the overall energy density of the battery. If successful, this project will enable self-forming and self-healing SEI containing alkali and/or alkaline earth halides that can suppress dendrite formation and improve CE. This will eventually enable high-energy-density (> 400 Wh/kg) and long cycle-life (> 500 cycles, 80% capacity retention) Li-metal batteries.

Approach. The project approach involves the following: (1) identify suitable combinations of solvents, Li-electrolyte salts, and halide and other additives that can produce highly Li-ion conducting, mechanically robust, and self-healing SEI, (2) use integrated theory and experiment, and (3) assemble and test symmetric and asymmetric cells and Li-metal batteries comprising a high areal-capacity cathode (> 3 mAh/cm^2) and a capacity-limited Li-metal anode (< 30% lithium excess).

Out-Year Goals. The project will down-select electrolyte compositions, develop designs for prototype full cells of >10 mAh capacity, and fabricate and deliver cells to DOE-specified laboratories for testing and evaluation.

Collaborations. This project collaborates with 4M Technologies Inc. (18 cm^2/80 cm^2 pouch cell fabrication and tests).

Milestones

1. Complete initial computations and halide solubility studies and construct experimental matrix of halides and solvents. (Q1 – Complete)
2. Demonstrate cell designs and electrochemical testing parameters that allow clear differentiation of dendritic and non-dendritic behavior of lithium electrodes. (Q2 – In progress)
3. Deliver characterization results for morphological evolution of Li-metal surface showing that halide additives diminish lithium dendrite formation. (Q3)
4. Demonstrate Li-Li symmetric cell using halide additives that outperforms additive-free cell according to criteria in Q2 and Q3. (Q4 – Go/No-Go milestone)

Progress Report

This quarter, results are reported for trends of solubility of lithium halides in different nonaqueous solvents that may be used to prepare lithium battery electrolytes.

A methodology was developed for predicting the trends of solubility of lithium halides in different solvents. To determine the trends, computed values of free energy of solvation for lithium and the halide anions, the free energy of formation of the halides, and the permittivity of the solvent were used. The solvation free energies are taken from the dataset from the work of Korth and co-workers. The free energies of solvation were calculated using COSMO (COnductor-like Screening MOdel) solvation model, which utilizes semi-empirical quantum mechanical (SQM) methods. The free energy of formation for the halides and dielectric constants for different organic solvents were taken from the CRC handbook of chemistry and physics.

The following trends for solubility of different lithium halides (LiF, LiCl, LiBr, LiI) in various solvents are predicted:

$$\mathrm{LiF} < \mathrm{LiCl} \ll \mathrm{LiBr} < \mathrm{LiI}$$

DMSO > Acetonitrile > Ethyl Acetate > THF > Dimethyl Carbonate > Propylene Carbonate > 1,3-dioxolane > 1,2-dimethoxyethane.

The predicted solubility trend for LiF in organic solvents is largely consistent with the previous experimental work [Wynn et al. *Talanta*, 31, no. 11 (1984): 1036]. Additional solubility tests were conducted to verify the predicted trend. Different amounts of lithium halides were dissolved into acetonitrile, dimethyl carbonate (DMC), 1,3-dioxolane, 1,2-dimethoxyethane, EC/DMC (1/1 by volume), and 1,3-dioxolane/ 1,2-dimethoxyethane (1/1 by volume) under inert atmosphere. LiI and LiBr were found to be quite soluble (LiI > 3 M and LiBr > 1 M in all the solvents tested), while LiCl and LiF dissolve very little (both < 0.05 M). Furthermore, the direct-current plasma emission spectroscopy technique was used to determine lithium concentration in a LiF-saturated DMC solution. The lithium concentration was found to be below the detection limit of the instrument used, which is 0.002 mM. These results suggest that if LiF is used as the electrolyte additive, its concentration may be too low to effectively passivate the Li-metal anode. Alternative options may be using more soluble lithium salts that can produce LiF *in situ* by reacting with lithium metal, such as $LiPF_6$, $LiBF_4$, LiFSI, and LiTFSI.

Additionally, the electrochemical window for different lithium halides in EC/DMC (1/1 by volume) was investigated. It was found that LiI, LiBr, and LiCl are oxidized at the potentials of > 3.0 V, > 3.4 V, and > 3.5 V vs Li^+/Li, respectively, while LiF is stable at least up to 4.5 V (electrolyte decomposition potential). These results suggest that LiI, LiBr, and LiCl additives may better be used for cathode materials with operation voltage lower than ~3 V, such as sulfur and TiS_2. LiF is suitable for intercalation cathode materials, such as LFP, LCO, NMC, and NCA.

TASK 8 – LITHIUM–SULFUR BATTERIES

Summary and Highlights

Advances in Li-ion technology have been stymied by challenges involved in developing high reversible capacity cathodes and stable anodes. Hence, there is a critical need for development of alternate battery technologies with superior energy densities and cycling capabilities. In this regard, Li-S batteries have been identified as the next flagship technology, holding much promise due to the attractive theoretical specific energy densities of 2,567 Wh/kg. In addition, realization of the high theoretical specific capacity of 1,675 mAh/g corresponding to formation of Li_2S using earth-abundant sulfur renders the system highly promising compared to other available cathode systems. Thus, the research focus has shifted to developing Li-S batteries. This system, however, suffers from major drawbacks, as elucidated below:

- Limited inherent electronic conductivity of sulfur and sulfur-compound based cathodes;
- Volumetric expansion and contraction of both the sulfur cathode and lithium anode;
- Soluble polysulfide formation/dissolution and sluggish kinetics of subsequent conversion of polysulfides to Li_2S, resulting in poor cycling life;
- Particle fracture and delamination as a result of the repeated volumetric expansion and contraction;
- Irreversible loss of lithium at the sulfur cathode, resulting in poor CE; and
- High diffusivity of polysulfides in the electrolyte, resulting in plating at the anode and consequent loss of driving force for lithium diffusion (that is, drop in cell voltage).

These major issues cause sulfur loss from the cathode, leading to mechanical disintegration. Additionally, surface passivation of anode and cathode systems results in a decrease in the overall specific capacity and CE upon cycling. Consequently, the battery becomes inactive within the first few charge-discharge cycles. Achievement of stable high capacity in Li-S batteries requires execution of fundamental studies to understand the degradation mechanisms in conjunction with devising engineered solutions. This Task addresses both aspects with execution of esoteric, fundamental *in situ* XAS and *in situ* electron paramagnetic resonance (EPR) studies juxtaposed with conducting innovative applied research comprising use of suitable additives, coatings, and exploration of composite morphologies as well as appropriate engineered strategies. Both ANL and LBNL use X-ray based techniques to study phase evolution and loss of CE in S- and S-Se based electrodes, primarily by the former during lithiation/delithiation while understanding polysulfide formation in sulfur and oligomeric PEO solvent by the latter, respectively. Work from PNNL, U Pitt, and Stanford demonstrates high areal capacity electrodes in excess of 4 mAh/cm^2. Following loading studies reported this quarter, PNNL performed *in situ* EPR to study reaction pathways mediated by sulfur radical formation. Coating/encapsulation approaches adopted by U Pitt and Stanford comprise flexible sulfur wire (FSW) electrodes coated with LIC by U Pitt, and TiS_2 encapsulation of Li_2S in the latter, both ensuring polysulfide retention at sulfur cathodes. BNL work on the other hand, has focused on benchmarking of pouch cell testing by optimization of the voltage window and study of additives such as LiI and $LiNO_3$. *Ab initio* studies at Stanford and U Pitt involve calculation of binding energies, diffusion coefficients, ionic conductivities and reaction pathways determination, augmenting the experimental results. Similarly, AIMD simulations performed at TAMU reveal multiple details regarding electrolyte decomposition reactions and the role of soluble polysulfides (PS) on such reactions. Using kinetic Monte Carlo (KMC) simulations, electrode morphology evolution and mesostructured transport interaction studies were also executed. Studies over the last quarter at PNNL suggest that proper control of electrode porosity/thickness is essential for obtaining high-energy Li-S batteries. Porosity shows strong dependence on calendering pressure because of low tap densities of electrode components such as sulfur and carbon. Increasing the calendering-pressure from 0.2 to 1.5 ton (T) leads to rapid decrease of electrode porosity, resulting in improvement of electrode volumetric energy density. Measured electrode volumetric energy density increased from 650 Wh L^{-1} for as-cast electrode (120 μm thick) to 1300 Wh L^{-1} for electrode compressed to 60 μm.

Additionally, Penn State has shown use of dimethyl disulfide as a functional co-solvent, demonstrating its ability to show an alternate electrochemical reaction pathway for sulfur cathodes by formation of dimethyl polysulfides and lithium organosulfides as intermediates and reduction products. Further, University of Wisconsin has conducted high-performance liquid chromatography (HPLC)-MS studies and has determined the distribution of polysulfides at various discharge and recharge reactions. UT Austin, at the same time, has shown that by integrating polysulfide filter coated separators fabricated with carbon nanofibers, the cells retain 50% of the initial capacity after storing for one year and exhibit a low self-discharge rate of only 0.14% per day.

Each of these projects has a collaborative team of experts with the required skill set needed to address the EV Everywhere Grand Challenge of 350 Wh/kg and 750 Wh/l and cycle life of at least 1000 cycles.

Highlights. This Task reports the following project highlights for this quarter:

1. Studies at U Pitt (Kumta) have shown directly doped sulfur assembly (DDSA) electrodes with 1305 mAh/g and a very low fade rate of ~0.0014%/cycle.
2. Using sulfide catalysts, Li_2S electrodes were demonstrated with capacities (S-VS_2@G/CNT electrode) of 830 mA h g^{-1} and the capacity remains at 701 mA h g^{-1} after 300 cycles with stabilized CE above 99.5% (Cui-Stanford).
3. Using electrodes of varying loadings, work at PNNL (Liu and Lu) has shown that the fade characteristics vary with electrode thickness, with thicker electrodes exhibiting higher fade. They note that the rapid capacity drop occurring in the early stage of cycling is possibly due to formation, free diffusion, and loss of soluble polysulfides when an excess amount of electrolyte (electrolyte/sulfur=10 µL/mg) is present. Using *in situ* EPR and HPLC tests, it has been identified that the electrolyte additive $LiNO_3$ (partly used for protection of lithium anode) can directly react with Li_2S/Li_2S_2/polysulfides and lose its function.

Task 8.1 – New Lamination and Doping Concepts for Enhanced Lithium–Sulfur Battery Performance (Prashant N. Kumta, University of Pittsburgh)

Project Objective. The project objective is to successfully demonstrate generation of novel sulfur cathodes for Li-S batteries meeting targeted gravimetric energy densities ≥ 350 Wh/kg and ≥ 750 Wh/l with a cost target of $125/kWh and cycle life of at least 1000 cycles for meeting the EV Everywhere Grand Challenge blueprint. The proposed approach will yield sulfur cathodes with specific capacity ≥ 1400 mAh/g, at ≥ 2.2 V, generating ~ 460 Wh/kg energy density higher than the target. Full cells meeting required deliverables will also be made.

Project Impact. Identifying new laminated S-cathode-based systems displaying higher gravimetric and volumetric energy densities than conventional Li-ion batteries will likely result in new commercial battery systems that are more robust, capable of delivering better energy and power densities, and more lightweight than current Li-ion battery packs. Strategies and configurations based on new LIC-coated sulfur cathodes will also lead to more compact battery designs for the same energy and power density specifications as current Li-ion systems. Commercialization of these new S-cathode-based Li-ion battery packs will represent, fundamentally, a major hallmark contribution of the DOE VTO and battery community.

Out-Year Goals. This multi-year project comprises three phases to be successfully completed in three years:

- Phase 1 (year 1) – Synthesis, characterization, and scale up of suitable LIC matrix materials and multilayer composite sulfur cathodes. (Complete)
- Phase 2 (year 2) – Development of LIC-coated sulfur nanoparticles, scale up of high-capacity engineered LIC-coated multilayer composite electrodes, and doping strategies to improve electronic conductivity of sulfur.
- Phase 3 (year 3) – Advanced high-energy-density, high-rate, extremely cyclable cell development.

Collaborations. The project collaborates with the following members: Dr. Spandan Maiti (U Pitt) for mechanical stability and multi-scale modeling; Dr. A. Manivannan (NETL) for XPS for surface characterization; and Dr. D. Krishnan Achary (U Pitt) for solid-state MAS-NMR characterization.

Milestones

1. Develop novel LIC membrane systems using *ab initio* methods displaying impermeability to sulfur diffusion, and demonstrate generation of novel sulfur 1D, 2D and 3D morphologies exhibiting superior stability and capacity. (June 2015 – Complete)

2. Prepare doped LIC with improved ionic conductivity. (January 2016 – Complete)

3. Apply ceramic filler incorporated CPEs to improve the specific capacity of commercial sulfur to ~ 812 mAh/g for over 100 cycles. (October 2016 – Complete)

4. Design and engineer high-capacity, LIC-coated sulfur nanoparticle. (January 2017 – Complete)

5. Generate integrated doped nanoparticulate sulfur-VACNT-LIC composite integrated electrode [comprised of DDSA-polysulfide trapping agent (PTA)]. (April 2017 – Complete)

6. Optimize doping composition and thickness to maximize capacity, rate capability, and cycling stability. Prismatic/pouch-type full cell assembly and testing of integrated electrode with optimum thickness. (In progress)

Progress Report

Phase 2 of the current project concluded with successful improvement in ionic conductivity of an LIC brought by doping, altering of the electronic structure of sulfur by incorporation of like-sized dopants, and designing effective methods for coating LIC onto sulfur cathodes. In Phase 1, commercial separator was replaced with an LIC that demonstrated complete prevention of polysulfide dissolution. The primary aims of Phase 3 are generation of integrated doped nanoparticulate sulfur-vertically aligned carbon nanotube, VACNT-LIC composite electrode, business value analysis and fabrication of the desired 4 mAh full cell. The first quarter of Phase 3 involved comprehensive physical and chemical property analysis of composite polymer electrolytes (CPEs) developed in the last quarter of Phase 2, which when tested against commercial sulfur cathodes demonstrated very stable capacity of ~ 812 mAh/g after 100 cycles, displaying minimal fade rate of 0.012%/cycle. This second quarter of Phase 3 involved development of DDSA electrode with very high sulfur loadings of ~ 18 mg/cm^2 and generation of PTA-coated DDSA electrodes with polysulfide trapping property, as depicted in Figure 89. The PTA-coated DDSA electrode shows excellent electrochemical cycling response with an initial capacity of 1305 mAh/g at 0.2C rate with less than 0.0014%/cycle fade in capacity for over 30 cycles, as shown in Figure 90a. Further, the PTA-coated DDSA electrode shows exceptional binding of the polysulfide species as confirmed by ultraviolet visible spectroscopy (UV/Vis), which explains the excellent cycling stability of these electrodes, as displayed in Figure 90b.

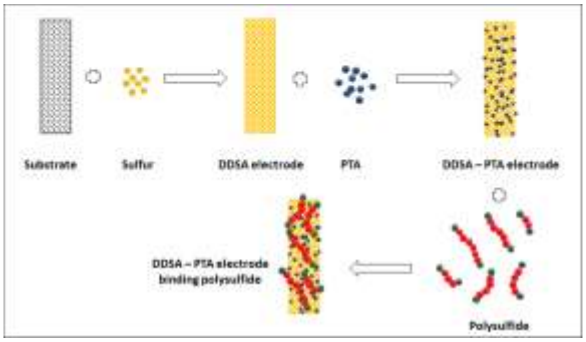

Figure 89. Schematic showing the interaction of polysulfide trapping agent with polysulfide.

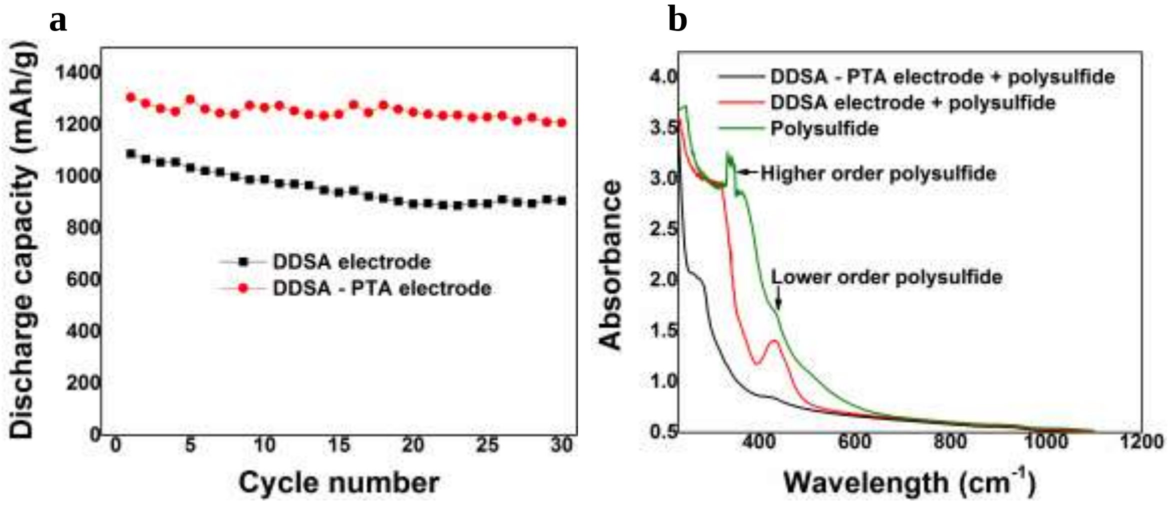

Figure 90. (a) Cycling performance of PTA-DDSA (polysulfide-trapping-agent-coated directly doped sulfur assembly) electrode. (b) Ultraviolet visible spectroscopy absorption studies on the electrodes treated in polysulfide solution.

Patents/Publications/Presentations

Patent

- Jampani, P. H., and B. Gattu, P. M. Shanthi, and P. N. Kumta. "Novel Electro-Spun Sulfur Wires for Fabricating Mattes of Li-Sulfur Batteries." International Patent Number: WO 2016/145429 A1, U.S. Provisional Patent, Application Number: PCT/US2016/022283. (Filing date: 03/14/2016)

Publications

- Jampani, P. H., and B. Gattu, P. M. Shanthi, S. S. Damle, Z. Basson, R. Bandi, M. K. Datta, S. K. Park, and P. N. Kumta. "Flexible Sulfur Wires (Flex-SWs) – A Versatile Platform for Lithium-Sulfur Batteries." *Electrochimica Acta* 212 (2016): 286–293.
- Shanthi, P. M., and P. H. Jampani, B. Gattu, M. Sweeney, M. K. Datta, and P. N. Kumta. "Nanoporous Non-Carbonized Metal Organic Frameworks (MOFs): Effective Sulfur Hosts for High Performance Li-S Batteries." *Electrochimica Acta* 229 (2017): 208–218.

Task 8.2 – Simulations and X-Ray Spectroscopy of Lithium–Sulfur Chemistry (Nitash Balsara, Lawrence Berkeley National Laboratory)

Project Objective. Li-S cells are attractive targets for energy storage applications, as their theoretical specific energy of 2600 Wh/kg is much greater than the theoretical specific energy of current Li-ion batteries. Unfortunately, the cycle-life of Li-S cells is limited due to migration of species generated at the sulfur cathode. These species, collectively known as polysulfides, can transform spontaneously, depending on the environment, and it has thus proven difficult to determine the nature of redox reactions that occur at the sulfur electrode. The project objective is to use XAS to track species formation and consumption during charge-discharge reactions in a Li-S cell. Molecular simulations will be used to obtain X-ray spectroscopy signatures of different polysulfide species, and to determine reaction pathways and diffusion in the sulfur cathode. The long-term objective is to use mechanistic information to build high specific energy lithium-sulfur cells.

Project Impact. Enabling rechargeable Li-S cells has potential to change the landscape of rechargeable batteries for large-scale applications beyond personal electronics due to: (1) high specific energy, (2) simplicity and low cost of cathode (the most expensive component of Li-ion batteries), and (3) earth abundance of sulfur. The proposed diagnostic approach also has significant potential impact, as it represents a new path for determining the species that form during charge-discharge reactions in a battery electrode.

Out-Year Goals. The out-year goals are as follows:

- **Year 1.** Simulations of sulfur and PSL in oligomeric PEO solvent. Prediction of X-ray spectroscopy signatures of PSL/PEO mixtures. Measurement of X-ray spectroscopy signatures of PSL/PEO mixtures.
- **Year 2.** Use comparisons between theory and experiment to refine simulation parameters. Determine speciation in PSL/PEO mixtures without resorting to ad hoc assumptions.
- **Year 3.** Build an all-solid lithium-sulfur cell that enables measurement of X-ray spectra *in situ*. Conduct simulations of reduction of sulfur cathode.
- **Year 4.** Use comparisons between theory and experiment to determine the mechanism of sulfur reduction and Li_2S oxidation in all-solid Li-S cell. Use this information to build Li-S cells with improved life-time.

Collaborations. This project collaborates with Tsu-Chien Weng, Dimosthenis Sokaras, and Dennis Nordlund at SSRL, SLAC National Accelerator Laboratory in Stanford, California.

Milestones

1. Continue *in situ* XAS and other spectroscopies to determine reaction products as a function of charge/discharge rate. (December 2016 – Complete)
2. Theoretical prediction of polysulfide solution composition based on thermodynamic calculations of polysulfide and disproportionation reaction Gibbs free energy. (February 2017 – Complete)
3. Employ carbon confinement strategies and demonstrate improved cycle life relative to all solid Li-S cells with unconfined sulfur. (June 2017 – On Schedule)
4. Perform *in situ* XAS on Li-S cells containing PFPE electrolytes; determine reaction products in absence of polysulfide dissolution. (September 2017 – On schedule)

Progress Report

In situ study of the reactions happening at the front of the cathode have been challenging due to the uncontrolled dissolution of lithium polysulfides into the electrolytes during cycling. The signals obtained when probing X-ray from the anode side, aimed to look at reactions happening at the front of the cathode, were complicated by the absorption from the polysulfides species in the electrolyte layer. The team has discovered a new solid electrolyte membrane that may overcome this issue. This cross linked PFPE has a good ionic conductivity (10^{-4} S/cm) at 90°C, and its fluorinated nature may prevent a significant amount of polysulfides dissolving outside of the cathode. The team examined polysulfide dissolution into the electrolyte with transmission UV/Vis spectroscopy, as shown in figure 91.

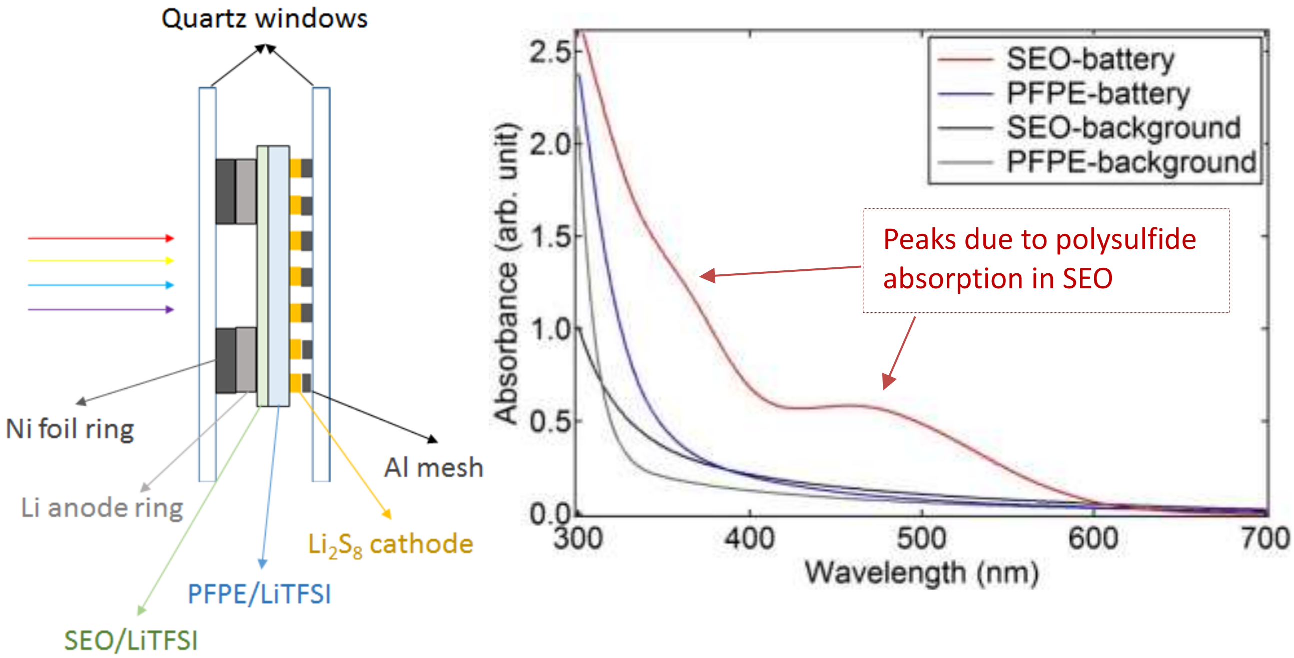

Figure 91. (left) Schematic of a Li-S cell used for transmission ultraviolet visible (UV/Vis) spectroscopy to examine dissolution of polysulfides out of the cathode. (right) UV/Vis absorption for the cell with and without the PFPE/LiTFSI layer.

Both the cathode and anode and current collectors are not light transparent. The electrolyte materials, however, allows UV/Vis light to go through. The left figure is a schematic showing the design to examine the amount of polysulfides dissolved into the electrolyte using a lithium ring as anode while the cathode is casted on an aluminum mesh material. On the right are the absorption results showing two cells after 5 cycles with and without the PFPE/LiTFSI layer. Lithium polysulfides absorb visible light strongly, as seen in the case of SEO battery without the PFPE layer. However, when the PFPE layer is added, there is no absorption peak. The background of pure PFPE/LiTFSI layer and SEO/LiTFSI layer present no absorption peaks in the range of interest, indicating that the absorption peak must come from the polysulfides dissolved into the SEO electrolyte. The lack of absorption peak indicates that the dissolution of lithium polysulfides out of the cathode is strongly limited using a PFPE layer. With this material, the team can study the reactions in the front of the cathode without the confusion of any polysulfide signal coming from the electrolyte.

Patents/Publications/Presentations

Publication

- Pascal, T. A., and I. Villaluenga, K. Wujcik, D. Devaux, X. Jiang, D. R. Wang, N. Balsara, and D. Prendergast. “Liquid Sulfur Impregnation of Microporous Carbon Accelerated by Nanoscale Interfacial Effects.” *Nano Letters*, (2017). Accepted.

Task 8.3 – Novel Chemistry: Lithium Selenium and Selenium Sulfur Couple (Khalil Amine, Argonne National Laboratory)

Project Objective. The project objective is to develop a novel S_xSe_y cathode material for rechargeable lithium batteries with high energy density and long life, as well as low cost and high safety.

Project Impact. Development of a new battery chemistry is promising to support the goal of PHEV and EV applications.

Approach. The dissolution of lithium polysulfides in nonaqueous electrolytes has been the major contribution to the low energy efficiency and short life of Li/S batteries. In addition, the insulating characteristics of both end members during charge/discharge (S and Li_2S) limit their rate capacity. To overcome this problem, sulfur or Li_2S are generally impregnated in a carbon conducting matrix for better electronic conductivity. However, this makes it difficult to increase the loading density of practical electrodes. It is proposed here to solve the above barriers using the following approaches: (1) partially replace sulfur with selenium and (2) nano-confine the S_xSe_y in a nanoporous conductive matrix.

Out-Year Goals. When this new cathode is optimized, the following result can be achieved:

- A cell with nominal voltage of 2 V and energy density of 600 Wh/kg.
- A battery capable of operating for 500 cycles with low capacity fade.

Collaborations. This project engages in collaboration with the following: Professor Chunsheng Wang of University of Maryland, Dr. Yang Ren and Dr. Chengjun Sun of APS at ANL, and Dr. Luis Estevez at PNNL.

Milestones

1. Investigating the impact of fluorinated solvents for Se-S systems. (December 2016 – Complete)
2. Investigating the effect of the pore volume of carbon matrix on high-loading Se-S systems. (Complete)
3. Investigating the effect of the pore size and specific surface area of carbon matrix on high-loading Se-S systems. (Q2 – In progress)
4. Exploration of novel electrolytes for high-loading Se-S systems. (Q3)
5. Synthesis of Se-S/carbon composites with high loading such as 7 wt% and high performance. (Q4)

Progress Report

Last quarter, the team initiated the study of high-loading selenium-sulfur for rechargeable Li-S batteries, which is crucial for their ovell energy density. It is well known that the pore structure of the carbon matrix plays a critical role on the electrochemical performance of S-C composites. Therefore, the team designed and synthesized three kinds of hierarchical porous carbon (HPC) materials with different pore size distribution and pore volume as well as specific surface area.

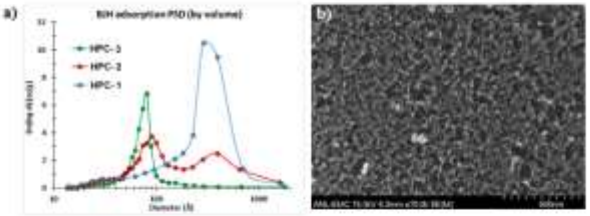

c)

	Pore size	Specific surface area, m^2/g	Pore volume, cc/g
HPC1	40 nm	1446	6.053
HPC2	10 nm, 40 nm	1039	2.671
HPC3	8 nm	818	1.464

Figure 92. (a) Pore size distribution of hierarchical porous carbon (HPC) materials and (c) the calculated specific surface and pore volume. (b) A typical scanning electron microscopy image of HPC1.

As shown in Figure 92a, the HPC1 has a main pore size distribution of around 40 nm and a ultra-high pore volume of 6.053 cc/g. The porous structure was further evidenced by its SEM image in Figure 92b. The high pore volume can benefit the high loading of sulfur, while it is generally considered that the relatively larger pore size will weaken its confinement on soluble polysulfides due to the capillarity effect. Therefore, HPC2 and HPC3 with smaller pore size distribution were furter synthesized. However, it was found that their pore volume also decreased to 2.671 and 1.464 cc/g, respectively. Based on melt-diffusion method, the team prepared three kinds of S/HPC composites with a sulfur loading of 70 wt% and further evaluated their electrochemical performance using the ANL-1 electrolytes developed in FY 2016.

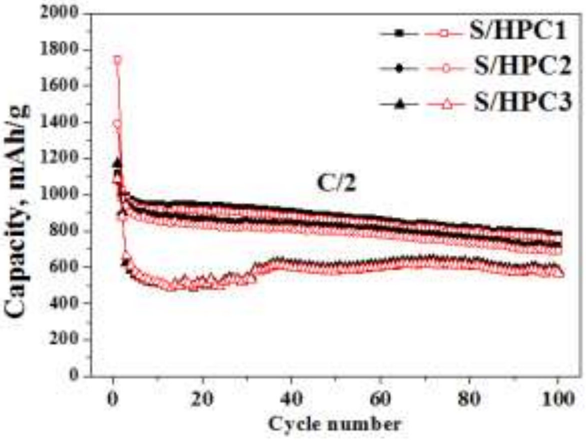

Figure 93. Cycle performance of Sulfur/hierarchical porous carbon composites with sulfur loading of 70 wt% as cathode of Li-S batteries at C/2.

As shown in Figure 93, S/HPC1 can still maintain a reversible capacity of around 800 mAh/g after 100 cycles of charge/discharge at C/2 (0.84 A/g), demonstrating excellent cycle stability. The reversible capacity of S/HPC2 was slightly lower than S/HPC1, which can deliver a reversible capacity of around 700 mAh/g after 100 cycles. However, the reversible capacity of S/HPC3 was significantly decreased to around 500 mAh/g and slightly recovered to 566 mAh/g after 100 cycles, presenting the poorest electrochemical performance. Nevertheless, it can be found that the polysulfides shuttle effect was suppressed, further evidencing the advantages of ANL-1 electrolytes of low polysulfides/polyselenide dissolution. The reversible capacity difference amongst different S/HPC composites should be attributed to their pore volume difference. The HPC3 can only theoretically load 60 wt% sulfur based on its pore volume. Therefore, extra sulfur will be distributed on the surface of HPC1, and then dissolved in the electrolytes and further led to its lower reversible capacity. In comparison, HPC1 and HPC2 can theoretically encapsulate 90 wt% and 75 wt% sulfur. Therefore, most of the sulfur can be well confined in the pores of HPC1 and HPC2, leading to better cycle stability.

Therefore, the team concluded that high pore volume is necessary for high Se-S loading systems, while it is not necessary for the pore size to be small (2-10 nm). The team plans to further increase the sulfur loading to 85 wt% to approach the theoretical limit of HPC1. It also plans to conduct surface coating to simultaneously enhance the electronic conductivity and confine the soluble polysulfides. Results will be provided next quarter.

Patents/Publications/Presentations

Publication

- Xu, Gui-Liang, and Jianzhao Liu, Zonghai Chen, and Khalil Amine. "Selenium and Selenium-Sulfur Chemistry for Rechargeable Lithium Batteries: Interplay of Cathode Structures, Electrolytes, and Interfaces." *ACS Energy Letters* 2, no. 3 (2016): 605–614.

Task 8.4 – Multi-Functional Cathode Additives for Lithium–Sulfur Battery Technology (Hong Gan, Brookhaven National Laboratory; and Co-PI Esther Takeuchi, Brookhaven National Laboratory and Stony Brook University)

Project Objective. Develop a low-cost battery technology for PEV application utilizing Li-S electrochemical system by incorporating multi-functional cathode additives (MFCA), consistent with the long-term goals of the DOE EV Everywhere Grand Challenge.

Project Impact. The Li-S battery system has gained significant interest due to its low material cost potential (35% cathode cost reduction over Li-ion) and its attractive 2.8x (volumetric) to 6.4x (gravimetric) higher theoretical energy density compared to conventional Li-ion benchmark systems. Commercialization of this technology requires overcoming several technical challenges. This effort will focus on improving cathode energy density, power capability, and cycling stability by introducing MFCA. The primary deliverable is to identify and characterize the best MFCA for Li-S cell technology development.

Approach. TM sulfides are evaluated as cathode additives in sulfur cathode due to their high electronic conductivity. Electrochemically active additives are also selected for this investigation to further improve energy density of the sulfur cell system. In the first year, the project established individual baseline sulfur and TM sulfide coin cell performances, and demonstrated strong interactions between sulfur and various MFCA within the hybrid electrode. During the second year, the project identified TiS_2 as the best MFCA candidate and demonstrated the particle size/BET surface area effect on Li-S cell electrochemical performance. In addition, sulfur electrode binder and carbon additives were optimized to achieve high sulfur loading up to 10 mg/cm^2 with good mechanical integrity. This year, the project targets to achieve optimized Li-S cell electrochemical performance by incorporating TiS_2 additive into the cathode formulation with new binder and new carbon additive. Electrode preparation process conditions and cell design factors will also be examined. The cell activation and cycling conditions will be defined, and 4 mAh sample cells will be built for DOE evaluation.

Out-Year Goals. This is a multi-year project comprised of two major phases to be completed in three years. Phase 1 was successfully completed during year 2, with selection of TiS_2 as the leading MFCA. Entering Phase 2, the project has completed binder and carbon selection. In the third year, tasks include cathode formulation optimization, process optimization, cell design optimization, cell activation, and testing optimization. At the end, the project will build 4 mAh sample cells for DOE testing. The mechanistic studies of MFCA and sulfur interaction will continue throughout the year to advance fundamental understanding of the system.

Collaborations. This project collaborates with Dong Su, Xiao Tong, and Yu-chen Karen Chen-Wiegart at BNL and with Amy Marschilok and Kenneth Takeuchi at SBU.

Milestones

1. Cathode formulation and process optimization with TiS_2. (Q1 – Complete)
2. Cathode loading/density effect and power optimization. (Q2 – Complete)
3. Cell design and cell activation procedure development. (Q3 – In progress)
4. 4 mAh cell samples preparation and confirmation study. (Q4 – On schedule)

Progress Report

Last quarter, the team defined the optimized sulfur electrode formulation with TiS_2 as cathode additive. In addition, the cathode preparation process to achieve uniform TiS_2 distribution was determined. This quarter, the team focused on electrode optimization, including carbon particle size, sulfur loading, and cathode density.

Carbon Particle Size Effect. Carbon particle size has significant impact on the mechanical integrity of the electrodes with high sulfur loading. The team achieved 10 mg/cm^2 sulfur loading by selecting M97 carbon. To improve the sulfur electrode rate capability or sulfur utilization, the M97 carbon sample was milled to reduce its particle size (see Figure 94). With both carbon samples, the electrodes of sulfur loading ranging from 1.2 to 5.5 mg/cm^2 were processed with good mechanical integrities. Interestingly, the carbon particle size effect is not linear on the discharge rate capability for the sulfur electrode. Under low discharge current density (< 1.0 mA/cm^2), sulfur electrodes with smaller particle size carbon do show higher sulfur utilization than the one with unmilled carbon. However, at the higher discharge current density (> 1.0 mA/cm^2), the opposite is observed (Figure 95). For now, the unmilled carbon is used for the following sulfur loading and electrode density study.

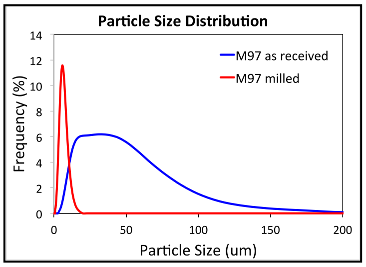

Figure 94. M97 carbon milling.

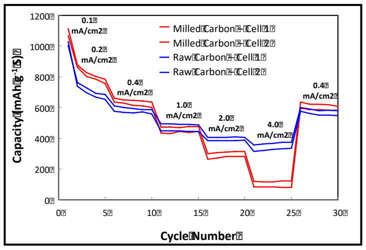

Figure 95. Carbon PS versus sulfur utilization.

Sulfur Loading and Electrode Density Study. The sulfur loading study is combined with electrode density effect evaluation to understand their interaction. With standard cathode formulation in the presence of TiS_2 additive, the electrodes of sulfur loadings ~2.7, ~4.9, and ~6.7 mg/cm^2 were prepared with good mechanical integrity. The as-coated pristine electrodes have density at ~ 0.8 g/cc for all three sulfur loadings. Higher electrode densities were achieved by hydraulic compressing of the electrodes under various pressures. The electrode density increases with increasing pressure and starts to level off at ~ 1.20 to 1.35 g/cc. The electrode density has profound effect on coin cell discharge performance, and the impact is more significant on the higher sulfur loading electrodes and at higher discharge rate (Figure 96). Low sulfur loading and low electrode density favor the high sulfur utilization during cell discharge at all current densities ranging from 0.1 mA/cm^2 to 4.0 mA/cm^2. The best electrochemical performance is derived from cells with pristine electrodes. Based on the team's estimation, the cathode porosity at density of 0.8 g/cc is ~ 65%, which is about 1.4 x the porosity of the 1.2 g/cc density electrode (47% porosity). The results suggest that maintaining the good ionic conductivity with increased electrolyte amount in the cathode pores and cell stack might be a critical factor for enhancing the sulfur electrode discharge power capability.

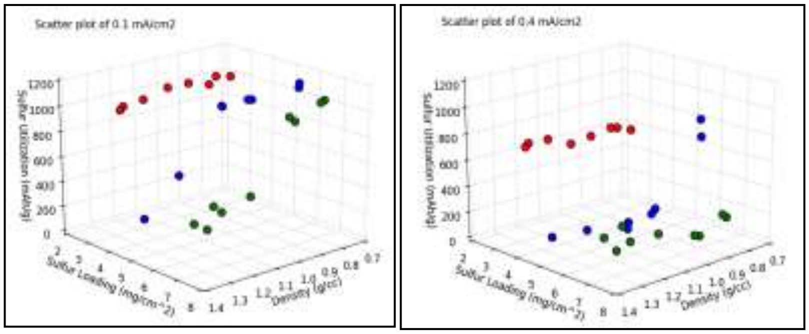

Figure 96. Sulfur utilization versus cathode density, sulfur loading, and discharge rate.

Patents/Publications/Presentations

Publications

- Zhang, Qing, and David C. Bock, Kenneth J. Takeuchi, Amy C. Marschilok, and Esther S. Takeuchi. "Probing Titanium Disulfide-Sulfur Composite Materials for Li-S Batteries via *In Situ* X-ray Diffraction (XRD)." *J. of Electrochem. Society* 164, no. 4 (2017): A897–A901.
- Sun, Ke, and Christina A. Cama, Jian Huang, Qing Zhang, Sooyeon Hwang, Dong Su, Amy C. Marschilok, Kenneth J. Takeuchi, Esther S. Takeuchi, and Hong Gan. "Effect of Carbon and Binder on High Sulfur Loading Electrode for Li-S Battery Technology." *Electrochimica Acta* 235 (2017): 399–408. http://dx.doi.org/10.1016/j.electacta.2017.03.023.

Task 8.5 – Development of High-Energy Lithium–Sulfur Batteries
(Jun Liu and Dongping Lu, Pacific Northwest National Laboratory)

Project Objective. The project objective is to develop high-energy, low-cost Li-S batteries with long lifespan. All proposed work will employ thick sulfur cathode (≥ 2 mAh/cm^2 of sulfur) at a relevant scale for practical applications. The diffusion process of soluble polysulfide out of thick cathode will be revisited to investigate cell failure mechanism at different cycling. Alternative anode will be explored to address the lithium anode issue. The fundamental reaction mechanism of polysulfide under the electrical field will be explored by applying advanced characterization techniques to accelerate development of Li-S battery technology.

Project Impact. The theoretical specific energy of Li-S batteries is ~2300 Wh/kg, which is almost three times higher than that of state-of-the-art Li-ion batteries. The major challenge for Li-S batteries is polysulfide shuttle reactions, which initiate a series of chain reactions that significantly shorten battery life. The proposed work will design novel approaches to enable Li-S battery technology and accelerate market acceptance of long-range EVs required by the EV Everywhere Grand Challenge.

Out-Year Goals. This project has the following out-year goals:

- Fabricate Li-S pouch cells with thick electrodes to understand sulfur chemistry/electrochemistry in the environments similar to the real application.
- Leverage the Li-metal protection project funded by the DOE and PNNL advanced characterization facilities to accelerate development of Li-S battery technology.
- Develop Li-S batteries with a specific energy of 400 Wh/kg at cell level, 1000 deep-discharge cycles, improved abuse tolerance, and less than 20% capacity fade over a 10-year period to accelerate commercialization of electrical vehicles.

Collaborations. This project engages in collaboration with the following:

- Dr. Xiao-Qing Yang (LBNL) − *In situ* characterization
- Dr. Deyang Qu (University of Wisconsin – Milwaukee) – Electrolyte Analysis
- Dr. Xingcheng Xiao (GM) – Materials testing
- Dr. Jim De Yoreo (PNNL) – *In situ* characterization

Milestones

1. Study thick sulfur electrode (≥ 4 mg/cm^2) with controlled porosity/thickness; demonstrate 80% capacity retention for 200 cycles. (Q1 – Complete)
2. Investigate electrolyte and additive degradation mechanism with thick sulfur electrode. (Q2 – Complete)
3. Identify approaches to minimize quick capacity drop and efficiency fluctuation occuring in thick sulfur electrode during initial cycles. (Q3 – In progress)
4. Complete pouch cell assembly and testing by using optimized high energy cathode and electrolyte/ additives. (Q4 – In progress)

Progress Report

Last quarter, effects of electrode porosity on the electrode energy density, cell cycling stability, Li-anode interface, and electrolyte/sulfur ratio were investigated using high-loading sulfur electrodes. Effective approaches have also been demonstrated to address the electrode wetting issues associated with higher loading electrodes. Stable cycling of 200 cycles with capacity retention over 80% has been achieved for sulfur electrode with loading around 4 mg cm^{-2}. However, one common issue observed for high-loading sulfur electrodes is rapid capacity and efficiency decay in the first 5 to 10 cycles. This quarter, the team efforts focused on fundamental understanding of initial efficiency and capacity drop by combining electrochemical method, XPS, Raman, HPLC, and *in situ* EPR.

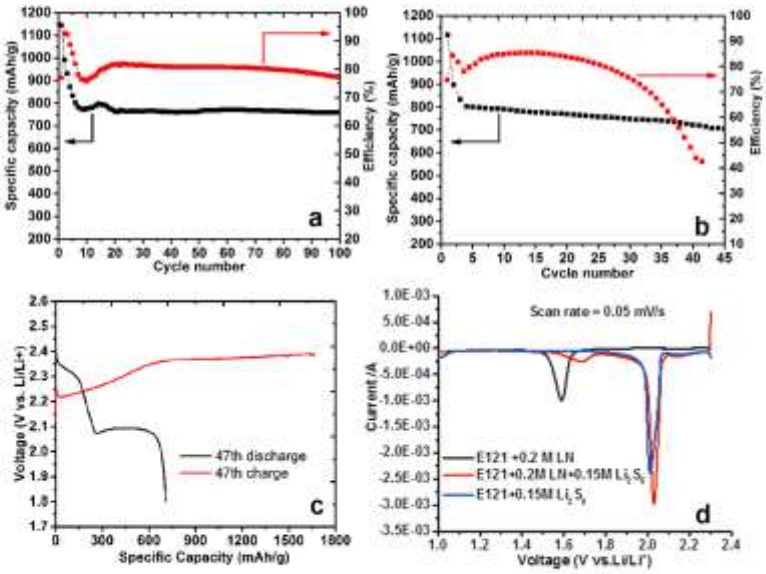

Figure 97. Cycling stability and Coulombic efficiency of thick electrodes with sulfur loadings of (a) 4 mg cm^{-2} and (b) 6.5 mg cm^{-2}. (c) The 47th cycle charge/discharge profiles of the failed Li-S cell in (b). (d) Cyclic voltammetry of carbon paper electrodes with electrolytes 1M LiTFSI/DOL/DME + 0.2M $LiNO_3$ (black), 1M LiTFSI/DOL/DME + 0.15M Li_2S_6 (blue), and stored 1M LiTFSI/DOL/DME + 0.2M $LiNO_3$ + 0.15M Li_2S_6 (red).

For sulfur electrodes with mass loadings of 1-2 mg cm^{-2}, both high capacity retention and CE (> 98%) can be obtained routinely (data is not shown). However, when sulfur loading is increased to above 4 mg cm^{-2}, significantly different cell performance is observed (Figure 97a). The rapid capacity drop occurring in the early stage of cycling is possibly due to formation, free diffusion, and loss of soluble polysulfides when an excess amount of electrolyte (electrolyte/sulfur = 10 µL/mg) is present. Accompanying capacity fading, the cell CE exhibits a similar evolution trend and quickly decreases to ca. 75% after 10 cycles (Figure 97a), which is much lower than that of thin-film electrodes. With further increase of sulfur loading (for example, 6.5 mg cm^{-2} in Figure 97b), efficiency decay is exacerbated remarkably, although the reversible capacities are still over 700 mAh g^{-1} after 45 cycles. A typical charge/discharge profile for a failed cell is shown in Figure 97c. A long charging plateau appears at around 2.4 V, which is caused by polysulfide “shuttle,” although 0.2 M $LiNO_3$ additive is used in the electrolyte. These results indicate accelerated depletion of $LiNO_3$ with increasing sulfur loading. A systematic investigation was performed to identify reasons behind this phenomenon. Results of *in situ* EPR and HPLC test indicate that besides reactions with lithium anode, oxidative $LiNO_3$ can directly react with Li_2S/Li_2S_2 and loses its function for lithium protection. This is exacerbated with the presence of more Li_2S/Li_2S_2, as shown in high-loading sulfur electrodes. Further study proves that $LiNO_3$ also reacts with some species of polysulfides. The stored electrolyte solution containing both $LiNO_3$ and Li_2S_6 shows much reduced peak intensity at 1.6–1.7 V, while slightly increased peak intensity at ~2.0 V compared to base electrolyte with same concentrations of $LiNO_3$ or Li_2S_6 individually (Figure 97d). This is due to direct reactions between $LiNO_3$ and certain species derived from Li_2S_6 polysulfide. From these results, more effective electrolyte additives for Li-anode protection or suppression of polysulfide shuttle are required for highly efficient and long-term cycling of Li-S batteries.

Patents/Publications/Presentations

Publications

- Lu, D., and Q. Li, J. Liu, J. Zheng, Y. Wang, S. Ferrara, S. Chen, J. Xiao, J. Zhang, and J. Liu. “Enabling High Capacity and High Energy Density Cathode for Lithium-Sulfur Batteries.” Submitted.
- Lu, D., and J. Tao, P. Yan, W. Henderson, Q. Li, Y. Shao, M. Helm, O. Borodin, G. Graff, B. Polzin, C. Wang, J. Zhang, J. Yoreo, J. Liu, and J. Xiao. “Formation of Reversible Solid Electrolyte Interface on Graphite Surface from Concentrated Electrolytes.” *Nano Letters* 17, no. 3 (2017): 1602–1609.

Presentation

- ACS National Meeting & Exposition, San Francisco, California (April 2–6, 2017): “Enhanced Performance of High Energy Sulfur Cathode for Lithium-Sulfur Batteries”; D. Lu, Q. Li, J. Liu, S. Wilson, J. Zhang, and J. Liu.

Task 8.6 – Nanostructured Design of Sulfur Cathodes for High-Energy Lithium–Sulfur Batteries (Yi Cui, Stanford University)

Project Objective. The charge capacity limitations of conventional TM oxide cathodes are overcome by designing optimized nano-architectured sulfur cathodes. This study aims to enable sulfur cathodes with high capacity and long cycle life by developing sulfur cathodes from the perspective of nanostructured materials design, which will be used to combine with Li-metal anodes to generate high-energy Li-S batteries. Novel sulfur nanostructures as well as multifunctional coatings will be designed and fabricated to overcome issues related to volume expansion, polysulfide dissolution, and the insulating nature of sulfur.

Project Impact. The capacity and the cycling stability of sulfur cathode will be dramatically increased. This project's success will make Li-S batteries to power EVs and decrease the high cost of batteries.

Out-Year Goals. The cycle life, capacity retention, and capacity loading of sulfur cathodes will be greatly improved (200 cycles with 80% capacity retention, > 0.3 mAh/cm^2 capacity loading) by optimizing material design, synthesis, and electrode assembly.

Collaborations. This project engages in collaboration with the following:

- BMR PIs,
- SLAC: *In situ* X-ray, Dr. Michael Toney, and
- Stanford: Professor Nix, mechanics; Professor Bao, materials.

Milestones

1. Demonstrate synthesis to generate monodisperse sulfur nanoparticles with/without hollow space. (October 2013 – Complete)
2. Develop surface coating with one type of polymer/inorganic material. (January 2014 – Complete)
3. Develop surface coating with several types of polymers; Understand amphiphillic interaction of sulfur and sulfide species. (April 2014 – Complete)
4. Demonstrate sulfur cathodes with 200 cycles with 80% capacity retention and 0.3 mAh/cm^2 capacity loading. (July 2014 – Complete)
5. Demonstrate Li^{2}S cathodes capped by layered metal disulfides. (December 2014 – Complete)
6. Identify the interaction mechanism between sulfur species and different types of sulfides/oxides/metals, and find the optimal material to improve capacity and cycling of sulfur cathode. (July 2015 – Complete)
7. Demonstrate the balance of surface adsorption and diffusion of Li^{2}Sx species on nonconductive metal oxides. (December 2015 – Complete)
8. The selection criterion of metal oxide is proposed to guide the rational design of cathode materials for advanced Li-S batteries. (April 2016 – Complete)
9. Demonstrate lithium polysulfides adsorption/diffusion on metal sulfides surface. (July 2016 – Complete)
10. Investigate the Li-ion diffusion mechanism in different types of metal sulfides. (October 2016 – Complete)
11. Identify the initial activation energy barrier of Li_2S on various metal sulfides. (December 2016 – Complete)
12. Demonstrate catalytic effect of Li_2S_x species on metal sulfides, enabling good performance of Li-S batteries. (April 2017 – Complete)

Progress Report

Last quarter, the team investigated the role of metal sulfides in catalytic decomposition of Li_2S on different types of metal sulfides, and the results indicate that the addition of CoS_2, VS_2, and TiS_2 significantly reduces the height of the potential barrier. The lower potential barrier and longer voltage plateau of the CoS_2-, VS_2-, and TiS_2-based electrodes compared to other metal sulfides indicate improved conductivity and reduced charge-transfer resistance. This quarter, the team further demonstrated the catalytic effect of Li_2S_x species on metal sulfides, enabling good performance of Li-S batteries.

Figure 98a shows the galvanostatic discharge/charge voltage profiles of S-VS_2@G/CNT electrode at various current rates from 0.2C to 4C in the potential range of 1.5–2.8 V. It exhibits excellent rate performance consisting of two discharge plateaus even at a very high current rate of 4C, which can be ascribed to the reduction of S_8 to high-order lithium polysulfides at 2.3–2.4 V and the transformation to low-order Li_2S_2/Li_2S at 1.9–2.1 V. In the reverse reaction, two plateaus in the charge curve represent the backward reaction from lithium sulfides to polysulfides and finally to sulfur. Based on the discharge curves at 0.2C, the sulfur electrodes containing G/CNT, SnS_2, Ni_3S_2, FeS, TiS_2, CoS_2, and VS_2 exhibit average discharge capacities of 685, 836, 845, 900, 1008, 1033, and 1093 mA h g^{-1}, respectively (Figure 98b). The higher discharge capacities of TiS_2-, CoS_2-, and VS_2- containing cathodes indicate the high utilization of sulfur due to the strong interaction between LiPSs and these sulfides. There are distinct differences in the voltage hysteresis and length of the voltage plateaus, which are related to the redox reaction kinetics and the reversibility of the system. The TiS_2-, CoS_2-, and VS_2- containing cathodes display flat and stable plateaus with relatively small polarizations of 177, 177, and 172 mV at 0.2C, much lower than G/CNT-, SnS_2-, Ni_3S_2-, and FeS- containing cathodes with values of 272, 244, 259, and 217 mV. This suggests a kinetically efficient reaction process with a smaller energy barrier promoted by the M_xS_y (TiS_2, CoS_2, and VS_2) catalyzing process, discussed previously. The charge/discharge plateaus obviously shift or even disappear for G/CNT-, SnS_2-, and Ni_3S_2- containing electrodes at high current rates, indicating high polarization and slow redox reaction kinetics with inferior reversibility.

Long-term cycling stability with high-capacity retention is crucial for the practical application of Li-S batteries. Figure 98c shows the cycling performance of the S@G/CNT and S-M_xS_y@G/CNT electrodes at 0.5C for 300 cycles after the rate capability test. The S-VS_2@G/CNT electrode delivers a high initial reversible capacity of 830 mA h g^{-1} and the capacity remains at 701 mA h g^{-1} after 300 cycles with stabilized CE above 99.5%, corresponding to a capacity retention of 84.5%, and slow capacity decay rate of 0.052% per cycle. The high LiPSs adsorbing capability and good catalytic conversion of sulfur species alleviate the shuttle effect and improve the CE. The S-CoS_2@G/CNT and S-TiS_2@G/CNT electrodes also retain reversible capacities of 581 and 546 mA h g^{-1}, respectively, accounting for 85.3% and 78.2% of their initial capacities, with low capacity fading rates of 0.049% and 0.073% per cycle. The remarkable improvements in cycling stability and CE can be ascribed to the immobilization of soluble polysulfide species through a strong chemical binding and facile redox reaction propelled by these metal sulfides. As for the S@G/CNT electrode, it only delivers an initial reversible capacity of 386 mA h g^{-1} at 0.5C rate and the capacity rapidly decreases to 218 mA h g^{-1} after 300 cycles, with a capacity retention of 56.5% and fast capacity decay rate of 0.145% per cycle. This suggests a weak affinity with LiPSs that cannot retard diffusion into the electrolyte and prevent active material loss. Compared with TiS_2-,

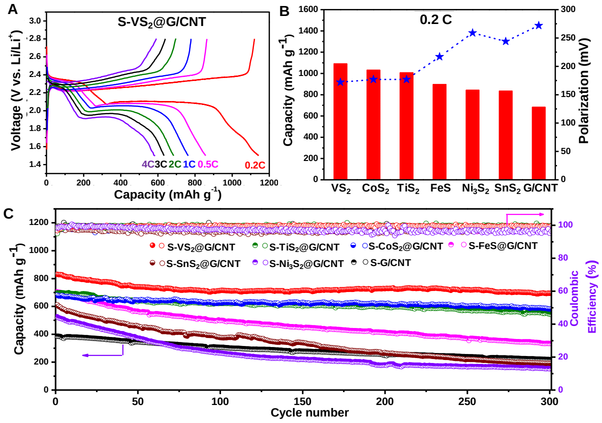

Figure 98. (a) Galvanostatic charge/discharge voltage profiles of the S-VS_2@G/carbon nanotube composite electrodes at different current densities within a potential window of 1.5~2.8 V versus Li^+/Li^0. (b) Comparison of the specific capacity and polarization voltage between the charge and discharge plateaus at 0.2C for different composite electrodes. (c) Cycling performance and Coulombic efficiency of the different composite electrodes at 0.5C for 300 cycles after the rate capability test.

CoS_2-, and VS_2- containing electrodes, the sulfur cathodes containing FeS (334 mA h g^{-1}, 47.4% capacity retention), SnS_2 (191 mA h g^{-1}, 31.3% capacity retention), and Ni_3S_2 (153 mA h g^{-1}, 29.1% capacity retention) demonstrate inferior cycling stability at 0.5C, with quick capacity degradation and unstable CE around 96%. The capacity fading rates reach 0.175%, 0.229%, and 0.236% per cycle for FeS-, SnS_2-, and Ni_3S_2- containing electrodes, respectively, much higher than the other three metal sulfides. These results imply that the selection of suitable polar hosts in the cathode that can (1) strongly interact with LiPSs, (2) rationally control Li_2S deposition, (3) enable fast Li-ion diffusion, (4) effectively transform sulfur to LiPSs/Li_2S, and (5) catalytically reverse the reaction process, is crucial and could significantly decrease polarization, improve sulfur utilization, and enhance rate performance and long-term cycling stability.

Patents/Publications/Presentations

Publication

- Zhou, G. M., and H. Tian, Y. Jin, X. Tao, B. Liu, R. Zhang, Z. W. Seh, D. Zhuo, Y. Liu, J. Sun, J. Zhao, C. Zu, D. Wu, Q. Zhang, and Y. Cui. “Catalytic Oxidation of Li_2S on the Surface of Metal Sulphides for Li-S batteries.” *PNAS* 114 (2017): 840–845.

Task 8.7 – Addressing Internal “Shuttle” Effect: Electrolyte Design and Cathode Morphology Evolution in Lithium-Sulfur Batteries (Perla Balbuena, Texas A&M University)

Project Objective. The project objective is to overcome the Li-metal anode deterioration issues through advanced Li-anode protection/stabilization strategies including (1) *in situ* chemical formation of a protective passivation layer and (2) alleviation of the “aggressiveness” of the environment at the anode by minimizing the polysulfide shuttle with advanced cathode structure design.

Project Impact. Through formulation of alternative electrolyte chemistries as well as design, fabrication, and test of improved cathode architectures, it is expected that this project will deliver Li/S cells operating for 500 cycles at efficiency greater than 80%.

Approach. A mesoscale model including different realizations of electrode mesoporous structures generated based on a stochastic reconstruction method will allow virtual screening of the cathode microstructural features and the corresponding effects on electronic/ionic conductivity and morphological evolution. Interfacial reactions at the anode due to the presence of polysulfide species will be characterized with *ab initio* methods. For the cathode interfacial reactions, data and detailed structural and energetic information obtained from atomistic-level studies will be used in a mesoscopic-level analysis. A novel sonochemical fabrication method is expected to generate controlled cathode mesoporous structures that will be tested along with new electrolyte formulations based on the knowledge gained from the mesoscale and atomistic modeling efforts.

Out-Year Goals. By determining reasons for successes or failures of specific electrolyte chemistries, and assessing relative effects of composite cathode microstructure and internal shuttle chemistry versus that of electrolyte chemistry on cell performance, expected results are as follows: (1) develop an improved understanding of the Li/S chemistry and ways to control it, (2) develop electrolyte formulations able to stabilize the lithium anode, (3) develop new composite cathode microstructures with enhanced cathode performance, and (4) develop a Li/S cell operating for 500 cycles at an efficiency greater than 80%.

Collaborations. This is a collaborative work combining first-principles modeling (Perla Balbuena, TAMU), mesoscopic level modeling (Partha Mukherjee, TAMU), and synthesis, fabrication, and test of Li/S materials and cells (Vilas Pol, Purdue University). Balbuena also collaborates with M. Vijayakumar from PNNL.

Milestones

1. Complete electrochemical modeling of cell performance with electrolyte and cathode properties. (Q1 – Complete)
2. Complete development of stable electrolytes. (In progress)
3. Produce 3-5 grams of C/S composite material.
4. Complete the scale-up of cathode composites, cell construction, and testing.

Progress Report

Development of Stable Electrolytes. Based on the *ab initio* molecular dynamics (AIMD) study of reactions at the surface of lithium metal at two different salt concentrations (1M and 4M), the project was able to conclude the following: (a) salts do not totally dissociate (not even at 1M solutions); (b) in 1M solutions, the coordination shell of the lithium ion is dominated by the solvent; (c) in 4M solutions, very complex networks are formed with mixed coordination shells (solvent and salt components); and (d) the kinetics of solvent decomposition (for DME and DOL) is much slower than those of typical anions (TFSI or FSI), and the extent of the reduction depends on the chemical nature of the salt. These conclusions have led to a hypothesis regarding plating of Li^+ ions inside the SEI layer. The project is testing effects of functional groups on the process of Li^+ plating. It aims to determine whether certain ion coordination shells are more favorable to induce lithium plating inside the SEI layer and how this plating compares with lithium deposition on the current collector.

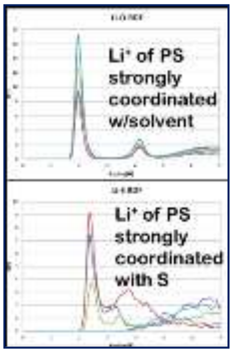

Figure 99. Radial distribution function $g_{LiO}(r)$ and $g_{LiS}(r)$ reveals the structure of the solvent near the lithiated polysulfide.

Migration of PS Species from Cathode to Anode. After extensive studies of Li^+ and long-chain polysulfide (PS) solvation, the team has concluded that PS anion species are not favored in most conditions; therefore, PS exists as a neutral species paired with lithium ions. This is evident from the radial distribution functions (rdf) (Figure 99). The Li-O rdf shows a clear first peak indicating the strong coordination of lithium ions of the lithiated PS species with the solvent, whereas the Li-S rdf shows that the same lithium ions are also well coordinated to the end-S atoms, and much less to those in the middle of the chain. However, under an electrical field, the PS ion pair will become at least partially dissociated, and the current estimate is that the monolithiated anion is the species that should migrate to the anode side.

Effects of Cathode Microstructural Complexation on Li/S Cell Performance. A comprehensive phase map, based on the Li_2S_2 and Li_2S precipitate morphology and cathode microstructure evolution, has been developed (Figure 100): (1) sulfur–to–electrolyte ratio: sets operational bounds on amount of sulfur without sacrificing cell capacity; (2) cathode initial porosity (before sulfur impregnation) determines sulfur loading and extent of surface passivation versus pore blockage; (3) controlling precipitate morphology, surface passivation can be deferred and greater cell capacity can be achieved; and (4) surface passivation found as the predominant mechanism of cell performance loss.

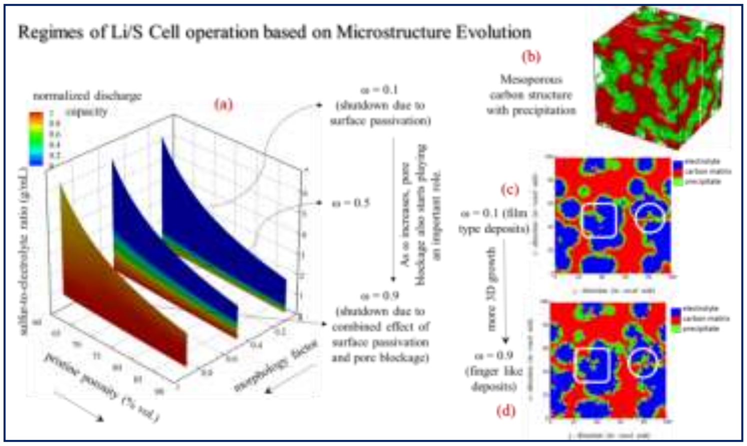

Figure 100. (a) Performance of a Li/S cell is a function of: sulfur-to-electrolyte ratio, pristine cathode porosity, and precipitate morphology. (b) Typical mesoporous structure with precipitation. Precipitate morphology affects discharge capacity (d) and obtainable cell capacity increases, as compared to film-like deposit (c).

Development of an Interlayer to Control PS Migration. A carbonaceous interlayer increases overall cathode conductivity, and impedes passage of large PS species through its pores. The interlayer was synthesized by nitric acid treatment of an interwoven carbon fiber membrane, in turn produced by pyrolysis of an electrospun polyacrylonitrile fiber membrane. The cathode was produced by physical mixing of carbon black, elemental sulfur, and PEO powder in the mass ratio 6:3:1. After cycle 200, the gravimetric capacity of the functional interlayer is almost double that of the same cathode without an interlayer. Similarly, the initial capacity of the interlayer-protected cathode is double (650 mAh/g) that of the unprotected cathode. The cycle 1 CE of the interlayer-protected cathode is very close to 100, suggesting effective PS migration suppression, and remains closer to 100 up to cycle 100.

Patents/Publications/Presentations

Publications

- Camacho-Forero, Luis E., and Taylor W. Smith, and Perla B. Balbuena. "Effects of High and Low Salt Concentration in Electrolytes at Lithium-Metal Anode Surfaces." *J. Phys. Chem. C* 121, no. 1 (2017): 182–194.
- Liu, Zhixiao, and Perla B. Balbuena, and Partha P. Mukherjee. "Revealing Charge Transport Mechanisms in Li_2S_2 for Li-Sulfur Batteries." *J. Phys. Chem. Lett.* 8 (2017): 1324–1330.
- Liu, Zhixiao, and Partha P. Mukherjee. "Mesoscale Elucidation of Surface Passivation in the Li-Sulfur Battery Cathode." *ACS Applied Materials & Interfaces* 9 (2017): 5263.
- Hong, S-M., and E. Jang, A. D. Dysart, V. G. Pol, and K. B. Lee. "CO_2 Capture in the Sustainable Wheat-Derived Activated Microporous Carbon Compartments." *Scientific Reports* 6 (2016): 34590.
- Tsai, C., and A. D. Dysart, J. Beltz, and V. G. Pol. "Identification and Mitigation of Generated Solid By-Products during Advanced Electrode Materials Processing." *Environ. Sci. Technol.* 50 (2016): 2627−2634.
- Nandasiri, M. J., and L. E. Camacho-Forero, A. M. Schwarz, V. Sutthanandan, S. Thevuthasan, P. B. Balbuena, K. T. Mueller, and M. Vijayakumar. "*In Situ* Chemical Imaging of SEI Layer Evolution in Li-S Batteries Using X-ray Photoelectron Spectroscopy." Under review.
- Liu, Z., and P. Balbuena, and P. P. Mukherjee. "Mesoscale Evaluation of Titanium Silicide Monolayer as a Cathode Host Material in Lithium-Sulfur Batteries." Under review.
- Chen, C.-F., and A. Mistry, and P. P. Mukherjee. "Correlating Impedance and Microstructure Evolution in Lithium-Sulfur Battery Cathodes." Under review.

Task 8.8 –Investigation of Sulfur Reaction Mechanisms
(Deyang Qu, University of Wisconsin Milwaukee; Xiao-Qing Yang, Brookhaven National Laboratory)

Project Objective. With the advantages of the unique analytical essay developed in 2016, the primary objectives are to further conduct focused fundamental research on the mechanism for Li-S batteries, investigate the kinetics for the sulfur redox reaction, develop electrolytes and additives suitable for Li-S chemistry, and optimize the sulfur electrode and cell designs. In these objectives, special attention will be paid to investigation of the redox reaction of sulfur cathode, management for the solubility of polysulfide ions, formation of SEI layer and dead lithium on the surface of lithium anode, rechargeability of lithium anode in the solution containing polysulfide, and exploration of electrode and cell designs. Through such investigations, the Li-S chemistry will be studied systematically, and scientific understanding of the reaction mechanism can be well utilized to guide system engineering design.

Project Impact. The unique *in situ* electrochemical HPLC/MS technique will identify the soluble polysulfides real-time during the charge/discharge of a Li-S battery; thus, the mechanism can be revealed in detail. The project results will guide development of sulfur cathode and Li-S designs.

Approach. This project will use *in situ* electrochemical-MS, electrochemical-HPLC/MS, XPS, SEM, and XRD to study electrochemical reactions associated with sulfur electrodes. Electrochemical techniques such as AC impedance, rotation ring disk electrode, and galvanostat will be used to study the electrode process kinetics. The project is developing an *in situ* electrochemical optical method to investigate the surface of lithium anode during cycling of a Li-S cell.

Out-Year Goals. The out-year goal is to establish tools to investigate the interaction between dissolved sulfur and polysulfide ions with lithium anode, exploring the additives that can migrate such interaction. In addition, gain further understanding of the chemical behaviors of the polysulfide in the electrolyte and propose a valid mechanism for the Li-S reaction.

Collaborations. The PI, Deyang Qu, is the Johnson Control Endowed Chair Professor; thus, the University of Wisconsin – Milwaukee and BNL team have close collaboration with Johnson Controls' scientists and engineers. This collaboration enables the team to validate the outcomes of fundamental research in pilot-scale cells. This team has been closely working with top scientists on new material synthesis at ANL, LBNL, and PNNL, with U.S. industrial collaborators at GM, Duracell, and Johnson Control as well as international collaborators in Japan and South Korea. These collaborations will be strengthened and expanded to give this project a vision on both today's state-of-the-art technology and tomorrow's technology in development, with feedback from the material designer and synthesizers upstream, and from industrial end users downstream.

Milestones

1. Complete design and validation of the *in situ* electrochemical – microscopic cell for *in situ* investigation of lithium anode during cycling. (Q1 – Complete)
2. Complete study of interaction between dissolved elemental sulfur and polysulfide ions with both the electrolytes and lithium anode. (Q2 – Complete)
3. Complete investigation of chemical equilibriums among dissolved polysulfide ions during the course of discharge and recharge of Li-S batteries. (Q3)
4. Complete the preliminary engineering design and test for the rechargeable Li-S battery including electrode design and cell design. (Q4)

Progress Report

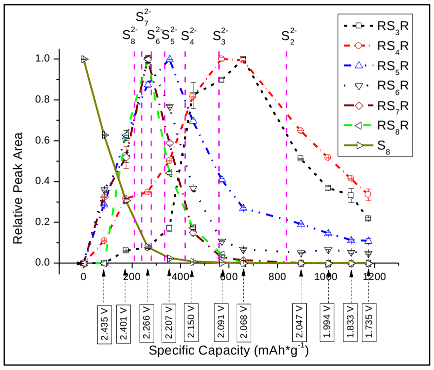

Figure 101. The normalized chromatographic peak for each derivatized polysulfide species ($R=CH_3$) from real-time high-performance liquid chromatography results during discharge of Li-S cell (from table S-3). The magenta dash lines indicate the stoichiometric species of polysulfides (also labeled on top of the dash lines) based on theoretical stepwise reduction.

This quarter, the team continued to utilize the unique HPLC-MS – electrochemical technique to investigate the mechanism of sulfur redox reaction. The distribution of polysulfide ions at various stages of discharge and recharge of a Li-S cell was determined. Figure 101 shows the change of distribution of polysulfide ions at various stages of discharge and potential. The change of polysulfide ions in the electrolyte from elemental sulfur, long-chain polysulfides to short-chain polysulfides can be clearly demonstrated as the discharge proceeds. It can be observed that the change of the abundance for S_8^{2-}, S_7^{2-} and S_6^{2-} was almost identical in the first discharge plateau, which was evident from the chemical equilibrium among those polysulfide species. The first flat discharge plateau could be a result from the equilibrium. Another interesting observation from Figure 101 is that even when the discharge reached the stoichiometric S_2^{2-} stage, the most abundant polysulfides in the electrolyte were S_4^{2-}, S_5^{2-} and S_3^{2-}. To the end of the discharge, even though the concentration decreased, the relative distribution of the three polysulfides remained. Based on the above discussion, Figure 102 (scheme 1) shows the mechanism of the 3-stage sulfur reduction reaction. The elemental sulfur became reduced to long-chain polysulfide ion (mainly S_7^{2-}, S_6^{2-}, and S_5^{2-}), and S_8^{2-} was formed through subsequent reaction between the long-chain polysulfide ions and sulfur. During this period, a chemical equilibrium was maintained among S_7^{2-}, S_6^{2-} , and S_5^{2-} until a substantial amount of S_7^{2-}, S_6^{2-} was consumed around 2.3 V, then the potential started to decrease. A sloped discharge profile was demonstrated between 2.3 to 2.1 V. Evidentially, as shown in Figure 101, almost all the polysulfides S_n^{2-} with $4 \le n \le 7$ were co-existing in the electrolyte during the reduction reaction; the concentration of the polysulfide changed independently, so no apparent equilibrium could be observed. The second reduction plateau started when almost all polysulfide species S_n^{2-} with $n \ge 6$ were consumed at about 2.1 V. During the second flat reduction plateau, the reduction rate of S_5^{2-}, S_4^{2-}, and S_3^{2-} remained almost the same, as shown by the parallel curves for these three species in Figure 101, which indicates a chemical equilibrium among the species. Even though the ratio of concentrations of these three polysulfides remained almost unchanged during the flat reduction region, the total amount of dissolved polysulfide ions decreased.

>2.3 V, first plateau, major species are bold

$$S_8 \xrightarrow{ne} (S_8^{2-} + \boldsymbol{S_7^{2-}} + \boldsymbol{S_6^{2-}} + \boldsymbol{S_5^{2-}} + S_4^{2-} + S_3^{2-})$$

$$\boldsymbol{S_7^{2-}} \rightleftarrows \boldsymbol{S_6^{2-}} \rightleftarrows \boldsymbol{S_5^{2-}}$$

Between 2.3 and 2.1 V, major species are bold

$$S_8^{2-} + S_7^{2-} + S_6^{2-} + \boldsymbol{S_5^{2-}} \xrightarrow{ne} \boldsymbol{S_4^{2-}} + S_3^{2-} + Li_2S_2 \downarrow + Li_2S \downarrow$$

<2.1 plateau, major species are bold

$$\boldsymbol{S_5^{2-}} + \boldsymbol{S_4^{2-}} + S_3^{2-} \xrightarrow{ne} Li_2S_2 \downarrow + Li_2S \downarrow$$

$$\boldsymbol{S_5^{2-}} \rightleftarrows \boldsymbol{S_4^{2-}} \rightleftarrows \boldsymbol{S_3^{2-}}$$

Figure 102. Scheme 1: The proposed discharge mechanism of sulfur in Li-S battery.

In the same way, the mechanism of the recharge process was also investigated. The change of the distribution of the dissolved polysulfide ions demonstrated that a single equilibrium remained in the charge process. The proposed mechanism is shown in Figure 103 (scheme 2).

Cathode potential <2.4 V

$$\boldsymbol{Li_2S_2 \downarrow + Li_2S \downarrow \xrightarrow{-ne} S_8^{2-} + S_7^{2-} + S_6^{2-} + S_5^{2-}}$$

$$\boldsymbol{S_8^{2-} \rightleftarrows S_7^{2-} \rightleftarrows S_6^{2-} \rightleftarrows S_5^{2-}}$$

Cathode potential > 2.4 V

$$\boldsymbol{S_8^{2-} + S_7^{2-} + S_6^{2-} + S_5^{2-} + S_4^{2-} + S_3^{2-} \xrightarrow{-ne} S_8}$$

$$\boldsymbol{S_8^{2-} \rightleftarrows S_7^{2-} \rightleftarrows S_6^{2-} \rightleftarrows S_5^{2-}}$$

Figure 103. Scheme 2: The proposed charge mechanism on the cathode in a Li-S battery.

Patents/Publications/Presentations

Publication

- Zheng, Dong, and Dan Liu, Joshua Harris, Tianyao Ding, Jingyu Si, Sergi Andrew, Deyu Qu, Xiao-Qing Yang, and Deyang Qu. "Investigation of Li-S Battery Mechanism by Real-Time Monitoring the Changes of Sulfur and Polysulfide Species during the Discharge and Charge." *ACS Appl. Mater. & Interface* 9 (2017): 4326–4332.

Task 8.9 – Statically and Dynamically Stable Lithium–Sulfur Batteries (Arumugam Manthiram, University of Texas – Austin)

Project Objective. The project objective is to develop statically and dynamically stable Li-S batteries by integrating polysulfide-filter-coated separators with a protected Li-metal anode through additives or a modified Li_2S cathode with little or no charge barrier during first charge. The project includes demonstration of electrochemically stable cells with sulfur capacities of > 1,000 mA h g^{-1} and cycle life in excess of 500 cycles (dynamic stability) along with positive storage properties (static stability) at > 70 wt% sulfur content and ~ 5 mg cm^{-2} loading.

Project Impact. The combination of polysulfide-filter (PS-filter)-coated separator, Li-metal-protection additives, and Li_2S cathode modifications offers a viable approach to overcome the persistent problems of Li-S batteries. This project is systematically integrating the basic science understanding gained in its laboratory of these three aspects to develop the Li-S technology as the next-generation power source for EVs. The project targets demonstrating cells with sulfur capacities of over 1,000 mA h g^{-1} and cycle life in excess of 500 cycles along with good storage properties at high sulfur content and loading that will make the Li-S technology superior to the present-day Li-ion technology in terms of cost and cell performance.

Approach. Electrochemical stability of the Li-S cells is improved by three complementary approaches. (1) The first approach focuses on establishment of an electrochemically stable cathode environment by employing PS-filter-coated separators. The PS-filter coatings aim to suppress the severe polysulfide diffusion and improve the redox capability of Li-S cells with high-sulfur loadings. The study includes an understanding of materials characteristics, fabrication parameters, electrochemical properties, and battery performance of the PS-filter-coated separators. (2) The second approach focuses on electrode engineering from two aspects. First, investigation of a Li-metal anode with coating- and additive-supporting approaches is aimed at improving the safety of Li-S cells. Second, research on activated-Li_2S cathode with little or no charge-barrier will promote performance and safety of the C-Li_2S cells. (3) Integration of the first two approaches would create statically and dynamically stable Li-S batteries for EVs.

Out-Year Goals. The overall goal is to develop statically and dynamically stable Li-S batteries with custom cathode and stabilized anode active materials. In addition to developing a high-performance battery system, a fundamental understanding of the structure-configuration-performance relationships will be established. Specifically, the optimization of the electrochemical and engineering parameters of PS-filter-coated separators aims at comprehensively investigating different coating materials and their corresponding coating techniques for realizing various high-performance custom separators. The developed PS-filter-coated separators can be coupled with pure sulfur cathodes with high-sulfur loading and content. Multi-functional PS-filter-coated separators, high-loading sulfur cathodes, stabilized-Li-metal anodes, activated-Li_2S cathodes, and novel cell design are anticipated to provide an in-depth understanding of the Li-S battery chemistry and to realize statically and dynamically stable Li-S batteries.

Collaborations. This project collaborates with ORNL.

Milestones

1. Analyze and improve dynamic electrochemical performances of Li-S cells. (Q1 – Complete)
2. Analyze and improve static electrochemical performances of Li-S cells. (Q2 – Complete)
3. Increase the sulfur loading of the cells. (Q3 – In progress)
4. *Go/No-Go*: Fabricate cells with high sulfur content/loading and good electrochemical stability. (Q4 – In progress)

Progress Report

Self-discharge is a serious problem in development of Li-S batteries. Unfortunately, the lack of literature on realities of self-discharge makes it a daunting challenge to develop a practically viable Li-S technology. Accordingly, the team focused this quarter to improve the long-term static electrochemical performance (shelf-life) of Li-S batteries (during resting) by employing (i) polysulfide-filter (PS-filter)-coated separators and (ii) advanced high-loading sulfur cathodes.

Specifically, the team focused on the PS-filter-coated separators fabricated with carbon nanofibers (CNFs) using a layer-by-layer (LBL) coating method. The LBL CNF-coated separators provide the Li-S cells an extended cell shelf-life of one year, which is the longest cell-storage period reported for Li-S cells in the literature (Figure 104a). In this extended low-self-discharge demonstration, the cells fabricated with the LBL CNF-coated separators retain 50% of the initial capacity after storing for 1 year, and exhibit a low self-discharge rate of only 0.14% per day, which is much lower than the target value (Figure 104b). In addition, the stored cells still display good cyclability. Figure 104c shows that the cell that is rested for 365 days keeps a high capacity with a low capacity-fade rate of 0.10% per cycle for 100 cycles. Thus, in developing Li-S batteries with a low self-discharge effect, the project has made in this quarter three significant accomplishments: (1) the longest shelf-life, (2) the lowest self-discharge rate, and (3) good cycle stability after resting (storing) for 1 year.

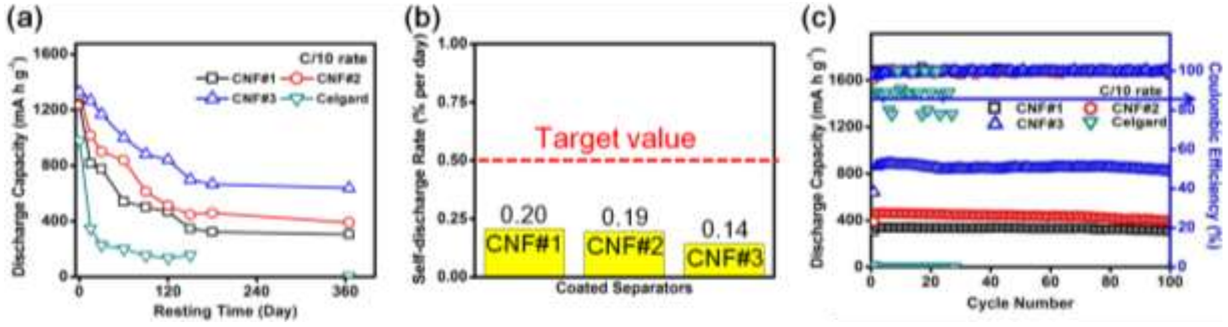

Figure 104. Static electrochemical analysis of the Li-S batteries fabricated (i) with the polypropylene membranes after resting for 150 days and (ii) with the layer-by-layer carbon nanofiber (CNF)-coated separators after resting for 365 days. (a) Static electrochemical stability. (b) Self-discharge rate. (c) Cycle stability.

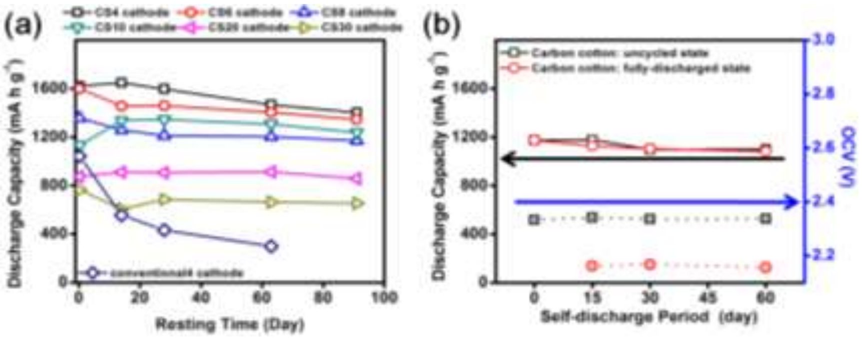

Figure 105. Static electrochemical analysis of the Li-S batteries with high-loading cathodes: (a) core-shell cathodes with sulfur loadings of 4-30 mg cm^{-2} and (b) carbon-cotton cathodes with sulfur loadings of 30 mg cm^{-2}.

With the fulfillment of all second quarter milestones, the team is also moving forward to study/reduce the self-discharge effect in cells fabricated with high-loading sulfur cathodes. Figure 105a-b shows the performances of the team's advanced high-loading sulfur cathodes fabricated with, respectively, pure sulfur powders in a shell-shaped carbon electrode as a core-shell (CS) cathode and polysulfide catholytes in a carbon-cotton electrode as a carbon-cotton cathode. Both have sulfur loadings reaching up to 30 mg cm^{-2}, which are the highest values reported so far; the corresponding cells exhibit low self-discharge rates. The core-shell cathode exhibits a self-discharge rate of only 0.07% per day with a shelf-life of over 3 months. The carbon-cotton cathodes hold 94% of their initial capacity (above 1,100 mAh g^{-1}) after resting for two months.

Patents/Publications/Presentations

Publication

- Chang, C.-H., and S.-H. Chung, and A. Manthiram. "Dendrite-Free Lithium Anode via a Homogenous Li-Ion Distribution Enabled by a Kimwipe Paper." *Advanced Sustainable Systems* 1 (2017): 1600034.

Task 8.10 – Electrochemically Responsive, Self-Formed, Lithium-Ion Conductors for High-Performance Lithium-Metal Anodes (Donghai Wang, Pennsylvania State University)

Project Objective. The project objective is to develop and deliver an electrochemically responsive self-formed hybrid Li-ion conductor as a protective layer for Li-metal anodes, enabling Li-metal anodes to cycle with a high efficiency of ~ 99.7% at high electrode capacity (> 6 mAh/cm^2) and high current density (> 2 mA/cm^2) for over 500 cycles. The project will also demonstrate prototype ~300 mAh Li-S battery cells with energy densities of ~200 Wh/kg and ~ 80% capacity retention for ~ 300 cycles at ~ 80% depth of discharge using Li-metal anodes with this protective layer.

Project Impact. This project aims to develop a new hybrid Li-ion conductor that enables safe and high-performance lithium metal anodes. The use of these high-performance Li-metal anodes in turn enables Li-S batteries with high energy density and long cycling life. Such anodes can also lead to a 50% increase in the energy density of conventional Li-ion batteries with Li-metal oxide cathodes. Meeting the technical targets will potentially develop a new high-energy-density lithium battery, promote increased adoption of EVs and PHEVs, and reduce petroleum consumption in the transportation sector by helping battery-powered vehicles become accepted by consumers as a reliable source of transportation.

Approach. The novel multiphase organo-Li_xS_y or organo-$Li_xP_yS_z$ hybrid ion conductors with tunable multifunctional organic components and controlled Li_xS_y and $Li_xP_yS_z$ inorganic components will be designed and prepared, and thus enable safe use of lithium metal with high CE. In the first year, the team will develop the organo-Li_xS_y lithium protection layers with tuned functionality: (1) finding appropriate composition and (2) developing appropriate synthesis and fabrication methods.

Out-Year Goals. Work will progress toward development of organo-Li_xS_y lithium protection layers with tuned functionality. Characterization, performance, and compatibility tests on materials and systems. Twelve baseline 300 mAh pouch cells using standard Li-metal anodes and high-performance carbon-sulfur cathodes will be delivered for independent verification.

Milestones

1. Development of the first-generation of organo-Li_xS_y lithium protection layers with tuned functionality. Conduct characterization and performance tests on the materials. (December 2016 – Completed)
2. Deliver 12 baseline ~ 300 mAh Li-S cells for independent verification. (Q2 – In Progress, 10%)
3. Optimize organo-Li_xS_y protective layer and demonstrate lithium anodes cycling with ~ 98.5% CE for ~ 200 cycles. (Q3)
4. Demonstrate lithium anodes with optimized organo-Li_xS_y protective layer and ~ 99% CE for ~ 200 cycles. (Q4)

Progress Report

Constructing a rechargeable prelithiated graphite/sulfur battery is a feasible strategy to address the issues of polysulfide shuttling and unstable lithium/electrolyte interface. A fluorinated ether of bis(2,2,2-trifluoroethyl) ether (BTFE) was blended with 1,3-dioxolane (DOL) for making a multifunctional electrolyte of 1.0 M LiTFSI DOL/BTFE (1:1, v/v) to enable high performance prelithiated graphite/S batteries. First, the electrolyte significantly reduces polysulfide solubility to suppress the deleterious polysulfide shuttling and thus improves capacity retention of sulfur cathodes. Second, thanks to the low viscosity and good wettability, the fluorinated electrolyte dramatically enhances the reaction kinetics and sulfur utilization of high-areal-loading sulfur cathodes. More importantly, this electrolyte forms a stable SEI layer on graphite surface and thus enables remarkable cyclability of graphite anodes. By coupling prelithiated graphite anodes with sulfur cathodes with high areal capacity of ∼3 mAh cm^{-2}, the team demonstrated prelithiated graphite/sulfur batteries that show high sulfur-specific capacity of ∼ 1000 mAh g^{-1} and an excellent capacity retention of > 65% after 450 cycles at C/10 (Figure 106).

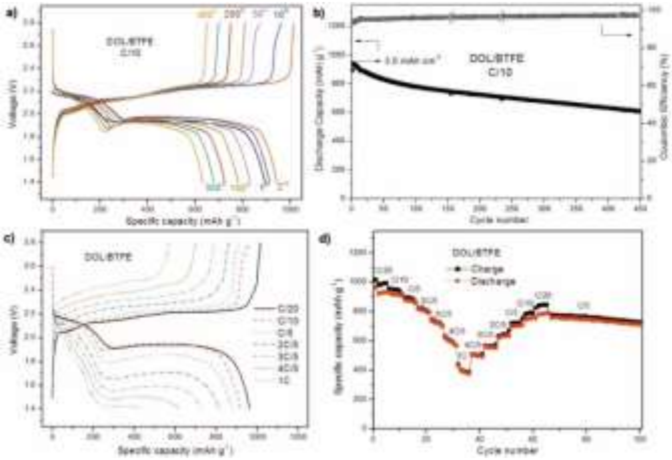

Figure 106. (a, c) Discharge−charge profiles and (b, d) cycling performance of prelithiated graphite/sulfur full cells at (a, b) C/10 and (c, d) different C rates in the DOL/BTFE electrolyte.

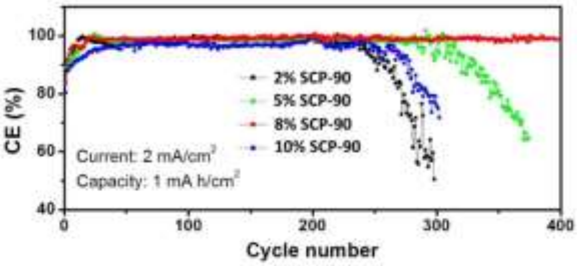

Figure 107. Cycling performance of cells using electrolytes containing different contents of sulfur-containing polymers.

For the protection of the Li-metal anode, the sulfur-containing polymers (SCPs), which contain the sulfur chains and organic units, are used for fabrication of organo-Li_xS_y lithium protection layers. The SCPs with 90 wt% sulfur (SCP-90) exhibited the best cycling performance. The content of SCP-90 as additives in the electrolyte affects the Li plating/stripping cycling performance. Comparing the Li plating/stripping performance of using electrolyte containing 2 wt%, 5 wt%, 8 wt%, and 10 wt% of SCP-90, the team found that cycling life is improved with increasing content of SCP-90 additive until reaching 8 wt% (Figure 107). When the content of SCP-90 in the electrolyte increased to 10 wt%, the cycling life deteriorated. Using SCP-90 as additives, the growth of lithium dendrite was effectively suppressed, and uniform and compact deposited lithium film could be obtained. After 100 cycles at a current density of 2 mA cm^{-2} and a deposition capacity of 2 mA h cm^{-2}, the deposited lithium exhibits very smooth and uniform surface and morphological compactness without any growth of lithium dendrites (Figure 108).

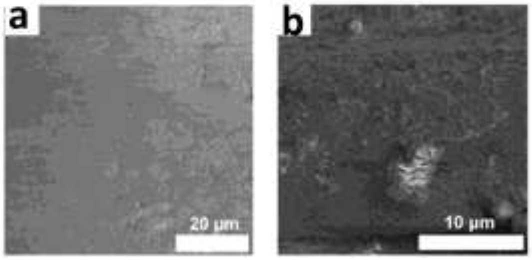

Figure 108. Scanning electron microscopy images of the deposited lithium after 100 cycles at a current density of 2 mA cm^{-2} and a deposition capacity of 2 mA h cm^{-2}.

Patents/Publications/Presentations

Publication

- Chen, S. R., Yu, Z. X., Gordin, M., Ran, Y., Song, J. X., and Wang, D. H. "A Fluorinated Ether Electrolyte Enabled High Performance Pre-lithiated Graphite/Sulfur Batteries." *ACS Appl. Mater. Interfaces* 9 (2017): 6959–6966.

TASK 9 – LITHIUM–AIR BATTERIES

Summary and Highlights

High-density energy storage systems are critical for EVs required by the EV Everywhere Grand Challenge. Conventional Li-ion batteries still cannot fully satisfy the ever-increasing needs because of their limited energy density, high cost, and safety concerns. As an alternative, the rechargeable lithium-oxygen (Li-$O_{2)}$ battery has the potential to be used for long-range EVs. The practical energy density of a Li-O_2 battery is expected to be ~ 800 Wh kg^{-1}. The advantages of Li-O_2 batteries come from their open structure; that is, they can absorb the active cathode material (oxygen) from the surrounding environment instead of carrying it within the batteries. However, the open structure of Li-O_2 batteries also leads to several disadvantages. The energy density of Li-O_2 batteries will be much lower if oxygen has to be provided by an onboard container. Although significant progress has been made in recent years on fundamental properties of Li-O_2 batteries, research in this field is still in an early stage, and many barriers must be overcome before practical applications. The barriers include:

- Instability of electrolytes—The superoxide species generated during discharge or O_2 reduction process is highly reactive with electrolyte and other components in the battery. Electrolyte decomposition during charge or O_2 evolution process is also significant due to high over-potentials.
- Instability of air electrode (dominated by carbonaceous materials) and other battery components (such as separators and binders) during charge/discharge processes in an O-rich environment.
- Limited cyclability of the battery associated with instability of the electrolyte and other battery components.
- Low energy efficiency associated with large over-potential and poor cyclability of Li-O_2 batteries.
- Low power rate capability due to electrode blocking by the reaction products.
- Absence of a low-cost, high-efficiency oxygen supply system (such as oxygen selective membrane).

The main goal of this Task is to provide a better understanding on the fundamental reaction mechanisms of Li-O_2 batteries and identify the required components (especially electrolytes and electrodes) for stable operation of Li-O_2 batteries. PNNL researchers will investigate stable electrolytes and OER catalysts to reduce the charging overvoltage of Li-O_2 batteries and improve their cycling stability. New electrolytes will be combined with stable air electrodes to ensure their stability during Li-O_2 reaction. Considering the difficulties in maintaining the stability of conventional liquid electrolyte, the Liox team will explore use of a nonvolatile, inorganic molten salt comprising nitrate anions and operating Li-O_2 cells at elevated temperature (> 80°C). It is expected that these Li-O_2 cells will have a long cycle life, low over potential, and improved robustness under ambient air compared to current Li-air batteries. At ANL, new cathode materials and electrolytes for Li-air batteries will be developed for Li-O_2 batteries with long cycle life, high capacity, and high efficiency. The state-of-the-art characterization techniques and computational methodologies will be used to understand the charge and discharge chemistries. The University of Massachusetts/BNL team will investigate the root causes of the major obstacles of the air cathode in the Li-air batteries. Special attention will be paid to optimization of high-surface carbon material used in the gas diffusion electrode, catalysts, electrolyte, and additives stable in Li-air system and with capability to dissolve lithium oxide and peroxide. Success of this project will establish a solid foundation for further development of Li-O_2 batteries toward their practical applications for long-range EVs. The fundamental understanding and breakthrough in Li-O_2 batteries may also provide insight on improving performance of Li-S batteries and other energy storage systems based on chemical conversion processes.

Highlight. The highlights for this quarter are as follows:

- ANL discovered that hydrolysis of solid LiO_2 differs significantly from that of NaO_2 and KO_2, and a new approach was developed that provides information on composition of a discharge product in a Li-O_2 battery.
- PNNL team developed a one-step, *in situ* electrochemical pretreatment method to generate thin protective films on the surfaces of CNTs air-electrode and Li metal anode at the same time. This method leads to significant improvement on the cycle life of Li-O_2 batteries.

Task 9.1 – Rechargeable Lithium-Air Batteries
(Ji-Guang Zhang and Wu Xu, Pacific Northwest National Laboratory)

Project Objective. The project objective is to develop rechargeable Li-O_2 batteries with long-term cycling stability. The FY 2017 objective is to stabilize Li-metal anode in Li-O_2 batteries and to investigate the temperature effect on ORR and OER processes of the Li-O_2 chemistry.

Project Impact. Li-air batteries have a theoretical specific energy that is more than five times that of state-of-the-art Li-ion batteries and are potential candidates for use in next-generation, long-range EVs. Unfortunately, the poor cycling stability and low CE of Li-air batteries have prevented their practical application. This work will explore a new electrolyte and electrode that could lead to long cyclability and high CEs in Li-air batteries that can be used in the next-generation EVs required by the EV Everywhere Grand Challenge.

Out-Year-Goals. The long-term goal of the proposed work is to enable rechargeable Li-air batteries with a specific energy of 800 Wh/kg at cell level, 1000 deep-discharge cycles, improved abuse tolerance, and less than 20% capacity fade over a 10-year period to accelerate commercialization of long-range EVs.

Collaborations. This project collaborates with Chongmin Wang of PNNL on characterization of cycled air electrodes by TEM/SEM and with Jinhui Tao of PNNL on characterization of Li-metal anodes by *in situ* AFM.

Milestones

1. Investigate temperature effect on ORR and OER of Li-O_2 batteries. (Q1 – Complete)
2. Identify factors that affect stability of Li-metal anode in Li-O_2 batteries. (Q2 – Complete)
3. Develop surface coating or electrolyte additive to stabilize Li-metal anode and improve cycle life of Li-O_2 battery. (Q4 – In progress)

Progress Report

This quarter, a simple one-step *in situ* electrochemical pretreatment method is further developed to generate thin protective films on the surfaces of CNT air-electrode and Li-metal anode at the same time. With the increasing pretreatment time from 5 min to 20 min, the thickness of the thin film formed on CNT air electrode surface increases from 1~2 nm to about 8~9 nm, as observed by TEM morphology shown in Figure 109. The protective films formed on lithium metal were also observed by *in situ* AFM technique (Figure 110) during the pretreatment process. The films formed on CNT air electrode and Li-metal anode contain the decomposition products of electrolyte (solvent and lithium salt) from XPS analysis. The electrochemical tests on these Li-O_2 cells show that the longest stable cycle life of 110 cycles is obtained at the pretreatment condition C. After cycling, the cells were disassembled, and the air electrodes and the Li-metal anodes were retrieved, cleaned, and characterized by SEM (Figure 111). It is seen that without pretreatment, the CNT air electrode has large breakages on the surface and thick side reaction products, and the Li-metal anode exhibits severe corrosion of most of bulk lithium and corrosion products are loosely packed on Li-metal anode. However, with pretreatment, the coating layers on CNTs are fewer and thin, the Li-metal anode still keeps thick bulk Li-metal layer without corrosion, and the surface layer is relatively flat and compacted with only a few cracks. Thus, the preformed protective films can significantly suppress and mitigate the well-known decomposition of carbon air electrode and severe corrosion of Li-metal anode upon cycling.

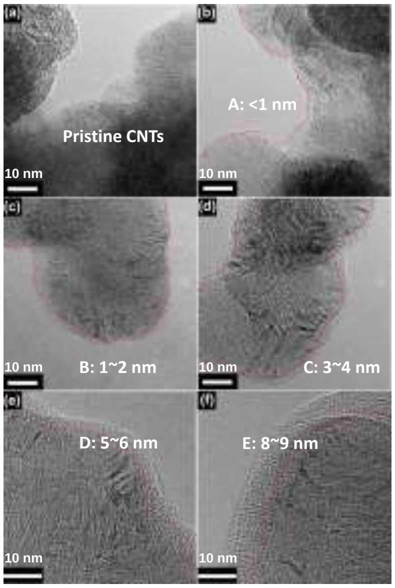

Figure 109. High-resolution transmission electron microscopy images of carbon nanotube electrodes at different pretreatment conditions.

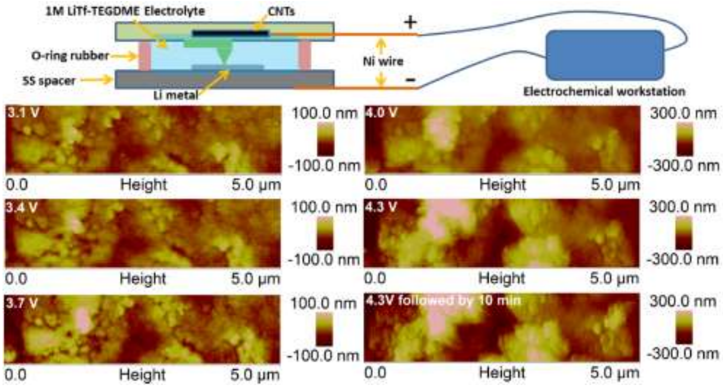

Figure 110. *In situ* atomic force microscopy observation of the formation of protective films on lithium metal during pretreatment.

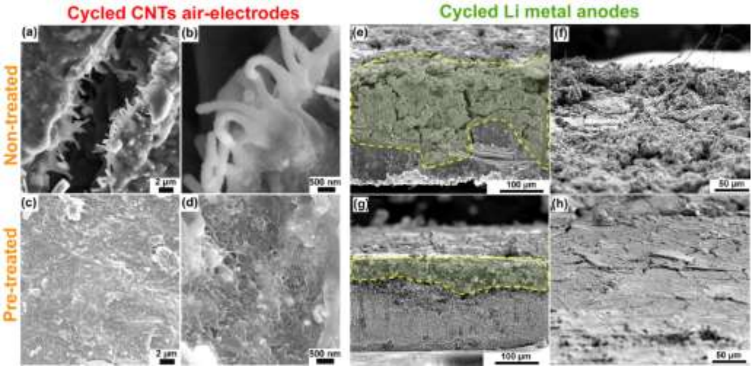

Figure 111. Morphological characterizations of the cycled carbon nanotube air electrodes without pretreatment (a, b) and with pretreatment under condition C (c, d), as well as the cycled Li-metal anodes without pretreatment (e, f) and with pretreatment under condition C (g, h).

Patents/Publications/Presentations

Publications

- Xu, W., and B. Liu, and J.-G. Zhang. "Preformation of Solid Electrolyte Interface on Lithium Metal Electrodes for Rechargeable Lithium Metal Batteries." PNNL Invention Disclosure Report 31087-E.
- Luo, L., and B. Liu, S. Song, W. Xu, J.-G. Zhang, and C. Wang. "Revealing the Reaction Mechanisms of Li-O_2 Batteries Using Environmental Transmission Electron Microscopy." *Nature Nanotechnology* (2017). doi: 10.1038/nnano.2017.27, in press.
- Liu, B., and W. Xu, P. Yan, S. T. Kim, M. H. Engelhard, X. Sun, D. Mei, J. Cho, C. Wang, and J.-G. Zhang. "Stabilization of Li-Metal Anode in DMSO-Based Electrolytes via Optimization of Salt-Solvent Coordination for Li-O_2 Batteries." *Advanced Energy Materials* (2017). doi: 10.1002/aenm.201602605, in press.
- Song, S., and W. Xu, J. Zheng, L. Luo, M. H. Engelhard, M. E. Bowden, B. Liu, C. Wang, and J.-G. Zhang. "Complete Decomposition of Li_2CO_3 in Li-O_2 Batteries Using Ir/B_4C as Noncarbon-Based Oxygen Electrode." *Nano Letters* 17 (2017): 1417–1424.
- Song, S., and W. Xu, R. Cao, L. Luo, M. H. Engelhard, M. E. Bowden, B. Liu, L. Estevez, C. Wang, and J.-G. Zhang. "B_4C as a Stable Non-Carbon-Based Oxygen Electrode Material for Lithium-Oxygen Batteries." *Nano Energy* 33 (2017): 195–204.

Task 9.2 – Efficient Rechargeable Li/O_2 Batteries Utilizing Stable Inorganic Molten Salt Electrolytes (Vincent Giordani, Liox)

Project Objective. The project objective is to develop high specific energy, rechargeable Li-air batteries having lower overpotential and improved robustness under ambient air compared to current Li-air batteries.

Project Impact. If successful, this project will solve particularly intractable problems relating to air electrode efficiency, stability, and tolerance to the ambient environment. Furthermore, these solutions may translate into reduced complexity in the design of a Li-air stack and system, which in turn may improve prospects for use of Li-air batteries in EVs. Additionally, the project will provide materials and technical concepts relevant for development of other medium temperature molten salt lithium battery systems of high specific energy, which may also have attractive features for EVs.

Approach. The technical approach involves replacing traditional organic and aqueous electrolytes with a non-volatile, inorganic molten salt comprising nitrate anions and operating the cell at elevated temperature (> 80°C). The research methodology includes powerful *in situ* spectroscopic techniques coupled to electrochemical measurements (for example, electrochemical MS) designed to provide quantitative information about the nature of chemical and electrochemical reactions occurring in the air electrode.

Out-Year-Goals. The long-term goal of this project is to develop Li-air batteries comprising inorganic molten salt electrolytes and protected lithium anodes that demonstrate high (> 500 Wh/kg) specific energy and efficient cyclability in ambient air. By the end of the project, it is anticipated that problems hindering use of both the lithium anode and air electrode will be overcome due to materials advances and strategies enabled within the intermediate (> 80°C) operating temperature range of the system under development.

Collaborations. This project funds work at Liox Power, Inc.; LBNL (Prof. Bryan McCloskey: analysis of air electrode and electrolyte); and California Institute of Technology (Prof. Julia Greer: design of air electrode materials and structures).

Milestones

1. Demonstrate discharge specific energy and energy density ≥ 500 Wh/Kg and ≥ 800 Wh/L, respectively, based on air electrode mass and volume. (Q1 – Complete)
2. Scale-up downselected cell components for 4 mAh and 10 mAh cells. (Q2 – Complete)
3. Demonstrate ≥ 10 cycles at ≥ 90% round-trip energy efficiency in laboratory-scale Li-air cells comprising a molten nitrate electrolyte and protected lithium electrode. (Q3 – In progress)
4. Fabricate and test 4 and 10 mAh cells. (Q4)

Progress Report

This quarter, the project investigated the Li-metal anode/SEI. Molten nitrate electrolytes are known to slowly decompose onto lithium metal, and therefore a solid electrolyte is required to prevent such reaction and improve battery cycle life. LLZO garnet-type pellets (10 mm OD, 0.5 mm thickness) were hot-pressed and sintered for 6 h at 1050°C under inert gas. Li/LLZO/Li symmetric cells were constructed in an Ar-filled glove box and operated at lithium melting point (185°C). Figure 112 shows lithium stripping/plating cycling data at 0.1 mA/cm^2 and 2 h per each half cycle with EIS recorded every 80 hours of cycling.

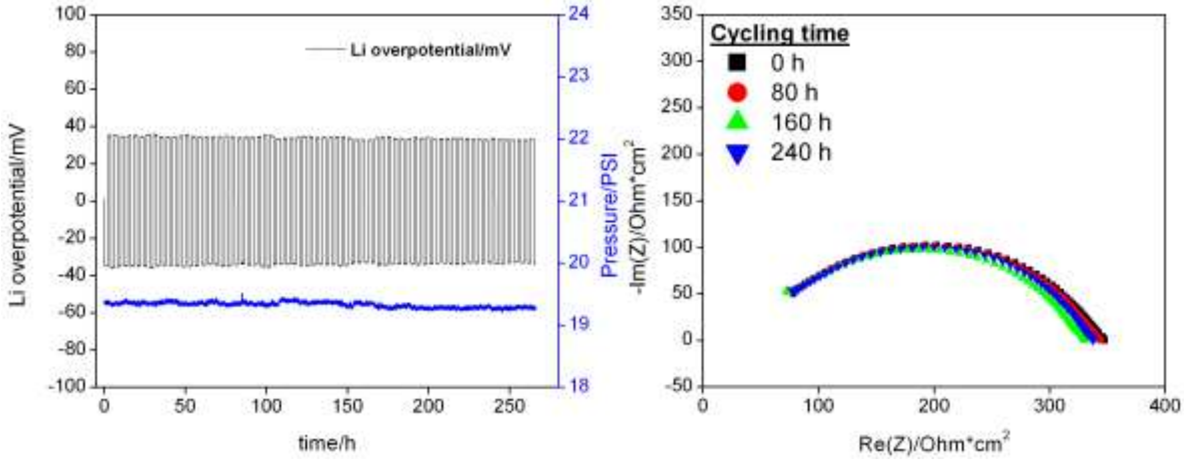

Figure 112. Li/LLZO/Li symmetric cell cycling at 185°C (with *in situ* pressure analysis) at 0.1 mA/cm^2 with corresponding electrochemical impedance spectroscopy analysis.

Typical bulk electrolyte and interfacial resistance were found to be roughly 40 Ω.cm^2 and 300 Ω.cm^2, respectively. Ongoing work includes improving interface between LLZO and Li-metal anode at 100 to150°C, as well as reducing LLZO electrolyte thickness while maintaining good mechanical properties. Li/O$_2$ cells using LLZO-protected lithium anode were also tested. The air cathode/catholyte consisted of a 2-to-1 mixture $LiNO_3$:KNO_3 eutectic with Super P Carbon (5% PTFE). Tests were conducted at 185°C to ensure good Li-LLZO-catholyte contact. It is expected that the elevated temperature may lead to rapid carbon degradation in presence of ORR products as well as enhanced Li_2O_2 solubility (leading to poor rechargeability). Figure 113a shows Li/O$_2$ cell discharge curve using a LLZO-protected lithium anode and a molten nitrate catholyte (j= 0.05 mA/cm^2, 185°C, m_{carbon}= 5 mg/cm^2, $m_{nitrate}$= 10 mg/cm^2). Separately, the project analyzed ORR discharge product morphology using a boron carbide air cathode. Boron carbide O$_2$ cathodes were collected from OCV and discharged molten nitrate Li/O$_2$ cells, rinsed in an organic solvent to remove excess nitrate salt, and analyzed by SEM (Figure 113b-c).

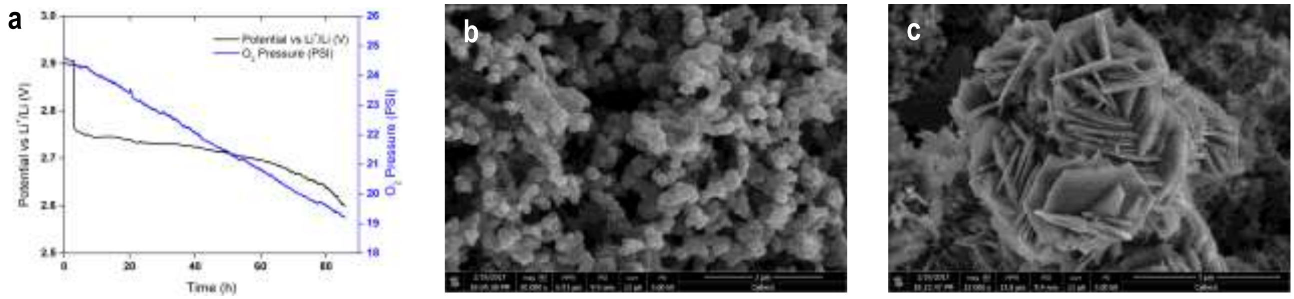

Figure 113. (a) Li/O^2 cell discharge curve using a LLZO-protected lithium anode and a molten nitrate catholyte (j= 0.05 mA/cm2, 185 °C, m_{carbon}= 5 mg/cm^2, $m_{nitrate}$= 10 mg/cm^2). Scanning electron microscopy analysis of boron carbide air electrode (b) before and (c) after discharge under O$_2$ in $LiNO_3$-KNO_3 eutectic at 150°C.

Task 9.3 – Lithium–Air Batteries
(Khalil Amine and Larry A. Curtiss, Argonne National Laboratory)

Project Objective. This project will develop new cathode materials and electrolytes for Li-air batteries for long cycle life, high capacity, and high efficiency. The goal is to obtain critical insight that will provide information on the charge and discharge processes in Li-air batteries to enable new advances to be made in their performance. This will be done using state-of-the-art characterization techniques combined with state-of-the-art computational methodologies to understand and design new materials and electrolytes for Li-air batteries.

Project Impact. The instability of current nonaqueous electrolytes and degradation of cathode materials limits the performance of Li-air batteries. The project impact will be to develop new electrolytes and cathode materials that are stable and can increase cycle life and improve efficiency of Li-air batteries.

Approach. The project is using a joint theoretical/experimental approach for design and discovery of new cathode and electrolyte materials that act synergistically to reduce charge overpotentials and increase cycle life. Synthesis methods, in combination with design principles developed from computations, are used to make new cathode architectures. Computational studies are used to help understand decomposition mechanisms of electrolytes and how to design electrolytes with improved stability. The new cathodes and electrolytes are tested in Li-O_2 cells. Characterization along with theory is used to understand the performance of the materials used in the cell and make improved materials.

Out-Year Goals. The out-year goals are to find catalysts that promote discharge product morphologies that reduce charge potentials and find electrolytes for long cycle life through testing and design.

Collaborations. This project engages in collaboration with Professor Kah Chun Lau (University of California – Norridge), Professor Amin Salehi (University of Illinois – Chicago), Professor Yang-Kook Sun (Hanyang University), Professor Yiying Wu (Ohio State University), and Dr. Dengyun Zhai (China).

Milestones

1. Investigation of new architectures for platinum catalysts using hollow nanocarbon cages. (Q1 – Complete)
2. Design and synthesis of new catalysts for cathode materials based on metal organic frameworks for low charge overpotentials. (Q2 – In progress)
3. Development of new characterization techniques for determination of the composition and conductivity of discharge products in Li-O_2 batteries. (Q3)
4. Investigation of uniformly synthesized metal clusters as catalysts and nucleation sites for controlling efficiency of Li-O_2 cells. (Q4)

Progress Report

Fundamental understanding of reactions of lithium peroxides and superoxides is essential for the development of Li-O_2 batteries. In this context, an investigation is reported of the hydrolysis of lithium superoxide, which has recently been synthesized in a Li-O_2 battery. Surprisingly, the hydrolysis of solid LiO_2 is significantly different from that of NaO_2 and KO_2. Unlike KO_2 and NaO_2, the hydrolysis of LiO_2 does not produce H_2O_2. Similarly, the reactivity of Li_2O_2 toward water differs from LiO_2, in that Li_2O_2 results in H_2O_2 as a product. Based on this a titration method that depends on the reaction of a Li-O_2 discharge product with a Ti(IV)OSO_4 solution, has been developed that provides a useful diagnostic technique to provide information on the composition of a discharge product in a Li-O_2 battery.

Initially a Li-O_2 cell with an Ir-rGO (reduced graphene oxide) cathode was used to produce a LiO_2 discharge product. The reaction of the LiO_2 discharge product with water was investigated using a spectrophotometric method to assess the amount of hydrogen peroxide produced. In this procedure, the team first establishes a calibration curve by adding incremental amounts of Li_2O_2 to the test reagent Ti(IV)OSO_4 as shown in Figure 114. The discharge product LiO_2 on the Ir-rGO cathode is then reacted with the acidic solution of Ti(IV)OSO_4 after removal of the electrolyte, but with the cathode material still present. Under the experimental conditions, Ti(IV) exists as TiO^{2+}(aq) complexed with SO_4^{2-} ion in 1.0 M H_2SO_4. If hydrogen peroxide is present, a color change to yellow/orange occurs due to the formation of a titanium peroxide complex, TiO_2SO_4. When the acidic solution of Ti(IV)OSO_4 was added to the LiO_2 discharge product, the liquid remained colorless and no notable UV/Vis intensity change was observed, as shown in Figure 115. From the UV/Vis spectra, the absorbance intensity is essentially negligible based on a calibration curve, which indicates the absence of hydrogen peroxide. The LiO_2 results are in contrast to the case for KO_2 and NaO_2 where an obvious color change is observed for this procedure, consistent with the presence of a hydrogen peroxide product. It is also in contrast to the case of a known discharge product of Li_2O_2 where the same titration test shows a positive result (that is, color change) for the presence of H_2O_2.

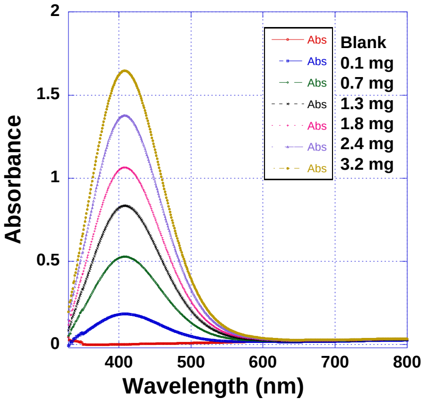

Figure 114. Ultraviolet/visible measurements (dual beam) of Li_2O_2 powders (Aldrich) added to 50 mL of $TiOSO_4$ reagent (aq).

Figure 115. Photograph of the cathode (Ir-rGO/LiO_2) discharged to 1000 mAh/g, dried under argon for 1 h and then soaked in 3.00 mL of $TiOSO_4$(aq); no apparent color change occurred upon titration indicating no Li_2O_2 is present.

Patents/Publications/Presentations

Publication

- Wang, H., and Y. Lee, R. S. Assary, C. Zhang, X. Luo, P. C. Redfern, J. Lu, Y. Lee, D. Kim, T. Kang, E. Indacochea, K. Lau, K. Amine, and L. A Curtiss. "Lithium Superoxide Hydrolysis and Relevance to Li-O_2 Batteries." *J. Phys. Chem. C* (2016). doi: 10.1021/acs.jpcc.6b12950.

TASK 10 – SODIUM–ION BATTERIES

Summary and Highlights

To meet the challenges of powering the PHEV, the next generation of rechargeable battery systems with higher energy and power density, lower cost, better safety characteristics, and longer calendar and cycle life (beyond Li-ion batteries, which represent today's state-of-the-art technology) must be developed. Recently, Na-ion battery systems have attracted increasing attention due to the more abundant and less expensive nature of the sodium resource. The issue is not insufficient lithium on a global scale, but what fraction can be used in an economically effective manner. Most untapped lithium reserves occur in remote or politically sensitive areas. Scale-up will require a long lead time, involve heavy capital investment in mining, and may require the extraction and processing of lower quality resources, which could drive extraction costs higher. Currently, high costs remain a critical barrier to the widespread scale-up of battery energy storage. Recent computational studies on voltage, stability, and diffusion barriers of Na-ion and Li-ion materials indicate that Na-ion systems can be competitive with Li-ion systems.

The primary barriers and limitations of current state-of-the-art of Na-ion systems are as follows:

- Building a sodium battery requires redesigning battery technology to accommodate the chemical reactivity and larger size of sodium ions.
- Lithium batteries pack more energy than sodium batteries per unit mass. Therefore, for sodium batteries to reach energy densities similar to lithium batteries, the positive electrodes in the sodium battery need to hold more ions.
- Since Na-ion batteries are an emerging technology, new materials to enable sodium electrochemistry and the discovery of new redox couples along with the diagnostic studies of these new materials and redox couples are quite important.
- In sodium electrochemical systems, the greatest technical hurdles to overcome are the lack of high-performance electrode and electrolyte materials that are easy to synthesize, safe, and non-toxic, with long calendar and cycling life and low cost.
- Furthermore, fundamental scientific questions need to be elucidated, including (1) the difference in transport and kinetic behaviors between sodium and lithium in analogous electrodes; (2) sodium insertion/extraction mechanism; (3) SEI layer on the electrodes from different electrolyte systems; and (4) charge transfer in the electrolyte–electrode interface and Na+ ion transport through the SEI layer.

This task will use synchrotron-based *in situ* X-ray techniques and other diagnostic tools to evaluate new materials and redox couples, to explore fundamental understanding of the mechanisms governing the performance of these materials, and provide guidance for new material developments. This task will also be focused on developing advanced diagnostic characterization techniques to investigate these issues, providing solutions and guidance for the problems. The synchrotron based *in situ* X-ray techniques (XRD and hard and soft XAS) will be combined with other imaging and spectroscopic tools such as HRTEM, MS, and TXM.

Task 10.1 – Exploratory Studies of Novel Sodium-Ion Battery Systems
(Xiao-Qing Yang and Seongmin Bak, Brookhaven National Laboratory)

Project Objective. The primary objective is to develop new advanced *in situ* material characterization techniques and to apply these techniques to explore the potentials, challenges, and feasibility of new rechargeable battery systems beyond the Li-ion batteries, namely the Na-ion battery systems for PHEVs. To meet the challenges of powering the PHEV, new rechargeable battery systems with high energy and power density, low cost, good abuse tolerance, and long calendar and cycle life must be developed. This project will use synchrotron-based *in situ* X-ray diagnostic tools developed at BNL to evaluate the new materials and redox couples, exploring the fundamental understanding of the mechanisms governing the performance of these materials.

Project Impact. The VTO Multi-Year Program Plan describes the goals for battery: “Specifically, lower-cost, abuse-tolerant batteries with higher energy density, higher power, better low-temperature operation, and longer lifetimes are needed for the development of the next-generation of HEVs, PHEVs, and EVs.” If this project succeeds, the knowledge gained from diagnostic studies and collaborations with U.S. industries and international research institutions will help U.S. industries develop new materials and processes for a new generation of rechargeable battery systems beyond Li-ion batteries, such as Na-ion battery systems, in their efforts to reach these VTO goals.

Approach. This project will use synchrotron-based *in situ* X-ray diagnostic tools developed at BNL to evaluate the new materials and redox couples to enable a fundamental understanding of the mechanisms governing the performance of these materials and to provide guidance for new material and new technology development regarding Na-ion battery systems.

Out-Year Goals. The out-year goals are as follows: (1) Complete the synchrotron based *in situ* XRD and absorption studies of MXene type material V_2C as new cathode material for Na-ion batteries during charge-discharge cycling, and (2) complete the preliminary synchrotron based X-ray absorption studies of $NaCuMnO_2$ as new cathode material for Na-ion batteries.

Collaborations. The BNL team has been working closely with top scientists on new material synthesis at ANL, LBNL, and PNNL, with U.S. industrial collaborators at GM and Johnson Controls, and with international collaborators.

Milestones

1. Complete the *in situ* XRD studies of one type of MXene material V_2C as new anode material for Na-ion batteries during charge-discharge cycling. (December 2016 – Complete)
2. Complete *in situ* hard X-ray absorption studies at vanadium K-edge of one type of MXene material V_2C as new anode material for Na-ion batteries during charge-discharge cycling. (March 2017 – Complete)
3. Complete soft X-ray absorption studies at vanadium L-edge, carbon, and oxygen K-edge of one type of MXene material V_2C as new anode material for Na-ion batteries at different charge-discharge states. (June 2017 – In progress)
4. Complete the synchrotron based X-ray absorption at copper and manganese K-edge for a new $NaCuMnO_2$ cathode material for Na-ion batteries during charge-discharge cycling. (September 2017 – In progress)

Progress Report

This quarter, the second milestone for FY 2017 was completed. BNL has been focused on the studies of a new cathode material for sodium-ion batteries. A V_2C material, as a new member of the two-dimensional TM carbides, so-called MXenes, was synthesized in a way containing surface functional groups (denoted as V_2CT_x, where T_x are surface functional groups) and studied as anode materials for Na-ion batteries. V_2CT_x anode exhibits reversible charge storage with good cycling stability and high rate capability through electrochemical test. In the second quarter, the *ex situ* hard X-ray absorption studies at vanadium K-edge of MXene material V_2C as new anode material for sodium ion batteries during charge-discharge cycling has been carried out. The *ex situ* V *K*-edge XANES spectra presented in Figure 116a were measured on samples harvested from cells discharged and charged to different voltages during the first cycle (OCV→0.1V→3V), as shown on the charge/discharge curve in Figure 116b. The V *K*-edge XANES spectra presented in Figure 116a show a relatively weak pre-edge peak (marked as A) at 5470 eV and a strong main absorption peak (marked as B) at around 5485 eV. The pre-edge absorption is associated with the transition to hybridized electronic states of the metal 3*d* and carbon 2*p* orbitals. The pre-edge peak of V_2CT_x spectra can be assigned to the transition of a 1*s* electron to the hybridized t_{2g} (V 3*d* + C 2*p*) and e_g (V 3*d* + C 2*p*) orbitals. And the main absorption peak “B” involves the dipole allowed transition of 1*s* electrons to unoccupied V 4*p* states. The spectra for V_2CT_x at different discharge/charge states do not show significant differences in shapes, but the edge shift is clearly observable during both discharge and charge process (inset in Figure 116a). A plot of the V *K*-edge energies, at half height of normalized XANES spectra, as a function of sodiation/desodiation state in Figure 116c clearly show the consistent energy position changes from one voltage step to the next. During first sodiation process from OCV to 0.1 V, the edge shifts to lower energy, which reflects the reduction of vanadium. During desodiation process from 0.1 V to 3 V, the edge shifts back to the higher energy indicating the oxidation of vanadium.

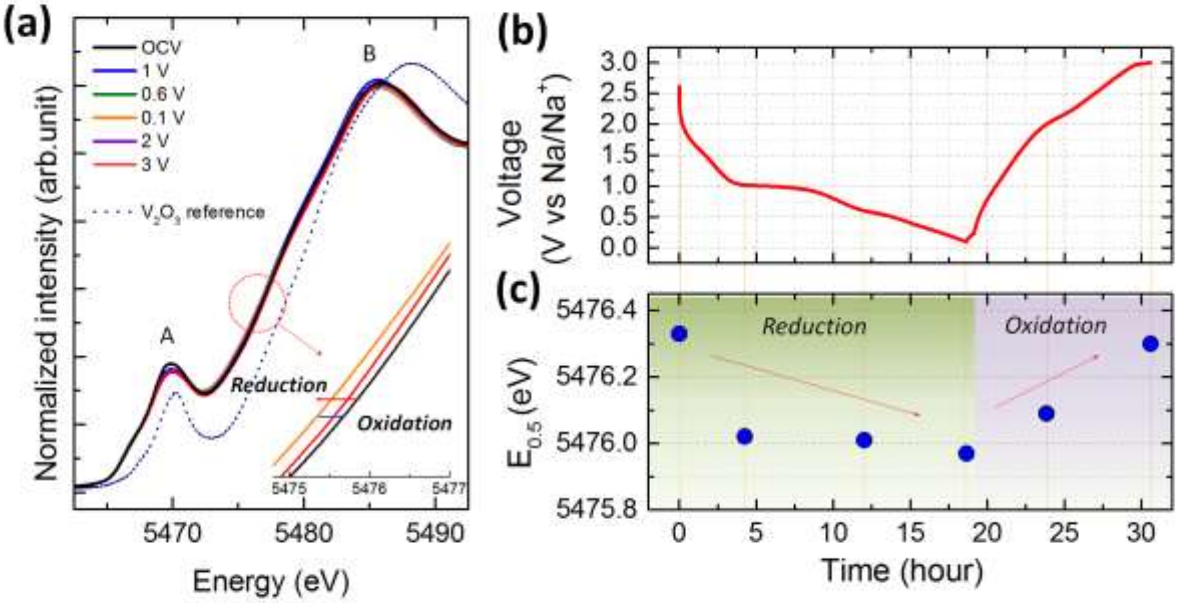

Figure 116. (a) *Ex situ* V K-edge X-ray absorption near edge spectroscopy (XANES) spectra of V_2CT_x at selected cell voltages during first sodiation/desodiation process (OCV→0.1V→3V). (b) Corresponding voltage profile. (c) Variation of V edge energy (at half height of normalized XANES spectra) at selected cell voltage.

Patents/Publications/Presentations

Publication

- Cao, Ming-Hui, and Yong Wang, Zulipiya Shadike, Ji-Li Yue, Enyuan Hu, Seong-Min Bak, Yong-Ning Zhou*, Xiao-Qing Yang,* and Zheng-Wen Fu.* "Suppressing the Chromium Disproportionation Reaction in O_3-Type Layered Cathode Materials for High Capacity Sodium-Ion Batteries." *J. Mater. Chem. A* 5 (2017): 5442–5448. Doi: 10.1039/C6TA10818K.

Presentation

- IBA 2017 Conference, Nara Kasugano International Forum, Nara, Japan (March 5–10, 2017): "Studies of New Electrode Materials for Next Generation of Batteries Using Synchrotron Based *In Situ* X-ray Diffraction and Absorption as well as TXM Techniques"; Enyuan Hu, Xiao-Qing Yang*, Yongning Zhou, Xiqian Yu, Seong-Min Bak, Hung-sui Lee, Yijin Liu, Hong Li, Xuejie Huang, and Liquan Chen. Invited.